DEVELOPING A LOW-COST CERAMIC MICRO-POROUS WATER FILTER FOR REMOVAL OF MICROORGANISMS THAT CAUSE COMMON DISEASES

by

Author: Jean Jacques Simonis

submitted to the

Faculty of Science

in fulfilment of the requirements of the degree of

Doctor of Philosophy

in the Department of Hydrology at the University of Zululand

Supervisor: Prof. B.E. Kelbe

Co-Supervisor: Prof. N. Revaprasadu

Co-Supervisor: Dr. A.K. Basson

Date submitted: November 2012

APPROVAL

Supervisor: Prof. B.E. Kelbe_____Date:_____

Co-Supervisor: Prof. N. Revaprasadu_____Date:_____

Co-Supervisor: Dr. A.K. Basson_____Date:_____

ABSTRACT

Africa is one of the most water-scarce continents on earth and the lack of potable water is responsible for the death of approximately 4 900 children every day. Water can be effectively decontaminated by using a household ceramic water filter. The local production of low-cost water filters suitable for the removal of suspended material and pathogenic bacteria from water sources, especially in rural areas, provides a promising solution to the problem and is therefore important to pursue.

The traditional slip casting process was used develop a micro-porous ceramic water filter. The method was found to be more suitable than either extrusion or die casting for manufacturing a locally suitable, low cost ceramic water filter. Slip casting, requiring limited expensive equipment, usage of locally available raw materials, labour and expertise makes this the only promising method for manufacturing ceramic filters in a rural, non-technical setting.

Using milled lithium alumino-silicate had the main advantages of thermal shock resistance and dimensional stability because of the material's zero thermal expansion at firing temperatures. Milling tests based on the Andreasen packing model were used for obtaining the best particle packing for the raw material recipe. The material also provides dilatant rheology matching the rheology of the organic carbon pore-former. The candle- type filter required less raw material compared to the other low cost filter such as the pot- type filter from (PfP). The particle size of the pore-former provided us with small pores around 3 microns after firing for the elimination of bacteria from drinking water. These pores were much smaller and more effective when compared with Potters for Peace (PfP's) pore size of 16-25 micron. The zero thermal expansion (adopted ZTE product name) helped to prevent damage (cracking) to the product during heating and gave accurate control of the ultimate filter size after sintering.

The large apparent porosity results of between 67-73 per cent for the finished product provide a specific surface area of 7 m^2 g^{-1} and a high flow rate which explains the filtration efficiency of the filter. The 32 minute retention time of water further helps with the filtration effectiveness. Bacteriological testing exceeded all expectations. The product was tested using water contaminated with high concentrations of selected bacterial cultures as well as with water from local polluted streams.

The product complies with the WHO (2011) recommendation requirement for household water treatment (HWT) technologies of a LRV ≥ 4 (log reduction value).

With correct cleaning and basic maintenance, this filter can effectively provide clean drinking water for rural families affected by polluted surface water sources. This product can immediately be useful to families placed in situations where polluted drinking water causes distress. The filter could provide a low-cost solution for the millions of people without access to potable water in Africa.

Furthermore, such a project provides opportunities for local financing and innovation. The method of slip casting for the manufacture of porous ceramic used in this study has been showed to work very successfully. The filter requires fewer raw materials, energy for the shaping- and firing- process, finishing, storage space, it is small, compact, and more effective against bacterial load and has a flow rate 3-4 times faster than any other low cost manufactured filter. The low unit manufacturing cost, places *Outbac* in a strong position, to also compete on a price-only-basis with other low cost, ceramic filter producers in the world.

Keywords: bacteria; ceramic filter; micro-porous; slip casting; water filtration

ACKNOWLEDGEMENT

Thank you to my wife, Anita and children, Jean-Francois and Simone, who shared both the good and the bad times with me.

Thank you to Ron Wilkinson who agreed to edit the thesis for further enhancement of the work.

Thank you to Prof. Bruce Kelbe, Dr. Albert Basson and Prof. Nerish Revaprasadu for their excellent guidance and patience throughout the whole research project. Thank you to Dirk Kotze for his initial guidance and ceramic knowledge.

Thank you to God for the inspiration as well as the original idea to develop the water filter for improving the living conditions of thousands of poor in the world: “Let Your living water flow over my soul…”

STATEMENT OF ORIGINALITY

I declare that the research : "DEVELOPING A LOW-COST CERAMIC MICRO-POROUS WATER FILTER FOR REMOVAL OF MICROORGANISMS THAT CAUSE COMMON DISEASES" done and reported in this dissertation is original work done by himself, and was not copied from any source, unless referenced clearly.

Signed:_____Date: 13th of April 2013

Jean Jacques Simonis

CONTRIBUTION TO THE BODY OF KNOWLEDGE

The results from the research have been published in three peer-reviewed journals for which the papers are attached in the APPENDIX:

1. **Paper I**: Evaluation of a low-cost ceramic micro-porous filter for elimination of common disease microorganisms. Elsevier's **Physics and Chemistry of the Earth**, 36 (2011), pp. 1129-1134.
2. **Paper II**: Manufacturing a low-cost ceramic micro porous filter and filter system for elimination of common pathogenic bacteria. Elsevier's **Physics and Chemistry of the Earth**, 50-52 (2012), pp. 269-276.
3. **Paper III**: Manufacture Of A Low-Cost Ceramic Microporous Filter For The Elimination Of Microorganisms Causing Common Diseases, IWA **Journal of Water, Sanitation and Hygiene for Development**, 03.1, 2013, pp. 42-50.

The development, manufacture and evaluation of the ***OUTBAC*** ceramic water filter has been demonstrated and presented at Symposia and other important venues during the past 4 years:

1. Research Project Registration (UNIZUL): Project Registration No. S 462/09- developing a low-cost ceramic micro-porous filter for the elimination of common disease microorganisms
2. Oral presentation: UNIZUL 4th Annual Postgraduate Symposium (October 2009) which qualified as the best presentation of the Symposium.
3. Oral presentation: UKZN Durban– Society for Microbiology Symposium (November 2009)
4. Oral presentation: UNIZUL 5th Annual Postgraduate Symposium (November 2010)
5. Poster presentation: 11th International WATERNET Symposium, October 2010, Vic Falls, Zimbabwe
6. Poster presentation: International Young Water Professionals Conference, June 2011, Pretoria
7. Poster presentation: GWSSA 2nd Regional Conference on Groundwater, September 2011, Pretoria
8. Poster presentation: 12th International WATERNET Symposium, October 2011, Maputo, Mozambique
9. Practical demonstration: COP 17, Durban: where a stall was manned for a two day demonstration and display of the ***OUTBAC*** and ***BACSTER*** ceramic filters to international delegates.
10. Poster presentation at 13th International Waternet Symposium in Johannesburg in October 2012: Viral removal through precipitation of nano-sized metallic salts on a low cost micro-porous ceramic water filter.

11. Oral presentation: IWA Regional Conference on Membrane Technology, December 2012 in Beunos Aires, Argentina: Making a low-cost ceramic microporous filter for the elimination of microorganisms causing common diseases.

TABLE OF CONTENTS

LIST OF FIGURES

LIST OF TABLES

Chapter 1: Introduction

1.1 Background

In 2006 it was reported by WHO (2006) that of the 735 million people living in sub Saharan Africa, only 44 percent had access to potable water. Du Preez *et al* (2008) indicate that in 2000, 66 percent of families in South Africa had access to a reliable water supply. It is therefore not surprising that in South Africa diarrhea is responsible for 11 percent of the deaths among children under the age of 5. In the rest of the developing world this number increases to 21 percent, resulting in 2.5 million deaths per annum. Lemons (2009) estimates that 40 percent of all child deaths resulting from diarrhea occurs in sub-Saharan Africa. According to Lemons (2009), most of Africa is therefore not going to meet the Millennium Development Goals and therefore drastic action plans have to be drawn up. Pruss *et al* (2002) and Moszynski (2006) state that "Unsafe drinking water contributes to a staggering burden of water-related disease in developing countries, borne primarily by the poor". According to McAllister (2005), more than 4 percent of all worldwide deaths occur as a result of diarrhea caused by bacterial pathogens.

According to Brown *et al* (2007), the word "diarrhea" is derived from an ancient Greek word meaning "leakage" or "flowing out/through". The symptoms of diarrhea vary with age, immune status and nutritional status. The impact of pathogens is unequally distributed in the population, with the children, elderly, pregnant and immune-deficient patients suffering the most. At any moment in time, half of the people in the developing world have a health problem related to inadequate water and sanitation (Brown *et al* 2007).

According to du Preez *et al* (2001), serious diarrheal disease is normally related to the pathogens *Salmonella-*, *Shigella-* species and *Vibrio cholerae*, resulting in an estimated 4.5 million loss of life annually due to diarrhea. The World Health Report (2008) lowers this number of deaths from polluted water, lack of sanitation and poor hygiene to 1.6 million diarrheal deaths, mostly of children under the age of five. This is mostly attributable to fact that 1.1 billion people are without access to potable water

sources (WHO 2009).

The recent cholera epidemic in Zimbabwe and the RSA has again shown that poor sanitation levels and insufficient water supply leads to increased diarrheal infection levels which, in turn, leads to death, poor health and a deteriorating socio-economic situation in our society. The WHO (2009) reported that 3 759 people lost their lives from the outbreak with another 80 250 people being infected. People were infected so quickly that half of the deceased never even made it to the 365 cholera centers. The open sewage and untreated drinking water resulting from a dysfunctional infrastructure in Zimbabwe was generally seen as the cause of this outbreak.

The situation in South Africa is no better with the government spending in 2008 slightly more than one percent of the R180bn needed for upgrading the water purification and sewerage infrastructure (FTE 2008). People are therefore starting to look for alternative solutions to their drinking water. The poor, however, do not have the luxury of choice but have to use polluted water as drinking water.

According to the National Water Resources Strategy, as quoted by Tarton (2008), South Africa has already allocated around 98 percent of the national water resources at a high assurance of supply to rural and urban requirements, mining and industrial users, power generation, irrigation, afforestation and transfer of water (DWA 2004).
Our water resources are therefore insufficient to consistently dilute pollutants and effluent in our streams (Tarton 2008). This has led to increased eutrophication, treatment complexity and purification/treatment costs. Van Vuuren (2008) estimates that 35 percent of total storage available in our dams are either eutrophic or hypertrophic (extremely nutrient enriched). This fact was practically illustrated in the 2008 Duzi Canoe Marathon when more than 40 percent of the participants contracted chronic diarrhea as a result of contact with the contaminated water of the Duzi River (FTE 2008).

1.2 Conventional water treatment

Standard bulk-water purification methods applied in high income countries are neither cost effective nor technically adoptable to low-income countries (Clopeck *et al* 2006). In developing countries, household-scale ceramic filters are being used as a better treatment option for both unpurified and insufficiently disinfected water at household level (Lantagne 2005; Clasen and Biosson 2006). Their use is becoming widespread, especially with the involvement of governments and international NGOs. Organisations such as Potters for Peace (http://www.potterswithoutborders.com), have established production facilities in a number of developing countries.

In short, the reasons why the traditional water treatment and delivery approach cannot meet the demands of the 1 – 2 billion people who still need potable water are as follows:

- They require high capital investment
- They require concentrated populations
- They require on-going maintenance (costs)
- They require a high quantity water source
- They require fee-paying users
- They lack adequate chlorination, mostly due to monetary issues
- They result in water losses (> 40 percent)
- They result in supply pressures that are too low

This results in the need for the poor to collect their own water outside their homes and then clean and store it for use at household level (Sobsey 2002).

The WHO (2009) states that of the 1.1 billion people without access to safe water, 84 per cent live in rural areas where centralised water distributions and treatment systems are often too complicated or too expensive to install. Even in areas with piped systems, treatment plants often do not function well. Contamination of drinking water also takes place between the tap point and the point of use. In all such cases water can be made safer to drink by treatment at the household level by means of Point of Use (POU) House Water Treatment Systems (HWTS) or ceramic water filters (CWF).

1.3 Advantage of using POU, CWF and HWTS

According to the WHO (2007), a growing body of research has confirmed the key role that POU water quality interventions can play in reducing diarrheal disease in a cost-effective manner.

The WHO report makes a strong case for managing water quality in the house. WHO (2009) have established a network aimed at promoting House Water Treatment Systems (HWTS). The network has led to HWTS format that optimizes flexibility and participation and supports coordinated action. The revised Sphere Standards for emergency relief promote household water treatment as an option in emergencies as well as in development settings (Sphere Project, *2004*).

What alternatives are there to traditional approaches in the developing world, especially where piped, high quality water systems for households are still decades away? Point of use (POU) systems at household level can provide such a solution. The lack of access to piped water has sparked interventions into alternative POU technologies. Sobsey (2002) reports that out of 37 water treatment options available, ceramic water filters (CWF) are one of the five best treatment options for reducing turbidity and bacterial levels by more than 99%. In developing countries, household-scale ceramic filters are being used as a better treatment option for both unpurified and insufficiently disinfected water at household level (Lantagne 2001; Clasen and Boisson 2006). Their use is becoming widespread, especially with the involvement of governments and international NGOs. Brown and Sobsey (2010) highlight a number of both published and unpublished microbial investigations of locally produced ceramic filters worldwide. Clasen *et al* (2005, 2006 and 2007) shows that more expensive commercially manufactured filters are effective against microbial pathogens. Brown and Sobsey (2010) provide further evidence that low-cost ceramic filters (CWF) can reduce bacteria concentration by 99 percent under laboratory conditions but find a lower effectiveness rate when tested under actual field conditions.

Eisenberg *et al* (2007) explains that the burden of diarrheal diseases resulting from inadequate water quality, poor sanitation practices and hygienic conditions remains high and that there is still limited understanding of the integration of these environmental control strategies. Eisenberg *et al* (2007) subsequently tested a household-level stochastic model designed to capture the interdependent transmission pathways of enteric pathogens. The model accounted for 5 different transmission pathways.

In an effort to find which diseases are preventable by water treatment, households that had been fully exposed to contaminated drinking water were compared to households that had benefited from water quality intervention. It was found that the benefits of water quality intervention depended on sanitation and hygienic conditions. The conclusion of the study showed that reduction and elimination of diarrheal disease is only possible through integrated control strategies[1].

The Eisenberg *et al* (2007) survey has proven that household water treatment and safe storage (HWTS) interventions can lead to dramatic improvements in drinking water quality and reduction in diarrheal disease, thus making an immediate difference to the lives of those who rely on water from polluted rivers, lakes and, in some cases, unsafe wells or piped water supplies. To accelerate health gains to people without reliable access to safe drinking water, research in the area of POU filtration and specifically ceramic filters is a necessity and not a luxury.

One of the options recommended by the WHO and UNICEF (2006) and the WHO (2009) is ceramic filters. The WHO and UNICEF is increasingly seeing ceramic filters as a user friendly and commercially attractive option to improve the quality of drinking water at the household level such as in India and Brazil where high cost commercial ceramic filters are in use.

[1] more than one control strategy used in series: flocculation followed by filtration or filtration followed by UV treatment

Clasen *et al* (2005) give an example from 2003 of how effective CWF can be in disaster areas. Poor land-use and heavy rains resulted in flooding of the Montecristi District in the Dominican Republic. Clean water had to be supplied to thousands of families whose normal water resources had been destroyed. Oxfam initiated a pilot study in February 2004 to provide 431 families with household water treatment system (HWTS). The system was made up of two 20-litre buckets fitted with three ceramic candles (Ceramica Stefani) and a tap. Due to the success of the pilot study, more filters were distributed.

Chaudhuri *et al* (1994) randomly selected filters available commercially in India and investigated the performance of two ceramic filter candles and one silver-impregnated filter candle with a layer of activated carbon, using *Escherichia coli* and poliovirus challenge water and filtration tests that replicate household water treatment. They found not one of the filters to be reliable as viralogical water purifiers. They recommended additional strategies be combined with ceramic filtration during outbreak of waterborne diseases.

Doulton Filters (2009) furthermore explains that many ceramic water filters (CWF) are additionally treated with colloidal[2] silver to further incapacitate bacteria and to prevent the growth of mould and algae in the body of the filter. Pore size reduction, metallic and metal oxide coatings as well as addition of slow release iodine resins are receiving attention as viralcides. By reducing the filter pore size to less than one micron for bacterial removal also make filters more effective in turbidity removal.

1.4 Cost benefit using HWTS

According to Fewtrell *et al* (2005), as more evidence is being gathered, the results show HWTS to be more effective and cost efficient than conventional treatment approaches.

[2] small, finely divided material that stays dispersed in a liquid as a result of their small size

Potters without Borders (2009) became involved in HWTS by using a low-cost press to manufacture ceramic pot filters. The micro-porous ceramic filters kept out bacteria and could, with the addition of a colloidal silver layer (fired into the ceramic), neutralise the build-up of microorganisms and make the filter effective over a longer time period.

Non-governmental organizations (NGOs) have used both commercial and locally-made units to improve the drink ing water of communities in at least 17 countries over the past five years. Filters have been shown to offer certain advantages over chemical and other approaches of water treatment, including their high microbial mortality, low cost, long life, efficacy in a wide variety of water conditions (temperature, pH, turbidity), and high levels of acceptability by the target population. Clasen and Boisson (2006) furthermore explain that in order to ensure that the systems continue to provide sufficient protection against microbial pathogens, programme implementers must convince householders of the need to replace the ceramic filter elements periodically. Equally important is the establishment of a means by which householders can obtain access to affordable replacement filter elements. This cost may not be a major obstacle, as in follow-up interviews most householders reported their willingness to pay for replacement filters (Clasen and Boisson 2006).

Clasen *et al* (2007) used the filtration effectivity data from a recent systematic review, cost data from programme implementers and World Health Organization databases to conduct a cost-effectiveness analysis. In the study they compared the cost-effectiveness of piped (bulk treatment) with non-piped, at source based (dug well, borehole and communal stand post) and four types of household-based interventions (chlorination, ceramic filtration, solar disinfection, flocculation/disinfection) to improve the microbial quality of water for prevention of diarrhoeal disease. When their results were measured against international benchmarks, it was found that source- and household based interventions were generally cost effective or highly cost effective even before considering the estimated saving in health costs that would offset the cost of implementation. It is also important to ensure that water quality interventions are guided by local conditions, user preferences, potential for cost recovery from beneficiaries and other factors (Clasen *et al* 2007).

Clasen *et al* (2007) highlight a UN result that shows how diarrhea morbidity can be decreased by up to 25 percent by providing potable water. The cost benefit for water and sanitation improvement at a global level is huge, especially if it results in significant reduction in disease incidence. The costs of halving the proportion of people without potable water by using roof rain water collection, borehole or protected springs, productivity improvements and healthcare costs savings results in a financial benefit of R 600 for every R10 invested.

1.5 Water filtration methodology

According to Green by Design (2009), water filters have been manufactured and used for ages. The earliest attempts to filter water date as far back as 2000 BC and included such methods as boiling water, placing hot metal instruments in water, and sand and charcoal filters. These old designs predate knowledge about the existence of bacteria and toxic chemicals. Only with the invention of the microscope, have scientists identified the harmful waterborne bacteria that can be removed by sand filtration to reduce diseases. It was only in 1804 that large scale sand filters were introduced in a municipal water treatment plant in Scotland and later throughout England. Further advances followed in England with the addition of chlorine to treated water. The use of chlorine then spread to the USA and afterwards to all parts of the world. The side effects of using chlorine as a disinfectant has only been investigated in recent times (Green by Design 2009).

Doulton Filters (2009) explains that with most filtration methods, water is introduced from one side of the filter, which acts to block the passage of particulate material. Only water and dissolved constituents will pass through to the other "clean" side of the filter. According to the USFilter (2012) there are 7 mechanisms involved in filtering particles from water:

1. Blocking: particle blocked by a physical barrier
2. Bridging: linked particles prevented from entering together
3. Sieving: particle size prevents access through pores and is retained on filter surface
4. Inertial impaction: particle enters but loses momentum and is entrapped in the

pores

5. Molecular dispersive interception: particle trapping due to the random movement of the molecules.
6. Electro-kinetic adhesion: particle and filter medium charge results in particle adherence
7. Stoke's settling: particle density results in gravitation settlement.

Figure 1.1 differentiates between a membrane and a ceramic micro filter. A membrane can be defined as a selective barrier between two phases (Mulder 1996). In membrane filtration the feed is separated into two streams, the retentate (waste stream) and permeate (product) streams. In ceramic micro filtration all of the feed permeates through the membrane to become permeate.

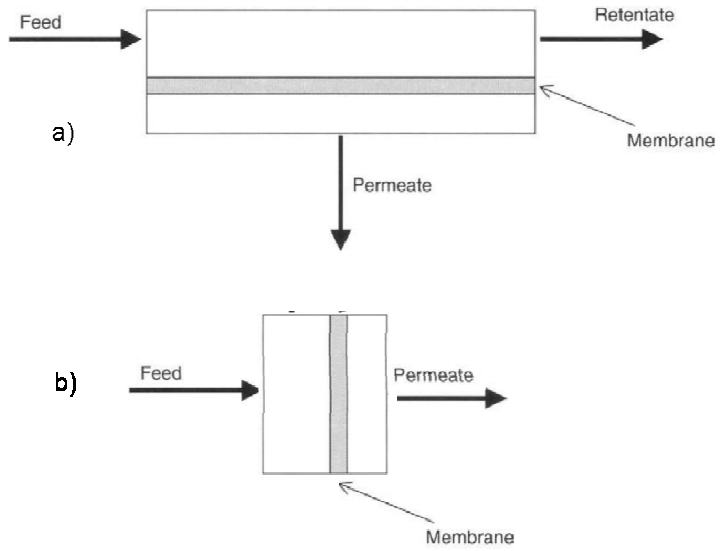

Figure 1.1: (a) Membrane and (b) microfiltration: (ceramic) separation processes (Tsuru 2003)

The process of water filtration can therefore be described as the elimination of suspended material (organic and inorganic) from water by flow through a membrane (porous or semi permeable). Filtration by means of a candle type filter (or disk type filter, see Figure 1.2) takes place as the water passes, due to a pressure gradient caused by a head difference, through the candle (or disk) and housing and is influenced by flow rate, water density, ceramic density and pore size (USFilter, 2012).

1.5.1 Ceramic water filters (CWF)

Sobsey (2002) explains that ceramic filters consist of a ceramic material with a high level of porosity. Porosity lends certain physical properties to ceramic filters, such as high specific surface area, high permeability and high tortuosity.

Pore size can be created to sub-micron sizes, making porous filters effective in the removal of suspended solids, pathogenic bacteria and other organisms in drinking water. Other advantages of CWF include the fact that they are free of chemicals, are light in weight, portable, low cost and gravity fed without the need for any external energy sources. They furthermore provide safe water storage, require only periodic cleaning and have a filter life of at least 0.5 – 1 year.

1.5.2 Making a ceramic water filter

Water filtration methods have been used since antiquity, primarily for removal of suspended solids, later for odour and taste improvement and when using ceramic water filters for the removal of suspended solids, pathogenic bacteria, organisms or other disease causing agents in drinking water. The manufacturing process of ceramic water filters produces the small pore size in the ceramic material to filter dirt, debris, and bacteria out of water.

Prior to the shaping of the ceramic water filter, ceramic raw materials (powders) are selected, prepared and mixed with processing additives (pore former, deflocculants and water). The mixing stage is then followed by the shape forming stage.

a) Raw material selection and preparation

Raw material are selected and prepared to provide the optimum characteristics such as particle shape (spherical, irregular) and particle size and particle size distribution to determine the flow properties during shaping, ceramic grain size and the amount and size of the pores.

b) Shaping (compaction)

The range of applied pressure, the type of compaction (method: pressing, slip

casting, etc.) and the type and amount of additives (deflocculants, water etc.) determine the pores size and the pore size distribution as well as the residual stress.

c) Sintering

Sintering involves the process of atomic diffusion. The diffusion occurs at high temperature and fuses the particles together into a solid ceramic filter. The powder grows during the sintering process and therefore will determine the final particle and pores size and the physical and chemical properties of the ceramic.

d) Main shaping methods

Three common shape forming processes can be used for the shaping of porous ceramics: pressing, extrusion and slip casting (Hbalze and Gaukler 2003). Each fabrication method results in a specific range of pore size, porosity, as well as varying levels of interconnectedness among the pores (Dobrovolskiy 1977). The number, size and shape of defects in the ceramic filter are also dependent on the processing method used. Finally, each fabrication method differs in terms of its overall investment and product cost.

Figure 1.2 illustrates the various low cost filter system options that are currently being utilized in developing countries. The pot and disk filter element designs, which are shaped using a hydraulic press, are being used by Potters for Peace and Filtron systems, respectively (Lantagne (2001). The candle element design is being utilized in this current study (*OUTBAC*).

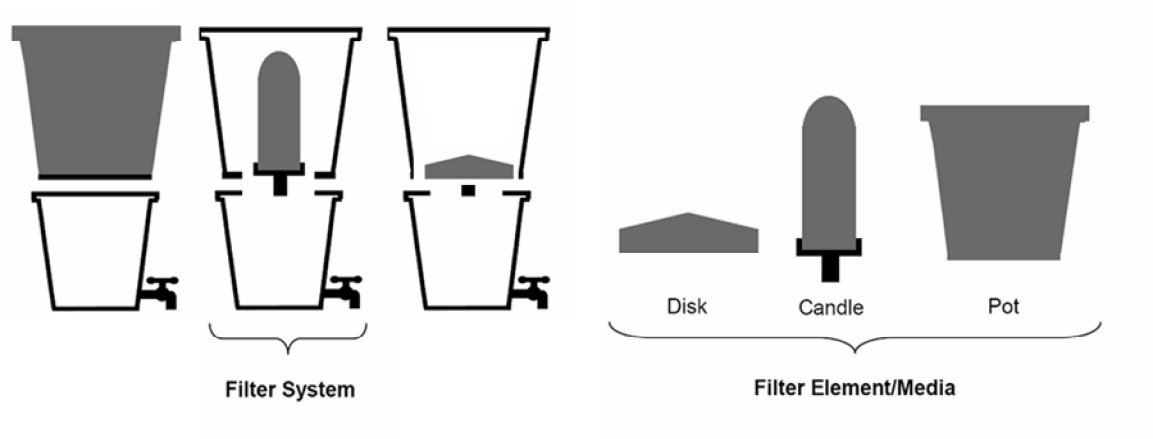

Figure 1.2: Filter elements and filter system (adapted from Dies 2000)

e) Pore formers

Weiguang *et al* (2005) explain that pores in ceramics can be made by burning out the pore former[3] in a sintering[4] process. There are two general kinds of pore formers, inorganic materials (such as ammonium bicarbonate and carbon powder) and organic materials (such as starch, PVA[5], PVB[6]). Weiguang *et al* (2005) fabricated porous SiC ceramics using yeast as pore former and investigated their sintering behaviour. Lyckfeldt (1998) lists some of the main methods of obtaining the pores in porous ceramics:

- sponge (polymer) method: sponge is filled with ceramic slip, dried, and then burnt out, and the ceramic material fired, forming an open pore body.
- foaming method: foaming agent is mixed into slip[7] and by further agitation foam increasingly builds up; it is dried, building up a pore structure, and fired, forming a closed pore body (dead end pores)
- ceramic powder blend method: material with a narrow particle size distribution for obtaining a porous structure

The three forming methods each have both advantages and disadvantages, and factors that have to be controlled during production. Problems arising from production mostly include material property and shrinkage (dimensions) variations (Kingery *et al*, 1976).

1.5.3 Ceramic filter properties

Porous ceramics have porosity that result in properties such as high specific surface area, high permeability and high tortuosity. These factors make porous filters effective by physically (non-chemical process) removing suspended solids, pathogenic bacteria and other organisms in drinking water.

[3] pore formers are materials that may be removed by a thermal or chemical process which results in the creation of a pore or pores approximately equal in volume to the material that was removed.

[4] agglomeration or sticking together of raw materials through heating

[5] polyvinyl acetate

[6] polyvinyl butyral

[7] suspension in water of clay or other raw materials

Ceramic water filters can be grouped according to various key factors that have a direct bearing on their properties:

1. Type of raw material and additions (clay, talc, feldspar etc.)
2. Production method (slip casting, press or extrusion)
3. Filter shape (Figure 1.2);
4. Pore former (organic carbon, resin, sawdust)
5. Sintering temperature
6. Function (chemical contaminant and/or bacterial removal: Lantagne (2001))
7. Construction: unit consists out of two main components: *filter element (candle or pot)* through which water passes and the *filter system* into which the element is mounted, normally constructed as a two bucket system for storage of water.

Mulder (1996) summarises the main filtration processes, pore size ranges, and main driving force responsible for filtration in Table 1.1.

Table 1.1: Filter types based on pores size and driving force with microfiltration the process used by low cost filter producers (Mulder 1996)

Membrane process	Phase		Driving force	Pore size
	Feed	Permeate		
Microfiltration	L	L	ΔP	0.1–10 μm
Ultrafiltration	L	L	ΔP	2–100 nm
Nanofiltration	L	L	ΔP	1–2 nm
Reverse osmosis	L	L	ΔP	<1 nm
Gas separation	G	G	ΔP	<0.5–1 nm
Vapor permeation	G	G	ΔP	<0.5–1 nm
Pervaporation	L	G	ΔP	0.5–2 nm
Electrodialysis	L	L	$\Delta \Phi$	
Dialysis	L	L	ΔC	
Membrane distillation	L	L	ΔT	

L, liquid phase; G, gas phase; ΔP, (partial) pressure difference; $\Delta \Phi$, electrical potential difference; ΔC, concentration difference; ΔT, temperature difference.

***OUTBAC* filter pore size range**

Oyanedel-Craver and Smith (2008) however found a large variability in pore structure (size) among the local ceramic filters tested by them. The majority of the pores sizes were found to be in the range 12 to 20 micron. Fahlin (2003) also found that the pore size distribution from these CWF varied widely due to the variety of raw materials and methods used in their local production.

The filter properties are crucial in maintaining effective protection against contaminated water but maintaining consistency (quality control) during the manufacturing process is inhibited by lack of universal quality control standards. Filter production variables have to be investigated to determine their impact contaminant removal.

1.5.4 Standards applied to water filters

Although there are standards for POUs in the USA and in some other countries, no international standards exist for POU devices. Protocols and standards for products made in developed countries cannot be applied to developing country conditions as such standards do not take local use and storage conditions into consideration. Incremental improvements should be encouraged together with more flexibility and consideration of local needs and conditions (Brown *et al* 2007). Duke *et al* (2006) and Lemons (2009) both agree that household water treatment and safe storage of water (HWTS) can be considered as low cost alternatives that are effective when compared to the more centralised water treatment systems (municipal systems) in the reduction in diarrheal diseases. Hwang (2003) made use of field testing on CWF in use for a six month period in Nicaragua to show that the CWF were able to eliminate 89.3 percent of total coliforms and 97.6 percent of *Escherichia coli*. The POUs have resulted in dramatic decreases in diarrheal infection rates and death in some developing countries (Sobsey 2002).

However, Brown *et al* (2007) contend that the microbiological effectiveness of the CWF in laboratory and in field testing remains limited. According to them field testing of ceramic water filters lack most of the following requirements:

- matched pre- and post-treatment samples
- information on analytical methods used
- appropriate sample handling and processing
- sufficient volume sampled
- proper replicate samples
- dilutions descriptions
- incubation periods
- detection limit details

A summary of worldwide testing done on low cost CWF for developing countries for the period 2000 to 2010 is presented in Table 6.11. The average benchmark standard for *Escherichia coli* (*E coli*) reduction effectiveness was 97 (± 3) whereas virus testing reduction effectiveness was limited. This compares poorly with the USA EPA standard log reduction value[8] (LRV) of 6 (99.9999 percent), but at least provides a starting point for establishing a useful guideline for the testing of low cost CWF. The factors mentioned by Brown *et al* (2007), however, have to be included in all protocol for future testing.

1.5.5 Local clean water provision solutions

Clean drinking water has always been a major issue in many developing countries, but with the onset of climate change and droughts, this may become a problem for industrialized countries as well. There is a simple solution for clean water: ceramic water filter. Using such a filter people everywhere can drink clean water using locally available material such as clay.

[8] LRV is used to report microbiological filter performance The formula is stated as follows: Log (No.of bacteria in feed/ No. of bacteria in filtrate)

The Millennium Declaration (2000) and commitment by the International community show a political will for increasing access to safe drinking water. Solutions at country and local level are making progress but dependent on many factors. Laying pipe for access to water needs a large capital investment and takes a large concentrated population to justify the investment in construction and suitable method of treatment. Aid organisations, NGO's and others are seeking local solutions at point of use (POU), such as the ceramic water filter made locally, from local materials. Methods of POU water treatment such as the units developed by Potters for Peace (PfP) creates a local, low cost solution of creating a ceramic filter from local materials which the general population can use. Such a solution achieves the goal of rapidly increasing access to clean water at the lowest possible cost through a local solution. Such as filter should be simple to create, inexpensive and made out of local materials. The filter should allow water, but not pathogens or suspended material, to pass and effectively remove in excess of 99% of a variety of bacteria from water. One filter should also provide 3 to 5 liter of drinkable water in one hour. Such an invention should purposely not be patented so that everyone could create their own water filters. Other organisations such as Engineers Without Borders and Potters for Peace have introduced similar filters using clay as raw material.

1.6 Aim

The main aim is to develop and evaluate a ceramic micro-porous filtration system using the slip casting technique for application in domestic water supply.

1.7 Objectives

1. Conduct a literature study and evaluation of the best method available for making ceramic micro-porous material
2. Source, investigate and test (rheology) ceramic materials for their suitability in the slip casting method
3. Produce ceramic samples for filtration testing and evaluation
4. Evaluate the effectiveness of the micro filtration system for removal of pathogenic bacteria
5. Design and create an effective micro filtration systems for household use

1.8 Hypothesis

Ceramic filters are effective in reducing microbial incidence by enabling rural households to reduce life threatening bacterial contaminants in drinking water. Local manufacture of such filters can provide a practical solution to households requiring clean water and provide a livelihood for the unemployed.

Chapter 2: Filter Forming Processes

2.1 Introduction

The manufacture of ceramic products takes place in different types of kilns with a wide range of raw materials and in numerous shapes, sizes and colours. The general process of manufacturing ceramic products, however, is rather uniform, besides the fact that, for the manufacture of wall and floor tiles, table and ornamental ware (household ceramics), sanitary ware and also porous ceramics, often a multiple stage firing process is used (Figure 2.1).

In general, raw materials are mixed and cast, pressed or extruded into shape. Water is regularly used for assisting in thorough mixing and shaping. This water is evaporated in dryers and the products are either placed by hand in the kiln (especially in the case of periodically operated kilns) or placed onto carriages that are transferred through continuously operated kilns. In most cases, the kilns are heated with electricity, natural gas, but liquefied petroleum gas, fuel oil, coal, petroleum coke and biogas/biomass are also used.

An irreversible ceramic structure for the product is reached during the firing process in the kiln. This demands a very accurate temperature gradient during firing to ensure that the products obtain the right treatment. Afterwards controlled cooling is necessary, so that the products release their heat gradually and preserve their ceramic structure. Then products are packed and stored for delivery.

In this chapter the most important shaping methods for porous ceramic manufacturing are explained. A literature survey is used to examine and select the most suitable ceramic forming process for the manufacture of a low cost, porous, ceramic water filter. The plant, as well as the basic steps and variations in the production processes are shown in Figure 2.1 and porous ceramic manufacturing will be further explained in Chapter 3.

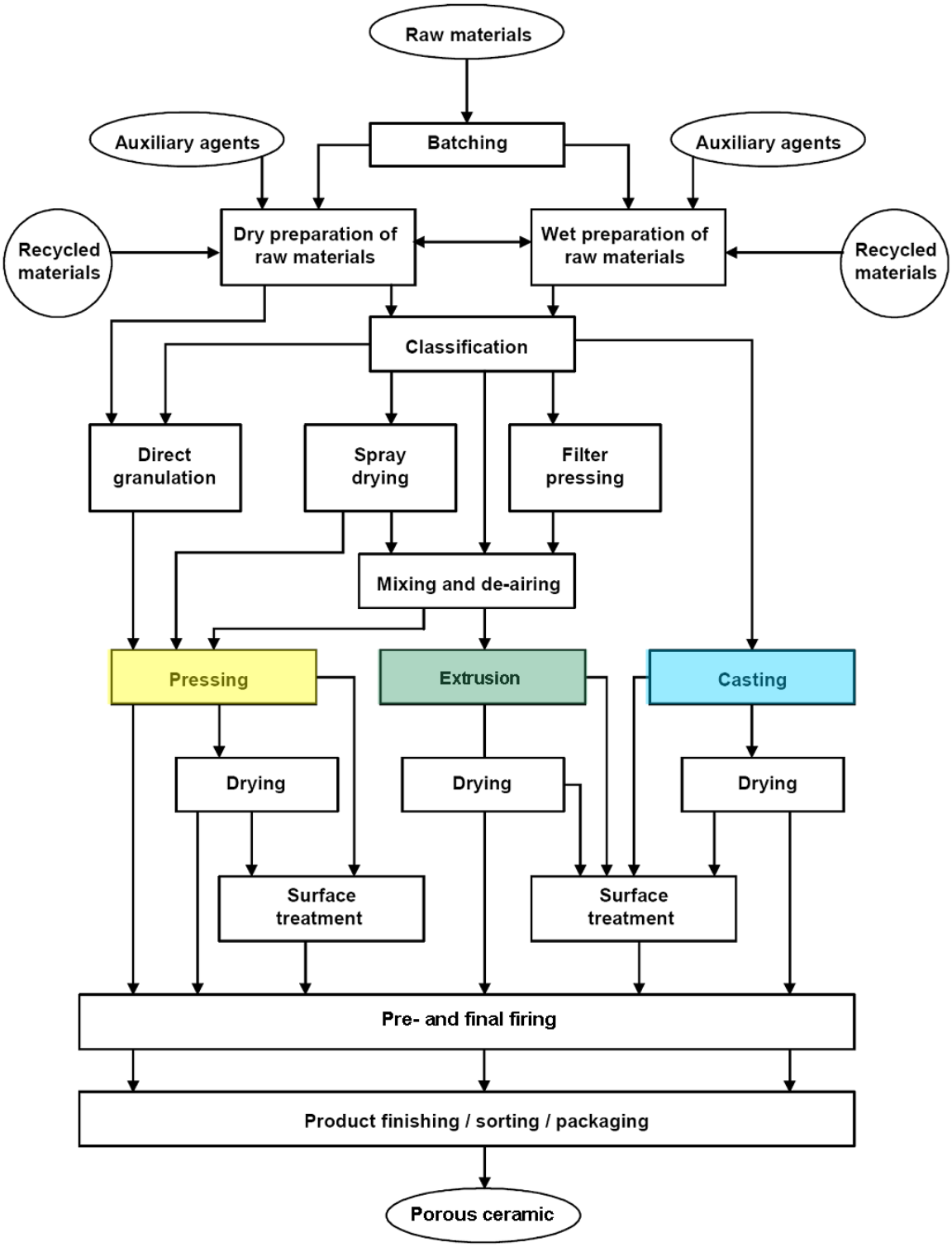

Figure 2.1: General forming process flow for ceramic manufacturing process (modified from EC 2007)

Traditional ceramic products were always shaped from raw materials in the plastic state, and for several millennia, this was a manual operation. At the present time, the demand is forever more stringent technical specifications covering such properties as dimensional tolerance, density, strength, durability and refractoriness[9]. In many cases, aesthetic qualities are also of prime importance. The method of forming the ware can have a profound effect on their ultimate properties and wide ranges of shaping techniques have evolved in the various sectors of the ceramic industry.

Three main shaping processes were investigated using a literature study:

a) die pressing

b) slip casting

c) extrusion

In the survey, each of the following requirements was examined for the three forming methods:

a) availability of raw materials with suitable particle size and particle size distribution properties required from the ceramic raw material

b) pore forming materials (which provide porosity for filtration)

c) milling requirements (to obtain required particle size distribution)

d) forming (shaping) requirements

e) mixing requirements (to obtain uniformity of properties within the body)

f) drying (to control shrinkage)

g) firing (characteristics of the fine fraction, particle size)

h) testing requirements (characterization and product evaluation)

According to Kingery *et al* (1976), the most critical factors affecting forming and firing are the raw materials and their preparation. The main influences will be the grain size and grain size distribution of the powders.

[9] difficult to melt and therefore resistant to heat

The fine grained powders, mostly less than 1 micron, are essential for the forming process since slip suspensions, plastic mixes and dry pressing all depends on small particles flowing over one another or staying in suspension. This is particularly important in suspensions where the settling aspect is proportional to the particle density and particle size. Coarse material (larger than 1 micron) should, however, form part of the mix as it allows the fines to fill the pores between the medium and coarse particles. The best size ratio for obtaining maximum particle packing is a 70 percent coarse to 30 percent fine material ratio (Kingery *et al* 1976).

When a semi dry powder, slip or plastic powder is taken and shaped or formed into a shape and fired, a ceramic product is the result. High green[10] density for restricting firing shrinkage is the main aim of the shaping process, which limits crack formation (less rejects) and leads to energy savings (higher density requires a lower firing temperature and therefore a shorter firing cycle). Shaping processes that do not end in high green density are therefore put in an unfavourable position.

2.2 Main forming methods

Most ceramic forming operations require raw materials with defined water or bonding content, and minor additives such as pigments and binders must be accurately dosed and then uniformly distributed in the mix.

The oldest method of forming malleable clay is by adding sufficient water to dry, clay powder and kneading the mixture by hand. Hand pressure is usually sufficient to shape coiled African pottery ware and clay can also be thrown and shaped by hand on a potter's wheel. This process can be taken further by simply pressing soft, plastic clay into a plaster or metal mould. The main forming processes for the shaping of porous ceramic are shown in Figure 2.1.

Pressing: When the material to be pressed, in dry or slightly moist raw material (less than 10 per cent moisture), mixed with an organic binder, is compacted in a metal die (the mould) at high pressure, a dense, strong product is formed.

[10] object that has been shaped and dried but not yet fired for conversion into ceramic

The most commonly used methods of pressing include cold or hot uniaxial pressing[11] and cold or hot isostatic pressing[12], and vibratory compaction (Yang *et al* 2003). The pressing method is extensively used when requiring a large number of simple shapes with very tight tolerances. Pressures used ranges between 3 to 30 kbar with the higher pressures used for harder oxide materials.

Extrusion: Plastic moulding is accomplished by extrusion, jiggering, or powder injection moulding. Extrusion is used in manufacturing structural porous ceramics, clay products and some refractory products. For products having elongated shape of fixed cross section (bricks, cylindrical filters and tiles), a stiff plastic mix is extruded (forced through under pressure) through a die orifice, with the desired cross section using a vacuum auger (continuous feed and mixing) or hydraulic piston (batch process). Jiggering is made by making a pancake of clay know as a bat on a revolving disk. The clay bat is then thrown into a plaster mould which shapes the front of the plate and a metal tool is lowered into the mould to form the back of the plate. Powder injection moulding is used for making small complex shapes.

The extrusion mix consists of a fine ceramic powder with the appropriate additions of binder(s) and plasticiser(s) to give the desired flow properties (rheology), either cold or when heated prior to being shaped into a mould or forced through a die. The raw materials, however, have to be well mixed with 10 to 20 percent water before it can be forced through the hardened die orifice. In extrusion, vacuum is applied for eliminating air from the mixture.

Slip casting: Slurry forming of ceramics generally is accomplished using slip casting, gel-casting, or tape-casting. A suspension or slip forms when more than 20% water, mixed with a deflocculant, is added to well mixed, powdered, micron sized, materials. In slip casting, the slip is poured into a porous mould (a negative of the desired shape and normally made out of plaster-of-Paris), water is absorbed by the plaster from the contact area, forming a rigid layer on the plaster surface.

[11] process of applying pressure in one direction to achieve densification

[12] process of using fluid (liquid or gas) pressure to densify raw materials

By continuing this process the mould interior can be either completely filled (solid casting) or filled up to the desired wall thickness, inverted (drain casting) to remove excess slip (Bowen *et al* 1972).

Gel-casting uses *in situ* polymerization of organic monomers to produce a gel that binds ceramic particles together into a shape. Tape-casting consists of forming a thin film of ceramic slurry of controlled thickness onto a support surface using a knife edge. For very thin layers; there are also new techniques, such as chemical and physical vapor phase deposition as well as molecular beam epitaxy (

Ohring (2000).

Each of the processes, from pressing to slip casting, requires increased amounts of water for the shaping process. Forming water has to be removed with a carefully controlled drying step to strengthen the body and to prepare it for firing. Ultimately, the water added contributes to the final porosity of the finished product.

The final step in producing ceramics product involves a heat treatment step (sintering or firing) where the shaped body is transformed or sintered into a dense solid. In sintering the micro structure development depends mainly on the variables that include temperature, grain size, particles size distribution and firing atmosphere. Because of the pore formers, a two stage firing process is normally required, which includes a burn out phase and the final sintering phase. Both of these are responsible for providing the highly porous structure.

Test methods, to characterize the raw materials and the porous ceramic product, give insight into their properties, which in turn provides clues to the history of the ceramic – how it was made, processes that occurred during its making, and its environmental interactions during use. The analytical measurements also provide the opportunity to compare it with desired standards. Important parameters that are tested include chemical composition, micro structure, specific surface area, temperature, particle size, pore size (distributions), and particle classification measurements (Figure 2.2).

2.2.1 Die Pressing

The typical process flow used in the pressing of porous products is shown in Figure 2.2.

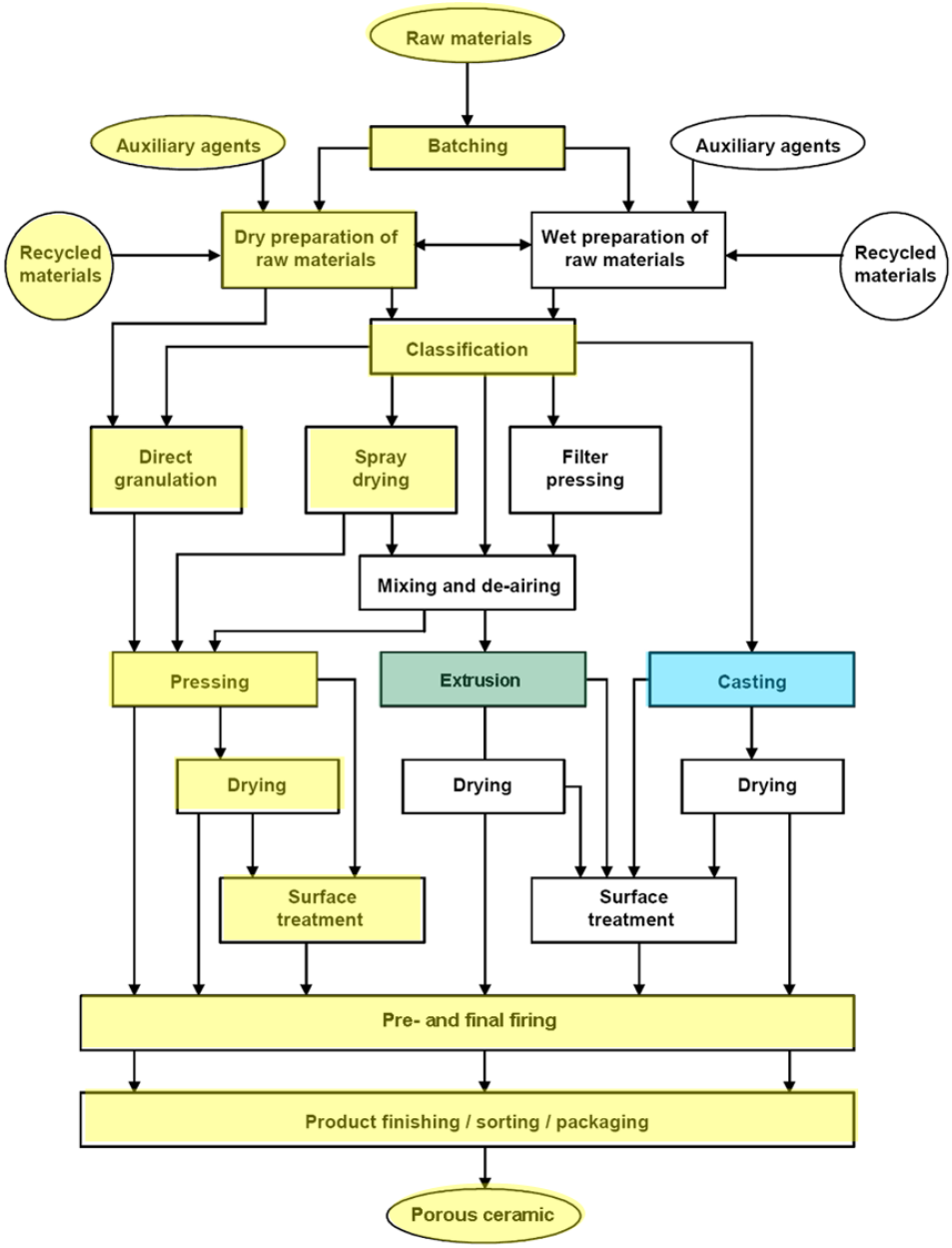

Figure 2.2: Process flow for the pressing of ceramic products (modified from EC, 2007). *Colour coded pressing route.*

Mechanical pressing

This method is still employed for the manufacture of bricks (e.g. semi-dry pressing) and of refractory products. Die boxes are charged with a pre-set volume of clay granules, and pressure is usually applied from above and below, with pistons being driven by camshaft action and aided by heavy flywheels.

Hydraulic pressing

Modern hydraulic presses can provide high compaction force, high productivity, consistency and easy adjustment. Many presses are now fitted with electronic control units, which can check the height of units and automatically adjust the cycle to ensure size uniformity. Such presses can be readily adjusted to meet a variety of requirements, including complicated press programs such as those used in forming complex refractory shapes. Hydraulic pressing is widely adopted for the shaping of tiles. In the case of ceramic tiles, the moist powder (at 5 – 7 % moisture content) is pressed in shallow dies, whereas clay roof tiles are usually formed by pressing plastic clay ‘bats’ cut from an extruded column.

Impact pressing

This involves a high energy rate forming via pneumatic mechanical impact between a high velocity ram striking powders in a die. The technique is employed in the manufacture of special refractory products.

Friction pressing

Mechanically driven friction (screw) presses are, in general, used for producing refractory shapes, although they are gradually being replaced by hydraulic presses.

Spray drying

This process is widely employed in the wall and floor tile industry and also carried out for the manufacture of tableware, technical ceramics and refractory products.

The aqueous suspension of raw material resulting from wet ball milling (solids content ~ 60 to 70 %) is sprayed under pressure to produce fine droplets which contact a stream of hot air. Drying of the droplets produces highly uniform, more or less spherical hollow granules (with moisture content of typically 5.5 to 7 %). This form of powder has high flowability, facilitating accurate filling of the press dies and the subsequent pressing of large single tiles.

In die pressing, stress is orientated in uniaxial direction to the ceramic grains loaded in the mould, to form loose bonds between the grains, giving the particles just enough strength for handling (Reed, 1995). Stress applied from one side of the mould only (upper side of the mould), is referred to as uni-axial die pressing. During pressing, three things (stages) happen to the shape of the ceramic powder (Figure 2.3):

a) granule packing

b) granule deformation

c) granule sliding to reduce the voids between deformed granules

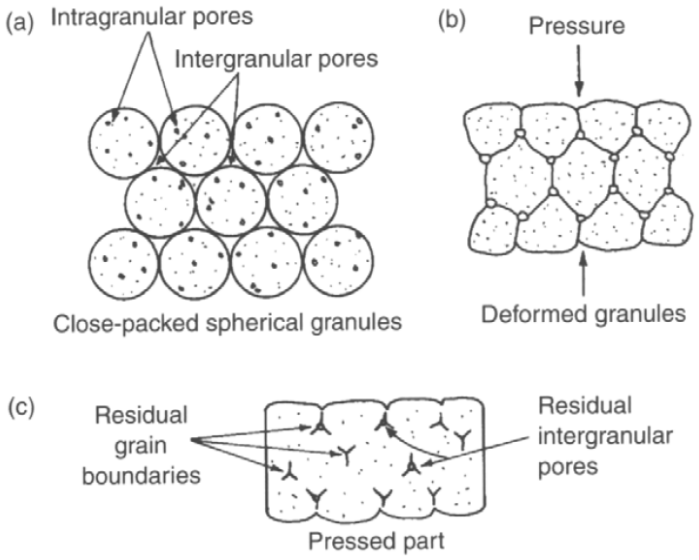

Figure 2.3: Granule shape change during die pressing (Reed 1995)

The advantage of die pressing is rapid and easy automation but with the disadvantage of leaving pressure gradients behind during the green stage of the product. Figure 2.4 shows how the increase in the applied pressure results in the varying stages of green density (compaction).

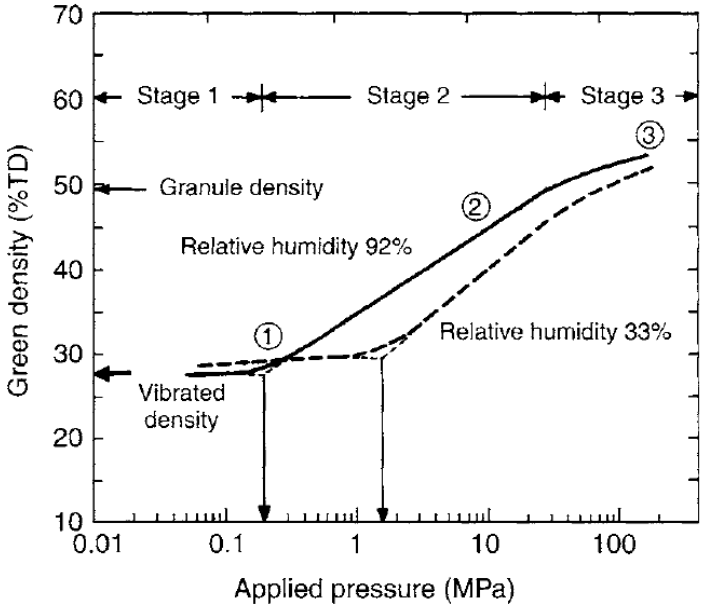

Figure 2.4: Compaction stages during pressing: Stage 1 granule packing; Stage 2 granule deformation and Stage 3 granule sliding (Reed 1995)

Yang *et al* (2003) explain that to prepare the raw material for a press, a suspension is usually first prepared which then has to be dried to form agglomerates. Various drying methods are available of which spray drying[13] is the most common. This drying method, however, is dependent on the requirements of the press mixture or the desired property of the pressed body. Some of the more important drying methods used to provide a uniform, free flowing mixture, are the following:

a) Pan drying: evaporation of water from a heated stainless or glass pan – results in segregation of the coarse and fine materials and requires further processing to obtain free flowing mixture

[13] process of making a dry powder by spraying a slip/slurry into hot air for rapid drying

b) Spray drying: a slip pump sprays the slip through a nozzle into a drying chamber fitted with a conical collection base. Cyclone separation is necessary to classify the particles. The slip feed rate, air temperature and air movement have to be managed. Figure 2.5 show the spherical nature of the particles.

c) Solvent drying: the mixing water is replaced by a solvent. The first step is the recovery of the solids through sedimentation, filtering, centrifuging or pouring into a plaster mould. The recovered material is then remixed using a solvent (acetone or methanol) and dried (solvent removal).

d) Rotary drying: feeding wet material into a heated, rotating cylinder. Agglomeration and adherence to the walls are a problem.

e) Freeze drying: where the water is sublimated negating the agglomeration of the powder. The process involves casting slip into containers (shallow), freezing and sublimating the water by keeping the temperature just above that of the cooling coil (all temperatures below freezing point). Like pan drying, freeze dried powders require further processing to obtain a free flowing mixture.

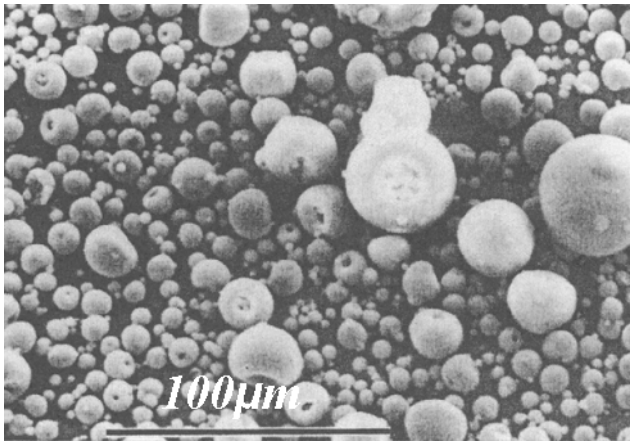

Figure 2.5: Scanning electron microscope (SEM) image of a spray dried mixture for pressing (King, 2002)

2.2.1.1 Die

According to King (2002), tolerances between the top and bottom punch and the die body (Figure 2.6) are tightly controlled to prevent powder from entering the gap. Dies are manufactured from hardened steel or cemented carbides. Die parts are then positioned and bolted to a press shaft. The cylindrical die assembly is illustrated in Figure 2.6.

Figure 2.7 shows the various steps of the die process, from filling to pressing the body out: remove top punch, meter (weight or volume based) press mix into die cavity and screed off the top of the die; lower punch and mix by removing a shim, insert top punch and press die to part of the final load; release pressure and allow trapped air to escape; Double-end press (both punches move) to full pressure; maintain pressure for a few seconds, release and strip.

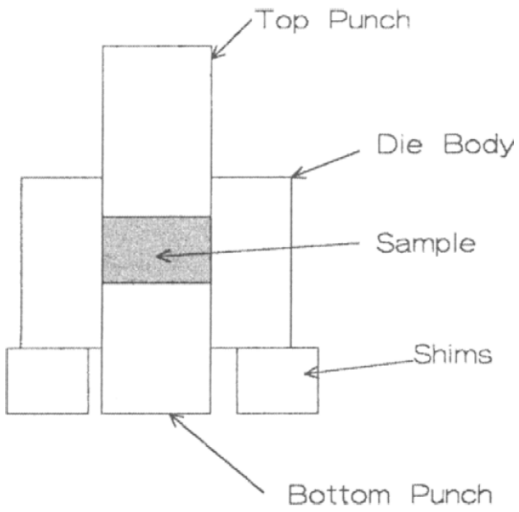

Figure 2.6: Die assembly, which includes a die body and two punches (King 2002)

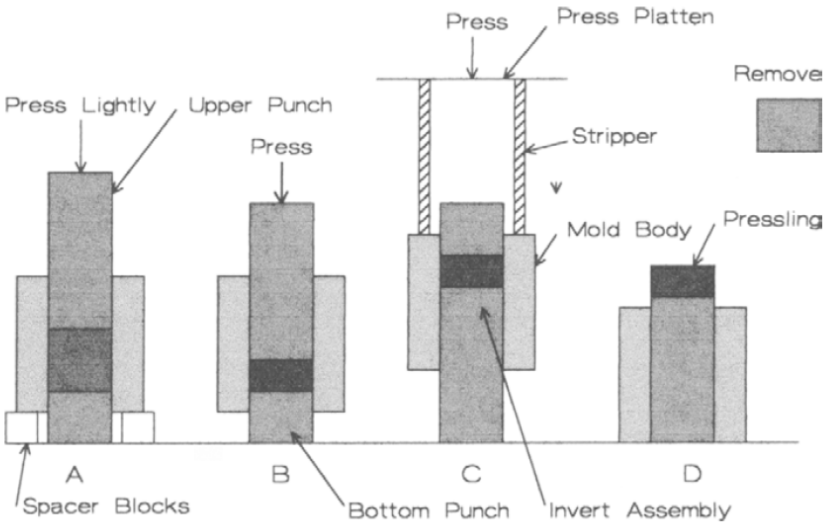

Figure 2.7: The four die stripping steps: A. Fill die and insert top punch - B. remove shim press - C. Invert die and position stripper on top - D. Press body out of die (Thompson 1981)

2.2.1.2 Die pressing problems

Some of the more serious defects that can occur when pressing ceramics include (Thompson 1981):

a) Laminations: cracks parallel to press top and bottom punch, caused by entrapped air

b) End capping: fracture crossing from top edge to center, caused by frictional forces parallel to punch surface

c) Sticking: press mix sticks to the punch faces, leading to rejects – resolved by polishing faces, using release agents or a paper divider

d) Hour glassing: density gradients with the center leading to higher firing shrinkage – resolved by using a more yielding mix, increasing the pressing pressure or by machining in green state prior to sintering

e) Warping: green density variations results in distortions and product warping – resolved by more even filling

f) Cracking: cracks form during pressing due to uneven cross-sections, die corners or differences in thickness – resolved by tooling geometry changes, pressing rate, binder strength, slow firing through critical stage.

2.2.1.3 Examples using die pressing to make porous ceramics

An example of using a simplified die pressing process for developing a porous ceramic filter, Bell (1988) prepared a hand mouldable mixture consisting of silica (5g with d_{50}[14] of 12 micron) and a-olefin oligomer[15] (16.4g). The mixture was hand mixed and hand filled into a mould, and then moulded using a pressure of 200 $kg.cm^{-2}$.

The firing cycle used by Bell (1988) was as follows:

- from room temperature the body was heated to 300°C at rate of 10°C h^{-1}
- 300°C to 850°C at a rate of 70°C h^{-1}
- dwell at 850°C for 12 hours

The resulting product had a porosity of 90 percent and average pore size of 80 micron.

In contrast Liu (1991) used the technique of powder injection moulding (PIM) to mould an alumina filter. In PIM, 30 to 50% polymeric binders are pre-mixed with ceramic powders. The mixture is subsequently heated in an auger-fed barrel and forced under pressure into a die cavity, where it cools and is subsequently ejected. The polymer is then removed and the component sintered to the required density. Lui used a range of solids loading from 55 to 70 percent and compression moulded cylindrical samples at a pressure of 10 MPa at 75°C. From experimentation he showed that green and sintered density improved linearly up to an optimum of 65 percent of theoretical density, and decreased linearly by increasing the coarse to fine ratio. The coarse particles slow down the densification process.

Die pressing is a complicated and expensive process for the manufacturing of porous ceramic water filters. Such a process requires expensive equipment, technical skills and know-how as well as specially prepared raw materials.

[14] for particle size distributions the median is called the d_{50}

[15] clear, water-white liquid used in the production of polyethylene and has the formula C_xH2_x

This technology is therefore outside the scope of producing low cost ceramic water filters.

2.2.2 Extrusion

Extrusion is commonly used for any three dimensional body and forms parallel straight lines such as round, square, rectangular, oval or honeycomb shapes. Examples of extrusion are bricks, solid cylinders and tubes. The extrusion process flow diagram is illustrated in Figure 2.8.

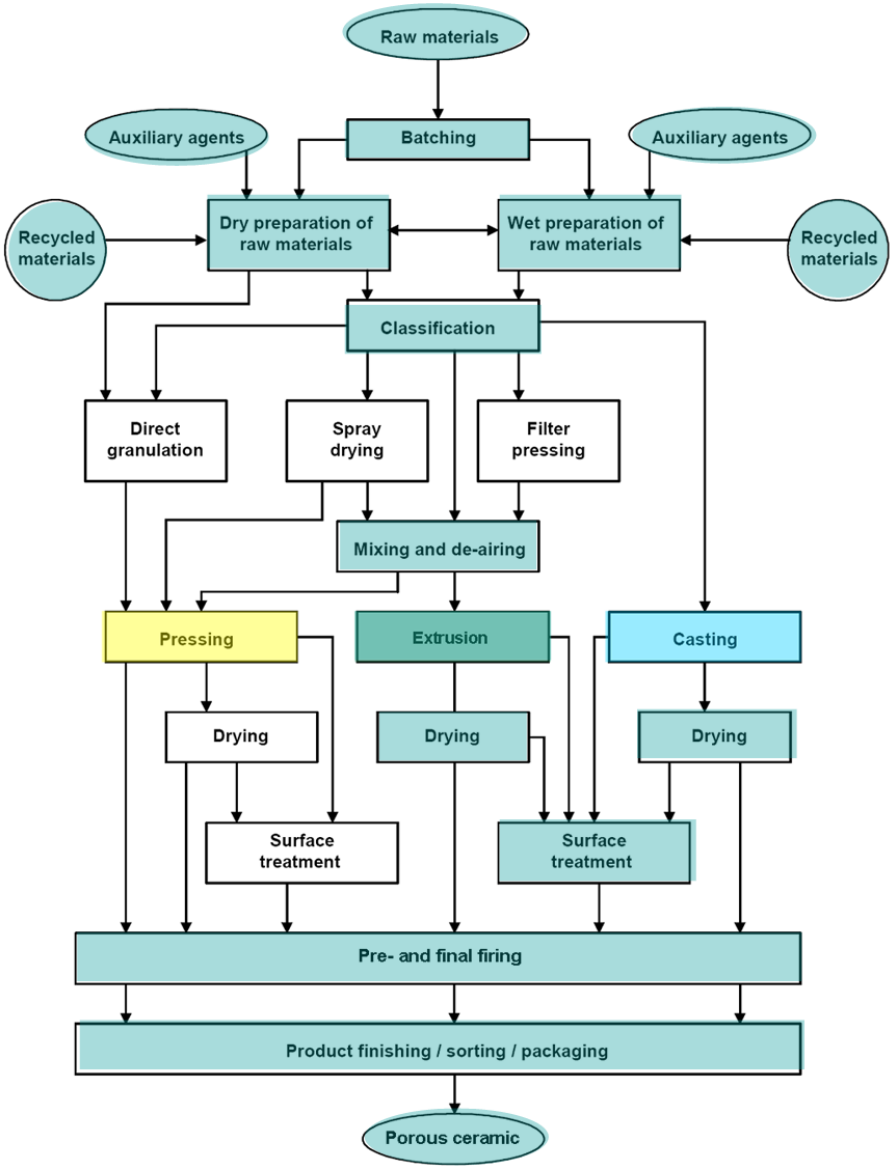

Figure 2.8: Forming process flow for the extrusion of ceramic products (modified from EC, 2007. Colour coding of the extrusion route ( ).

This forming process consists of forcing a ceramic powder through a constricting die to produce elongated shapes that have a constant cross section. The powder mix consists of a fine ceramic powder with the appropriate additions of binder(s) and plasticiser(s) to give the desired flow properties (rheology), either cold or when heated prior to being forced through the die.

The mixture is required to be plastic, deflocculated and stiff. Plasticity can usually be increased by adding ball clay, such as Hectorite[16] (alumina silicate) or long chained organic polymers or alginates[17]. The extrusion has to be kept straight as it exits from the die onto a flat surface before being trimmed to correct length (Von Hoy *et al* 1998 and Wright and Reed 2001).

2.2.2.1 Auger extrusion

An extruder has an entry port for feeding the mix into the auger, and an auger for both mixing and extrusion out of a die. Figure 2.9 illustrates a process flow and the equipment needed for the extrusion process.

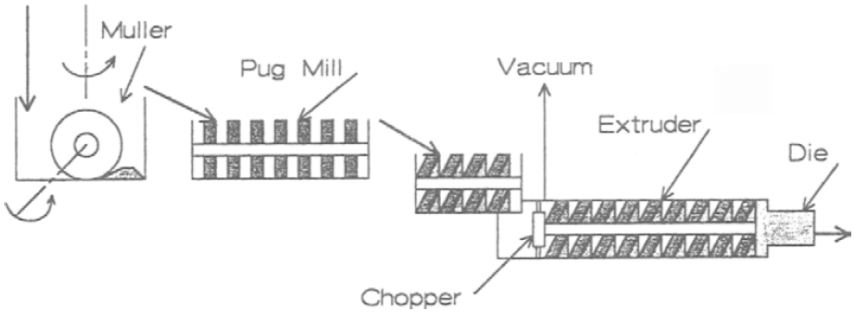

Figure 2.9: Extrusion processes, which include mulling, pug milling and a vacuum extruder (King 2002)

The material is batched into a muller[18] and then moved to the pug mill. The functions of the various extruder parts are as follows:

[16] soft, plastic, light coloured clay mineral with formula of $Na_{0.3}(Mg,Li)_3Si_4O_{10}(OH)_2$.

[17] polysaccharide found in the cell walls of algae when mixed with water forms a gum capable of absorbing 200-300 times its own weight in water

[18] muller is a high intensity mixer that applies both compression and shear to a plastic mixture using a weighted wheel to breakdown agglomerates

- muller: distributes the mix ingredients uniformly and de-agglomerates the fines

- pug mill[19]: homogenizes the material by shear, providing a uniform batch for the extruder

- twin compartment extruder[20]: a) forces material into the extruder and from there into the hopper under vacuum for air removal and b) chopped mix is discarded into the extruder auger, from where it undergoes intense shearing and mixing and c) auger flights move the material through the extruder die under pressure to compact the mix and to shape through the die.

Wear is extensive and auger barrels, liners and blades have to be coated with a wear resistant material. Another type of extruder is the ram extruder that uses a hydraulic cylinder in the place of an auger for pushing the mix through the die (Mutsuddy and Ford 1995 and Ring 1996).

Yang and Tsai (2008) state raw material can be shaped by extrusion only if the mixture has the rheology of clay. Plasticity is the key to consistent extrusion and this can be measured by using Atteberg limits. Young and Tsai (2008) extruded cylindrical porous ceramic filters from a mixture of alumina (d_{50} of 4 micron), bentonite (d_{50} of 74 micron) and starch (d_{50} of 53 micron used as pore former). Additional organic additives, such as methocel[21], amijel[22] and polyethylene glycol, were also added for mechanical strength. The firing cycle used was as follows:

- body heated from room temperature to 500°C at 1°C min^{-1}
- 500°C to 1200°C at 1.67°C min^{-1}
- dwell at 500°C for 4 hours
- dwell at 800°, 1000° and 1200°C for 2 hours respectively

[19] extruder-type machine where raw materials are both ground and mixed with a liquid.

[20] process of making items with a fixed cross-sectional profile. Raw material is forced through a die with the required cross-sectional profile.

[21] ethers derived from cellulose that are water-soluble

[22] pre-cooked starch that thickens instantly in cold water - pregelatinised starch

2.2.2.2 Examples using die pressing to make porous ceramics

Zuberi *et al* (2009) in their US patent (C04B3503FI) used mullite fibres (71.2g), isofrax fibres[23] (21.9%), $MgCO_3$ (5.3%) and $CaCO_3$ (1.5%) to form their target composition of $Ca_{0.1}Mg_2Al_4$ $0.1Si_5O_{18}$. For the extrudable mixture (binder and rheology modifier) hydroxypropyl methyl cellulose (16g) was added, and for the pore former, carbon particles (smaller than 45 micron, 65g) together with de-ionised water (130g) were added. The mixture was then vacuum extruded, samples cut to size, dried and fired resulting in a honeycomb structure with 88 percent porosity. Most of the fibres were aligned along the extrusion direction with a low thermal expansion coefficient and orthorhombic structure.

Hamidi *et al* (2008) used raw material recipes (F1 and F2 in Figure 2.10) to develop two extrudable mixtures for making porous samples. They used combinations of silica (62 and 64 percent), bentonite clay (12 and 9 percent) and carboxymethyl cellulose (26 and 27 percent). The results of the extrusion, sintered at various sintering temperatures, are shown for product F1 and F2 in Figure 2.10. The higher flexural strength in product F2 is due to the higher fiber content.

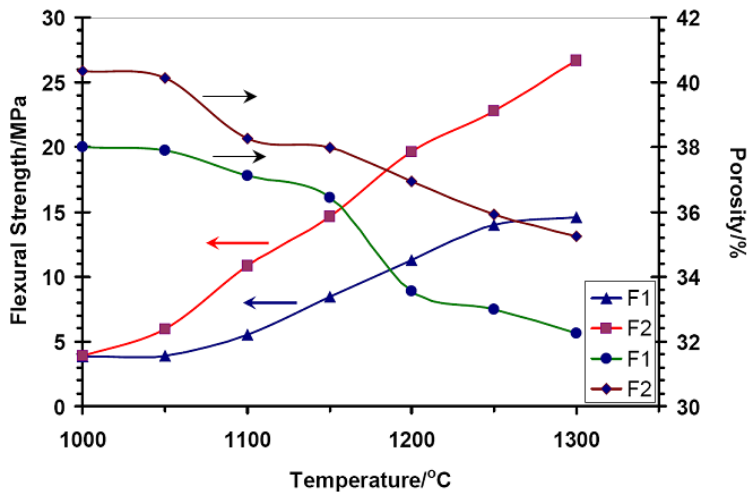

Figure 2.10: Porosity and flexural strength of filter samples at various sintering temperatures (Hamidi et al 2008). Left facing arrows indicate flexural strength and right facing arrows the porosity

[23] alkaline earth silicate wool (fiber) that can withstand high temperatures

Wittemore (1999) used extrusion for making ceramic filters and had to overcome a number of problems during the process such as the use of extrusion aids to lessen the abrasiveness of silica grains. The extrusion aids also allowed trapped air to be released during extrusion, which together with narrow pore size and particle size distribution controls, they arrived at a more consistent mixture for extrusion. The material was weighed into a muller type mixer and mixed for 1 hour before extrusion into hollow cylinders. His recipe for preparing a 25kg extrusion batch was as follows:

- 20kg diatomaceous earth
- 5kg bentonite clay
- 12.5kg water
- 12.5 kg gel Methocel[24] (mix water with Methocel powder, first disperse in hot water and then gel by quenching in cold water)

Wittemore (1999) showed the advantages of using extrusion as a shaping method for porous ceramic water filters. Where using extrusion meant that little finishing was required and that any size and length could be extruded without increasing the manufacturing costs. Extrusion however requires expensive equipment, technical skills to operate the equipment as well as additives necessary for raw materials without the necessary plasticity. Producing low cost ceramic filters using the extrusion process is therefore not recommended without consideration of the above mentioned factors.

2.2.3 Slip Casting

Wet forming methods are characterized by the direct consolidation of the green body from a homogeneous suspension with optimally dispersed powder particles. This type of shaping method – also called colloidal shaping method – is particularly preferred for ceramic powders in the nanometer or sub-micrometer range in order to use the advantages of ultra-fine powders in terms of microstructure and properties.

[24] water-soluble polymers derived from cellulose

Conventional slip casting is a widespread and cost effective shaping method for the production of complex shaped, large sized components made of advanced ceramics. Pressure slip casting is an established method and has been used for sanitary and table ware for many years. In the field of advanced ceramics pressure slip casting is only used for the production of complex shaped, large size parts made of low price raw powders in large quantities. The process flow diagram for a typical casting operation is shown in Figure 2.11.

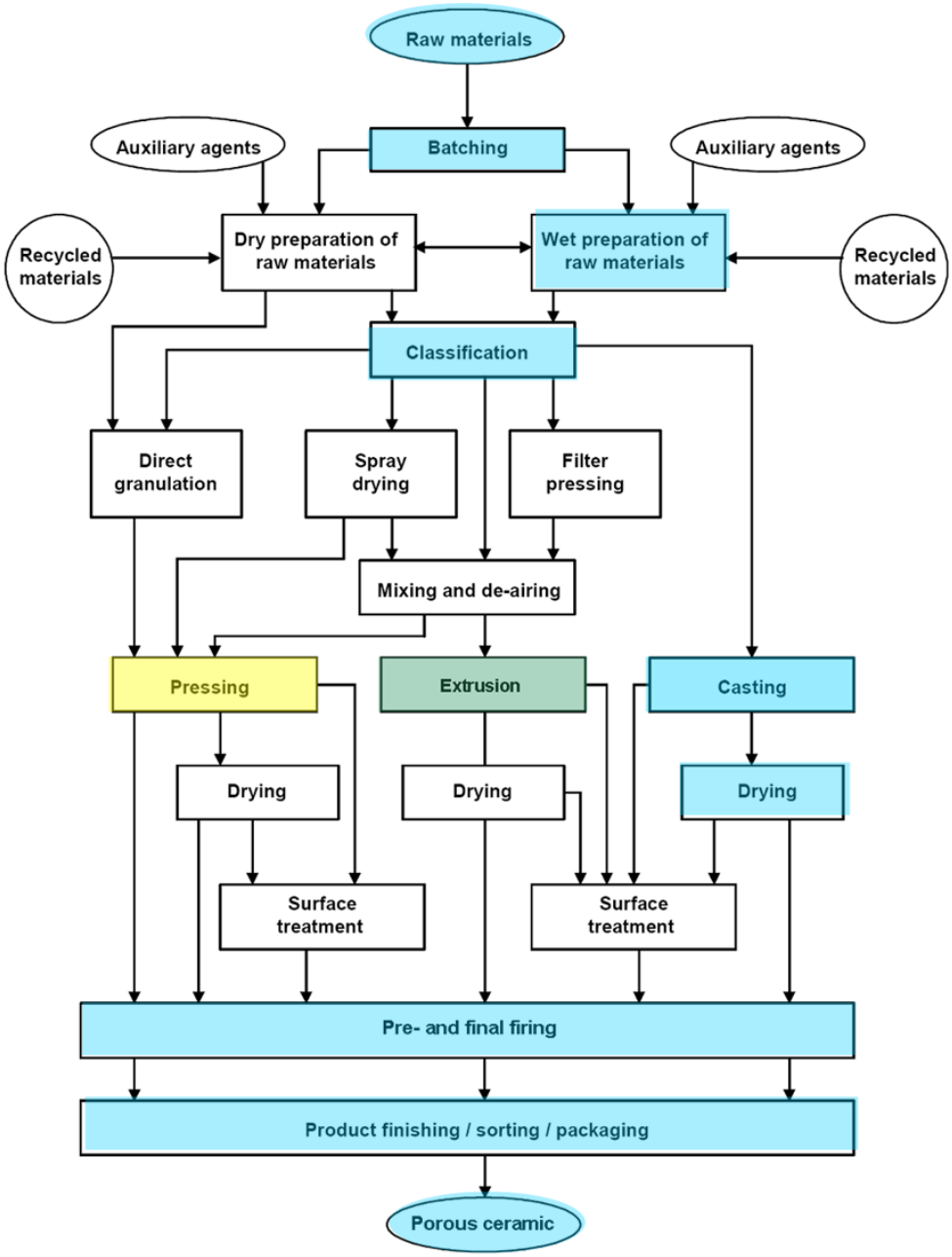

Figure 2.11: Forming process flow for the casting of ceramic products (modified from EC 2007). Colour coded casting route (■).

For alternative slip casting methods such as gel-casting the green body is consolidated by polymerization of a monomer solution. Using this method, components of any shape and with a high level of success can be produced.

According to Ramachandra and Rao (1999), who reviewed the history of slip casting, this method originated in the 18th century when clay materials were used exclusively. The first non-clay material used in slip casting was alumina followed by other oxides, such as silica, magnesia, zirconia and calcia. This was followed by slip casting of non-oxides, such as carbides, nitrides and borides. Today slip casting is used as a major forming method for both large scale monoliths and composite ceramics manufacturing.

Slip casting refers to the filling of a porous mould, a negative of the desired shape, with a slip consisting of a suspension of micrometer size ceramic particles in liquid. Slip usually also contains additional material, binders (organic carbon), pore formers (fibres) and pH modifiers. The capillary action due to the pores in the mould withdraws the liquid from the slip. As the liquid filters into the mould a cast is formed on the mould surface (excess slip is then removed: drain casting) or continued into a solid part (mould is kept full of slip: volume casting). Stable slips with high solids contents and low viscosities can be prepared by careful adjustments of the chemistry of the slip by adding deflocculants (King 2002). The main purposes of slip are for slip casting and for making spray dried mixes for pressing.

2.2.3.1 Drain and Volume Casting

Yang *et al* (2003) divide casting into two categories, namely drain and constant volume casting. In drain casting, the slurry becomes solidified by removal of dispersed liquid accompanied by shrinkage of the consolidated product. In contrast, in constant volume casting, the slurry becomes solidified while maintaining the dispersing liquid.

Wet-processing is the most convenient avenue for producing quality ceramic products from ceramic powders. As a result of homogenous particle packing, fewer defects develop during further processing compared with dry (extrusion and die pressing) processing.

Recently more improved wet processing techniques have been developed that work by either consolidation or by coagulation[25] of the suspended grains (Balzer and Gauckler 2003).

2.2.3.2 Consolidation of slips

Consolidation aims to produce a near net shape part with sufficient strength for subsequent handling by removal of the liquid phase. A number of methods (gel-casting, freeze casting, electrophoretic deposition etc.) have been developed for the removal of the liquid phase. Solvent drainage through porous walls of a mould is used as the main process for slip casting.

A pressure gradient between the porous wall and the liquid is created by capillary forces (***Pc***) resulting from particle size (*a*) and surface tension (γ_{LV}) at the liquid-vapour interface for driving the liquid flow according to the relationship:

$$P_C = -\frac{2\gamma_{LV}}{a}$$ (Guo and Lewis 1999)

The parabolic decreased growth with time (initially rapid growth, but as the layer thickness increases it becomes more difficult for water to migrate through the layer) of the slip cast layer makes slip casting slow and not appropriate for thick layer castings.

According to Guo and Lewis (1999), osmotic consolidation makes use of osmotic pressure (higher than capillary pressure in slip casting) between the slip with a polymer solution and a semi-permeable membrane. With the osmotic consolidation method the chemical potential gradient, *Π*, between polymer solutions and membrane forces the flow of the solvent through the membrane. The formulation for the above process is given by the following relationship:

$$\Pi = \frac{\mu_s - \mu_P}{V_m}$$

Where μ_s, and μ_p, are the chemical potential of the solvent in the ceramic slip and the chemical potential of the polymer solution, respectively, and V_m is the molar volume of the solvent.

[25] process where well dispersed colloidal particles agglomerate

Alternatively the solvent can be removed through a filter membrane using externally applied, mechanical pressure, such as filter pressing[26], where the applied pressure is several orders of magnitude larger than in normal slip casting. This leads to increased consolidation rates. In this case the liquid flux, described by Darcy's law, *J*, through the porous layer is dependent on the pressure gradient, ▼*p*, liquid viscosity, η, and permeability, *D*, as given by the following equation from Yang *et al* (2003):

$$J = -\frac{D}{\eta}\nabla P$$

Gravitational forces can also result in segregation of the solid and liquid phases in a dispersed slip using a mould fitted to a centrifuge. The settling velocity for an individual spherical grain in a centrifuge[27] can be determined using the following adaptation from the Stokes equation, ***v***, from Yang *et al* (2003) for slips :

$$v = \frac{2\Delta\rho R^2\omega^2 z}{9\eta}$$

where, ω, is the angular velocity of the centrifuge, $\Delta\rho$ is the solid liquid to density difference, *R*, is the particle radius, liquid viscosity, η, and *z* the linear distance between particle and rotating axis. The linear relationship between layer growths and casting time provides for easy numerical solution.

In electrophoretic deposition[28] an electric field is used to accelerate suspended particles carrying a surface charge. As in centrifugal casting, steady state particle velocity, ***v***, is balanced by the viscous forces as described by Yang *et al* (2003) in the following equation:

$$v = \frac{\varepsilon_r\varepsilon_0\zeta E}{f_H\eta}$$

Where:

- ε_r, is the dielectric constant of the liquid
- ε_o, is the permittivity of free space[29]

[26] separates the solids from the liquids (de-waters) for further processing of the raw material

[27] process that uses centrifugal force for the sedimentation of mixtures

[28] process where clay particles in a slip migrate under the influence of an electric field and are deposited onto an electrode.

[29] how space effects the forces between two charges: physical constant equal to approximately 8.85 x

- ς, is the particle zeta potential[30]
- E, is the applied electric field strength
- f_H, is the Henry constant (values between 1-1.5 dependent on particle size and ionic strength)

The role of particle (and indirectly the pore diameter which is dependent on the particle diameter) diameter in the various adhesive forces is shown in Figure 2.12 below. The *OUTBAC* ceramic filter pore size (filter developed in this study) is also indicated as a comparison.

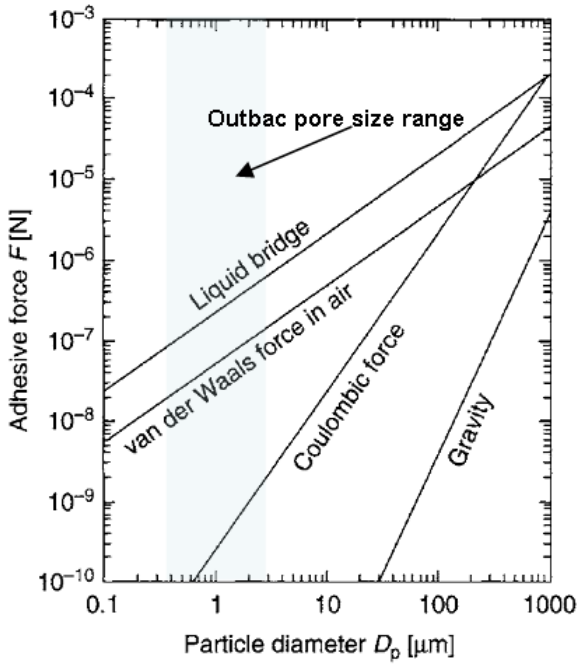

Figure 2.12: Comparing the particle size (pore size) to the adhesive surface forces (Yang et al 2003)

In summary some alternative slip consolidation techniques of suspended particles discussed above include:

- gel-casting (Janney 1990; Young *et al* 1991 and Omatete *et al* 1992): this method makes use of monomers in suspension which are polymerized; alternatively, polymer gelation is induced by using temperatures increases (Sarkar and Greminger 1983), UV radiation (Landham *et al* 1987 & Tormey *et al* 1984) or by catalyst use.

10^{-12} farad per meter (F/m)

[30] defined as the potential at the surface of an electro-kinetic unit (particle) moving through the liquid

- freeze-casting: this method uses dispersed particles which are frozen then stripped from the mould by sublimation (Cowan 1976; Bollman 1957; Grala 1957 and Maxwell *et al* 1954).
- electrophoretic deposition: where colloidal particles suspended in a liquid move under the influence of an electric field (electrophoresis) and are deposited onto an electrode. All colloidal particles that can be used to form stable slips and that can carry a charge can be used in electrophoretic deposition. This includes materials such as polymers and ceramic materials.

2.2.3.3 Slip control

In ceramic processing it is the smaller, colloidal particles that have to be controlled. To produce slip with required properties, a number of slip parameters have to be carefully controlled. Stability is the most desired property in a ceramic slip where inter-particle forces play the most important role in determining slip stability. Particles suspended in a liquid spontaneously agglomerate as a result of the attractive van der Waals forces amongst the particle surfaces. Preventing such spontaneous settling requires modification of the particle surface to produce a repulsive force that counteracts the attractive van der Waals force. High solids loading is another requirement for slip stability. Normally a high as possible solids loading is preferred together with a low as possible viscosity for mould filling. Table 2.1 summarises some of the other important properties necessary for slip stability (Yang *et al* 2003).

Table 2.1: Parameters required to keep slip stable (Yang et al 2003)[31][32]

Property	Characteristics
pH	• ion absorption from solution results in particle surface charge
	•at low pH, H+ ions results in positively charged surfaces
	•at high pH, absorption of anions produce a negatively charged surface
	•neutral charged surface is called point of zero charge
	•iso-electric point is reached for a pH value with zero Zeta potential
particle size distribution	•important only with high solids loading and packing close to theoretical density which impacts on viscosity
	•with high percent of finer particles results in lower solids loading and thixotropic in character (increased SSA binds more water and dispersant instead of making available to slip)
	•with high percent of large particles results in dilatancy reducing the flow and lowers solids loading
	•with large percentage of medium size particles narrow particles size distribution and traps water in the pores of the larger particles
coagulation	•irreversible getting together and adherence due to van der Waals attraction
	•flocculation is a reversible adherence
double layer repulsion	•colloidal particles contact with similar charge
	•overlap of ionic cloud causes increase in ionic strength
	•causing depletion of water in the area
	•causing an increase in osmotic pressure
	•diffusion of water into this area to maintain equilibrium causes the particle repulsion- slip stability

Fish (2001) further illustrates the packing arrangement of particles in flocculated[33] and deflocculated slip systems when controlled by pH (Figure 2.3).

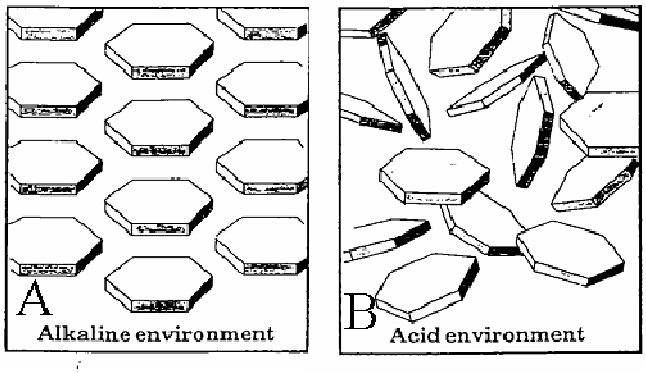

Figure 2.3: Illustration of a deflocculated slip system (A: alkaline pH) and a flocculated slip system (B: acidic pH) - Fish (2001)

[31] SSA: specific surface area

[32] thixotropic slip: inverse relationship between shear rate and viscosity

[33] process wherein colloids (clay particles or fines) come out of suspension in the form of floc when adding a flocculating agent (opposite for deflocculation where particles are suspended using a deflocculant)

2.2.3.3.1 Particle packing

Particle packing is based on the perception that with perfect packing of the individual particles, a minimum amount of water is needed to make it a stable slip. During the last 100 years or more, quite an extensive amount of work has been undertaken in order to determine theoretical packing models, Andreasen in 1930 proposed a model that is simple to use and with proven results (Furnas 1931 & Hüsken and Brouwers 2008):

$$CPFT = \left[\frac{d}{D}\right]^{q} \cdot 100$$

CPFT: Cumulative Percent Finer Than
d: Particle size
D: maximum particle size
q: distribution coefficient (q-value) [34]

Funk and Dinger (1994) using the above ideal packing system equation state that the use of a wide particles size distribution system yields a better packing efficiency compared to a monosize system (The ideal packing system model will be further developed in Chapter 3).

Even where flowability is not an issue, efficient particle packing leads to increased mechanical strength and reduced liquid addition during processing.

2.2.3.3.2 Particle size distribution (PSD)

A slip is in the simplest case a mixture of raw materials from the fine to the super fines with submicron particle size. The significance of a proper particle size distribution has been widely recognised in recent years. A precise grading of the particle sizes enables one to make a slip which is easily mixed and placed and also has the desired mechanical properties.

The ability to control the particle size distribution is important also in quality control and production. More flexibility of raw materials choice and reduced costs of the raw materials are some of the concerns when making slip.

[34] d: average particle size

In Chapter 5 the section on particle size distribution will be further developed to show how to construction a composite particle size distribution of the raw materials giving highest packing density, was used to obtain the best material recipe, and by manipulating the particle size distribution, shown how to obtain slip with suitable flow and packing.

Should a milled fraction for some reason change characteristics, it is relatively simple to adjust the recipe so that the desired PSD can be maintained.

2.2.3.4 Slip dispersion (deflocculation)

Ramachandra and Rao (1999) state that dispersion of ceramic particles can be obtained as follows:

- controlling electrostatic surface charges through pH adjustments (maintaining either a positive or negative charge on particles, therefore preventing flocculation)
- dispersant absorption by particles (deflocculant added to the slip results in absorption of the deflocculant charge on the particles)
- polymer with long chains absorbed to grain surface (chain results in separation of the particles)

According to them such well dispersed slips produce homogenous, high density green products with only minor defects.

2.2.3.5 Raw material requirements for slip casting

The most critical factors affecting formation and firing processes are the raw materials and their preparation (King 2002). Selection of raw materials forms the first part in slip preparation process. Essential properties in developing a good slip will include (Sakar-Deliormanh and Yayla 2002):

- rheology control suitable fluidity (low viscosity and minimum water addition)
- particle dynamics (particle density and shape),
- diffuse double layer interaction, and
- colloidal interaction

Rheology control: It is important to control the rheology[35] to ensure proper processing by controlling slip viscosity through variables such as particles size distribution, total solids concentration, and particle packing (Dobrovolskiy, 1977). These factors determine the amount of water addition and optimum flow properties during the shaping. Slip viscosity must be manipulated to be high enough to minimise particle segregation and low enough for mould filling and bubble release (entrained during the mixing process). Viscosity also affects the shrinkage and ultimate product density. By optimizing the flow properties, risk of product deformation or breakage through the various handling steps is minimised.

Particle dynamics: Ceramics are derived from powders which have to be handled and processed before sintering. To obtain the desired properties, particle sizes in the submicron size-range are used. With particle sizes smaller than 100 micron, surface forces equal to gravity result in agglomerates and settling.

When particle sizes decrease from 1 micron to 1 nm, the size of the surface forces also increased to 3 to 10 orders of magnitude higher than gravity, as shown in Figure 2.4. To control ceramic powders during processing, a full knowledge of the origin and quantitative measurement of the surface forces are required (Yang *et al* 2003).

[35] study of the deformation and flow of materials in a liquid

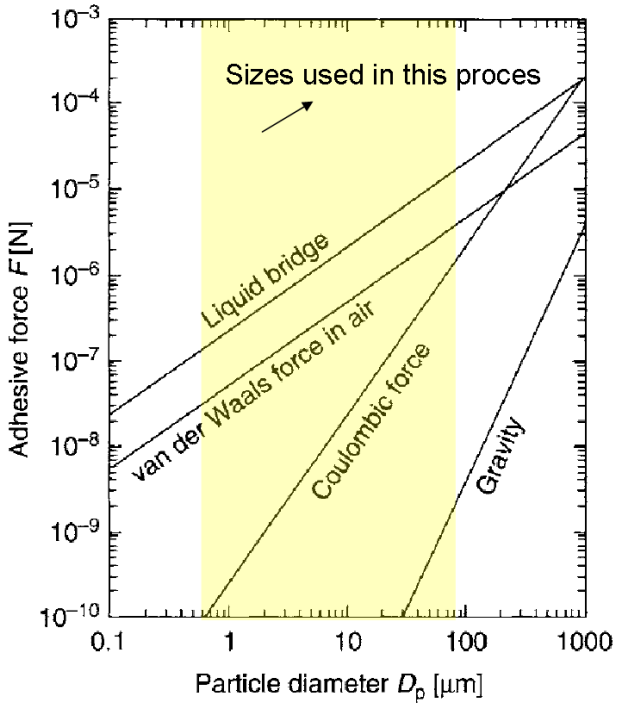

Figure 2.4: Comparing the surface attraction forces, particles size distribution and particle sizes used in their study (Gotoh and Higashitani 1997)

Diffuse double layer: By having a diffuse double layer surrounding a grain, the shear slippage occurs at some distance away from its surface. The electric potential at this shear slippage surface can be quantified by using the zeta-potential. According to Rahaman (2003), silicate particles adsorb ions from solution to form a surface charge. During hydration at the surface of the silicate particles, at low pH, H^+, ions form a positive charge, whereas at high pH OH^- ions produce a negatively charged surface. The point of zero charge occurs at a pH where the surface is neutral as shown in Figure 2.5.

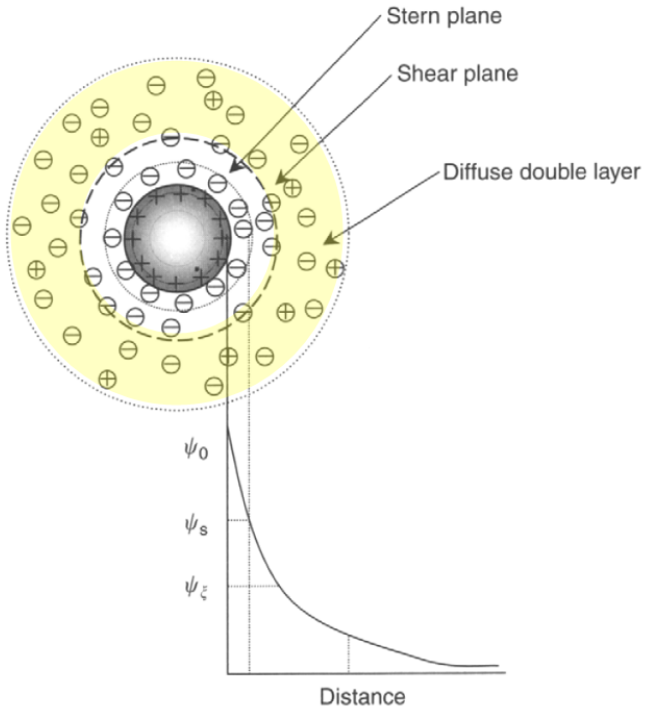

Figure 2.5: Distance from the particle surface impacts on the electric potential, with ψ_s *as the surface potential* ψ_ξ *as the zeta potential and* ψ_0 *as the zero potential (Hunter and White 1987)*

The pH value at which the zeta potential is zero is called the iso-electric point (IEP). Some of the more important ceramic compound's IEPs are shown in Table 2.2 below.

Table 2.2: Iso-electric points (IEP) of the main oxides from Hunter and White (1987)

Material	Iso-electric point
α-Alumina (Al_2O_3)	9 - 9.5
Silica (SiO_2)	3 - 4
Zinc oxide (ZnO)	9
Titania (TiO_2)	4 - 5
Calcium Carbonate ($CaCO_3$)	9 - 10
Lead oxide (PbO)	10
Magnesia (MgO)	12 - 13
Zirconia (ZrO_2)	4 - 5
Stannic oxide (SnO_2)	4 - 7

Colloidal interaction: Colomban (1989) explains that colloids develop in range from 1 micron to 1 nm. The word is derived from the Greek word for "glue," because the grains in this size range have a tendency to stick together.

These sticking forces have to be controlled during the shaping process to obtain a stable slip. To prevent the spontaneous agglomeration due to the van der Waal's attractive forces, the particle surfaces have to be modified to form repulsive forces to negate the attractive van der Waal forces – slip stability. This is done either by absorbing polymer chains onto the surfaces (stearic stabilization) or by adding charged ions or dipoles to the surface (electric double layer stabilization). It is furthermore desirable to increase the solids loading at a viscosity low enough for mould filling and spray drying (pressing).

Hunter and White (1987) state that, in a slip, it is the charge on the surface of a colloidal particle that results in double layer stabilization. The repulsion between particles depends on the size of the surface charge and therefore the stability of the slip. The "diffuse double layer" then forms when oppositely charged ions and polar molecules in solution are then attracted to this charge. The electric potential at this surface where shear slippage occurs is called the zeta potential. A local increase in ionic strength is caused by two particles of like charge approaching one another resulting in an overlap of their respective double layers. This results in a depletion of water and osmotic pressure development in this area. Water molecules diffuse into this area, resulting in particle repulsion, which stabilizes the slip.

When two colloidal particles of like charge approach, their double layers start to interact and the repulsion, V_R, will oppose the van der Waals attractional forces, V_A, should the repulsive potential be larger than the attractive van der Waals potential, double layer stabilization results, V_T, as indicated in Figure 2.6.

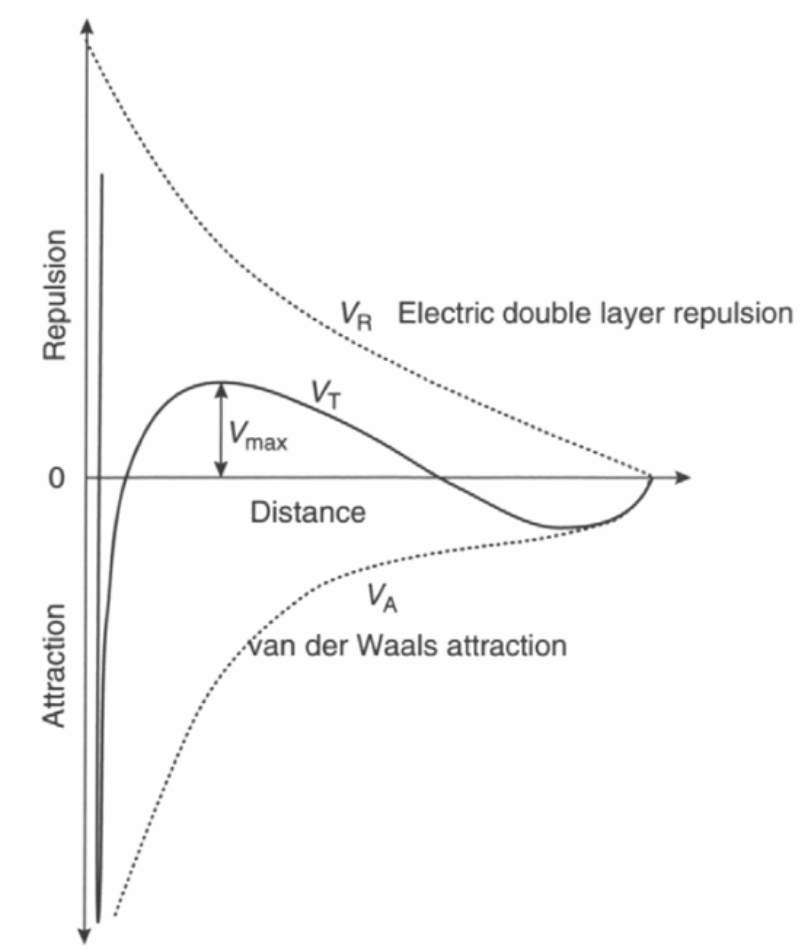

Figure 2.6: The influence of the van der Waals attractive forces and the electric double layer repulsion on the potential energy of two approaching particles in a slip (Yang et al 2003)

2.2.3.6 Gel-casting

Colomban (1989) presents an overview of the sol-gel[36] technology. This manufacturing route has been used for centuries in earthenware and china production as a means of sintering at low temperatures. The drawbacks of this route are as follows: costs, toxicity, solvent recycling, grain growth and the need for special mould formers.

[36] process of forming material with specific properties (porosity) at room temperature compared with conventional glasses needing much higher melting temperatures

Gyger *et al* (2007) explain that gel-casting was initiated in the 1990s to create complex ceramic shapes. Gel-casting is a sol-gel mixture where ceramic powders are mixed with a monomer solution to form a high solids loading, low viscosity slip that can be cast or injected into moulds with complex shapes. This is then followed by a low temperature treatment to polymerise the product and so immobilise the particles. Gel-casting advantages are as follows:

- high solids loading and green density without the need for pressure
- uniform particle and density distribution
- removal of green gel-cast body with retention of complex shapes requiring minimal finishing
- tailor made porosity, mechanical properties and specific applications

Gregorová *et al* (2004b) found that during gelation there is a continuous rheological change from viscous to elastic (viscoelastic behaviour), and this transition can be used as a new shaping process. Gregorova *et al* (2006) explain that using organic or bioorganic components in slips requires a focus on viscoelastic behaviour. This is necessary because gelation (rheological change from viscous, viscoelastic, to elastic) is important in casting with polypeptides (gelatin) or polysaccharides (starch, agar, and carrageen). According to them, starch consolidation (rapid starch swelling with temperature increase) has more than one mechanism for body formation; a change in rheology after swelling accounts for the total time needed to produce strong green bodies. A slip of silicon nitride (volume solids loading: 43 percent) and alumina (volume solids loading: 50 percent) where prepared and consolidated with carrageenan and other agroids.

Padilla *et al* (2005) contrasts gel-casting with slip casting. Gel-casting is processed by gelling (polymerisation) of a concentrated slip, suspended in a monomeric solution, where the organic polymers surround the ceramic particles, resulting in a high strength green product. In slip casting the porous mould withdraws water which results in the solidification of the product. The disadvantage of slip casting is that fluid flow due to capillary action is slow with a weak green body due to a density gradient especially in thick walled bodies. This contrast with gel-casting where green bodies are uniform and strong.

2.2.3.6.1 Gel-casting types

The binders in gel-casting forms a continuous, strong gelling network that binds the ceramic particles permanently in position preventing the formation of inconsistencies during the subsequent drying and firing processes. A number of authors presented below have used a variety of binders in gel-casting porous ceramics.

Tulliani *et al* (2009) list the following gel cast monomers that have been used in the past:

- acrylamide (withdrawn due to neurotoxicity), and
- gelling agents – agar, carrageenan gums, egg white and gelatin

In their study, natural food-grade gelatin (pig derived) was used as gelling agent. This allowed temperature induced polymerisation – without having to use catalyst and initiator (used in synthetic monomers) and creating a low environmental impact. The gelatin was first dissolved in de-ionised water at 60°C before stirring it into the ceramic suspension, which is also kept at 60°C. The optimum amount of gelling agent in respect to water concentration of 3 percent gave continuous polymerisation and strong green product for de-moulding. A de-airing step was added as gelatin tended to foam. The mixture was poured into non porous Plexiglas and cooled to room temperature for gelation development. The cast samples were then dried under controlled humidity and at room temperature before stripping.

Akhondi *et al* (2009) used sodium alginate (natural product from brown sea weed) to gel ceramic particles into a solid network. Sodium alginate is first dissolved in water (room temperature), added to the ceramic mix and then the mixture is gelled using Ca^{2+}. Their process for gel-casting alumina powders is shown in the flow chart (Figure 2.7) below.

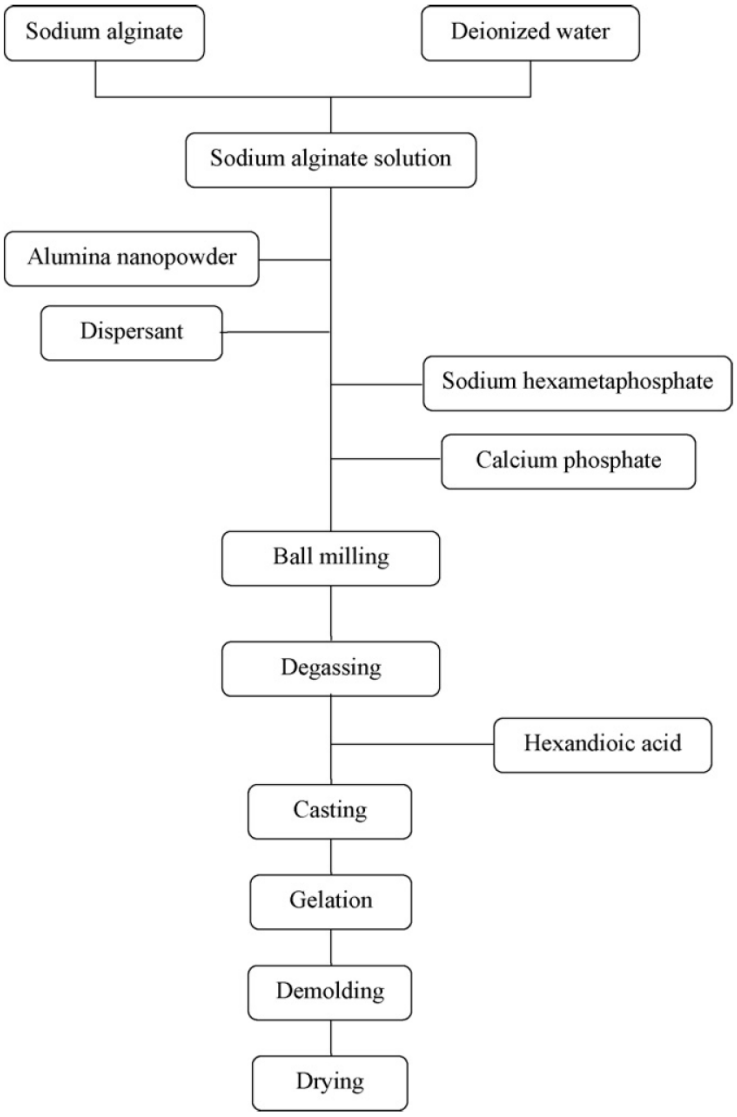

Figure 2.7: Gel-casting process by Akhondi et al (*2009)*

Thermo gravimetric analysis (TGA: in air with 10°C min^{-1} heating rate to 700°C) and DTA (differential thermic analysis) results of the authors are presented in Figure 2.18 that demonstrates the 4% weight reduction at 130°C due to evaporation of the retained water. Most of other additives burnt out between 280–450°C. By increasing the temperature from 25°C to 600°C resulted in a 17% weight loss. This rapid loss can cause cracking in the green body during the burn out of the binder.

The DTA and TGA results were then used to design the slow heating rate at 1°C.$min.^{-1,}$ allowing the binder volatiles to be slowly released and prevent cracking.

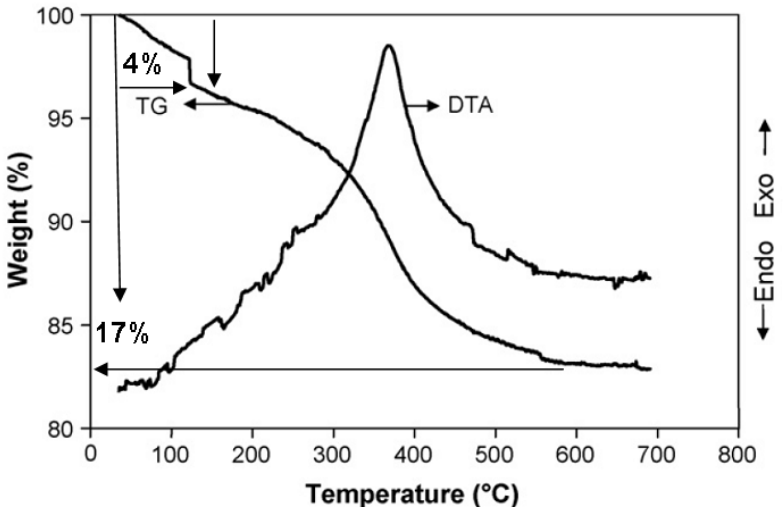

Figure 2.18: TGA and DTA plots for green bodies in air (Akhondi et al 2009)

Bartuli *et al* (2009) used fluka agar to produce slip with a solids loading of 55 percent. Their zirconia suspension was prepared using de-ionised water with 1.22 weight percent (wt) Dolapix PC 33 (dispersant) added. A portion of water was used for dispersion of the zirconia and the remainder was used for dissolving the agar (2.38 wt percent) at 90°C for 1h. The agar solution was cooled to 60°C before adding to the warmed ceramic suspension (60°C). When foaming occurs a de-airing step was added to remove trapped air. The slip was poured into non porous resin moulds at a temperature of 60°C. Cooling of the product to room temperature caused the gel structure to develop. The gelling agent resulted in 7 percent porosity after first firing.

Takahashi *et al* (2009) used gelatin to gel-cast a double layered porous ceramic filter (see Figure 2.19) using waste material and a non-toxic monomer. The product was fired under reducing conditions to pyrolise[37] gel cast ceramics. The formulation used for ball milling was as follows: water, broken glass (42 to 45 percent), mica mineral (18 to 22 percent), mining waste (18 to 22 percent), spent alumina (12 to 15 percent) and gelatin.

[37] process of removing organic volatiles at tempatures ranging between 200 and 900° C under reducing conditions

The slip was heated to 80°C and aggressively mixed to a produce a foamed slip, cast into moulds, and allowed to cool and solidify into a product strong enough for de-moulding.

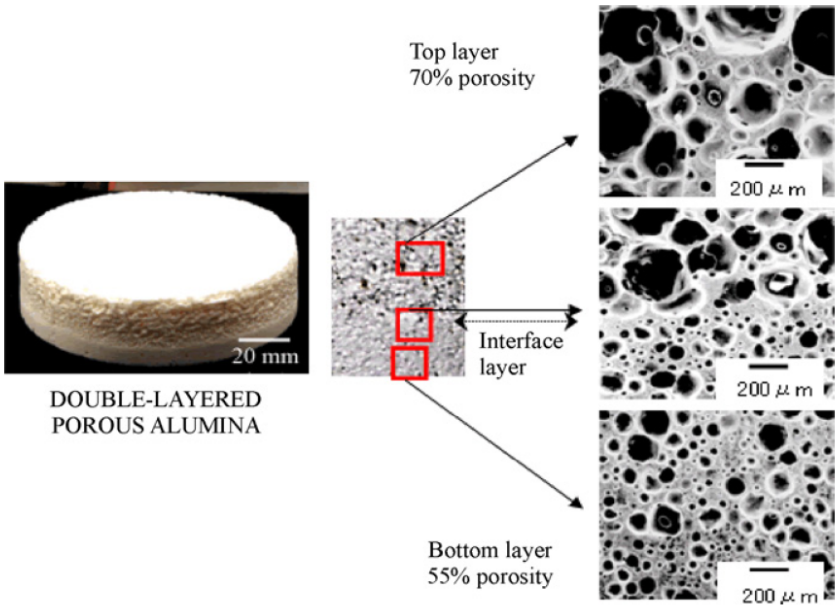

Figure 2.19: Double-layered porous filter (Takahashi et al 2009)

Liu *et al* (2001) used gel-casting to shape porous mullite with open porosity of between 58.5 – 63.9 percent and average pore size ranging between 0.8 – 1.3 mm. The gelled mixture consisting of kaolinite and $AlOH_3$ was sintered at 1300- 1600°C. By varying the raw material ratios and firing temperature, the average pore size, pore size distribution and hydraulic conductivity could be controlled.

Ganesh *et al* (2009) used alumina powder with d_{50} of 0.8 micron, zirconia powder with a d_{50} of 0.43 micron together with an AlN powder with d_{50} of 0.33 micron as gelling and consolidation agent[38].

[38] set or bind the suspension making it strong enough for further processing

2.2.3.7 Freeze casting

Freeze-casting, the shaping of porous structures by the solidification (freezing) of a solvent (water into ice), have seen a number of developments during the last few years. Of particular interest for water filtration are the unique structure and properties exhibited by porous freeze-cast ceramics, which opened new opportunities in the field of porous ceramics (Hbalze and Gaukler 2003).

In summary Hbalze and Gaukler (2003) emphasized the fact that wet processing has a better potential to produce high quality ceramics than dry processing because it results in better particle-to-particle contact, which produces a more homogenous packing, leading to limited defects in the final microstructure. Two newer slip casting forming techniques of consolidation of dispersed slip and coagulation of suspended particles, were discussed. Consolidation is applied in the gel-casting with monomer polymerisation in the slip (or induced polymerisation by UV, heat or catalyst use), whereas in freeze-casting and quickset, the dispersed medium is solidified (by freezing) and then sublimated for removal. The liquid to solid change can therefore be initiated through either heating, changing the pH or by increasing the suspension's ionic strength.

2.2.3.8 Slip casting benefits

Fish (2001) gives a number of reasons why slip casting is still a suitable or preferred ceramic shaping method. Slip-casting methods provide superior surface quality, density and uniformity in casting high purity ceramic raw materials over other ceramic forming techniques. The raw materials used for slip casting are also a mixture of components that helps reduce the firing temperature.

Masaaki and Kurita (1997) identify conventional slip casting as a method of choice in Japan for casting near net-shaped castings and suggest the use of polypropylene moulds instead of the conventional plaster moulds. In thin castings a homogenous green body is possible but as the wall thickness increases the density decreases further away from the mould. It is impossible to use a plaster core as the product shrinks around the core leading to stresses that make stripping difficult or results in rejects (Takahashi and Kurita 1997).

To overcome the stresses, they developed a self-hardening slip that rapidly sets in the mould, making it possible to remove the core. A hardening resin and hardener was added by the authors to disperse the slip. After de-airing, the slip was cast into a polypropylene mould. After de-moulding and drying at room temperature, drying was completed at 80°C in a drier for 12h. The green product was fired at 600°C for 1h to burn out the organics and then at 1500°C for 1h (Figure 2.8).

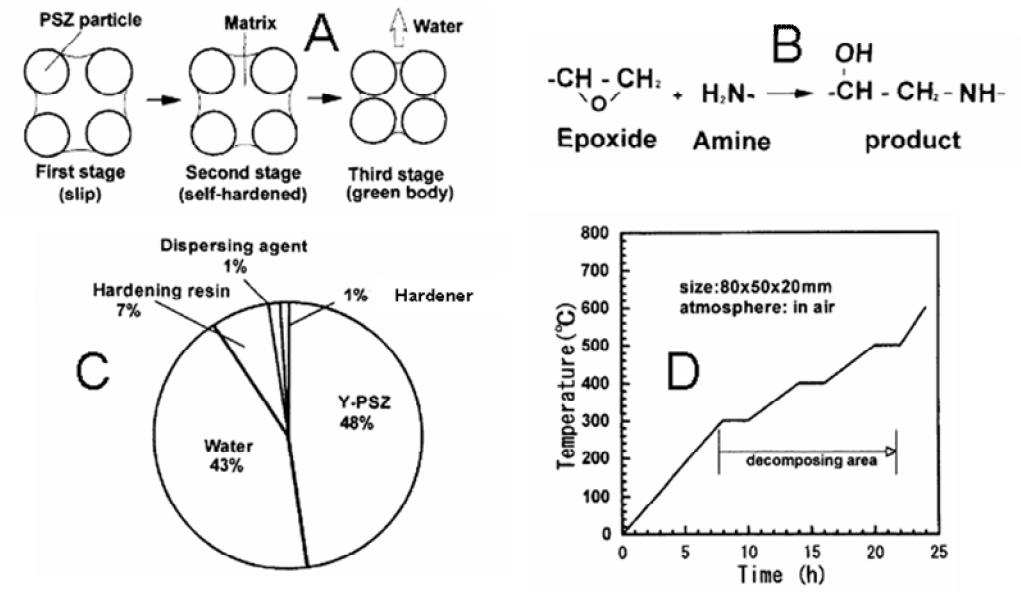

Figure 2.8: A- Model for the forming of the self-hardening slip; B- Equation for the reaction between epoxy and amine hardener; C- Volume fraction of materials and D- Burn-out schedule for resin (Masaaki and Kurita, 1997)

The advantage of using self-hardening casting slips in the manufacture of ceramic water filters include:

- forming thick bodies (use of non-porous moulds)
- forming sintered bodies with high strength
- reduced firing temperatures (energy savings)

Ozgur and San (2009) found it possible to develop a fine particle migration technique for forming a multi-layered, varied pore size filter by using the slip casting technique. By combining a varying sized mixture of quartz-zeolite-glass particles (10 percent mass by weight loading) the method was used to make ceramic filters with a 350 micron pore size.

They also improved the filling method as illustrated in Figure 2.9 which resulted in reducing the time necessary for the labour intensive refilling of the plaster moulds during casting.

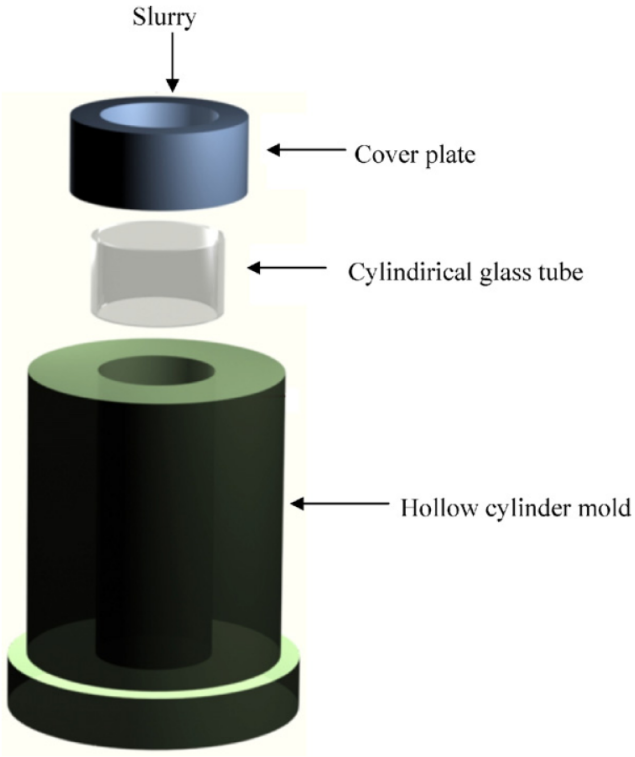

Figure 2.9: The Ozgur and San (2009) mould system for slip casting

Darcovich *et al* (2003) describe the benefit of using the slip casting technique to develop a single step sedimentation method for obtaining an asymmetric porous microstructure. Surface chemical control allows a fine alumina powder slip to consolidate onto a plaster mould forming an increasing mean pore size from top to bottom. This structure is made possible by the use of a broad particle size distribution powder. Normally, sintering of such a structure results in warping. The authors examined warpage by using a sintering modeling technique that incorporates particles size distribution as a variable. The model ensured that the particles size distribution was broad, overlapping and occurred with a significant tailing of fines.

Hotta *et al* (2005) were able to benefit from using a poly-acrylic ammonia acid dispersant (CELUNA D-305) to cast a low soda alumina (AL-160SG-4). The process flow chart used in their process is indicated in Figure 2.10 below.

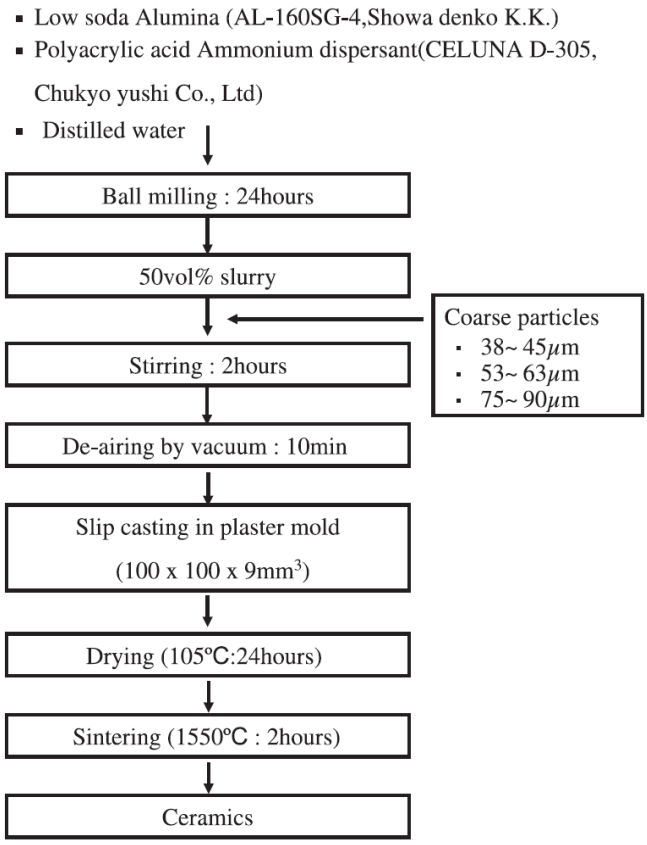

Figure 2.10: Fabrication process for alumina ceramics (Hotta et al 2005)

2.2.3.9 Forming method application summary

In the forming step, dry powders, plastic bodies, pastes, or slips are consolidated and moulded to produce a cohesive body of the desired shape and size.

Dry forming consists of the simultaneous compacting and shaping of dry ceramic powders in a rigid die or flexible mould. Dry forming can be accomplished by dry pressing, isostatic pressing, and vibratory compaction.

Plastic moulding is accomplished by extrusion, jiggering, or powder injection moulding. Extrusion is used in manufacturing structural porous ceramics, clay products and some refractory products. Jiggering is widely used in the manufacture of small, simple, axially symmetrical white ware ceramic such as cookware, fine china, and electrical porcelain. Powder injection moulding is used for making small complex shapes.

Slurry forming of ceramics generally is accomplished using slip casting, gel-casting, or tape-casting. In slip casting, ceramic slurry, which has a moisture content of 20 to 35 per cent, is poured into a porous mould. Capillary suction of the mould draws the liquid from the mould, thereby consolidating the cast ceramic material. After a fixed time the excess slurry is drained, and the cast is dried.

Slip casting is widely used in the manufacture of sinks and other sanitary ware, figurines, porous thermal insulation, fine china, and structural ceramics with complex shapes. Gel-casting uses *in situ* polymerization of organic monomers to produce a gel that binds ceramic particles together into complex shapes such as turbine rotors. Tape-casting is used to produce thin ceramic sheets or tape, which can be cut and stacked to form multilayer ceramics for capacitors and dielectric insulator substrates.

Table 2.3 highlights the three main forming methods with their respective material requirements, equipment, problems and advantages.

Table 2.3: Summary of the forming characteristics

Forming Method	Material requirement	Moisture Content	Equipment Type	Problems	Advantages
Die Pressing	Fine/coarse grained	Dry or slightly moist	Die, die assembly, hydraulic press. Isopressing (hydrostatic)	Laminations, edge capping, sticking, hour glassing, warping & cracking	No drying required
Extrusion	Stiff, plastic mixture (add clay or hectorite) & extrusion aids	12- 20% moisture	Extrusion die, vacuum auger, hydraulic piston & hand forming at low pressures	Dimensional controls	Productivity
Slip Casting	Flocculants & deflocculants (Sodium silicate to increase fluidity)	+ 20%	Plaster moulds	Settling, clogging of filter cake. Plaster mould drying	Homogeneity of properties, low input cost

2.3 Selection of the best forming (shaping) method

Currently ceramics are mostly produced through densification of ceramic raw materials (pressing and extrusion) and sintering. All of these need expensive production equipment and high temperatures for sintering (Figure 2.11), which make manufacturing costly. Slip casting, in contrast, although still requiring high temperature for sintering, requires simple and low-cost equipment for production with less technical limitations in the type of raw materials than other methods. It is also hoped that through further development with cement based bonding (in contrast to high temperature sintering), that low-cost equipment can be combined with lower firing temperatures.

Other processes, such as solid state burn-out of polymers and sol-gel processes have been developed and applied to non-oxide ceramics to further decrease firing temperatures and equipment costs (Segal, 1989 and Narula, 1995). In both developments, molecular formers are synthesized and changed into ceramics by heating at lower processing temperatures (see Figure 2.18 above).

Recently bio-mineralization processing (Lowenstam and Weiner 1989; Mann *et al*, 1989 and Baeuerlein 2000) has illustrated how nature makes intricate shapes and materials at standard temperature, pressure and atmospheric conditions – something that is not possible with current artificial processes.

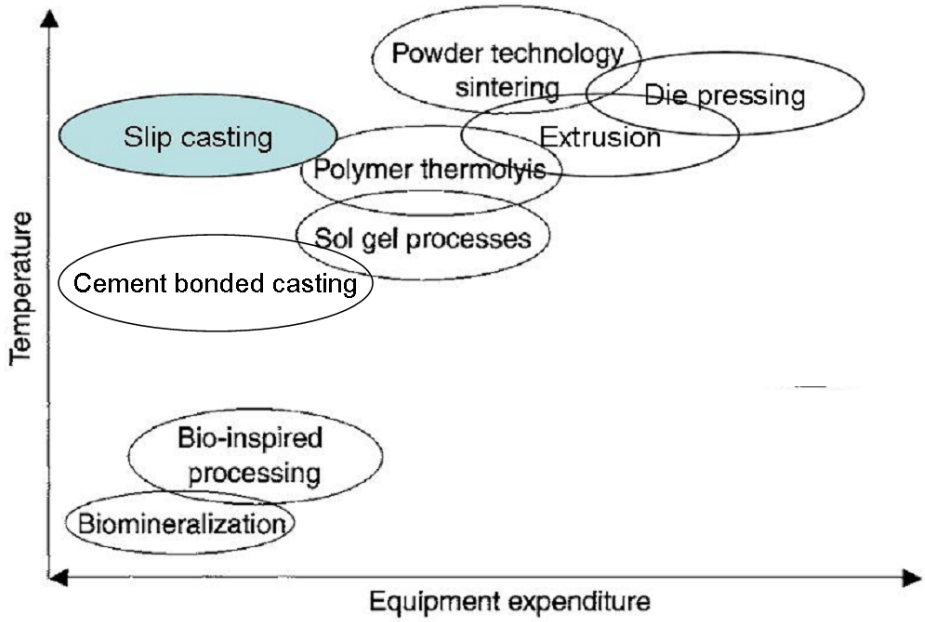

Figure 2.11: Ceramic forming processes organized according to equipment expenditure and processing temperature (Adapted from Bill et al 2003)

Guided by the literature study, the slip casting method was selected as the method of choice for this study as it is the most suitable low-cost (equipment expenditure), low technology method for shaping and forming ceramic water filters. The benefits of the slip casting process such as limited finishing, good size tolerance and obtaining high density castings also played a role in the selection process. It is also the only process that merely requires ceramic particles to be mixed into a dispersed suspension (slip), a porous mould to consolidate the aqueous suspension, a drying and burning-out process where the de-moulded (stripped) green body gains initial strength and finally the sintering process to give the pores and the final product strength.

Because processed silicates (clays) are not available throughout Africa and also vary widely in terms of chemistry, mineralogically and physical properties, it was decided to limit the initial research by sourcing material with more consistent properties, ability to flow and pack into a dense product and by selecting materials that could be purchased off-the-shelf and which required minimal further treatment. The selection of raw materials for the slip casting process is further described in Chapter 6.

Chapter 3: Processing of Porous Ceramics

The processing of porous ceramic products takes place in different types of kilns, with a wide range of raw materials and in numerous shapes, sizes and colours. The general processing of ceramic products, however, is rather uniform, besides the fact that, for porous ceramics, often a multiple stage firing process is used.

In general, raw materials are mixed and cast, pressed or extruded into shape. Water is used for thorough mixing and shaping. This water is evaporated in dryers and the products are placed by hand in the kiln. In most cases, the kilns are heated with electricity but natural gas, liquefied petroleum gas (LPG), fuel oil, coal, petroleum coke or biogas/biomass are also used. An irreversible porous ceramic structure for the product is reached during the firing process in the kiln which demands a very accurate temperature gradient during firing to ensure that the products obtain the right treatment. Afterwards controlled cooling is sometimes necessary so that the products release their heat gradually and preserve their ceramic structure.

In the following Sections 3.1 to 3.5, the most important units of a porous ceramic manufacturing plant, as well as the basic steps and variations in the production processes, will be explained.

3.1 Raw Materials

3.1.1 Background

According to Lange (1989), raw materials are one of the most important quality factors in ceramics. King (2002) views the manufacturing of a ceramic product as a raw material pyramid on which all the other steps are built. The use of the correct raw material is therefore critical in producing usable ceramics at a low cost.

Selection of the correct raw materials should be guided by envisaged forming method and end-product specifications. Further treatment, such as milling and mixing, also critically affects raw materials and must therefore be controlled. Naito *et al* (2003) provides a number of raw material factors that can be used as selection criteria (Table 3.1).

Table 3.1: Selection criteria for raw materials (Naito et al, 2003)

Material Properties	Selection criteria
Chemistry	
Composition	Homogeneous
Impurity	None
Stoichiometry	Stoichiometric
Phase	Stable
Particle	
Shape	Uniform and spherical
Size	Small
Distribution	Adequate

Raw materials should be able to be formed into a physically and chemically uniform green shape, and with further heat treatment into the final finished product. Uematsu *et al* (1995) and Uematsu (1996) provides an example of a green body where the absence of defects was only due to an inadequate identification tool for identifying important defects.

Figure 3.1 shows the green body examined by Uematsu *et al* (1995) and Uematsu (1996) using a sensitive optical method that detects small defects. The large defects (at this detection range) are clearly visible. It is clear from this example that the compact was far from uniform (homogeneous) as it contained a number of structures (aggregates and coarse particles) that could have resulted in unpredictable variations in the final product had they not been identified.

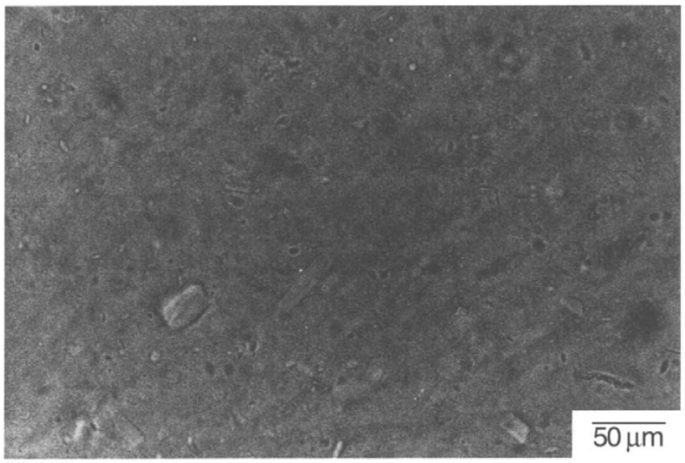

Figure 3.1: SEM image of green compact defects identified using the liquid immersion technique (Uematsu 1996)

From the above example it should be clear that the raw material quality is often outside specification and for this reason unexpected variations could occur between batches. The problems introduced during the green body stages are likely to develop into defects during later stages, such as sintering, which will ultimately result in product strength reduction and porosity variations (Naito *et al* 2003).

The following sections examine raw material characteristics as well as raw material treatment processes, such as milling and mixing, necessary for raw material forming requirements.

3.1.2 Raw material characteristics

3.1.2.1 Chemical composition

The aim here is to keep the chemical composition fixed and constant. For simple oxides and silicates, the stoichiometries stated in datasheets are seldom achieved in raw material containing transitional metal elements. This can critically affect the composition and subsequent product properties (Naito *et al* 2003).

An example given by Hegenbart (1995) describes how chemistry can affect flow properties for starch grains during slip casting. Starch and oil are the two forms in which plants can store their unused energy. Starch is stored in both underground plant bodies, such as tubers (potatoes), roots (cassava), and corms (bulbs), and in above ground fruits and seeds (for example corn).

Legumes (beans and peas) and cereals (corn, amaranth, millet, rice, wheat, and sorghum) are plant groups with seeds containing large concentrations of starch. Starch grains are important pore-formers that exist in two different chemical configurations:

a) Amylose which forms linear chains
b) Amylopectin which forms branched chains

Starches mostly consist of the two forms in a ratio determined according to the plant type. Amylose supplies the gelling character of slips, while amylopectin supplies the slip viscosity. The higher the concentration of amylopectin, the more water is absorbed by the starch lowering the gelatinization temperature of the starch grains. Both starch configurations therefore provide very different slip casting properties.

3.1.2.2 Impurities

Impurities are minor components that occur in raw materials; some of the impurities can govern the production properties of ceramics and limit their applications.

The standard example of the impact of impurities is the occurrence of sodium in alumina raw materials. Dispersion in slips and the sintering behaviour are affected by sodium concentrations that critically influence product quality. Similarly, according to Handwerker *et al* (1989), calcia and silica in alumina, separate at the grain boundary, causing irregular crystal growth in alumina during firing, which affects both the physical and chemical properties at the boundary of the grains. However, certain elements, especially elements in the same group in the periodic table, often have minor effects (Bae and Baik 1994).

3.1.2.3 Phase change

Raw materials containing similar chemistry are significantly affected by phase changes during heat treatment. The phase changes result in a change in volume with heating. Karagedov (2006) gives the example of zirconia, which exhibits a cubic phase at high temperatures and a monoclinic phase at lower temperatures.

The change in volume between the high temperature phase and low temperature phase can result in cracking should uncontrolled cooling cycle occur.

3.1.2.4 Grain size

Small grains form persistent aggregates that are difficult to disperse in a slip (Singh *et al* 2009). Fractures tend to originate from aggregates and are problematic in ceramic production. The dispersant must cover the whole grain surface (proportional to the surface area) to produce repulsion amongst the grains. Large amounts of dispersant will be needed for very fine grains (large surface area). PH and the use of low molecular weight dispersants can, however, effectively disperse fine powders.

Rate and temperature of sintering are hugely affected by particle size (Naito *et al* 2003). In Figure 3.12 various alumina powder grain sizes were sintered for equal time steps at various temperatures. Theoretical density was achieved at sintering temperatures of 1600°C and at 1300°C for powders with grain size of half a micron and one tenth of a micron respectively. According to Coble and Gupta (1967), the sintering rate varies at 3rd to 4th power of grain size in bulk diffusion and grain boundary mechanisms, therefore the sintering rate for finer grain size can be up to between 10- 60 times faster. In contrast, the mass transport rates rapidly slows down (lower activation energy for the solid state diffusion mechanism) at lower temperatures, which is compensated for by the faster sintering rate and higher product density achieved by the smaller grain size as illustrated in Figure 3.2.

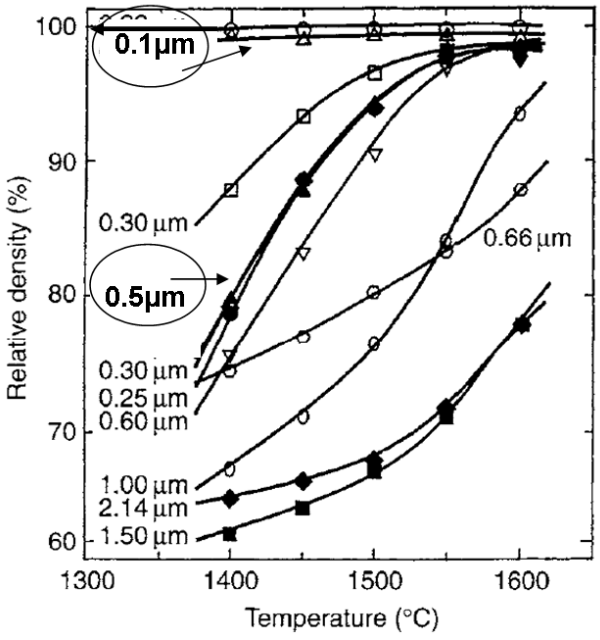

Figure 3.12: Effect of grain size on sintering rate and product density (Coble and Gupta 1967)

3.1.2.5 Particle size distribution

According to Reed (1995), particle size distribution is the main factor in the achievement of higher packing densities. Between 70 and 80 percent density can be achieved for a mono-deflocculated powder. A too broad particle size distribution system is however liable to develop extreme grain growth due to nuclei formation of the larger particles leading to negative property impacts such as low product density and the development of cracks (Kingery *et al* 1976). Although large particles are always present and are poorly identified by particle size analyzers (when their concentrations are below 1 percent), they can be detected by using the liquid immersion technique as explained in the previous section (see Figure 3.1 – Uematsu *et al*, 1995 and Uematsu 1996). Such large particles are either single crystals or aggregates consisting of fine grains.

Particle size distribution measurements stay illusive and are dependent on particle size analyzer type and operator input. Figure 3.3 illustrates the case where the mean particle size (d50) for the same sample varied between 0.4 to 0.9 micron in one type of analyser and even more when other analyser types were used.

The significance of a proper PSD has become widely recognised in recent years. A precise grading of the particle sizes enables one to make slip which is easily mixed and placed and also has the desired mechanical properties. Incorrect analyses can complicate the adjustment of the recipe where composite particle size distributions of the raw materials are used in obtaining desired PSD.

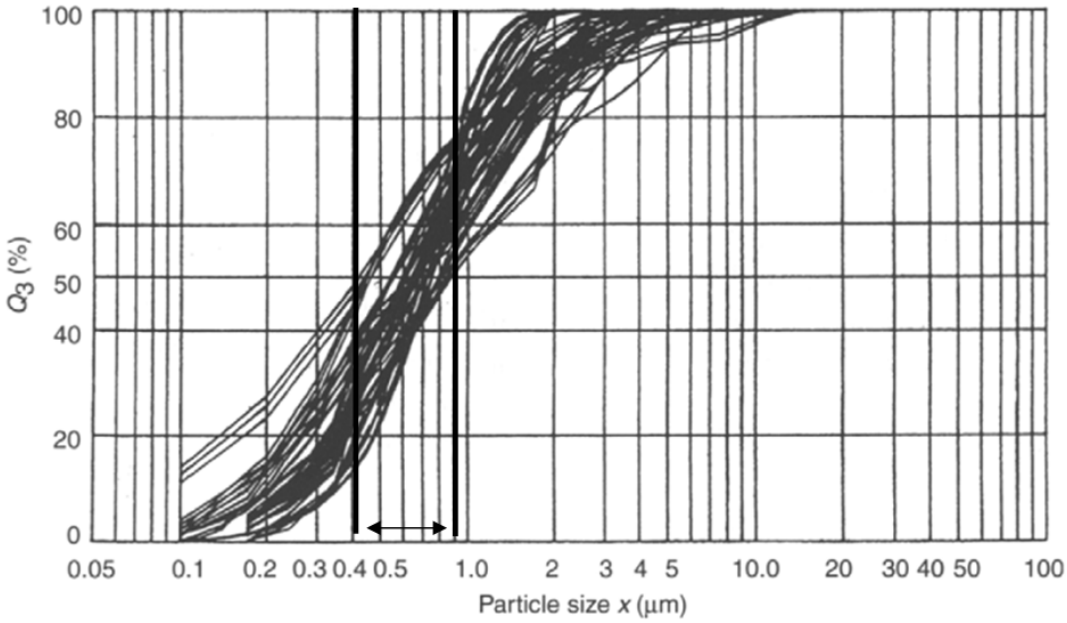

Figure 3.3: The same silicon carbide powder analysed by various laser diffraction type analysers (Uematsu et al 1995)

3.1.2.6 Grain shape

The packing structure of green compacts is highly affected by particle shape. Spherical grains nearly always give good packing density whereas it is impossible to obtain similar packing with platelet or needle shaped grains. This is well illustrated in Figure 3.4 where SEM images for starches are indicated. The forming method (extrusion) can orientate non spherical particles through shear stress resulting in anisotropic properties after sintering. This happens, when a non-uniform shear stress exits with movement away from the die wall (Reed 1995).

The shape of a particle (due to anisotropic property on forming) can also affect sintering and product density (Shui *et al* 2001).

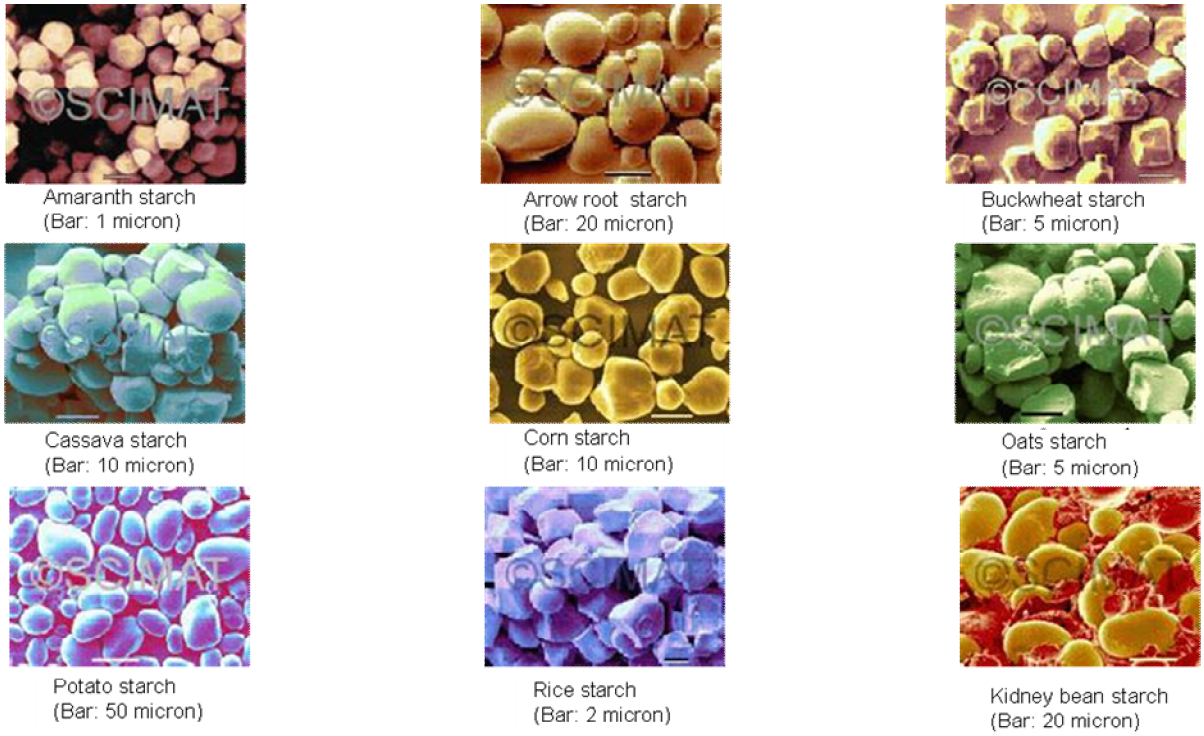

Figure 3.4: Particle shape and size of starches (Shui et al 2001)

3.1.2.7 Agglomerates

Agglomerates develop due to attraction (capillary forces, van der Waals forces, and electrostatic forces as discussed in Chapter 2) between particles (

Lange *et al*, 1983).

Addition of dispersants and mild mechanical forces (milling) can break down aggregates into primary particles (reversible process). If aggregates are not dealt with during the formation process it can have a negative effect on green-compact structure and therefore the micro structure of the end product, forming localized density gradients (

Lange *et al* 1983 and Zheng, and Reed 1989).

3.1.2.8 Aggregates

In contrast to agglomerates, aggregates form due to strong bonded particles that develop during the manufacturing process (sintering) of some raw materials. Such aggregates cannot simply be broken by gentle stirring or by adding dispersants; severe milling is required for breakdown and use in ceramics (Cutler 1978).

There is also a difficulty in identification of aggregates (coarse fraction) using particle size analysers in concentrations below 1 per cent as discussed earlier.

Grains formed from aggregates, with size equal to the outer diameter of the aggregate, have a negative effect on the production of ceramics as they tend to cause defects in the green body and in the sintered product. Aggregates tend to slow down the densification process during sintering. Aggregate identification and removal will help in the sintering process and help in final product quality (Rhodes and Wench 1973 and Dynys and Holloran 1984).

3.1.2.9 Material impact on slip rheology

For raw material selection we can distinguish between the following 2 slip grain sizes:

1. coarse grained slip (grains size up to 2 mm with some added fines)
2. fine grained slip (grain size range between 0.1 and 5 micron)

For both coarse and fine grained slips there are a number of effects that raw material fractions play in controlling the rheology of slips during production (Dinger 2002):

a) solids content of the slip
b) particle morphology
c) particle size distribution of the slip
d) flocculation of the slip
e) type and intensity of particle-to-particle collisions

3.1.2.10 Solids Content

In suspensions, the percentage of solids in the solution has an important effect on rheology. At low solids content suspension viscosity is similar to that of the liquid

viscosity. At higher solids content, the fractions control the slip viscosity. For every slip the limiting solids content depends on the particle size distribution and the ability of the particles to pack together.

3.1.2.11 Particle morphology

According to Dinger (2002) the fine, medium and coarse fractions result in opposing rheological effects during production and sintering.

The coarse fractions result in:

a) unwanted settling during casting
b) blockages
c) abrasion
d) coarse fractions have much lower specific surface area (SSA), which needs an increased firing temperature – resulting in coarser crystal grains, reduced firing density, and shrinkage

The finer fractions in contrast result in:

a) larger specific surface area of the fines during firing, increases the viscosity but produces a small crystal grain size that allows lower firing temperatures, increase fired density, and therefore increased ceramic strength
b) absorption and inter particulate forces in ultra-fines, which changes the rheology resulting in processing difficulties and lower density (green) and higher shrinkage[39] (fired)

The medium sized fraction, in contrast, results in the best compromise with relatively low firing temperature, medium fired shrinkage, and good fired density.

The sizes of particles affect the stability of suspensions. Clay or colloidal particles remain suspended within liquid whereas large particles settle out when suspensions are at rest or at low flow velocities (shear). Settling severity is therefore dependent

[39] shrinkage takes place as a result of water loss (evaporation) during drying and atomic diffusion and reduction in porosity during the sintering process thereby increasing the density (fired density)

on both size and flow velocity of the suspension.

The grain surface properties also impact on the rheology when higher solids content is used:

a) smooth surfaces (natural or due to organic/polymeric coatings) result in particles that slide easily past one another
b) rough surfaces increase particle-to-particle friction, resulting in increased suspension viscosities
c) electrostatic surface potentials can result in particles repelling one another (deflocculation) or attracting one another (flocculation). Both of these effects are dependent on mineral type, pH or chemical additives that alter surface properties.

An example of casting difficulties is given by Ozgur and San (2009) who used quartz, natural zeolite and lead borosilicate glass to slip cast ceramic filters. The limiting factors in their slip production were the relative concentration of the powders and the size ratio of powder (fine grains) and granules (coarse grains). After sintering, the pore walls were hydrophilic, due to the glassy coating. Large particle size differences, however, resulted in fines migration and cracking during drying and firing. Finer particles resulted in a loss of structural integrity. They found that the combination of a fraction (with a median particle size of 650 micron) with a fraction with grain size interval between 1.25 and 2.50 mm, worked best for the multilayer glassy ceramic filter. Pressure casting could also overcome the problem of fines migration.

3.1.2.12 Particle Size Distribution

Particles size distribution affects the rheology as well as determining the packing density. It forms a key ingredient in most slip, green and fired properties of ceramics. Funk and Dinger (1994) and Dinger (2002) looked for three packing requirements for improved flow when selecting raw material fractions:

1. grains had to be well sorted and well-rounded in shape

2. ability to fill the gaps (gap size) using fractions that could fit smaller sizes into the openings created by the next bigger grain size (use a ratio of 10:1)
3. making use of the natural particles size distribution of fractions and blend two to three fractions together.

A particle size distribution that packs well with a low porosity when packed will remain fluid even with high solids concentrations. Particle size distribution, flow and porosity are therefore directly related. The role of the carrier fluid (water) in this relationship has 2 functions:

1. saturates the pores, and
2. excess fluid separates the particles

When particle size distribution changes from batch to batch in suspensions where solids content is controlled, constant correction to either increase or decrease the particle separation (IPS) will be necessary to increase or decrease the viscosity (Dinger 2002).

According to Hüsken and Bouwers (2008) controlling solid particle packing is essential when working with granular materials with a mixture of size classes. Their work concurs with the results from the work on PSD done by Dinger (2002). Controlling particle packing allows the user to control behaviour and characteristics of the end product based on the granular PSD. The complexity of particle size, shape, surface texture results in a variation in packing for various systems (Hüsken and Bouwers 2008). Therefore improving the packing capability, by manipulating the particle size distribution (PSD) of a forming body or slip, allows one to achieve acceptable rheology and the desired solids content.

Denser packing leads to lower porosity resulting in less carrier fluid needed to initially fill the pores therefore providing more fluid for particle separation. This translates into larger inter-particle spacing (IPS- average distance between particles in suspension), lower viscosities and therefore better flow and less forming problems. Improved packing densities can result in lower green body moisture content, lower drying and firing shrinkage (Dinger 2001). These improvements are only possible when slip is well deflocculated, particles are not tied up by inter-particle attraction and gelation (Dinger 2001).

3.1.2.12.1 Particle packing

In each of the forming methods discussed earlier, whether a body will be extruded, plastically formed, pressed and slip cast, the solid particle packing potential (determined by the PSD) is the main parameter that influences all the other parameters.

Optimum packing for slip casting can be obtained by comparing the PSD of the mix with a continuous distribution packing model where particle size, shape, position and orientation of particles are recorded.

3.1.2.12.2 Packing models

As discussed in Chapter 2, the Furnas and Anderegg model (Furnas, Anderegg 1931), Andreassen and Andersen model (Andreassen and Andersen 1930) and the modified Dinger and Funk model (Dinger and Funk 1993) are models that have been used in the past for obtaining an optimum PSD for dense packing and improved flow properties. The Furnas and Anderegg model is difficult to use while the Andreassen model is easier (more empirical) and does not require a shape factor (particles should be of the same shape) but presumes infinitely small particles (which is impractical). Dinger and Funk model is a modification of the Andreassen model (presented in Chapter 2) making it more workable. Both models used for obtaining dense packing are shown below:

Andreassen model

$$CPFT = (d/D)^q \cdot 100$$

Dinger and Funk model (modified Andreassen model)

$$CPFT = [d^q - d_m^q)/(D^q - d_m^q)].100$$

where; CPFT: Cumulative per cent finer than

d: particle size (mm) as shown in Figure 3.5

d_m: minimum particle size (mm)

D: maximum particle size (mm)

q: distribution coefficient (q-value)

According to Dinger (2001) and Husken and Bouwers (2008) both the maximum and minimum particle size play an important role in determining the packing density. The finer particles (powders) help to optimise the grading of the entire mix (slip) by fitting in between the maximum particle size grains and contribute to the green strength of the demoulded items. The distribution coefficient, q, has an impact on the ratio between the maximum and minimum particle sizes. A coefficient with values larger than 0.5 results in coarse mixtures whereas values smaller than 0.25 results in mixtures high in fines.

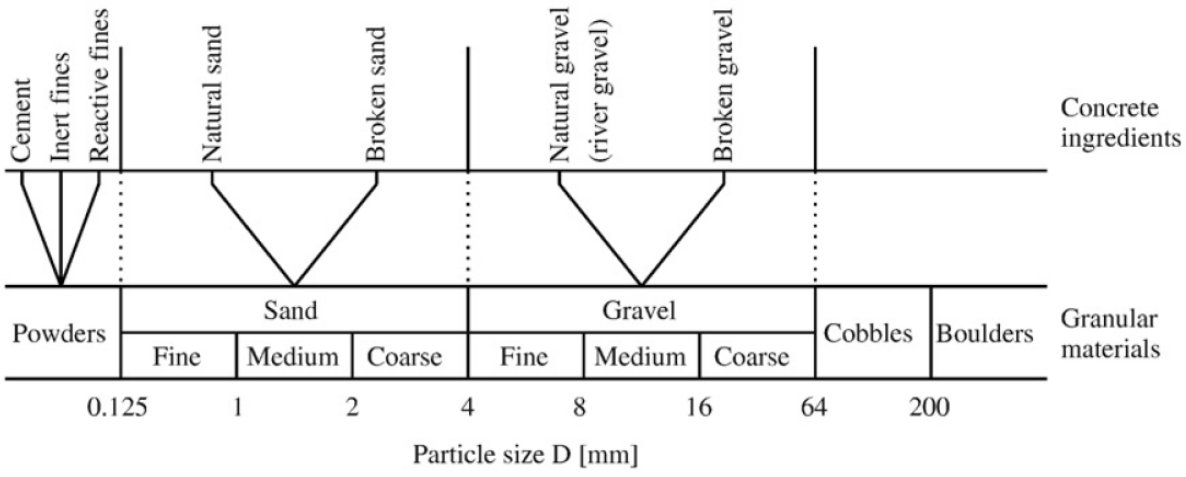

Figure 3.5: Particle sizes for granular packing (Husken and Bouwers 2008)

In summary Subbanna *et al* (2002) state that the conventional thought process of forming densely packed, uniformly distributed, fine pores, is necessary for slip (colloidal processing) casting or pressure casting.

Factors such as the firing cycle, shrinkage, residual porosity and microstructure do not only depend on the size distribution and reactivity of the raw materials but also on the physical properties of the green product. Packing is a function of size distribution and through size distribution manipulation, researchers have tried to obtain dense green compacts.

3.1.2.13 Slip flocculation

In slip processing, certain important interactions can change the inter particle forces, including attractive van der Waals, capillary and steric forces, and repulsive electric double layer and steric forces. Figure 3.6 is a schematic of the relationship between the slip, inter particle forces and slip flocculation.

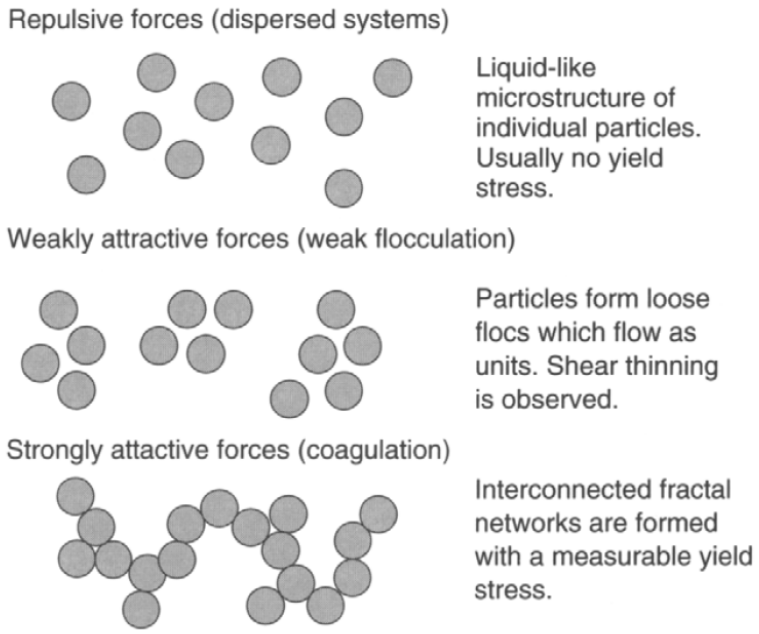

Figure 3.6: Slip microstructure, inter particle forces and suspension structure (Sigmund et al 2000)

Yang *et al* (2003) gives examples of low molecular weight organic chemicals dispersants with functional groups for anchoring on particle surfaces include acids such as citric acid. Other organic dispersants include polymers and poly-electrolytes. The particle size and the dispersing medium control the van der Waals forces.

Yang *et al* (2003) identify typical polar or dissociable functional groups for dispersant as hydroxyl (OH), carboxyl (COOH), sulfonate (SO_3), sulfate (OSO_3), ammonium (NH+), amino (NH_2), imino (NH), and poly-oxyethylene (CH_2 .CH_20) groups (Sigmund *et al*, 2000). Some of the main deflocculants are shown in Table

3.2.

Table 3.2: Common deflocculants used in ceramics (Naito et al, 2003 and Sigmund et al, 2000)

Low molecular weight	High molecular weight
Sodium borate	Poly(acrylic acid) (PAA)
Sodium carbonate	Poly(methacrylic acid) (PMAA)
Sodium pyrophosphate	Ammonium polyacrylate
Sodium silicate	Sodium polyacrylate
Citric acid	Polyisobutene
Ammonium citrate	Menhaden fish oil
Sodium citrate	Phosphate ester
Sodium tartrate	Sodium polysulfonate
Sodium succinate	
Glyceryl trioleate	

As discussed previously in Chapter 2, stabilisation of slip occurs through an electrostatic process by pH control (NaOH and HCl addition). Low pH (pH <5) results in positively charged particles and high pH (>9) particles are negatively charged. Like charges repel, and particles are therefore dispersed or stabilized. The degree of stabilization from the repulsive forces is dependent on the type of mechanism generated which normally originates from the electrical double layer overlap. By adjusting the pH to the isoelectric point of the slip particles will result in flocculation of the slip as a result of van der Waals forces (Silakate *et al* 2008). Normally, a slip is adjusted to the condition of "controlled flocculation" staying fluid, yet ensuring that the finer particles stay agglomerated and in suspension. Slips should therefore be less fluid than they could be because a totally deflocculated slip results in free movement of the particles resulting in segregation.

The fines migrate toward the mould surface resulting in changes in the particle size distribution which causes differential drying shrinkage of the wall resulting in drying cracks.

An example is given by Silakate *et al* (2008) where deflocculant as well as pH changes had a strong impact on both the particle surface charge and particle size of the slip. When making porous alumina filters using slip casting, they found that the flocculation increased particles size and slip viscosity through the mechanism of polymer bridging of the electrolyte on the surface of the particles. Their product had

an average pore size range of 0.3 to 0.4 micron after firing to 1500ºC.

Complications when using casting clays include the ageing properties of a clay body which will change according to the composition. The biggest problem is the usual time necessary for the clay to age in order to become stable just before casting. Other factors to consider included: poor filling (too long to fill moulds), flabby casts (soft casts – difficult to handle), brittle casts (hard casts – difficult to fettle), poor draining after casting, wreathing (unevenness on the slip side of casting), pinholes (air-holes below casting surface), cracking, casting spot (poor flow), and casting flash (discolouration on the side of the mould). To overcome some of the problems normally require minor adjustments in deflocculation and flocculation.

3.1.3 Additional raw materials

3.1.3.1 Pore-formers

Porous ceramics can be made through a number of methods such as using particle size distribution, the impregnated sponge method and the addition of pore former. In this study the pores for the porous ceramic were produced by burning out the pore former during the sintering process.

Chi (2004) identifies two types of formers, inorganic materials (NH_4HCO_3 and carbon powders) and organic materials (starch, polyimide, polyvinylidene chloride, cellulose, polyacrylonitrile, phenolic resin, microorganisms and yeast).

In order to obtain high porosity, large volumes of pore former have to be added to the ceramic phase. The decomposition of the binders and pore formers normally result in the development of large quantities of volatiles (gas) during the burn-out phase. Burn-out temperatures between 300-700 ° C should be maintained for achieving slower decomposition and good control of the debinding process (Lu and Lannutti, 2000).

Maintaining the burn-out temperature at this level reduces the risk of cracking in the green body. But the gas released during the burn-out phase (amount generated and temperature) also controls the forming of either closed pores or connected (open)

pores (Colombo, 2008).

3.1.3.2 Examples of pore-formers

The following authors provide examples of various organic and inorganic pore formers used in developing porous ceramics.

Yeast: Chi (2004) looked at the sintering behaviour of yeast as pore former in pressed SiC ceramics. To prevent segregation glycerol was used to slow down gravity segregation. Glycerol has high viscosity that binds the pores on yeast surface. The heating rate used was 60°C h^{-1} to a holding temperature of 900°C for yeast removal and then heating at a rate of 300°C h^{-1} with a 1 to 5h soak in air. A three step yeast decomposition (shown in thermo gravimetric analysis (TGA) graph, Figure 3.7) was established:

- normal drying up to 100°C
- step 1 from 140 to 200°C with little change in weight,
- step 2 from 200 to 900°C complete oxidation of yeast with volatile release resulting in fast weight loss and
- step 3 with temperature >900°C where no further weight loss occurred.

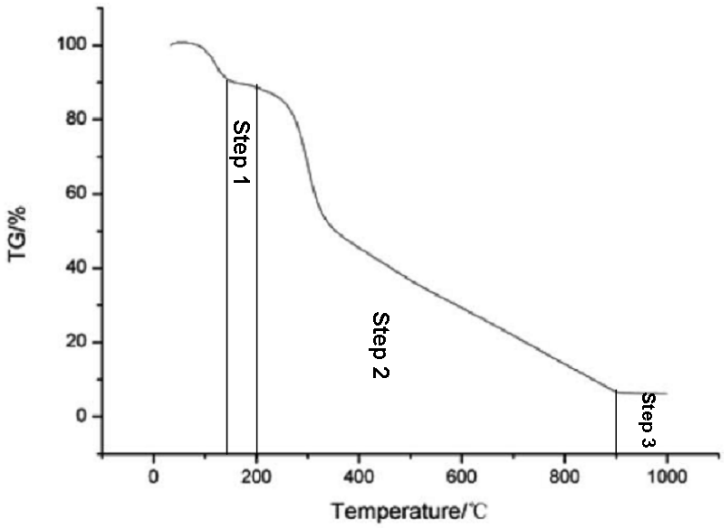

Figure 3.7: Thermo gravimetric (TGA) curve for yeast using a firing rate of 10°C h

Starch: Yin *et al* (2009) used starch as binder, consolidator and as organic pore former in preparing their porous ceramic. They confirmed that amylose causes gelling of starch slips. Starch can be added in volume fractions from 20 to 50 percent without resulting in critical defects.

From studies on the impact of starch on the gelling and flow properties of alumina slips, it was determined that albumin controlled the gel while starch allowed the viscosity of the slip to increase. With very high concentrations of starch, in an alumina system, hydraulic forces played a big role and viscosity was dominated by particle size distribution, solid loading and starch alumina ratio as shown in Figure 3.8. The starch impact on the slip rheology is clearer in the slip with increased alumina contents. The viscosities of 52 and 55 vol. % alumina slips showed sharp increases, with added starch exceeding 3.3 wt. %.

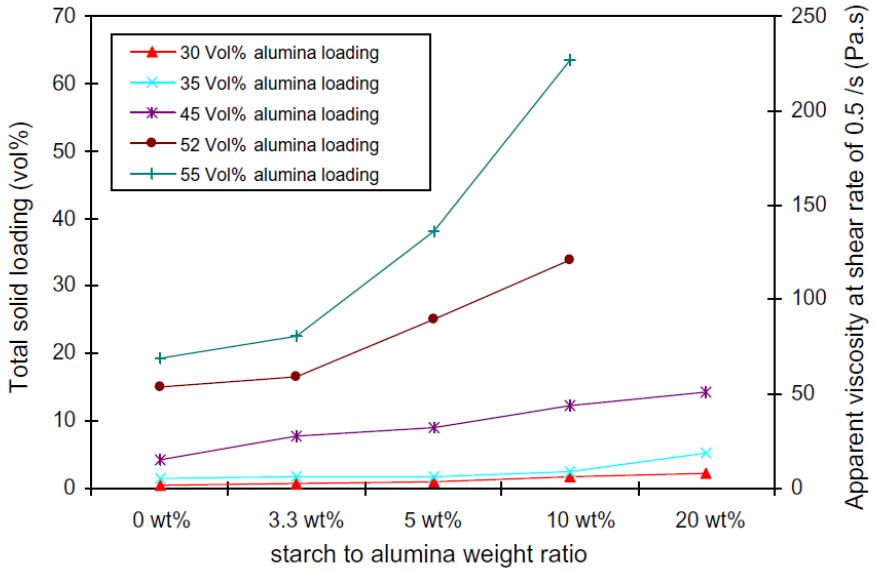

Figure 3.8: Impact of starch to alumina ratio on viscosity at a constant shear rate (Yin et al 2009)

Rice starch: Yeh and Li (1996) used a polarizing microscope, with a hot stage and image analyzer, to examine rice starch. A small change in granule size, between temperatures of 35 to 55°C, occurred with a more rapid size increase at 65°C. Finally, a 16 micron increase resulted at 65°C. The viscosity changes resulted from the increased volume fraction of swollen granules.

At low concentrations the particles are far enough apart to not affect the viscosity but at larger concentrations the interactions due to swelling became more accentuated, resulting in a higher viscosity.

Paraffin: Neirinck *et al* (2009) used paraffin as a pore former. This had the advantage of eliminating the burn-out phase of firing. They consolidated alumina powder, using a solution of paraffin in ethanol, onto a porous object using electrophoresis. By evaporating the paraffin prior to sintering, the time consuming first firing process (burn-out) was eliminated and large spherical pores 20 to 200 micron could be customised. By altering the emulsion composition, both open and close cell porosities could be obtained.

3.1.3.3 Coating

Coating of porous ceramic is an additional step added to augment ceramic filter by coating for improved reduction of viruses in drinking water. The coating can either result in sorption or the inactivation of viruses on the modified ceramic surfaces. In this study the porous ceramic filter was coated with a finely milled non-porous, lithium-alumino-silicate coating.

Masuda *et al* (1994) gives an example of coating an alumina ceramic with a thin, dense zeolite film on the outside of the filter. The zeolite's silica source was sodium silicate (Na_2SiO_3). They used a two-solution slip of sodium silicate and aluminates in a reactor to thinly coat a zeolite coating, hydro-thermally, on an alumina filter. The structure and composition were tested using the following methods: X-ray diffraction, nuclear magnetic resonance and electron probe microanalysis.

3.1.3.4 Activated carbon

Granular Activated Carbon (GAC) is a charcoal (various sources) treated with oxygen (steam) which creates millions of tiny pores in between carbon atoms. The large specific surface area of GAC provides an infinite number of chemical bonding sites. Chemicals (organic) in water that passes through the GAC are absorbed to the activated carbon surface and become trapped.

The high surface area (texture) and porous nature of the GAC is clearly visible from the SEM images illustrated in Figure 3.9. Haarhof and Olivier (2002) made the following conclusions for the use of granular activated carbon GAC) in water purification during their study of three South African water treatment plants:

- absorption of coal based activated carbon was much better than wood based activated carbon
- organic constituents in water differed substantially between each site
- high levels of organics in water due to indirect re-use as well as extremely naturally high humic and fulvic acid in coastal areas
- limited use of GAC in SA water plants, only used as an emergency measure

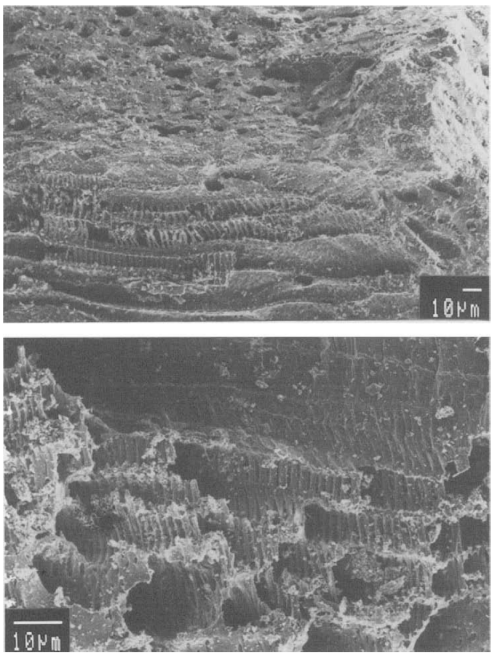

Figure 3.9: SEM images of GAC prepared from coconut shells (Haarhof and Olivier 2002)

Using a ceramic water filter in combination with GAC enables suspended matter to be removed first by the ceramic and before allowing the clean water to pass through the GAC, thereby effectively removing organic material (humus, algae, fungi), highly concentrated chemicals (chlorine, trihalomethanes, fluoride) as well as microscopic contaminants such as pesticides and herbicides (Water Filter Info, 2012) from the contaminated water.

3.2 Material Preparation

3.2.1 Grinding (Milling) of ceramic raw materials

The physical process of milling produces de-agglomeration and a specific particle size distribution in powders. The milling process results from crushing, impact and shear between two hard surfaces to produce the desired particle size. The work necessary to fracture a solid particle results from the increased surface area of the powder which releases energy. Agglomerates result from mining, fusion, and sintering and are normally milled and screened into various fraction sizes by the supplier. Even after the initial milling by the supplier the powders may need further milling to achieve specific particle size requirements.

Definition: According to Zaspalis *et al* (2003) grinding is the mechanical breakdown of solid grains into fine powders. Milling of ceramic materials provides powder with a certain particles size distribution and no agglomerates. The mechanical breakdown includes the following physical processes:

- impact
- shear
- crushing

In the milling process, energy is released in the form of heat as a result of fracturing and friction by mill equipment and the creation of new surface areas. The largest contribution of heat comes from energy released during the creation of new surface area.

Through the process of mining and beneficiation, lumpy materials are obtained which have to be crushed, milled and screened by the supplier into different sized fractions. The milling is normally done as a dry milling process as this eliminates an additional drying process and the associated hard lumps (agglomerates) that form during drying. Material requirements then dictate whether further milling (usually wet ball milling) is required by the user to obtain optimum particle size and distribution.

Yokoyama, *et al* (1987) furthermore classify milling (grinding) into two categories (Figure 3.10):

a) volume grinding through impact: breaking larger agglomerates into smaller agglomerates

b) surface grinding by frictional forces: fines are formed from grain-to-grain surfaces more effective in delivering sub-micron powders

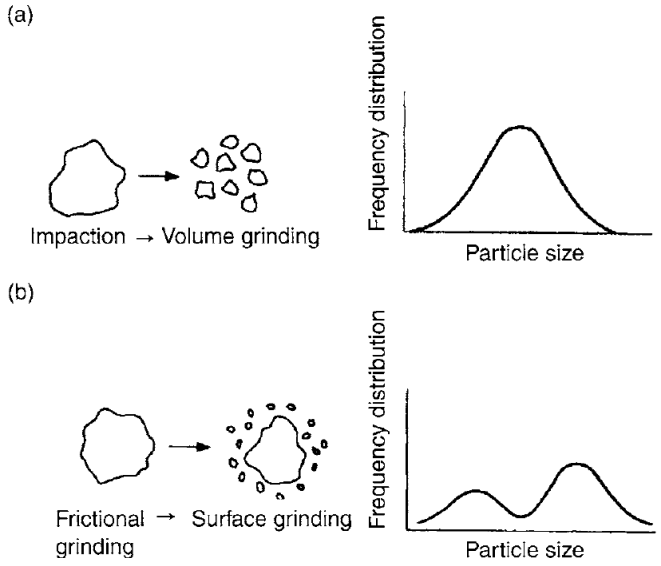

Figure 3.10: Mechanism of grinding materials- a) impact- and b) friction grinding (Ohmori 2003)

Naito *et al* (2003) lists some of the factors that have to be taken in consideration in grinding:

a) choice of production of submicron powders in dry and wet form: volume grinding and surface grinding (fine grains due to frictional forces between surfaces of the particles) see Yokoyama, *et al* (1987) above

b) types of grinding aids for milling improvements (the aids are added to increase the surface area- grinding surfaces)

c) cake formation (where dead spots form in the mill where no particle reduction is taking place)

d) quality control of ground materials (important to produce raw materials with consistent properties)

Dry and wet milling: The most common type of milling is done in a ball mill using grinding media of appropriate size. Ball milling can be either done dry, for pressing, or wet, with water added for slip preparation. Dry milling in contrast to wet milling is less effective in smaller mills with less energy to break apart the grains.

There exists a lower particle size limit that will not change even with increased dry grinding times (Yokoyama *et al* 1988). This smallest particle size is known as the equilibrium particle size (Jimbo 1992). The equilibrium particle size limitation can grouped into the following two categories:

a) Equipment issues: particle evasion from the grinding zone and coating of grinding media resulting in cushioning of the grains (Rumpf 1959).

b) Grain size issues: Limitation in brittleness below 1 micron (Schoenert and Steier 1971) and agglomeration of newly produced fines.

Dry milling: According to Kingery *et al* (1976), dry milling is a great tool for avoiding an extra drying step (wet milling) and resultant agglomerate formation (during drying). Dry milled raw materials are normally used in pressing. Dry milling in a ball mill with grinding media can become ineffective if certain precautions are not taken. These precautions include prevention of the caking of dry powder on the sides of the mill, which prevents further reduction in grain size.

Wet milling: According to King (2002), wet milling is more frequently applied than dry milling for slip preparation.

Grinding aids: Grinding aids materials can be in a solid, liquid or gas phases. The following mechanisms can be used to explain the function of grinding aids (Naito and Jimbo 1985):

a) Strength reduction of the solids using additives prior to milling to reduce aggregate or agglomerate bond strength

b) Mechanical properties control of the raw material:

   i. Wet grinding: liquids are added as grinding aids to deflocculate materials and reduce viscosity of the slip in the mills.

   ii. Dry grinding: a variety of aids are added to both disperse (fine powder) and lubricate (liquid) the materials.

Cake forming: According to Naito (2003), both types of milling (dry or wet) can result in serious under milling (not achieving the pre-determined PSD) of raw materials. In dry milling material, caking forms in the dead corners of the mill (outside the grinding media contact zone), which limits further size reduction. Only through a complete discharge of the mill (both grinding media and milled material), and the scraping of the material from the corners can the problem be reduced. In wet milling, dead spots normally occur at the lid end of the mill, which results in un-milled slip contaminating the rest of the slip during discharge.

Ground powder quality control: It is important to accurately determine the milled material particle size distribution. The size range between 5 – 95 percent can determined without problems, but determination outside this range proves to be difficult (alternative methods are required for accurately identifying low concentration of coarse grains) and time consuming (dispersing, and slow settlement – fines). Figure 3.11 shows the effect that factors such as grinding media size and milling time have on a + 45micron starting powder. From the PSD seems like there were no particles in excess of 20 micron after 4h of milling but from Figure 3.12 it is clear that a small quantity of (+45 micron) coarse particles were still present even after milling for 24 hours (Naito *et al* 1998).

Combining grinding media sizes, grinding aids, regular cleaning (cake forming)) and ball mill design (reduce the number of dead spots) could therefore give better result in achieving the necessary amount of fines and reducing the coarse particles present.

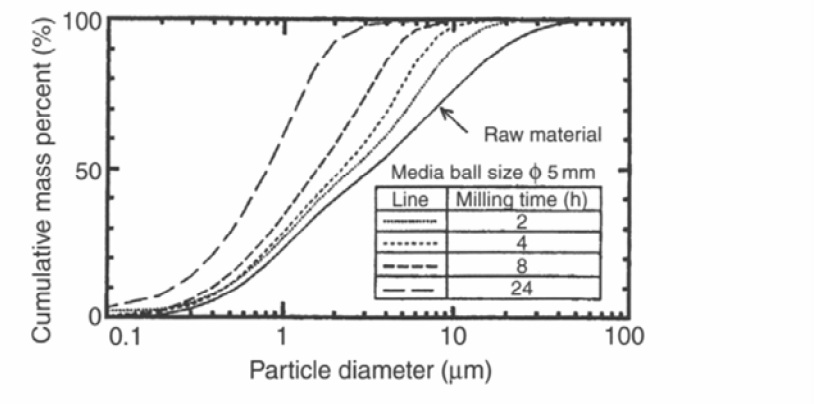

Figure 3.11: Impact of grinding media and milling time on particle size of a +45 micron starting material (Naito et al 1998)

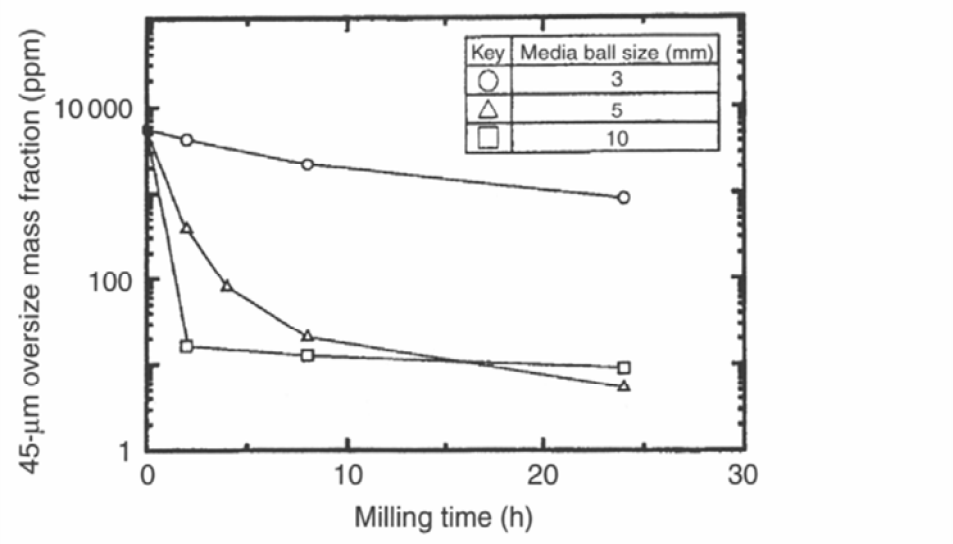

Figure 3.12: Impact of milling time, ball size and milling time on particles size (Naito et al 1998)

Furthermore contamination due to wear in the lining, grinding media, and previous milling waste in the milled powders affect the quality of the final product and should therefore be minimized.

Milling equipment: Table 3.3 identifies the features of some of the existing grinding equipment available from which a large range of particle sizes can be obtained (Naito *et al* 1998). The table summarises the different types and features of grinding equipment available today.

Table 3.3: Classification and features of milling equipment (Naito, 2003)

Classification	Types of machines	Examples
Primary crusher	Compressive crusher	Jaw crusher
		Cone crusher
	Shearing crusher	Cutter mill
	Impact crusher	Hammer crusher
Secondary crusher	Roller mill	Roll crusher
		Edge runner mill
		Cage mill
	Hammering type	Stamp mill
	High-speed impact mill	Hammer mill
		Pin mill
		Disc mill
Fine grinding mill		Centrifugal classifying type mill
	Roller mill	Roller mill
		High-pressure roller mill
	Frictional grinding mill	Angmill
	Autogeneous mill	Aerofall mill
	Ball mill	Tumbling ball mill
		Vibration ball mill
		Planetary ball mill
		CF mill
		UF mill
	Agitating ball mill	Tower mill
		Mixing vessel type
		Tube type
		Annular type
		Annular agitating type
	Jet mill	Jet mill
		Liquid jet mill
	Wet grinding mill	Colloid mill
	Others	Mortar
		Stone mill

Summary: Particle size and particles size distribution of raw materials obtained by milling are critical factors for both the drying and firing stages of ceramics. The fine particle fraction is also critical to the forming processes since colloidal suspensions (slip); plastic mixes (extrusion) and dry pressing all depend on the small particle flow or particles remaining in suspension. In addition to particle size and particle size distribution, milling also assists in intimately mixing the material and for obtaining uniformity of properties during the forming process.

3.2.2 Small Scale Milling Equipment

Small wet mills (jar mills) are cylindrical in shape with a capacity of about 10 to 20 liter and have been used in preparing slip in this project. Mill racks, rather than an individual drive, provide the rotation propulsion for small jar mills (Figure 3.113). Steel is normally used for manufacturing these mills because of its strength and low price. Mills are normally lined with polyurethane to prevent contamination (wear from the lining) from the steel lining. The mill consists of a cylinder, lid (lined with polyurethane) and a clamping system to keep lid in position. The mill is half filled with grinding media that together with the rotation propulsion is responsible for milling the material. The type of grinding media is normally selected to prevent contamination and sized to provide maximum impact energy for fracturing the particles. High alumina (> 90 percent Al_2O_3) is the most common choice for grinding media.

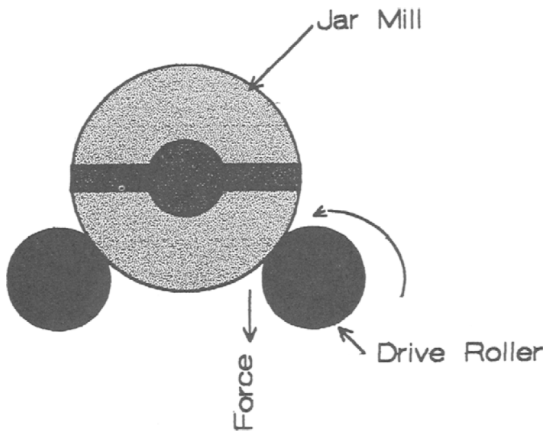

Figure 3.113: Mill rack and motion (King 2002)

Factors affecting the milling rate of the raw material include the grinding media shape and size, grinding media specific gravity, grinding media type and mill type. Smaller media are more efficient (due to the greater contact area) than larger media but lack the energy (by mass) of larger media (Table 3.4 and Figure 3.12).

Table 3.4: Mill and Media requirements and advantages (King 2002)

Media/Mill Property	Advantage/Requirement			
	1	2	3	4
SG	milling energy	determines media mass		
Size	Small: more contact area	Large: more energy due to mass	Select smallest size sufficient energy to grind	
Shape	Maximum contact area			
Type	Same composition as batch	Minimum wear (less contamination) makes TZP & Alumina most common		
Milling rate & Critical speed	gravity force > centrifugal force	60 – 75% critical speed		
Wet milling	Slip preparation	breakdown agglomerates	less dead spots	
Dry milling	No drying step	no dried lumps		
Mill rack	variable speed	roller with downward force vector on	adjustable idler roller	rubber lined roller

The grinding media SG determine the energy that is available for crushing and grinding. The higher the ball density (mass) the more energy can be transferred to the raw material. Table 3.5 below presents some of the most commonly used grinding media SGs.

Table 3.5: SG of important grinding media (King 2002)

Media Material Type	Ball SG g/cm^3
WC/Co (Tungsten carbide)	13.0- 15.0
Iron	7.8
TZP (Tetragonal Zirconia)	+ 6.2
Zircon	4.7
Alumina	3.98
Silicon Carbide/Silicon Nitride	3.21/3.18 +2.7
Porcelain	+ 2.62

Dinger (2002) established that smaller lab mills (jar) have to be more than half filled with grinding media to be effective. Overfilling, leads to increased media wear (chip and break) and insufficient energy for the fracturing process. In contrast, under filling results in media-to-media contact, this chips and breaks the grinding media.

3.2.3 Product Drying

3.2.3.1 Drying steps

In Chapter 2 it was noted that for each of the shaping processes the addition of water was required. In the drying step, the water is removed by careful control, especially for slip casting where a higher liquid content is used. In the dry pressing process the drying difficulties are minimised, which is a major advantage of using this method.

According to Puyate (2009), for firing to succeed, it requires a thorough drying process. Drying typically evolves through a series of processes:

- continuous water film on the surface
- evaporation of this film brings the grains closer together resulting in minor shrinkage which requires controlled drying to prevent additional warping and cracking
- diffusion of water through the pore matrix
- particle-to-particle contact allows for rapid drying until all absorbed water is diffused and evaporated allowing the product to be fired

Yang *et al* (2003) point out the importance of reducing the non-uniform drying stresses during the drying process in order to prevent cracks, differential deformation and density gradients in green structures. These differential drying stresses are related to pressure gradients in the pore liquid and gas phase in the unsaturated pores as well as to temperature gradients resulting in differential thermal expansion. These pressure and temperature distributions depend on transport processes such as diffusion of water molecules, water flow and heat conduction, whereas the particle network's inter-particle forces, frictional forces and particle visco-elastic properties result in particle repositioning and deformation due to drying stresses.

The pressure change between the liquid-vapour interfaces of a cylindrical pore is given as (Puyate 2009):

$$\Delta P = \gamma_{LV}/a$$

Where γLV, is the specific energy from the liquid-vapour interfaces and a, the radius of a cylindrical capillary.

This is derived from the Laplace equation with R_1 and R_2 as the curved radii of the liquid-vapour contact:

$$\Delta P = \gamma_{LV}\left(\frac{1}{R_1} + \frac{1}{R_2}\right)$$

The capillary pressure results in liquid being forced from inside the green body to the outside as the body shrinks. This volume change is equal to the volume of water evaporated from the surface. This shrinkage of the particle framework forms part of the first drying stage. The more shrinkage occurs, the stiffer the body becomes, resulting in maximum capillary pressure which could eventually lead to cracking of the green body during this stage of drying. Furthermore localised capillary gradients lead to localised shrinkage. These pressure gradients occur at the drying front where liquid tension is higher than in the saturated pores of the body.

From expression of the capillary pressure, P_c, for a circular capillary with radius, a, and θ is the contact angle, it can be shown that the magnitude depends on the pore size (a) expressed as follows:

$$P_C = -\frac{2(\gamma_{SV} - \gamma_{SL})}{a} = -\frac{2\gamma_{LV}\cos(\theta)}{a}$$

The equation shows that the capillary pressure is determined by the pore size. Smaller raw material particle size, green body thickness and drying rate will therefore all lead to an increased development of non-uniform drying stresses (related to pressure gradients in the pore liquid and in the vapor phase of unsaturated pore space, and to temperature gradients that cause differential thermal expansion, Yang *et al* 2003).

Figure 3.14 shows the position of water in a porous body during the various drying stages. During the CRP (Constant Rate Period[40] or Leather-hard Period) particle-particle compressive strength is larger than the capillary pressure. The drying rate is now controlled by external conditions and no further contraction occurs and the larger pores drain and fluid is forced into the smaller pores due to higher capillary suction and become partially filled with liquid. The body now enters the Funicular[41] or Falling Rate Period (FRP) with a lower weight loss rate compared with CRP and where a drying front is gradually moving into the interior (evaporation takes place from the fluid menisci).

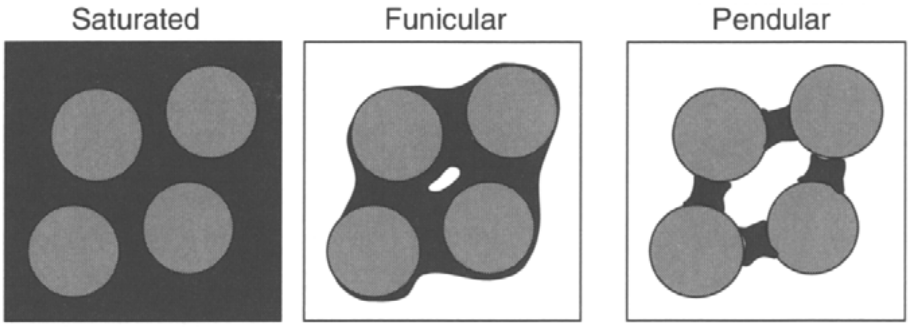

Figure 3.14: Model of solvent distribution in a porous body (Yang et al 2003)

Liquid movement is initially driven by evaporation from exterior surface which creates a pressure gradient toward outside surface described by Darcy's Law. At this stage vapour diffusion through the partially drained pores is minimal:

[40] period during which the green body mass reaches or decreases constantly

[41] continuous liquid phase distribution along pore walls

$$J = -\frac{D}{\eta}\nabla P$$

With *J,* the pressure driven fluid flux, D, as the porous structure permeability and, η, as the liquid viscosity. Higher pressure gradients are needed with lower permeabilities and higher flow resistance (viscosity) for draining the pores.

According to Yang *et al* (2003) the evaporation (outside surface) results in a lower temperature (endothermic) relative to the temperature inside the pores. This result in a surface tension decrease (temperature dependent) and vapour pressure increase on the surface. Both factors help to move the liquid from the inside to the surface. The drying front movement has an inverse relationship to time ($t^{-1/2}$).

At the stage that the pressure gradient is not sufficient to move the water (long distance between drying front and surface), the transition between funicular to pendular state[42] takes place with isolated fluid pockets. The dry pores that appear are not connected to the water film of the neighbouring pores (Figure 3.14). The water phase change in the pores (evaporation- vapour phase diffusion) now determines the rate of movement. Fick's Law relates the concentration gradient, *C,* to the diffusive flux, J_D. With D_C as a diffusive constant (Puyate 2009):

$$J_D = -D_C \nabla C$$

It is now clear that both heat and mass exchange processes work together to determine the kinetics for the total drying process. The control of these two mechanisms is important in controlling drying stresses, cracking and non-uniform deformation of the green body during drying.

Table 3.6 summarises the result, cause and equations necessary for understanding and controlling the various drying steps outlined above.

[42] state when insufficient water is left for maintaining a continuous film in the **pores**

Table 3.6: Drying steps: causes and equations (Summarised from the work of Yang et al 2003 and Puyate 2009)

Step	Result	Cause	Equation
Saturated	stresses due to local variations in water content; warping & cracks	independent of water concentration- continuous water film at surface; slow drying rate, temperature & pressure ▼develop- depends on water diffusion, water flow & heat conduction	Laplace Eq.: $\Delta P = \gamma_{LV}\left(\frac{1}{R_1}+\frac{1}{R_2}\right)$
Funicular	shrinkage until particle contact is made; volume change equals volume of evaporated water; maximum pressure capillary	particle contact free from water; more rapid drying rate	$P_C = -\frac{2(\gamma_{SV}-\gamma_{SL})}{a} = -\frac{2\gamma_{LV}\cos(\theta)}{a}$
Leather hard Point/Critical Point	pores partially drained, no further shrinkage	compressive strength > capillary pressure	Darcy's Law: $J = -\frac{D}{\eta}\nabla P$
Falling rate period	drying front moves into green body at rate $1/\sqrt{t}$	rate of weight loss decreases compared to CRP; evaporation at surface by water flow	
Pendular State	pressure▼ for water flow not enough to balance evaporation at surface	drained pores not connected by liquid film therefore liquid moves as vapour becomes the rate determining step	Fick's Law $J_D = -D_C\nabla C$

Units: R_1& R_2 radii of curved liquid-vapour interface; a- capillary radius; D- permeability of pores; η- liquid viscosity; J_D- diffusive flux & D_C- diffusive coefficient; ▼C- concentration gradient

3.2.3.2 Green body strength

It is important to note that green body strength should be sufficient to prevent cracking from taking place during the drying and subsequent handling processes. The microstructures that develop during this stage will continue through the firing and are therefore more likely to become the start of flaws during firing. It must however be remembered that pores are actually the main cause for the reduced fracture strength of the final product.

Kingery *et al* (1976) agrees with the notion that shrinkage occurs due to removal of the water film between the particles in the green body. However the film thickness is determined by the particle size, with the result that smaller particle sizes increase the number of films and therefore results in higher shrinkage, subsequent warping and reduction in green body strength. Apart from particle size and particles size distribution, proper mixing will ensure uniform properties within a green body, also helping with the subsequent reaction of the particles during the firing process.

King (2002) warns that permeability allows the evaporating water to escape from inside the green body during drying. The lower the permeability (finer particles) the higher the internal pressure build-up resulting in cracking and warping. Decreasing the drying temperature to 60°C reduces this problem. For coarse grained green bodies with a higher permeability, the final drying stage can be completed during the initial firing stage. Proper air flow in the drier, for the removal of the water vapor from the drier (open vents), is important.

As discussed earlier, Dinger (2002) emphasizes the importance of modifying the inter-particle space (IPS) in different production batches. This requires the particle size distribution of the raw material to be regularly monitored and adjustments to be made using slight changes in mixing recipes instead of chemicals to modify the changes. By keeping the IPS (particle size distribution of the mixture is kept constant) constant, instead of making unnecessary additions, the drying properties of the different production batches can be kept constant. Chemical additions, however, can result in change in the flocculated/de-flocculated rheology of the suspensions, resulting in changes in the drying rates.

3.2.3.3 Drying Conditions

King (2002) and Kingery *et al* (1976) describe what happens when a green body is being dried as well as actions to be taken during the drying process. Some of the points mentioned by King (2002) and Kingery *et al* (1976) include:

a) Particle packing (IPS and PSD) will determine the amount of shrinkage (most parts will shrink when dried)

b) Shrinkage starts at the outside and because of the resistance from the inside of the body, cracking may develop

c) A good drying program should ensure that tensile strength of the body is not exceeded by the differential shrinkage (surface and interior link)

d) Body permeability will determine the drying rate with enough allowance for the water vapour to diffuse to the outside (so preventing the body from explosive popping especially with fine grained, dense bodies – volume change ratio from $H_2O_{(liquid)}$: $H_2O_{(gas)}$ is 1: 1244).

3.2.3.4 Setting

During drying it is important not to set the wet body on an impervious surface as this creates a non-uniform drying rate, resulting in rejects due to distortion and cracking. It is best to place the drying body on a welded mesh surface, allowing air to reach all surfaces of the body and to regularly rotate it to expose all surfaces (King, 2002 and personal experience).

3.2.4 Types of Drying

3.2.4.1 Air Drying

Body parts are set outside in suitable area and on an open mesh or on porous material. Parts can dry slowly under ambient conditions. Parts should also be protected from rain and covered from dust (Kingery *et al* 1976).

3.2.4.2 Laboratory Oven Drying

The standard laboratory oven should have ventilation, correct shelving and temperature control and temperature indicator. According to King (2002) it helps to place thermocouples at various levels to identify cool spots that can mostly be resolved using proper air circulation (air blower and air vents). It also helps to have the heating elements at the bottom for hot air to then rise through the stack.

3.2.4.3 Humidity Driers

Humidity driers should have humidity and temperature controls to better maximize drying. Humidity can be slowly lowered as the parts dry and, together with temperature control, these safeguard parts that warp or crack easily.

3.3 Firing

After drying, the ceramic body is fired to temperatures ranging between 700 to 1800°C depending on the composition and properties required. The heat treatment step is required for the shaped powder to be transformed or sintered into a dense solid final ceramic product (Kingery and Francois 1967).

In sintering one has to understand how production variables (particle size, particles size distribution, particle packing, temperature and firing atmosphere) influence the micro-structure formation. This section outlines the basic principles of sintering as applied to the production of ceramic filters.

3.3.1 Burn-out

As mentioned previously for pore formers, large concentrations of organic additives have to be burned out at lower temperatures, prior to final firing, to reduce the violent discharge of volatiles. Uncontrollable volumes of volatiles lead to an internal stress gradient that exceeds green body strength, resulting in cracked product (Lu and Lannutti 2000).

Slowing down the burn-out rate, lead to improved control during this phase. Ring (1996) recommends keeping the burn-out temperature at levels where the partial pressure of the volatiles is kept below 1 atm (atmospheric pressure). Tensile stresses develop at the surface when the pressure inside the pores exceeds the surface pressure at higher temperatures. Thompson and Harmer (1993) provide the alternative of increasing the surrounding pressure to thereby reduce the volatile partial pressure.

Pathways for the breakdown of organic components depend on a number of factors, including (Yang *et al* 2003):

- chemical structure of the organic polymers
- burn-out temperatures as well as rate and length of temperature steps
- solid and gas phase composition
- reaction products (liquid or gas)
- cause of the polymer breakdown (thermal activation or oxidation)
- reaction of polymer breakdown (endo- and exothermic reactions)
- green body pore size distribution and pore size

According to Ring (1996), the polymer elimination starts by chain separation caused either by thermal or oxidation degradation. This is followed by sublimation of the now lower molecular weight section of the separated chain. The slow diffusive movement of oxygen through the pores usually becomes the rate determining step. Oxygen levels in the pores can be enhanced through the presence of metallic oxides in the green body composition. It is important to note that the low molecular weight products volatilize instead of remaining as solid carbon in the product after burn-out. Residual carbon can only be removed in an oxidising atmosphere with temperatures in excess of 700°C (Yang *et al* 2003).

The initial stage (loss of volatiles: temperature between 200- 300°C) must be controlled (slow firing rate) for the pyrolising[43] (carbonisation) of the pore former (German 1996). This will decrease stresses and flaws in the ceramic body during the latter sintering process. Air intake into the kiln has to be minimised during this stage for the proper development of the carbon skeleton. Controlled (rate and air intake) burn-out of the carbon framework can then proceed with a temperature increase to 600°C (Chi 2004; Almeida 2009).

3.3.2 Final firing (sintering)

After the burn-out stage, the body is ready for the final firing process. In this stage the ware is fired in an oxidizing atmosphere to the final temperature of between 950°C and 1250°C. This is the stage where the oxidizing atmosphere drives off the carbon framework, leading to a highly connected, highly porous ceramic product. The temperature depends on the composition and final properties that will be required.

It is the rise in temperature that makes the atoms more mobile in the solid state for grain growth, chemical reactions, and sintering to proceed – allowing the forces of surface tension to strengthen the ware and lower the porosity. Dwell[44] at high temperature can lead to changes in porosity unless it is controlled (Kingery *et al* 1976).

[43] decomposition of organic material at high temperatures under reducing conditions

[44] holding temperature

Composition and phase changes of the constituents during sintering will determine the four sintering categories that develop during heat treatment (Evans and De Jonge 1991; Rahaman 1995; German (1996) :

a) Solid state: heating the shaped green body to 50-90 percent of the body melting point, but without the presence of liquid where atomic diffusion joins the grains and reduces the porosity.

b) Liquid phase: sintering temperature results in a liquid of small volume (relative to the volume of the solid material). The liquid does not fill the pores and is therefore insufficient to achieve full density. This category forms the basis of industrial ceramic production.

c) Vitrification[45]: sintering temperature resulting in a volume one quarter smaller than the original. Product density is achieved through liquid formation, diffusion into the openings which crystallises (vitrifies) from cooling.

d) Viscous: where a mass of glass grains are heated to their softening point (or above) and densification develops through viscous flow forced by the surface tension.

e) Another category called pressure sintering can be applied when product density cannot be achieved through the other categories (conventional sintering). Pressure is applied during heating (example: hot isostatic pressing or hot pressing)

Only solid state vitrification which is more applicable to filter production will be further explained.

3.3.3 Solid State Sintering

The main driving force for the sintering of a product is the lowering of free surface energy as a result of the removal of internal surface area, from the pores. This process is small (± 100J/mol for grains with starting diameter of 1 micron) in comparison to other chemical reactions.

[45] process of changing or making raw material into a glass or a glassy substance through heat fusion

Sintering proceeds at a moderate rate at reasonable temperatures because of the short transport distances (grain diameter distance) required.

According to Rahaman (2003), it is the roundness of the grain surface and the specific energy of the grain that result in stress in the atoms just below the surface. For curved surfaces, the two main grain curvatures of r_1, r_2 and the stress, φ, is obtained from the Young and Laplace equation:

$$\sigma = \gamma_{sv}\left(\frac{1}{r_1} + \frac{1}{r_2}\right) \quad (1)$$

With, γ_{sv}, as the specific surface energy. Matter diffusion is driven by the diffusion potential, μ, which is determined by setting the mechanical work performed by the stress equal to the thermodynamic work required for the lowered free surface energy:

$$\mu = \sigma\Omega \quad (2)$$

Where Ω is the molecular volume. For polycrystalline ceramics, μ, is more complicated when the pores are in contact with particle boundaries (De Jonge and Rahaman 1988). Raj (1988) gives an equation, in the final firing stage, for spherical pores:

$$\mu = \Omega\left(\frac{2\gamma_{gb}}{G} + \frac{2\gamma_{sv}}{r}\right) \quad (3),$$

With, γ_{gb}, as the surface energy of the particle boundary, G, particle diameter, and, r, the pore radius. From equation 3, it is clear that the diffusion potential, μ, consists of the pores and boundary energy contributions.

This concept can be further developed (De Jonge and Rahaman 1988) by relating diffusion potential, μ, to an external stress, E, with similar impact on sintering as the rounded pore and particle boundaries. This stress provides a basis from which experiments for the measurement of sintering stress can be devised.

3.3.4 Sintering Stages

The initial discrete (unbonded, individual grains) grain structure (micro-structure) of a body changes constantly during sintering (De Jonge and Rahaman 2003). The micro-structural changes can be divided into three stages:

a) Initial stage: as a result of atomic mobility, concave necks form between individual grains (necking), resulting in ± 5 percent linear shrinkage (depending on grain growth)

b) Middle stage: the necking in stage one develops into a continuous framework of solid grains and cylindrical type pores. This stage contains most of the densification (linear shrinkage) and is valid up to the stage where the pre-fired body porosity is reduced to between 5 to 10 percent. Grain growth (agglomeration) becomes important.

c) Final stage: the pore channels develop into isolated pores and grain growth becomes more important, making it difficult to remove the remainder of the original (pre-fired) porosity and to therefore obtain theoretical constituent density.

3.3.5 Mechanism of sintering

According to De Jonge and Rahaman (2003) and Gordon (1973) crystalline raw material sintering takes place as a result of a number of atomic diffusion (transport) mechanisms as indicated in Figure 3.15:

1. surface diffusion
2. lattice diffusion from the surface
3. vapour diffusion
4. diffusion from the grain boundaries
5. grain boundary lattice diffusion
6. plastic flow

Gordon (1973) shows the sintering diffusion transport paths for two grains in Figure 3.15. Note that surface and lattice diffusion as well as vapour transport from the particle surface to the neck result in zero densification during the processes of neck growth and grain coarsening. It is however from the combined grain boundary and framework transport (between grain boundary to the neck), that most of the increase in density occurs.

It is from the grain boundary to neck transport that results in growth and densification (shrinkage) in the neck area. Grain creep[46], from firing stress, causes plastic flow which results in neck growth and shrinkage.

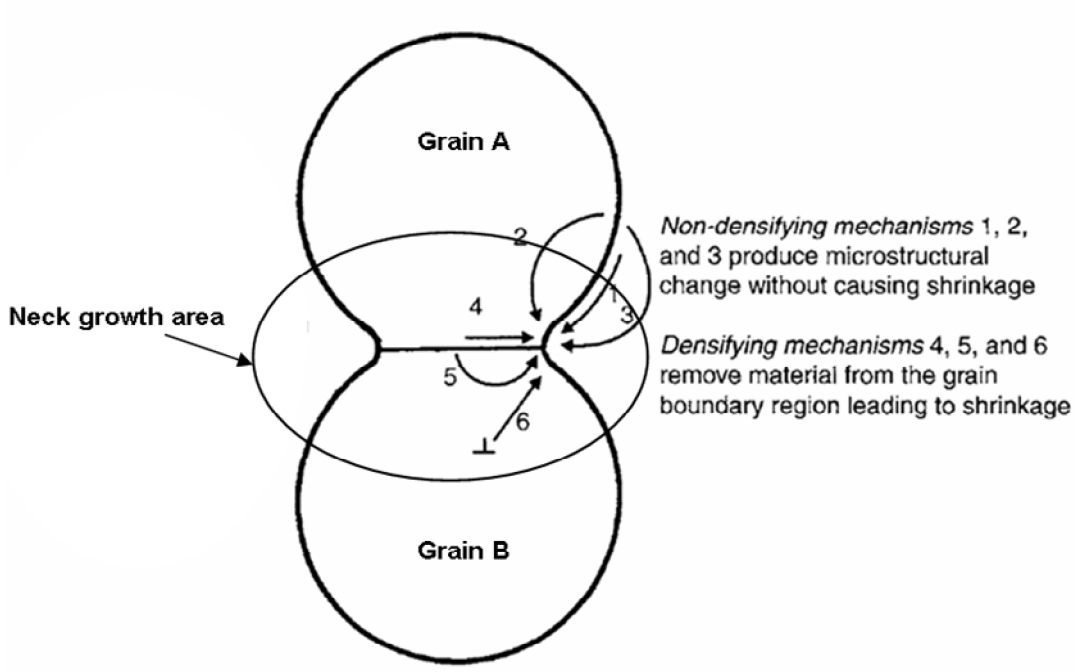

Figure 3.15: The main sintering mechanisms for two individual grains (Gordon 1973)

Additional complications result due to alternative mechanisms, such as different ionic species' diffusion rates and pathways, for the compound to form (Howard and Lidiard (1964); Ruoff (1965) and Readey (1966)). Gordon (1973) gives the diffusion coefficient, ***D***, for an oxide, M_xO_y, as:

$$\bar{D} = \frac{(x+y)[D_l^M + \pi\delta_{gb}D_{gb}^M/G][D_l^O + \pi\delta_{gb}D_{gb}^O/G]}{y[D_l^M + \pi\delta_{gb}D_{gb}^M/G] + x[D_l^O + \pi\delta_{gb}D_{gb}^O/G]} \quad (4)$$

with, ***D***, as the transport (diffusion) coefficient, δ, is the grain boundary thickness, ***G***, is the particle size, subscripts $_l$ and $_{gb}$ as lattice framework, grain boundary transport respectively, and ***M*** and ***O*** as metallic and oxygen ions. From equation 4 it should be clear that regardless of the magnitude of the four diffusivities types, rate is controlled by the slowest diffusion species and along its quickest path.

[46] deformation over a period of time

The rate controlling step for a particular raw material will change as particle size, chemical composition and temperature changes (

Coble and Cannon 1978).

3.3.5.1 Grain boundaries

It is the grain boundaries that will be determining the pore shape. For the chemical potential of the atoms at equilibrium to be the same is equivalent for the pore surface curvature to be the same right round the surface. The forces between the contact of the particle boundary and pore surface must be balanced. Figure 3.16 indicates the balance of forces which results in (Howard and Lidiard 1964; Ruoff 1965 and Readey 1966):

$$\cos\left(\frac{\psi}{2}\right) = \frac{\gamma_{gb}}{2\gamma_{sv}} \qquad (5)$$

With, ψ, as the dihedral angle, γ_{gb}, as the grain boundary specific energy and, γ_{sv}, as the surface specific energy. For concave pore surface during the firing (Figure 3.16(a)), the surface will move to the center and shrink. Whereas in Figure 3.16(b) with pores surrounded by numerous particles (coordination number[47] of the large pores) the pore surface will expand or become unstable (Kingery and Francois, 1967).

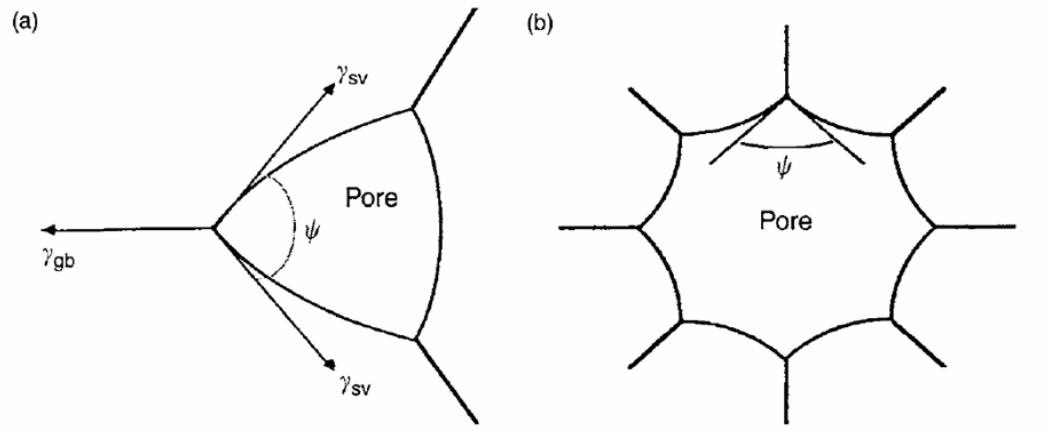

Figure 3.16: Shows the stability and shape of pores being controlled by the pore dihedral angle and coordination number

[47] grains packed around a pore

Figure 3.17 shows how control (maximizing) of particle packing result in high density. In the example for a ψ angle of 120^0, pores with N (number of grains surrounding a pore coordination number) of less than 12 (critical value- N_c) will reduce in size, while pores with $N>N_c$ will expand, resulting in increased porosity in the fired product.

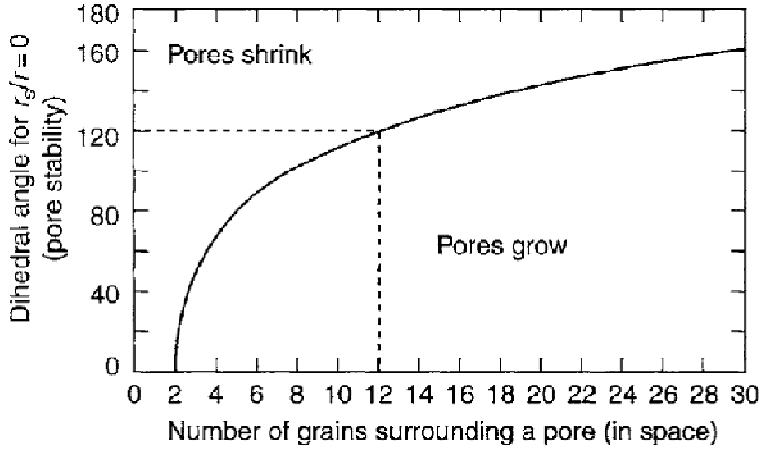

Figure 3.17: Responsibility of dihedral angle and pore coordination numbers for pore stability (Kingery and Francois 1967)

3.3.6 Heating Schedule

In determining the heating schedule, compositional phase diagrams (binary or ternary systems) have to be investigated that represent the various phases of a substance and the conditions under which each phase exists when fired. There are normally only four additional steps in firing the ceramics that have to be considered: binder or pore former burn-out, ramp-up, soak and ramp-down. Figure 3.18 shows a heating schedule with a number of control stages (soak):

- Stage 1- controls heat up rate for the binder burnout, volatiles such as water and polymers. A too rapid heat-up rate can result in bloating[48] or cracking.
- Stage 2- promotes chemical homogenisation or reaction of the raw material components
- Stage 3- heat-up (ramp-up) to the final firing temperature

[48] boiling and evaporation of organic additives from a too rapid heating in the specimen resulting in visual defects

- Stage 4- where most of the density increase and micro-structure occurs (soak)
- Stage 5- cool-down (ramp-down) where an additional step can be added to release stresses
- Stage 6- final cool-down

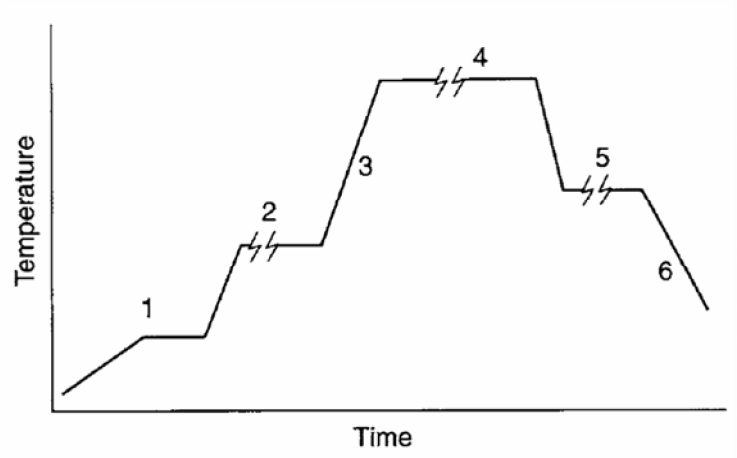

Figure 3.18: General heating schedule (Chu et al 1991)

Cracks can also develop when the stacked product is prevented from shrinking due to friction (free movement restrictions) and due to an uneven shrinkage rate. The firing rate, temperature distribution through the ware, as well as kiln atmosphere must be controlled to improve porosity and shrinkage variations. Important variables that have to be under control to best utilize such a firing schedule include: particles size distribution, particle size, particle shape and particle structure of the raw material as well as the green body particle packing.

3.3.6.1 Particle size

Equations 3 and 4 show the dependence of diffusion rates on the grain size of the raw material. For a heating schedule where densification is dominant (Figure 3.19), the densification rate varies with $1/G^m$, with grain size $\boldsymbol{G}$ and the exponent ($\boldsymbol{m}$) for grain boundary transport exponent is equal to 4 and for lattice diffusion is equal to 3 (Zhou and Rahaman 1993 and Rahaman and Zhou 1995. It has to be noted that packing problems can also lead to a lowering of the sintering rate due to particle size reduction. Nano-sized particles are more prone to packing difficulties and contamination, due to large surface area, which leads to lower green density.

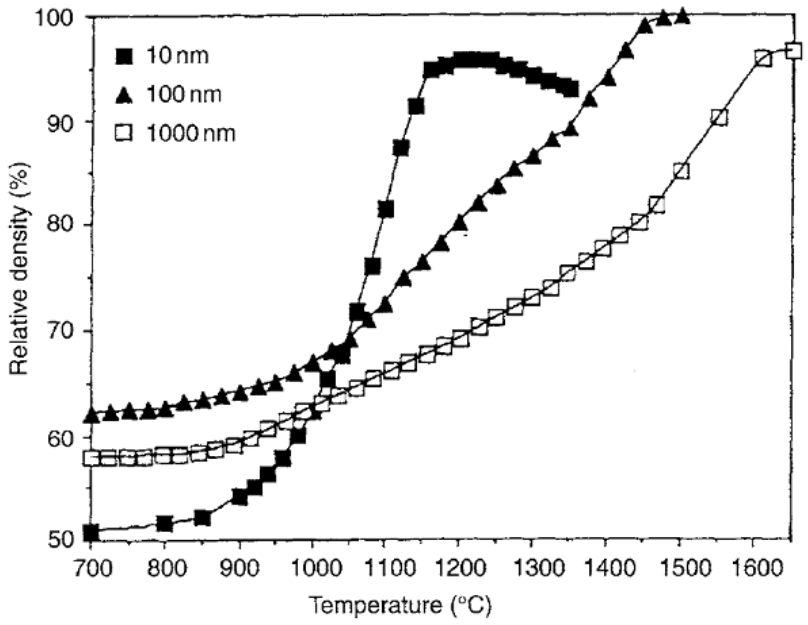

Figure 3.19: Particle size impact on CeO_2 powder firing with a constant heating rate of 10° C min^{-1} (Rahaman and Zhou 1995)

3.3.6.2 Particle size distribution

Because finer grains fit into the larger grains' openings, the use of a wide size distribution normally results in increased packing density and therefore reduced shrinkage. Shrinkage becomes a factor when firing large shapes. Figure 3.20 demonstrates the positive impact of small grains in a wide particles size distribution during early stages of sintering. The final stages of firing, in contrast, depend more on the green compact's particle packing (Patterson and Benson 1983; German 1992 and Chapell *et al* 1986). Particle size distribution effects, on firing rates, are in Figure 3.20.

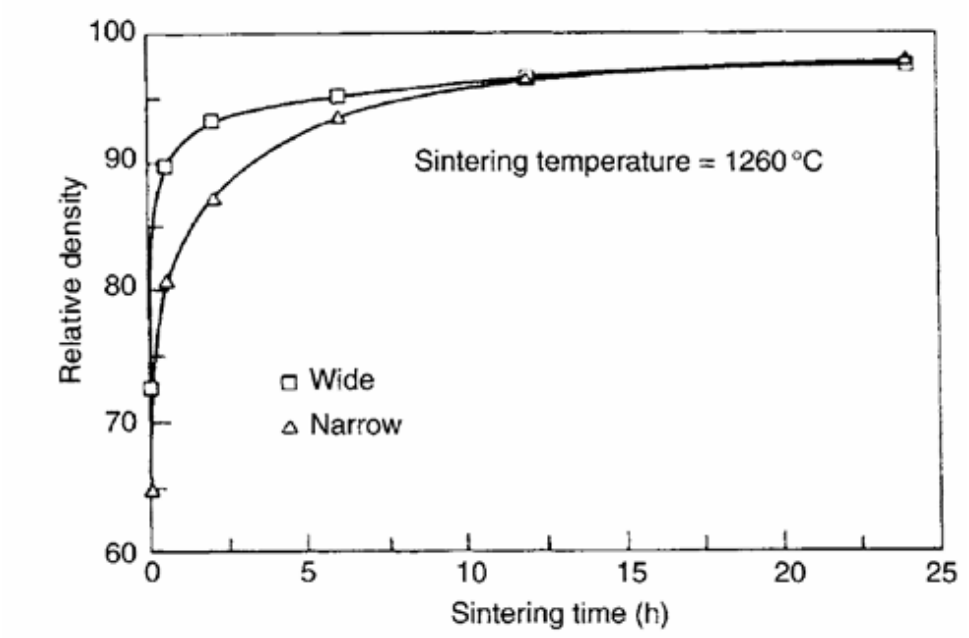

Figure 3.20: Particles size distribution impact on the sintering of Al_2O_3 slip, cast from a wide and narrow particles size distribution with similar median grain size (German 1992)

3.3.6.3 Particle shape and structure

Packing of green bodies is influenced by particle shape with divergence from spherical shape resulting in lower densification. Should tubular particles be aligned compacts can be sintered to higher density (Yamaguchi and Kosha 1981).

3.3.6.4 Particle packing

Rhodes (1981) states that homogeneous packing with good packing density results in improved sintering rates and high density. Such packing results in small, uniform pore size and a low pore coordination number (See Figure 3.21: shrinking pores). From Figure 3.21 it is clear that after 1h sintering at 1100°C (centrifuge forming method) nearly complete densification in contrast with die pressing where only 95 percent density was achieved after 1 h sintering at 1500°C.

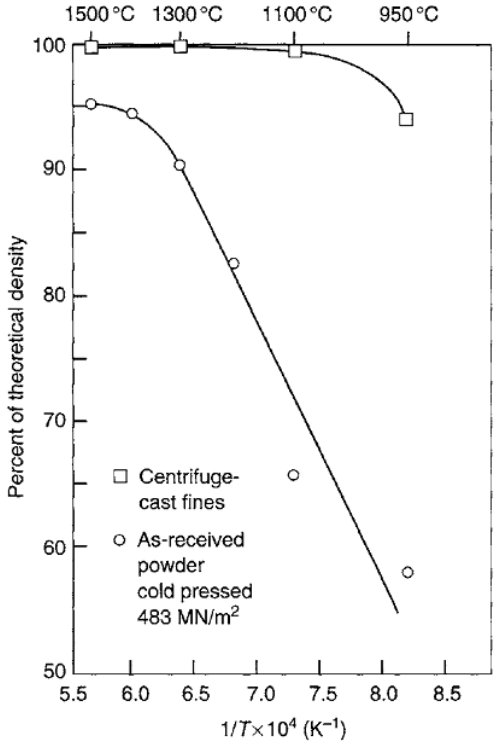

Figure 3.21: Particle packing and sintering for Y_2O_3- stabilised compacts at 1 h for various temperatures (formed by centrifuge and die-pressing) Rhodes 1981

3.3.6.5 Green density

According to Rahaman *et al* (1991), increased green density of a shaped compact, leads to a decrease in shrinkage and higher firing stress (smaller pore volume) during sintering. Research shows a correlation with green and sintered density where a decrease in firing density resulted, for green densities, in the range 50-60 percent of theoretical value. Products with green densities in the range lower than 40-50 percent of theoretical value were harder to densify during sintering (Palmour *et al* 1992). However, it has been found that the highest green densities delayed the onset of grain growth from large coordination number (reduced green density) pores together with an increase in non-homogeneous densification (Mansur and White 1963).

3.3.6.6 Examples of firing porous ceramic

Hung *et al* (2006) looked at the meso-porous structure at various calcination temperatures. By observing the shape of the isotherm, pore size, surface area and total pore volume, it was noticed that only small changes occurred in the meso-pore properties between 600- 700°C.

Above 800°C the pore walls surrounding the meso-pores started breaking down leading to an extensive pore-framework. The average pore size was higher, as the firing temperature increased to 900°C. It was only when temperature was increased to above 1000°C that meso-porous structure collapsed and the necking structure (Figure 3.15) started forming.

Chi (2004) in contrast coated cordierite ceramics with a polymer blend of furan resin (liquid) and polyethylene glycol (milled to -100 micron). 0.5 ml of HNO_3 (65 percent) was added to initiate polymerisation and acetone was used to adjust the viscosity of the blend. Trials were done using the following ratio of PEG: 0.3, 0.5 and 1.0. The carbon content of the 100 percent PEG was low and would have required repeated dipping.

After dipping, compressed air was used to remove the excess polymer from the pores. The curing and carbonisation temperatures were as follows:

- overnight curing at room temperature
- drying at 383°C for 24 hours
- carbonisation in an argon atmosphere at 973°C
- activation with CO_2 at 1073°C after 8hrs

This resulted in a carbon loading of 8 per cent with a carbon burn-off of 10 per cent.

Controlled firing is necessary to minimise the development of stress or build-up of pressure during the release of volatiles or phase changes that occur during firing. The firing cycle determined using techniques that will be described in Chapter 4. Once determined the firing cycle has to strictly adhere to, to minimise product defects.

3.4 Product shaping

3.4.1 Plaster

In the slip casting process, ceramic particles are mixed into a dispersed suspension (slip) which then has to be poured into a plaster mould to shape and form the aqueous suspension into a green body. Traditionally plaster of Paris moulds have been used for this type of forming process.

Plaster of Paris is derived from the calcination of gypsum where half a molecule of water remains in the structure. Care must be taken not to remove this crystal water during mould drying as the material then becomes anhydrous and useless for casting.

Ergun *et al* (2004) looked at various moulds types that could be used for slip casting. Plaster of Paris is usually used. Plaster moulds have an open cell structure with an average pore size of about 1 micron and uses capillary forces to absorb water from the slip. Although plaster moulds are inexpensive, plaster still has a number of disadvantages:

- long casting period
- low wear resistance and therefore limited life
- after use water has to be removed by drying

In contrast, open cell, polymethyl methacrylate moulds have high strength and can withstand the high pressures needed for pressure casting (13-15 bar). These moulds furthermore require shorter casting periods and the water can be removed by air pressure after casting.

3.4.2 Plaster preparation

Plaster moulds are prepared by mixing plaster at a set ratio into water. According to King (2002), the ratio of water to plaster is referred to as the plaster's consistency. Normal tap water is used to mix plaster to a consistency range 60-70 for slip casting.

For example, to prepare a 66 consistency, two parts of water is mixed into 3 parts of plaster. The plaster is mixed through the fingers and left to slake[49] for a few minutes allowing lumps to be easily broken with the fingers.

[49] absorbtion of water

Plaster is sensitive to mixing intensity, therefore a quick, but thorough mix is recommended.

Viscosity increases rapidly and once stirring motion is retained in the mixture, the plaster is ready for pouring into the master mould.

Figure 3.22 shows the impact that water addition has on plaster consistency where plaster strength decreases but water absorption increases.

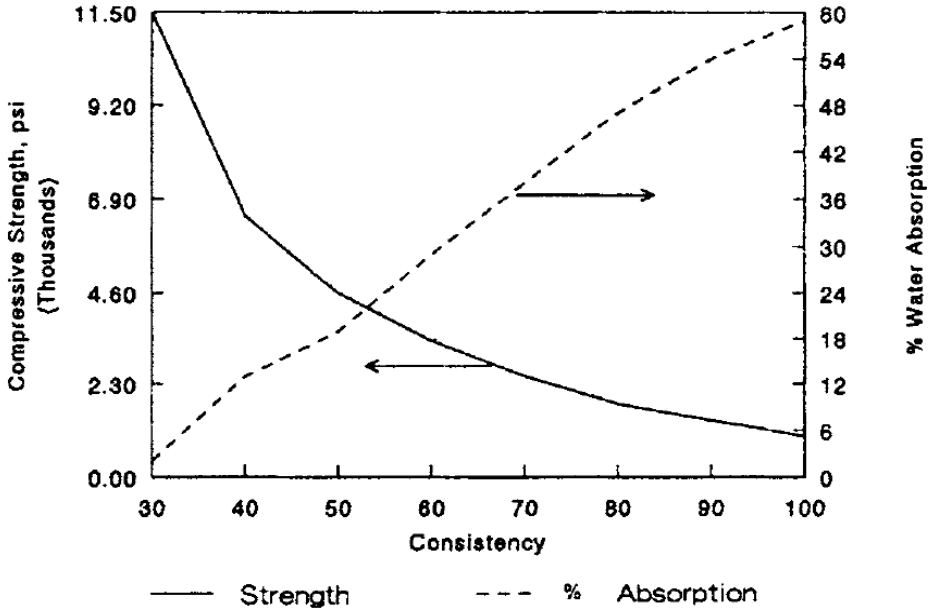

Figure 3.22: Impact of plaster consistency with a decrease in strength and absorption increase with more water addition (King 2002)

3.4.3 Master mould

A master mould is required from which a former can be prepared to cast the actual plaster mould. The master mould's dimensions and shape are determined by the geometry of the product and by making allowances for shrinkage (drying and firing). The master mould is precision turned on a lathe using non porous material suitable for turning (aluminium, plastics and wood). The base plate and the shell complete the assembly for simple moulds (See Figure 3.23). Mould release agent (silicone or lithium stearate) is applied to all mould surfaces that will be in contact with plaster.

The master is then positioned onto a glass, polished granite surface or base plate. The outer shell of the mould is centralised around the master. A thin fillet of mixed plaster is placed around the outer core and base contact and allowed to set. This will prevent plaster leaking through the edge. The plaster is now poured into the mould, de-aired by slight vibration, slightly overfilled and left to set.

Just before final set the upper surface is leveled using a flat scraper. Figure 3.23 below indicates all the mould parts necessary for successful plaster moulding. The set of the plaster is exothermic, resulting in the mould becoming warm to touch. After one to two hours the mould cools down and can be removed from the base plate and the master mould can be extracted from the plaster. This action is helped due to the fact that plaster expands slightly during curing. The mould is now turned upside down to prevent salts in the plaster from migrating onto the casting surface. After curing the mould is oven dried at a maximum temperature of between 50-60°C.

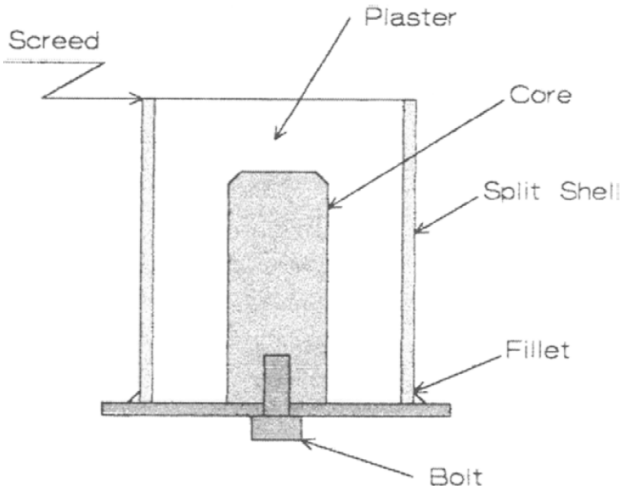

Figure 3.23: Master mould: cylindrical plaster former for casting a crucible shape

The porous nature of the plaster allows water to be absorbed by capillary forces from the slip during the casting process. Figure 3.24 shows an SEM photo of interlocking texture of plaster which allows for the movement of water.

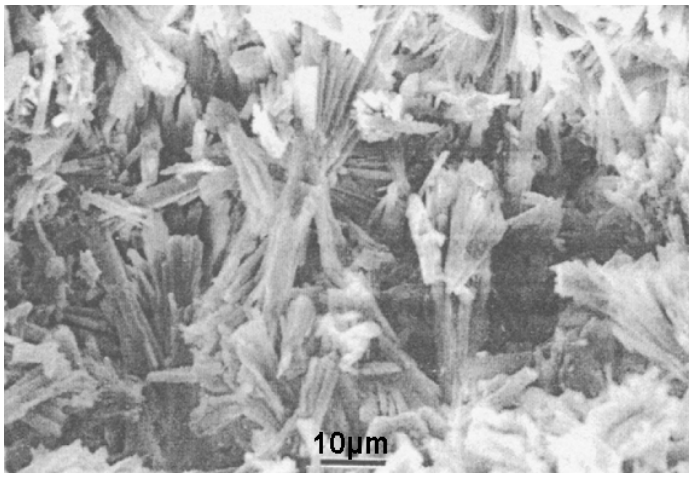

Figure 3.24: SEM image of set plaster (scale bar 10 micron) - (King 2002)

3.4.4 Using the mould

Casting is initiated by pouring slip into a plaster mould in such a way as to prevent the inclusion of air bubbles. On contact with the plaster a slip cast wall develops which subsequently affects the remainder of the cast. Sufficient plaster permeability and capillary pressure are necessary but it is the permeability of the initial casting wall (less permeable than plaster) that determines the casting rate.

The plaster mould saturation status will impact on the initial casting conditions which might then require minor modification:

- when the plaster is too dry it results in a too fast and irregular cast (fill mould with water, decant immediately and let it stand)
- when the slip is too deflocculated it results in a hard and impermeable cast which will be difficult to remove due to the negligible drying shrinkage (adjust slip pH, surfactant or binder concentration)
- then test the density and drying- and firing shrinkage – too hard rather than too soft is preferable: linear shrinkage < 20 percent is obtained when using fine- grained slip. Coarse-grained slips have densities in the range 65-90 percent, because of limited shrinkage.

3.4.4.1 Mould Filling

With water being withdrawn during casting, the slip level decreases and has therefore to be constantly topped up to prevent drying and later difficulty in removing the cast piece. For this reason it is the practice to position a non-porous ring over the casting opening to contain a reservoir of slip. (Chapter 2, Figure 2.21).

Segregation of coarse-grained slips result in a differentiation between coarse and fine particles that causes non-uniform drying and firing with cracking problems. Segregation can be prevented by increasing the slip viscosity by addition of organic thickeners, or by increasing the fines or by adding flocculants. Higher viscosities can lead to slower casting rates.

3.4.4.2 Air Drying Slip Cast Parts

Normally the cast part is left in the mould to first air-dry until it is strong enough for removal. As water vapour is denser than air, it is standard practice to invert the mould until the part self-separates from the mould (due to shrinkage as well as from the slight taper of the mould). This minimises any stress formation and prevents cracks from developing. Drying shrinkage for mould stripping can be manipulated by pouring a dilute water corn starch suspension into the mould and leaving for a few minutes before inverting and leaving to dry or it can be obtained by preparing a slightly flocculated slip (Dobrovolskiy 1977).

3.5 Summary

In this chapter, the production processes and factors influencing porous ceramic properties are summarised from the comprehensive literature survey and presented in the mind map as represented in Figure 3.25.

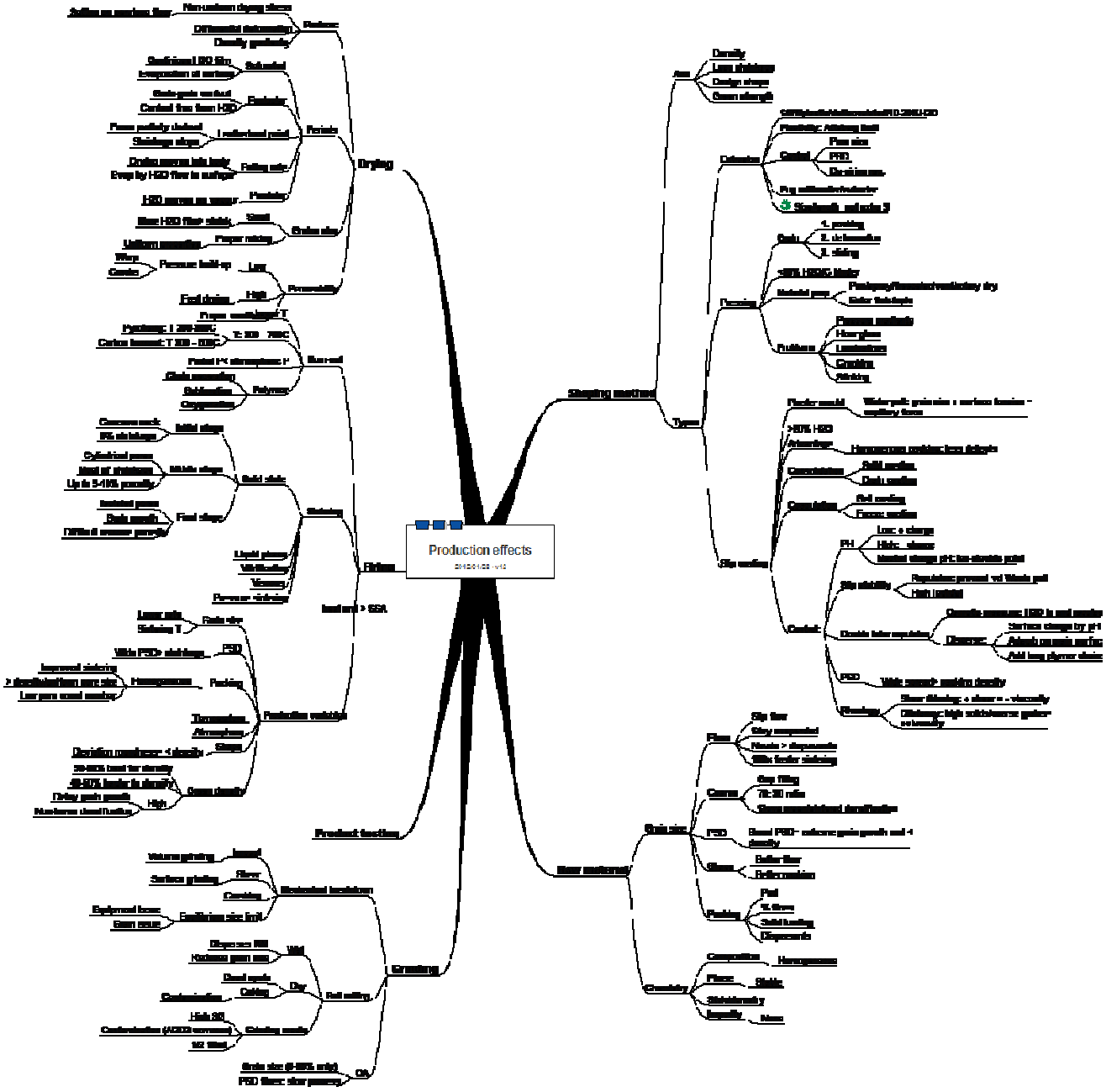

Figure 3.25: Mind map illustrating best practice impacts on product quality

Chapter 4: Analysis of Ceramic Filter Properties

4.1 Introduction

Low cost water filters are important in safeguarding household health where existing potable water such as bulk water supply or other sources, are left untreated, are poorly treated or become contaminated during use (WHO and UNICEF 2006). For this reason formulated and relevant test methods and performance specifications are needed for testing and evaluating ceramic water filters. This chapter identifies relevant production test methods as well as methods for evaluating final product (filter) performance. It covers the physical and analytical criteria against which the quality of the raw powder and solidified product can be measured. Properties manifested in the ceramic filter are the effect of temperature and time on the green structure made up of starting powder and water. These methods include surface analytical methods such as chemical composition, structure, surface area, thermal and particle size. The discussion concentrates on the use of these techniques in the manufacture of low cost ceramic water filters.

In-process testing is necessary for product certification and Van Halen *et al* (2009) provide the main criteria for the final testing and evaluation of a household filter:

a) filter system cost and accessibility to the user: cost for the filter system and filter replacements have to be kept low by providing local distribution networks close to the manufacturing facility.
b) guaranteed water quality improvement: filtrate quality is affected mainly by the maximal elimination of pathogenic microorganisms, heavy metals, nitrogen, turbidity, colour and odour, pesticides and pharmaceuticals from polluted water. The focus is to reduce incidences of diarrhea. The removal efficiency is checked by using indicator organisms such as *Escherichia coli* which should have a LRV value in excess of 2-3.
c) sufficient water production from filtration process: evaluate the clogging mechanism by selecting a suitable cleaning method. Some examples of cleaning method effectiveness are presented in Figure 4.1.

d) functionality: testing the filter flow rate, lifespan before replacement, filter breakage and cost of treated water

e) environmental footprint: comparing chemical and energy use relative to other water purification processes

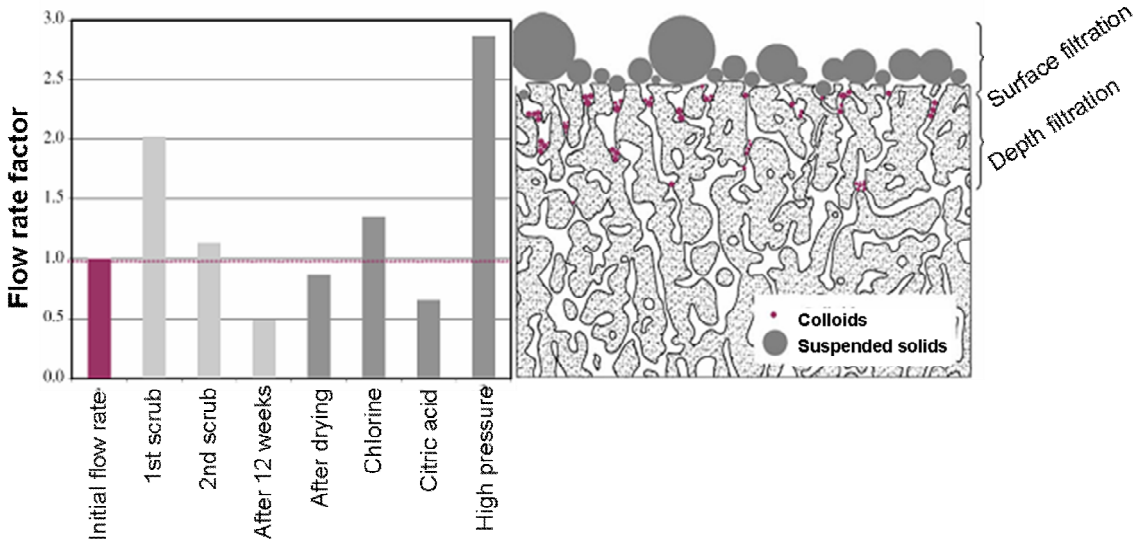

Figure 4.1: Filter cleaning methods and mechanisms (short-surface and long-term-depth cleaning) in terms of flow rate (relative to initial flow rate) improvement (Van Halen 2009)

4.2 In-process control

4.2.1 Particle Size

According to Darcovich *et al* (2003), one of the key characteristics of a ceramic material is the particle size and particle size distribution, as both controls the surface area of materials. These properties are determined by using screen analysis, a hydrometer or more sophisticated X-Ray or laser technology (discussed in Chapter 3 with their related problems in measurements of low concentration of agglommerates).

The results from an particle analysis is normally plotted on a graph with the cummulative % passed (finer than) on the verticle axis and the log of the particle size on the horisontal axis. A typical particle size distribution plot is shown in Figure 4.2.

As size decreases, surface area per unit mass of material increases rapidly. In order to change the specific surface area of a mixture, it is necesary to change the PSD through milling. The ability of particles to pack is directly related to the PSD. The broader the PSD, and the more size ranges of materials are available, the better the particles can pack, forming low viscosities even with high solids content. Very narrow PSD packs poorly and forms dilatant rheological properties resulting in lower solids content.

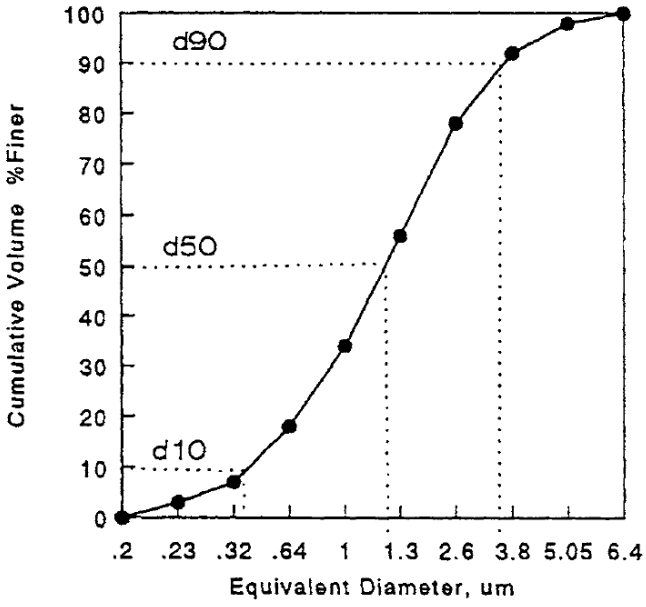

Figure 4.2: Cummulative particle size distribution plot (Dinger 2002)

The steeper the curve, the narrower the distribution, whereas the lower the angle the wider the distribution. As indicated in Figure 4.2 the measurements of d50, d10 & d90 are normally used to summarise the distribution.

Boisnolt *et al* (1999) graphically illustrate, in Figure 4.3, the impact of particle size distribution on flow properties contrasting single particle size slurry and with an optimised blend (packing model) of several particle sizes.

According to them the smaller particle size acts as a lubricant between the larger sizes. The analogy of pumping slurry or slip casting can be used as a comparison by contrasting a mono particle sized system with ternary particle sized system.

When combining at least 3 particle sizes (ternary system) higher packing density, lower cemented porosity (35% in contrast to the 75% of normal slurries), higher compressive strength (due to lower water content and thus higher cement: water ratio), lower permeability and increased solids per unit volume of slip can be obtained. Packing volume fraction (PVF) was used for optimising their distributions. The PVF is defined as the ratio of the sum of the absolute volumes of all the individual material components in the dry blend to the total bulk volume of the dry blended components together. PVF values of 0.64 - 0.74, for random and hexagonal packing when using identical spheres, can be obtained. According to Boisnolt *et al* (1999), PVF in excess of 0.8 was routinely obtained for the optimised blends resulting in the improved properties stated above. PVF values can also be seen as a packing model as discussed in Chapter 2 and 3. In Figure 4.3 below a simple example of using ping-pong balls, peas and sand combination is used to visually explain the relationship between their ternary optimised systems.

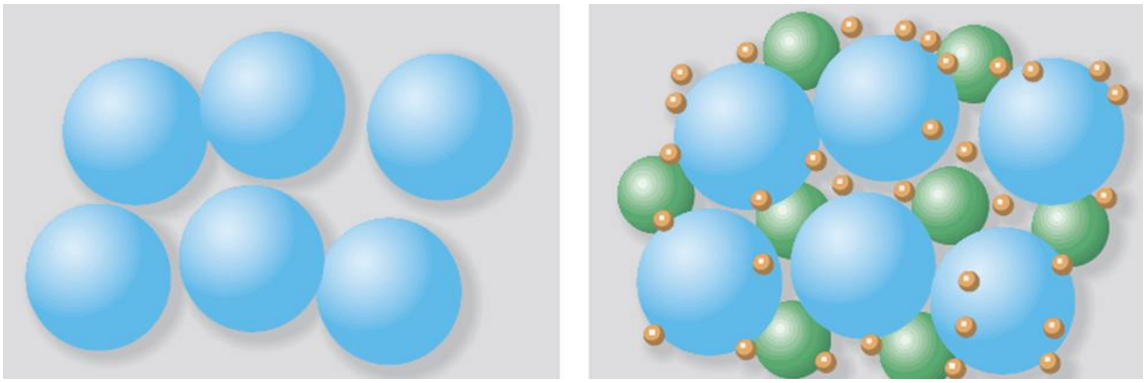

Figure 4.3: A slip made from particles of single size (left: ping-pong balls) where water fills the large pores, and a slip made by optimizing several particle sizes (right: peas and sand) where pore-size has been reduced because small particles fill the spaces and act as lubricating ball-bearings (Boisnolt et 1999)

Fahay (2009) provides a number of equations for the sedimentation method for particle sizes analysis as well as for the pipette method. A list of the instrumentation required for the hydrometer method is presented.

The Soil Moisture and Porous Ceramic Catalogue (2008) summarises the sedimentation method for determining the particle size distribution. Screen analysis is applicable only to particles larger than 60 micron. For particles below this size it is recommended to use the sedimentation methods (pipette or hydrometer methods), making use of Stoke's Law, Table 4.1, which depends on the buoyant sphere weight, sphere diameter and fluid viscosity.

Table 4.1: The equations and units for Stoke's Law and the Reynolds Number (Fahay 2009)

$$\text{Resistance} = 3\pi\eta v D = \text{Weight} = \frac{\pi}{6}(\gamma_s - \gamma_f)D^3 \Rightarrow \quad v = \frac{(\gamma_s - \gamma_w)D^2}{18\eta}$$

where γ_s and γ_f are the unit weights of the solid and the fluid (γ_w if water)

- Thus, a sphere of diameter D will fall distance h in water in time t_D:

$$t_D = \frac{18\eta h}{(\gamma_s - \gamma_w)D^2}$$

- where η is the fluid viscosity (1×10^{-6} kPa.s for water @ 20°C), γ_s is the unit weight ($= \rho g$) of the sphere material (26.5 kN/m³ for silica material), and γ_w is the unit weight of water (9.91 kN/m³ ≈ 10 kN/m³)
- This is the basis of the "pipette" method of determining the sizes of fine soils – easy to explain, but requires high precision
- Also the basis of the "hydrometer" method – more complex to explain, but simpler to do
- Only valid for Reynolds' Number $R_e < 1$ (Reynolds' Number determines if flow is 'laminar' or 'turbulent')

$R_e = \frac{\rho_f v D}{\eta}$ For water, $\eta \approx 1 \times 10^{-6}$ kPa.s. For $(\gamma_s - \gamma_w) = 16$ kN/m^3, and D = 103 µm, $t_D = 10.3s$, and $R_e = 1.0$

In the hydrometer method, which follows the Archimedes' Principle, which states that an object less dense than water will float to a depth equivalent to the mass of the water displaced. With mass being equivalent to density x volume, it is clear that an object floated in water of different densities, will displace different volumes of water. The hydrometer has a tube of constant mass calibrated to measure density by measuring readings on the stem showing the fraction of the hydrometer submerged (Figure 4.4). This reading is converted into density, and therefore the mass of material suspended in the water.

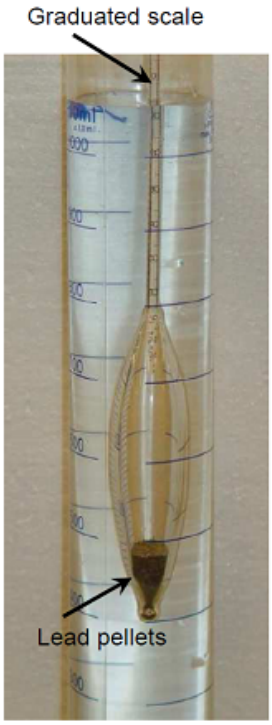

Figure 4.4: Hydrometer in use

4.2.2 Slip density (SG) measurements

Accorging to Funk and Dinger (1994), specific gravity (SG) of a sample is an important material property. Slip density or specific gravity (SG), is measured by weighing the 100cm^3 slip in a tarred measuring cylinder. Slip SG is an important measurement used in controlling slip quality during the production of porous ceramics.

A pycnometer[50] is the more expensive instrument used for the measurement of density. By measuring the gas displacement for a fixed volume, the sample volume can be obtained. The sample volume and weight is then used to determine the density (King 2002).

[50] container with a fixed volume used for determining the density of a liquid or powder

4.2.3 Slip rheology (viscosity)

Rheology is the science that measures the viscous behaviours of fluids, suspensions and forming bodies resulting from applied shear. The viscosity of a fluid characterizes how easily it will flow when sheared. Water, petrol, and paint thinners, for example, have low viscosities. In contrast, molasses and cooking oils have higher viscosities. We associate low viscosities with thin fluids that flow quickly, and we associate high viscosities with thicker fluids that flow slowly. The dynamic viscosity of any fluid under any set of conditions is the ratio of the measured shear stress to the measured shear rate (Dinger 2002).

Dinger (2002) illustrates the shear range in water, as follows: low shear can be pictured as water being stirred with a spoon, whereas high shear would be water passing through a garden spray nozzle, with most of it disintegrating into spray – or small droplets. When a fluid's viscosity changes with a change in the applied shear, the fluid is characterized by more complex rheology and is not a simple fluid. In such cases the rheology has to characterise and quantify the varying viscous behaviours of the fluid, slip or forming body.

Fluids, such as water, characterised by a single viscosity at constant temperature with applied shear it is called a Newtonian fluid and there is no need to quantify (define) the applied shear. But many fluids have viscosities that are NOT constant with the applied shear rate. These fluids are called non-Newtonian fluids and in such cases the shear rate at which viscosity was measured should be given. Non-Newtonian rheology's fall into several types of viscous behaviours (or categories). Each fluid exhibits a single, characteristic time independent rheology as illustrated in Figure 4.5:

- dilatant rheology: fluids with viscosities that increase as shear rates increase (Outbac rheology)
- shear thinning rheology: fluids which decrease in viscosity as shear rates increase exhibit pseudo plastic rheology's. Example is ketchup
- yield dilatant, Bingham, or yield pseudo plastic rheology's: suspensions which gel and exhibit yield stresses
- thixotropic: slip suspensions which decrease or increase in viscosity with time at constant shear rate

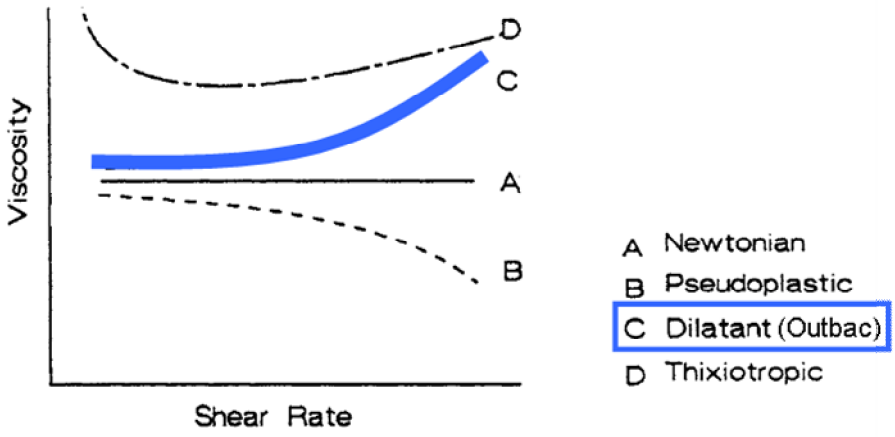

Figure 4.5: Slip Rheology Curves (King 2002)

Non-Newtonian fluids can, however, also simultaneously exhibit time dependent rheology's. Depending on their characteristic rheological behaviour, each fluid can exhibit a variety of measured viscosities as they are exposed to constant shear rates for periods of time.

King (2003) further simplifies rheology (viscosity of slip) definition in terms of its two common types by analogy of pouring slip out of a beaker or squirting from a syringe (makes large difference in subsequent processes- See Figure 4.6 below):

1. pouring from a beaker (low flow rate therefore low shear rate)
    a) high viscosity: pours slowly like molasses
    b) low viscosity: pours out like water.
2. squirting the slip out of a syringe (high shear rate):
    a) difficult to force out: making it more difficult to cast or extrude (dilatant)
    b) easier to squirt with increasing velocity: easy to cast, pump or extrude

4.2.3.1 Factors controlling viscosity

According to Funk and Dinger (1994), viscous behaviour is important in ceramic processing. Factors that can control viscosity are as follows:

- solids content (expressed in volume per cent solids) leads to a rapid in viscosity increase in excess of 50 volume per cent solids as particles-particle contact occurs in slip (Figure 4.6). The increased viscosity prevents settling, improves the tempo of casting, leads to a more uniform cast, and results in improved density.

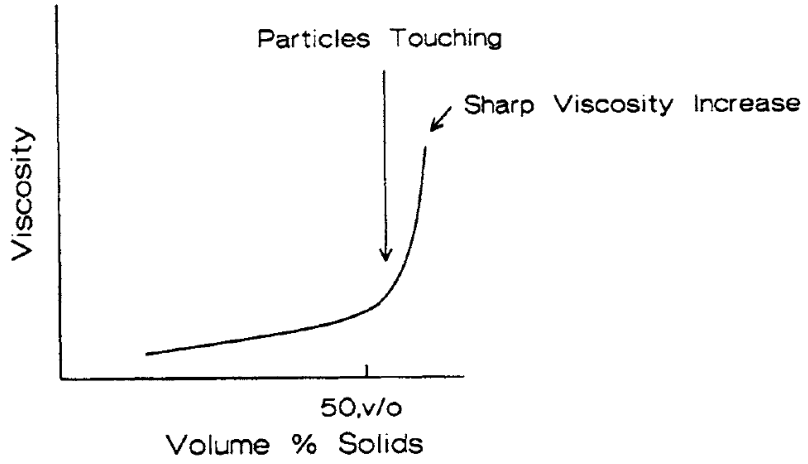

Figure 4.6: Viscosity increase (solid content) as a result of particle-particle contact (Dinger 2002)

- deflocculant concentration helps in keeping the casting permeable for drying and develops just enough shrinkage for stripping from the mould. Figure 4.7 indicates the relationship between viscosity and deflocculant amounts. With deflocculant addition the viscosity initially decreases rapidly before reaching a minimum (A) and then increases again (C- B). Some of the deflocculants available include acrylate compounds, sodium silicate, ligno-sulfonates, and some phosphates.

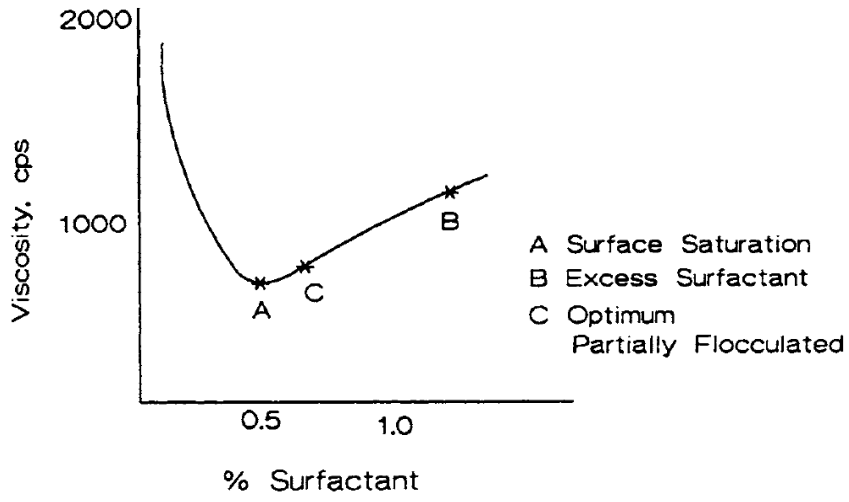

Figure 4.7: Viscosity increase (solid content) as a result of particle-particle contact (Dinger 2002)

- dissolved polymers (starch) act as a binder that increases green strength and provides porosity
- pH changes results in charges on the particle surface (Chapter 2 and 3). Similar charge repels, deflocculates and therefore decreases slip viscosity. Zeta potential and pH measurements can be determined to obtain S-shaped curves that can be used for determining the slip flocculation point for a specific pH value.
- packing of the grains where medium and fine grain sizes fill the pores (Chapter 3 packing models), will determine the slip volume. Solids content of above 80 per cent can be achieved although content for fine grained slips range from 50-55%. Figure 4.8 shows where coarse, medium, and fine fractions give the best particle packing
- ionic strength is determined by electrolyte concentration
- temperature increases during milling with the creation of new active surface area which results in an increase in slip viscosity.

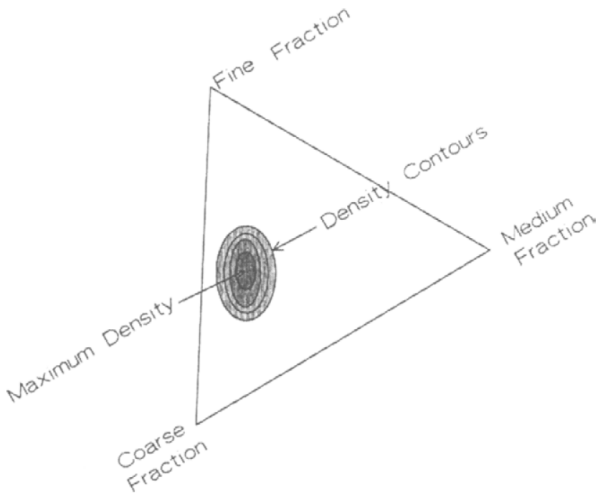

Figure 4.8: Maximum slip density for three size fractions (King 2003)

4.2.3.2 Measurement of Viscosity

4.2.3.2.1 Orifice Flow Viscometers

The inexpensive orifice flow viscometers make use of funnels or cylinders with an outlet in the center of the base (See Figure 4.9). The measurement is made by adding a set volume of slip to the funnel while keeping the opening closed with a finger, and then opening the hole and obtaining the time that it takes until the flow stops. This time (flow time/rate) number can be used for production quality control purposes but cannot be used for calibration purposes due to the change in strain rates (higher shear rate - full funnel and lower shear rate – as funnel empties).

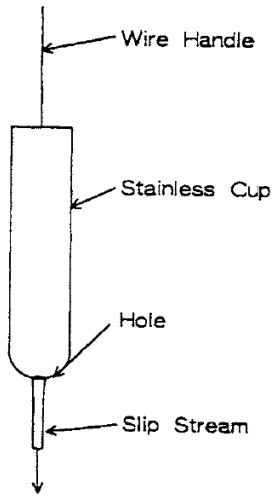

Figure 4.9: Orifice Flow Viscometers for measuring the slip flow time (BAMR Quality Control Instrumentation)

According to the supplier, BAMR Quality Control Instrumentation, flow cups (process of flow through an orifice) can be used as good relative measurement of kinematic viscosity. The flow time can be converted into centistokes through the use of a viscosity disc calculator. The slip cups, in contrast, provide the means of obtaining a quick viscosity measurement on the production floor. The cone-and-plate viscometer can be used for non-Newtonian liquids.

Fish (2001) suggests making an orifice flow viscometer by using a PVC pipe of 200 mm, with a 4 mm hole drilled in the end cap, for determining the casting rate (flow time viscosity). The larger the volume of slip tested the more accurate the reading becomes.

The author suggests a further improvement by drilling another 4 mm outlet hole just below the top of the PVC pipe. Slip is added constantly allowing excess slip to drain through the upper hole thereby resulting in a constant head viscosity flow measurement. In the normal variable head flow test the shear varies as the slip level in the PVC pipe declines resulting in a variable shear measurement of flow. The constant head allows the measurement of slip flow rate (viscosity) at constant shear rate. This overcomes the limitation of the flow cups and orifice flow viscometer and places this method one the same plane as the more expensive viscometers.

4.2.3.2.2 Viscometers and Rheometers

According to King (2002), several types of the more expensive viscometers are available for measuring rheological properties. Viscometers measure the viscosity of a fluid or slip. The two main types of viscometers are the rotor cup geometry type and the plate and cone geometry type, of which both are used for fine-particle size slurries. The rotor type works best for coarse particles. The viscosity is determined indirectly by measurement of the rotor's rotations per minute (rpm).

In contrast, a rheometer measures the shear rate. The two types of rheometers are a shear-rate-determined rheometer and a stress-determined rheometer. Rheometers are mostly shear-rate controlled, whereby the rotor speed is adjusted and shear stress determined. Strain-rate-controlled viscometers are the most effective for all ceramic slips.

Holdridge and Moore (1952) explain that the rotational viscometer consists of two concentric cylinders and uses the torque that is generated when one of them is rotated relative to the other for measurement. The shear stress varies inversely as the square of the distance from the rotational axis. Small differences in radii result in a small range of shear stress, which has a major advantage over the capillary type of viscometer, for non-Newtonian materials. This system also works better for thixotropic materials, where the material for the same sample can be repeatedly broken down and built up again and the thixotropic level related to the power input.

For fine-grained slips, special attention must be given to viscosity measurements, which helps in optimising some of the following production variables (King 2002):

- Milling time impact
- PSD and milling time
- Mill critical speed
- Effect of solids content
- Type and amount of deflocculant
- Selection and addition of the pore former
- Effect of pH, Zeta potential

4.2.4 Slip pH

pH is measured using a standard, calibrated pH meter. pH is one of the first properties of the interparticle fluid chemistry to check to control suspension rheology. The pH of suspensions is important because each particular powder material will have an isoelectric point at a pH controlled by the powder's composition. The isoelectric point is the pH at which the electrostatic surface charges on the clean powder surfaces are zero (King 2002).

Powders typically flocculate at the isoelectric point and they deflocculate as the pH increases or decreases away from that point. Depending on the nature and concentrations of impurities that occur in the raw material, suspension pH can fluctuate from batch to batch (Dinger 2002).

4.2.5 Thermal Analyses

Some of the more important techniques that can be used in thermal analysis include: thermal conductivity/expansion, differential scanning calorimetry (DSC), loss on ignition (LOI), differential thermal analysis (DTA), thermal gravimetric analyses (TGA) and specific heat (King 2002). These techniques are important for determination of the firing curve to match reactions that occur as a result of temperature.

4.2.5.1 TGA and DTA

Dinger (2002) states that TGA is used for determining the weight loss/change of a sample during heating in an oxidizing or reducing atmosphere (air, nitrogen or argon). TGA can be used to analyse for thermal decomposition in carbon burn-out, dehydration and desorption. In contrast, DTA determines the change in temperature between an inert material and the sample during heating. DTA is used for identifying melting, phase changes, and oxidation reaction temperatures. DTA is used for identifying temperatures at melting, phase changes, and for oxidation-reaction. The weight and temperature changes can be measured by both instruments.

4.2.5.2 Thermal Expansion

High thermal expansion results in thermal shock occurrence. Yang *et al* (2003) indicate that thermal expansion is obtained by measuring the difference between a predetermined length of sample and the same sample when heated. The expansion is measured with a dilatometer. Ceramics can have a wide variation in thermal expansions with alkaline earth oxides topping the expansion coefficient list. The expansion coefficient is determined by measuring the expansion percentage and multiplying it by the inverse of temperature ($°C^{-1}$) . Fused silica glass and Li aluminium silicate (lithium alumino silicate) have low coefficients of expansion and are generally used in applications where zero thermal expansion is required.

Thermal shock is determined by rapidly heating a ceramic filter to a red hot temperature and then rapidly cooling it in water. The filter either cracks or shatters or is resistant to thermal shock and can be applied under inceased temperature conditions (Hasselman 1969).

4.2.5.3 Loss on Ignition (LOI)

LOI is determined by measuring the weight loss caused by dehydration as a result of burn-off of the organics in the sample (Dinger 2002).

4.3 Final product testing

The most common analytical methods include surface and chemical analytical methods.

4.3.1 X-Ray Diffraction (XRD)

X-ray diffraction results in a series of peaks caused by the crystal lattice in contrast to spectra of wavelengths used to identify oxides in the X-Ray Fluorescent analysis. XRD is used for the identification of minerals in a ceramic sample. The mineral gives a characteristic (fingerprint) diffraction pattern that is used for identification purposes. X-ray analyses can furthermore be used for grain-size analyses (PSD). Sample preparation requires a powdered sample packed into a sample holder. The grains have to be randomly orientated for best results (not possible in elongated or planar particles). The lattice planes and their spacings diffract the X ray beam at different angles, resulting in the unique diffractogram.

In X-Ray Fluorescence, tests samples for the determination of major and trace elements in solids. When materials are exposed to short-wavelength X-rays ionization of the atoms take place which releases one or more electrons from the inner orbital of the atom. The release of an electron makes the structure of the atom unstable, and electrons in higher orbitals move into the lower orbital to fill the orbital left behind. In the process, a characteristic energy is released in the form of a photon, which is used for elemental analysis (Jenkins 1984)

4.3.2 Surface Area

The Brunauer-Emmett-Teller (BET) surface area analysis method is used for determining ceramic surface area (Brunauer *et al* 1938). For this method the sample is heated under vacuum to remove the absorbed water vapour and any other gasses. The material is then coated with a monolayer of nitrogen gas.

The amount of gas used is a reflection of the surface area. Sample heating is normally the most time consuming step.

Martin *et al* (1998) describes an *in situ* method of indirectly measuring the reduction of surface area during sintering. The technique makes use of longitudinal wave ultrasonic velocity measurements and has been measured in Al_2O_3 and ZnO systems. Martin *et al* (1998) found that PSD has an effect upon this correlation. They found that materials with a narrow particle size distributions exhibited a linear relationship between the longitudinal wave velocity and surface area reduction and the over sintering period. In contrast, materials having wide PSD exhibited a much larger decrease in the SSA during the early stages of vitrification. They attribute these influences to differences in the thermodynamics during vitrification of the particles.

4.3.3 Microscopy

King (2003) explains that the stereo-binocular or petrographic/metallographic microscopes have either reflected or transmitted light options. These microscopes are used to examine ceramic surface texture and structure with a magnification of up to 40x optically and 100x digitally. Lighting is oblique, shining on the surface and through the optics. Digital photo capability can be used for recording and quality control cases. The microscope can also be used for particle size and microstructure determination.

The method works by digitally projecting microscopic images of the grains to a screen for further viewing and processing. The screen is ruled into squares for convenience in counting and size determination (Dunn 1930).

Scanning Electron Microscopy (SEM) and Transmission Electron Microscopy (TEM) are microscope techniques which are fitted with analytical chemical capability by measuring the X-ray fluorescent or diffraction spectra radiating away from the sample location when receiving energy from the electron beam.

4.3.4 Density (ASG) Measurements

Accorging to Funk and Dinger (1994), apparent specific gravity (ASG) of a sample is an important material property for measurement of finished product. The density can be determined for a porous material by 2 methods: either by sealing the surface (wax or resin) or by saturation of the sample for the determination of bulk density and apparant porosity. For the ASTM C 20-87 (ASTM, 1988) method , the sample is boiled in water for 2 hours and then submerged for an addional 12 hours to saturate the connected pores with water.

4.3.5 Porosimeter (pore volume and pore size distribution)

Pore volume is measured with a porosimeter, by forcing a non-wetting liquid, such as mercury, into the pores of a sample in order to measure the pore sizes, pore distribution and pore volume. Mercury intrusion porosimetry involves placing a 1 cm^3 sample into a container and evacuating the air from the container for removal of air and water vapour. Mercury is allowed to enter into the container. The container is pressurised and the volume of mercury entering the pores is measured (van Halen 2006). For the apparatus used in our tests (Micrometrics Mercury Intrusion Autopore), a maximum of 210 MPa was used to fill pores with with sizes up to 0.006 μm. By calculating the mercury pressure and volume displaced, the pore size distribution can be calculated.

A number of alternative techniques for measuring pore dimensions and distributions are discussed below:

1. Roeek and Uchytil (1994) describe a technique of using only mercury for penetration of the inner part of sample. The Wasburn equation was presented as giving the change in pressure with which mercury is forced into a cylindrical pore of radius, r:

   $$r = 2\gamma\cos\phi / \Delta p$$

   with γ, as the mercury surface tension, ϕ, as the mercury and sample surface contact angle and Δp, as the change in pressure (mercury penetration).

By embedding the sample in mercury (on side testing) and using the Coulter porosimetry method, it is possible to compare sample porous structures as well as use it for membrane defect detection.

Palacio *et al* (2009) gives an example and shows results were they used Roeek and Uchytil (1994) technique for testing their pressed membranes. Palacio *et al* (2009) made ceramic membranes by pressing clay and phosphates from Moroccan ores with starch as the pore formers. Use of different starch contents resulted in filters with different hydrophilic properties. The results for a range of starch contents and the resulting pore diameters are shown in Figure 4.10.

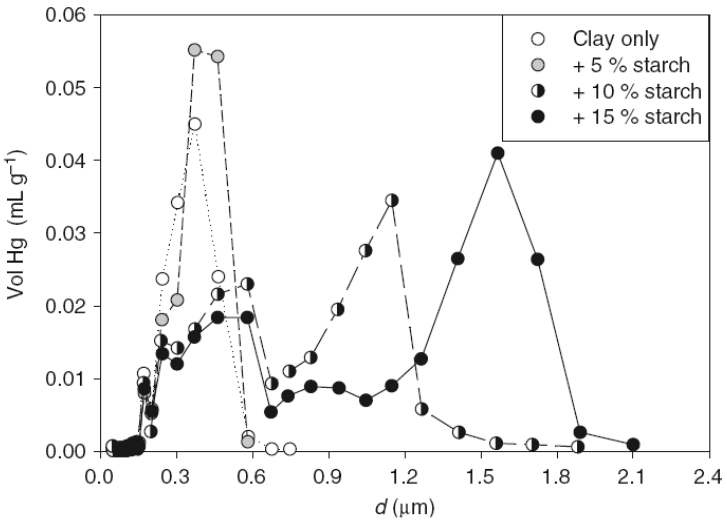

Figure 4.10: Volume of mercury intruded versus pore diameter for samples with varying starch contents (Palacio et al 2009)

2. Jena *et al* (2003) describes the capillary flow porosimetry method, where the sample pores infiltrated with a wetting liquid with a free surface energy less than free surface energy of sample. By increasing and measuring the pressure, the liquid is forced out of pores (see Figure 4.11).

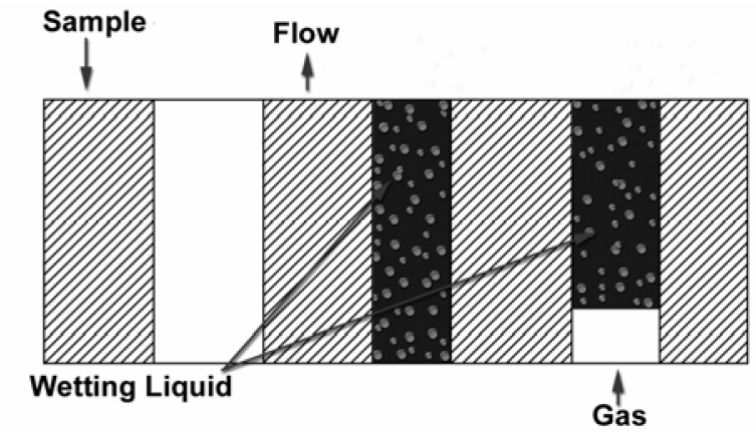

Figure 4.11: Capillary flow porosimetry method (Jena et al 2003)

The measured pressure needed to force wetting liquid out of pore is also calculated by using the Washburn equation explained by Roeek and Uchytil (1994) in the previous section.

A simplified equation is presented for the determination of the pore diameter (size) by defining the bubble point, using the following equation: $p = 30\gamma/D$ and conversely, the pore size of the ceramic by the equation: $D = 30\gamma/P$. The variables listed are as follows:

- D – pore diameter in micron
- γ – surface tension of water (dynes/cm) at 20°C $\gamma = 72$ dynes cm^{-1}
- p – bubbling point (air entry pressure) measured in mm Hg

From the equation it is clear that the bubbling point pressure will increase with smaller pores and decrease with larger pore sizes. The pore size of ceramics directly affects the bubbling pressure (pressure with which air breaks through a wetter pore channel) as well as the hydraulic conductivity, K, rate at which ceramic, of known thickness, conducts liquid from one surface to opposing surface. Water is normally used but K varies with liquid type used. According the Soil Moisture and Porous Ceramics Catalog (2008) the effective pore size is defined as the minimum opening within a channel or pore. The porous material behaviour is directly related to the pore properties as well as the material type used in the manufacturing of the ceramic.

3. Okada *et al* (2009) used Archimedes water method and the pore volume of the sample using mercury intrusion porosimeter[51] for testing porous ceramics. According to Okada *et al* (2009) the many applications for porous ceramics implies a large variation in properties that need to be tested. These include: surface, pore volume, pore size and pore size distribution of the pore.
4. Mohd (2002) made modifications to the Archimedes water method (ASTM Standard- C97-83) that required a test specimen to be immersed in water for 48 hours. They found however that the majority of absorption occurred during the first few hours, thereby confirming that 24 hours should be sufficient for water absorption, density and effective porosity determination, with the following variables:
    - bulk density (g cm^{-3}) - mass of oven dried sample/total volume including pore space
    - dry density (g cm^{-3}) - mass of oven dried sample/total volume by 24 h immersion
    - grain density- mass of oven dried sample/sample volume (excluding pore space)
    - water absorption: water absorbed (mass) in the sample after 24 h submerged in water/oven dried sample mass expressed as %
    - apparent porosity (%): % of void volume/total rock volume
    - effective porosity (%): connected pores volume – (water absorption x BD)
    - saturation (%): % pore volume filled with water after 24h immersion
5. Van Halem (2006) and Van Halen *et al* (2009) combined some of the techniques discussed above for testing porous ceramic filter properties. The samples for testing was taken from 3 positions in a pressed filter (bottom, middle and lip of filter wall) to determine how homogeneous the filter element had been pressed by determining the porosity (pressure used not equal over the length of the sample).

[51] injection pressure of 200MPa and a contact angle of 130° and surface tension of 0.485N/m

4.3.6 Hydraulics

Hydraulic conductivity (permeability), K, is defined as the ability to conduct water under a unit hydraulic gradient. The K is intrinsic to the ceramic and is determined by the pore size, pore size distribution, tortuosity and total porosity. K is normally expressed by Darcy's formula: $K = Q\,L\,A^{-1}\Delta h^{-1}\Delta t^{-1}$, where K, hydraulic conductivity (cm sec-1); Q, volume of water (cm^3) flowing through a given area in a given time; L, length through which water flows (cm)- or thickness of the ceramic filter; A, cross-sectional area through which water flows (cm^2); Δh, hydraulic gradient across which flow takes place (cm, height of water column) and t (sec), time interval during which flow was measured (Poehls and Smith, 2009).

A number of authors investigated the relationship between permeability and other pore related factors:

1. Zand *et al* (2007) pointed out the importance of permeability when they tested a range of natural and cement-based materials and showed that although porosity only varied between 0.1 and 0.3, permeability for construction materials varied by a factor of 100. This showed the sensitivity of permeability to pore size (length of the scale system). Zand *et al* (2007) further tested this variation by using a different approach to the measurement of permeability. They drilled a small opening (blind hole approach) in the material to be tested which was then filled with water. Calculations are illustrated in Figure 4.12 and the blind hole in Figure 4.13:

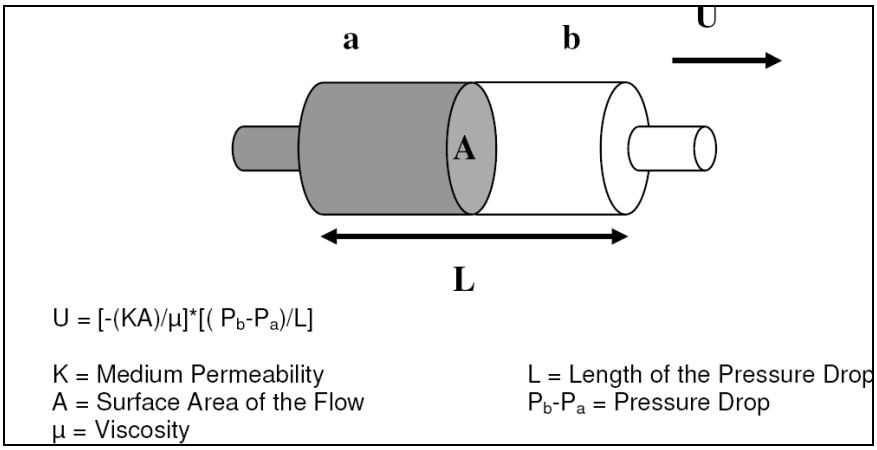

Figure 4.12: Using Darcy's Law to calculate K (Zand et al 2007)

From Darcy's law, that provides the radial water velocity, u, with viscosity, μ, through an isotropic porous filter of permeability, K, as:

$$u_r = -\frac{K}{\mu}\frac{dp}{dr} \qquad (1)$$

With dp/dr, pressure gradient across radius and radial velocity defined as $u_r = \varphi d_r/d_t$, and φ as the porosity of the filter. According to him the test can be conducted either using constant flow rate or constant pressure. In the constant pressure example, $\Delta\rho$, radius of the hole at $t = 0$, r_0, the radial flow front, r_f, moves with time as follows:

$$r_f^2\left(2\ln\left(\frac{r_f}{r_0}\right)-1\right)+r_0^2 = 4\frac{K\Delta p}{\mu\phi}t \qquad (2)$$

The linear form for equation 2 can be simplified to $Y(r_o, r_f) = \kappa t$.

Then permeability, κ, can then be directly determined from the slope of a straight line (linear) drawn through a best fit of the data points:

$$K = \frac{\mu\phi}{4\Delta p}\kappa \qquad (3)$$

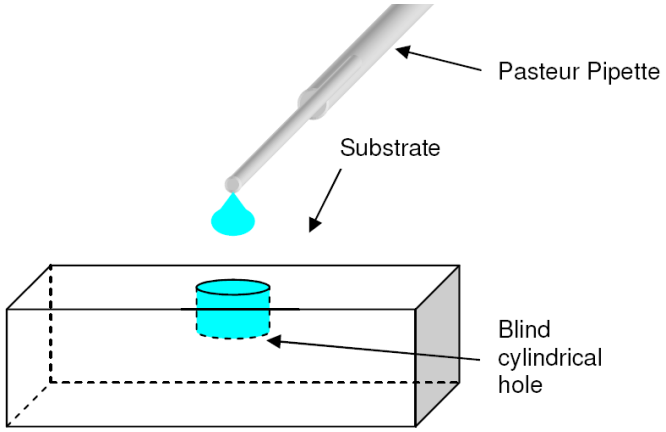

Figure 4.13: Blind hole approach for measuring permeability (Zand et al 2007)

2. Vidal *et al* (2009) looked at permeability and packing structure. They determined that porosity was not sufficient for describing the ceramic packing structure, but rather that permeability (hydraulic conductivity) was a much better indicator of packing structure, because of its sensitivity to structural differences. Permeability is furthermore uniquely defined at low Reynolds numbers by the Darcy's equation.

3. Fahlin (2003) determined the tortuosity of a ceramic filter by using bromine as a tracer and measuring the retention time of the bromine during a filtration test. The conclusion from the study indicated that water spent a minimum of 50 minutes within their filter before breakthrough of the tracer occurred. Table 4.2 lists the variables they used for calculating tortuosity and hydraulic conductivity (constant flow rate).

Table 4.2: Parameter definitions and equations (Fahlin 2003)

Parameter	Units	Description
Q	mL/min	Flow through the filter; $Q = KA\frac{\Delta h}{L}$
K	cm/min	Hydraulic conductivity (measure of how well water travels through the media)
A	cm^2	Cross Sectional Area of the filter the water travels through
? h	cm	Difference in head between the influent and effluent of the filter
L	cm	Shortest linear length the water travels through the filter
D	cm^2/min	Dispersion coefficient (movement of molecules away from each other); $D = D_m\tau + \alpha_L v$
D_m	cm^2/min	Molecular dispersion coefficient of the tracer used (bromide)
t	unitless	Tortuosity is the ratio of the actual distance the water travels over the shortest linear length; $\tau = \frac{Le}{Ls}$
a_L	cm	Longitudinal dispersivity, which is a property of the porous medium and is related to pore structure.
v	cm/min	Theoretical actual velocity of the water through the pores – should not be confused with Darcy's velocity
Le	cm	Theoretical actual distance the water travels
Ls	cm	Shortest linear length the water travels through the filter

4. Finally Li *et al* (2006) investigated the relationship between permeability and microstructure parameters for improving filtration. Microstructure (pore diameter and porosity) have a large impact on filtrate flux and retention.

In the past the ceramic filtration has been viewed as a black box with only product variables such as porosity and particle packing being tested. The importance of permeability and the relationship of permeability with these variables have been shown to be more important in filter characterisation.

4.4 Microbiological testing

4.4.1 Test criteria

This section identifies relevant water filter microbial performance specifications from literature that provides a microbial performance target and testing protocol for household water treatment systems (HWT).

Lantagne (2001) describes the three modes of waterborne disease transmittal and presents their worldwide impacts in Table 4.3 below:

a) waterborne diseases: from human or animal waste infected by pathogenic bacteria and viruses, transferred by drinking contaminated water or food
b) water-washed diseases: from lack of sanitation (lack of adequate supply of water) certain diarrheal diseases and communicable eye and skin infections can result
c) water-supported diseases: part of parasite life cycle development in water.

Table 4.3: World health impact from waterborne diseases (Lantagne 2001)

Disease	Morbidity (per year)	Mortality (deaths / year)	Population at risk
Waterborne & water-washed			
Cholera			
Diarrheal disease	1,500 million episodes in children under 5	4 million in children under 5	Over 2,000 million
Enteric fevers	500,000 cases	25,000	
Poliomyelitis	204,000	25,000	
Ascariasis (roundworm)	1,000,000	20,000	
Leptospirosis			
Trichuriasis			
Water-washed			
Trachoma	6 – 9 million blind		500 million
Leishmaniasis	400,000 new infections / year		350 million
Relapsing fever			
Typhus fever			
Water-based			
Schistosomiasis	200 million	200,000	500 – 600 million
Dracunculiasis	Over 10 million		Over 100 million

Lantagne (2001) furthermore presents an additional table (Table 4.4 and Table 4.5) with the waterborne bacteria types, sizes (A) and disease causing organisms (B):

Table 4.4: A- Bacteria types and sizes (Lantagne 2001)

Shape	Name	Size
Spherical	cocci, coccus	1 – 3 µm in diameter
Rod	bacilli, bacillus	0.3 – 1.5 µm in width 1.0 – 10 µm in length
Curved rod	vibrios	0.6 – 1.0 µm in width 2 – 6 µm in length
Spiral	spirilla	up to 50 µm
Filamentous		up to 100 µm and longer

Table 4.5: B- Waterborne disease causing organisms (Lantagne 2001)

Organism	Disease	Remarks
Bacteria		
Escherichia coli	Gastroenteritis	Diarrhea
Legionella pneumophila	Legionellosis	Acute respiratory illness
Leptospira	Leptospriosis	Jaundice, fever
Salmonella typhi	Typhoid fever	Fever, diarrhea
Salmonella	Salmonellosis	Food poisoning
Shigella	Shigelloisis	Bacillary dysentery
Vibrio cholerae	Cholera	Heavy diarrhea, dehydration
Yersinia enterolitica	Yersinosis	Diarrhea
Viruses		
Adenovirus	Respiratory disease	
Enteroviruses (67 types, including polio, echo, etc.)	Gastroenteritis, heart anomalies, meningitis	
Hepatitis A	Infectious hepatitis	Jaundice, fever
Norwalk agent	Gastroenteritis	Vomiting
Reovirus	Gastroenteritis	
Rotavirus	Gastroenteritis	
Protozoa		
Balantidium coli	Balantidiasis	Diarrhea, dysentery
Cryptosporidium	Cryptosporidiosis	Diarrhea
Entamoeba histolytica	Amebiasis	Diarrhea, bleeding
Giardia lamblia	Giardiasis	Diarrhea, nausea, indigestion
Helminths		
Ascaris lumbricoides	Ascariasis	Roundworm infestation
Enterobius vericularis	Enterobiasis	Pinworm
Fasciola hepatica	Fascioliasis	Sheep liver fluke
Hymenolepis nana	Hymenolepiasis	Dwarf tapeworm
Taenia saginata	Taeniasis	Beef tapeworm
T. solium	Taeniasis	Pork tapeworm
Trichuris trichiura	Trichuriasis	Whipworm

From Table 4.4 and Table 4.5, together with the WHO (2011) performance requirements for HWT technologies, it is clear that a standarised approach that combines microbial performance with health outcome targets are necessary for testing water filters.

Kupper *et al* (2009) list and compare alternative water disinfection methods (Table 4.6). They found ceramic water filters to be the only absolute safe disinfection method at higher altitudes.

Table 4.6: Water disinfection methods (Kupper et al 2009)

Procedure	Safe for				Remarks
	Viruses	Bacteria	Cysts (*Giardia*, amebic) & eggs of helminths	*Cryptosporidium*	
Boiling	+	+	+	+	Fuel consuming/ deforestation
Chemical disinfection[a]	+	+	(+)	+[b]	May be critical if water is very cold or contains organic substances[c]
Ceramic filter[d]	(+)[e]	+	+	+[f]	Type specific failures/ limitations may become clogged, need to clean
Chemical disinfection + ceramic filter	+	+	+	+[b,f]	The only absolute safe procedure at high altitude
Sand filter	−	(+)[e]	(+)[g]	n.d.	Fine sand and low flow necessary
Charcoal filter	−	(+)[e]	(+)[g]	n.d.	Low flow necessary
Sand + charcoal filter	−	(+)[e]	(+)[g]	n.d.	Fine sand and low flow necessary
Textile filter	−	(+)[e]	(+)[f]	n.d.	The tighter the textiles, the better the filter effect

(+: safe; (+): safe with some limitations, see footnotes; −: not safe; n.d.: no data available).
[a] With (hypo-) chlorite.
[b] High ct constant necessary.
[c] Longer disinfection time or higher concentration of disinfectant necessary.
[d] (or other filters with pores <0.2 μm).
[e] Not safe, but reduces concentration of microorganisms.
[f] Pore size <1 μm necessary.
[g] ''nearly safe'' (up to 100% elimination of most microorganisms, but a total remove of cysts and eggs cannot be guaranteed).

Some of the performance criteria for ceramic water filters, as derived from the literature, are as follows:

- According to Aqua Rain (1998), the US EPA standard for bacteria is the removal of 99.9999% (LRV = 6) of *Klebsiella terrigena* with a new filter.
- EPA (2006) shows the importance of pore size (the full stop at the end of this sentence is 500 micron in size). The recommendation is to use the criteria of absolute (largest) pore size and not nominal (average) pore size. An absolute one micron filter is recommended for removal of *Cryptosporidium*.
- According to Wegmann *et al* (2008a), there are a number of technologies (each of them aimed at providing proficient performance while reducing complexity and costs) available for eliminating viruses from water. Sometimes it is only by a combination of methods that virus removal is in excess of 99.9 per cent (LRV= 3).

Reverse osmosis membranes is the only technology that provides this high level of protection but it is also restricted in terms of low flow rate, membrane blockage and extreme costs.

- Holmes (1996) provides the South African drinking water testing criteria for heterotrophic, total- and faecal coliform plate count ranges (Table 4.7).

Table 4.7: Target ranges and effects of microbial infection (Holmes 1996)

Heterotrophic Plate Count Range (counts/1 m•)	**Effects**
Target Water Quality Range 0 - 100	***Negligible risk of microbial infection***
100 - 1 000	Indicative of inadequate treatment, post-treatment contamination or aftergrowth in the water distribution system. Slight risk of microbial infection
> 1 000	Indicative of poor treatment, post-treatment contamination or definite after-growth in the water distribution system. Increased risk of infectious disease transmission

Total Coliform Range (counts/100 m•)	**Effects**
Target Water Quality Range 0 - 5	***Negligible risk of microbial infection***
5 - 100	Indicative of inadequate treatment, post-treatment contamination or growth in the distribution system. Risk of infectious disease transmission with continuous exposure and a slight risk with occasional exposure
> 100	Indicative of poor treatment, post-treatment contamination or definite growth in the water distribution system. Significant and increasing risk of infectious disease transmission

Faecal Coliform Range (counts/100 m•)	Effects
Target Water Quality Range 0	***Negligible risk of microbial infection***
0 - 10	Slight risk of microbial infection with continuous exposure; negligible effects with occasional or short-term exposure
10 - 20	Risk of infectious disease transmission with continuous exposure; slight risk with occasional exposure
> 20	Significant and increasing risk of infectious disease transmission. As faecal coliform levels increase, the amount of water ingested required to cause infection decreases

The WHO (2011) takes the test criteria listed above a step further by providing $\log_{10}$ reduction criteria for reference microbes for interim, protective and highly protective performance. Table 4.8 presents health-based microbiological performance targets for HWT systems. Their testing protocol includes bacteria, viruses and protozoa and makes suggestions and recommendations for reference microbes to be used. WHO (2011) recommend that technologies should be as effective as possible against all three classes of microbes. Should they be effective against two and not three classes of microbes, the technology used should also show epidemiological evidence of improved health impacts.

Table 4.8: WHO (2011) performance requirements for HWT technologies and reduction criteria

Reference microbe used in dose–response model	Assumed number of microbes per litre used in risk calculations[a]	Pathogen class	$\log_{10}$ reduction required		
			Interim	Protective[c]	Highly[c] protective
			Requires correct, consistent and continuous use to meet performance levels		
Campylobacter jejuni	1	**Bacteria**	Achieves "protective" target for two classes of pathogens and results in health gains	≥ **2**	≥ **4**
Rotavirus	1	**Viruses**		≥ **3**	≥ **5**
Cryptosporidium	0.1	**Protozoa**		≥ **2**	≥ **4**

4.4.2 Ceramic filter microbial test results

Bielefeldt *et al* (2009) showed that meeting the criteria for ceramic filters to be difficult for low cost ceramic filter producers. They tested 6 different ceramic filters using a concentration of 10^6 CFU/ml of *E coli* influent water and obtained only a 3 to 4 Log (LRV) improvement.

For viral protection, Wegmann *et al* (2008b) went a step further by modifying commercial micro porous ceramic filters to adsorb viruses by coating the ceramic filter with ZrO_2 nano powders through dip-coating and heat treatment. The result was that the target virus was attracted to the positively charged filter surface. The coating changed the iso-electric point from pH 3 to pH range 5 to 9. The original uncoated filter retained 75 per cent of MS2 bacteriophages, whereas the coated filter resulted in a 7 log removal. The specific surface area also enlarged from 2 m^2 g^{-1} to between 12- 25 m^2 g^{-1}, providing a larger absorptive surface for virus removal.

4.4.3 Ceramic filter testing with the membrane filter technique

The membrane filter technique is one of the standard methods of water analysis; it is mainly used as a technique for measuring coliform density in water, as recommended by the American Public Health Association.

This technique is known to have various advantages over other techniques which could possibly be used for water analysis, including the pour plate technique and the spread plate technique. Advantages of these techniques include (Mathibela 2012):

- The ability to obtain results in a shorter time (24h)
- Permits a direct count of coliform colonies or colonies of other kinds of bacteria, e.g. *Salmonella.*
- Larger volumes of water can be tested (100ml or more)
- Accurate and reproducible results are possible
- Requires less procedures than many other equivalent methods, and is makes it possible to both isolate and enumerate microbes.
- A technique that is both effective and acceptable for monitoring drinking water.

According to Mathibela (2012), the principal behind the membrane filter technique is that a measured amount of the water sample is filtered using a sterile membrane filter (pore size of 0,45um or smaller), depending on the microbe to be isolated. The filter traps the bacterial cells on the membrane; it is then transferred from the filter assembly onto a selective medium to grow and to differentiate between different groups of bacteria (WHO 2009).

After incubation of the plates, the colony forming units (CFU) are counted to estimate the concentration of bacteria present in the water sample. The CFU should not be less than 20 and a maximum of 80 should be counted in order to confirm the accuracy of the test being conducted. However, if more colonies are detected on the plate containing medium, then tenfold dilutions with sterile water should be made to decrease the bacterial count to a sizable value. If the bacterial count is less than the minimum, then a larger sample should be used to ensure that more bacteria form on the plates for an accurate and effective count to be made (Mathibela 2012).

4.4.4 Challenge water verification of HWT

According to the WHO (2011), the experimental setup for testing the HWT systems should model actual use conditions as closely as possible. Enough test microbes must be present in, or be added to, the test water to enable quantification of the reduction required for the specified health-based target (Table 4.9). Sterile water is inoculated with known concentrations of microbes with different morphologies and filtered through the ceramic filters. Both the influent and effluent water are assayed (enumerative – counting colonies on agar medium) to determine the microbial reduction (WHO 2011).

Choice of microbes

The choice should be based on local and regional pathogens that either present the greatest waterborne disease risk or contribute the most risk. If the laboratory cannot test for such a pathogen, an indicator microbe can be used (*Vibrio chole*rae and be replaced by *E. coli* as indicator organism) Clasen *et al* (2007b).

Challenge water used for inoculation

The WHO suggests two challenges for water to be laboratory-tested (2011), as set out in Table 4.9. For test purposes, the water should model as closely as possible the whole range of possible untreated water sources.

Table 4.9: Recommended challenge water for inoculation of reference microbes (WHO 2011)

	Test water 1	Test water 2
Description	High-quality groundwater, surface water, caught (newly harvested) rainwater or other water free of disinfectant residual	High-quality groundwater, surface water, rainwater or other water free of disinfectant residual with 20% by volume primary wastewater effluent or 1% by volume untreated raw sewage, sterilized or pasteurized
Turbidity	< 5 NTU	> 30 NTU
pH	7.0–9.0	6.0–10.0
Temperature	20 °C ± 5 °C	4 °C ± 1 °C

NTU, nephelometric turbidity unit

4.4.5 Conclusion

The wet processing route was selected as one of the more promising methods of making high-quality ceramic filters. By better controlling the particle contacts, reduction in the size and number of defects could be expected in the finished product. This is as a result of increasing the homogeneity of particle packing in the wet processing stage compared to dry processing methods. Test methods more specific to wet processing evaluation and testing were therefore emphasised in this chapter.

Chapter 5: Experimental Procedure

5.1 Introduction

In this chapter a comprehensive description of the experimental procedure used in producing a porous ceramic filter using the slip casting technique is presented. A newly developed technique, a process formation map (PFM), is presented and used for illustrating the experimental procedure. The remainder of the section will concentrate more on the use and application of the methods used in the experimental procedure, sample preparation and the taking of measurements, whereas the PFM will provide a more detailed outline and methodology which was followed in the filter manufacture.

5.2 Process Formation Map

Putting together a Process Formation Map (PFM): A PFM has been developed as an easy guide through the ceramic water filter production and testing processes. A PFM is printed on a single sheet of paper, double-sided and typically laminated as illustrated in Figure 5.1. Once completed, the PFM two-pager represents the production process at various levels on the front and back pages (Figure 5.1):

a) Column 2: Block flow diagram with 4 to 8 major production steps called Logically Associated Tasks (LATs),
b) Column 3: Sub-steps within each major step with instructions and explanations, usually 1 to 6 sub-steps
c) Column 4 and back page: Supporting photos or graphics
d) Column 1: Defines all the safety and other symbols used (legend)
e) The back page has a variety of supporting information and is customizable

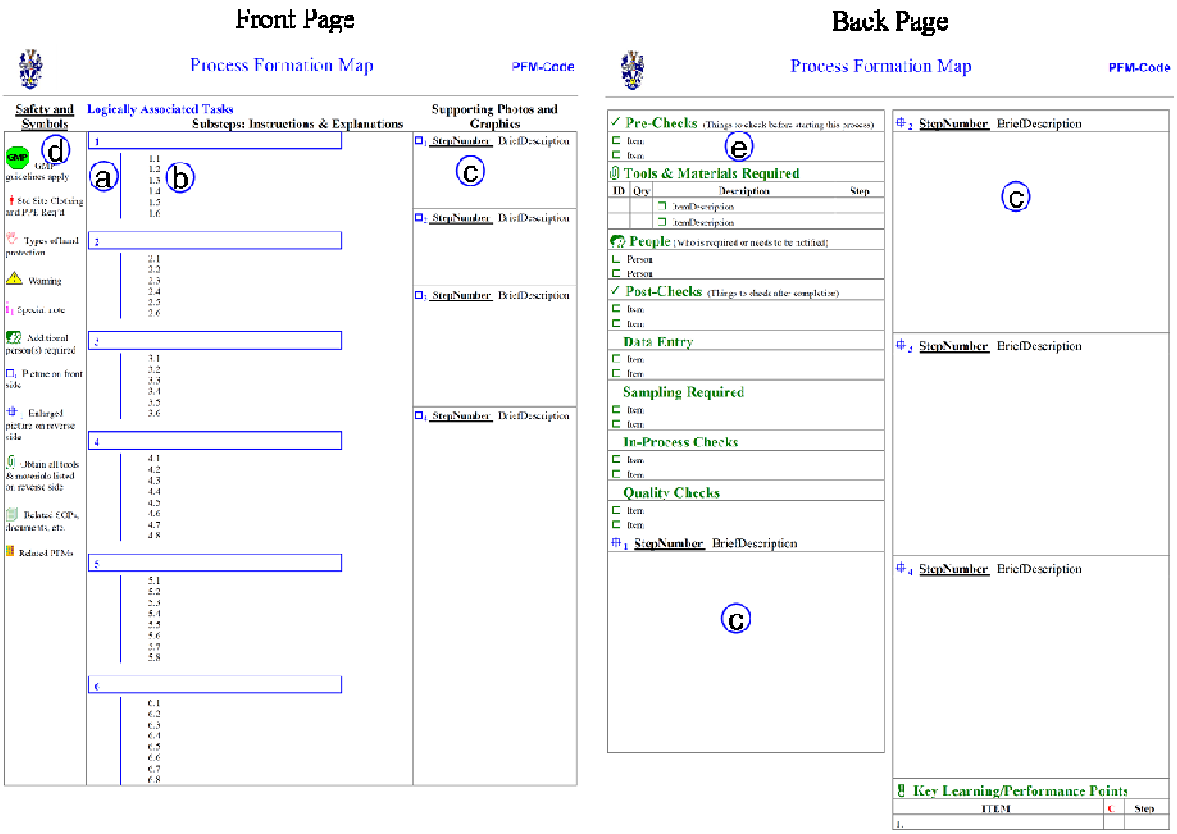

Figure 5.1: Illustration of the PFM layout

The PFM was used in this study to summaries the production process (Table 5.1: Experimental procedure) and the test methods used in the study (hydrometer test, immersion test, constant head permeability test and bacteriological testing).

Figure 5.2 explains the sequence of steps necessary in preparing a PFM for the experimental procedure of the filter manufacture process. The steps involved in preparing the PFM Experimental Procedure:

1. summarise the research and best practice (combination of literature review, practical experience and research)
2. identify and list the main manufacturing steps
3. observe task and take photos to simplify the manufacturing process
4. establish pre-checks, process checks and product tests
5. write procedures(front page): instructions and explanations, insert photos, cross-references

6. write additional information (back page): expand on the steps, include hazards and reminders
7. complete the PFM template
8. review for best practice: check against documentation and test procedures using PFM
9. use relevant symbols and place next to steps by using Copy & Paste.
10. present the final PFM procedure for producing the ceramic as shown in the Experimental Procedure,

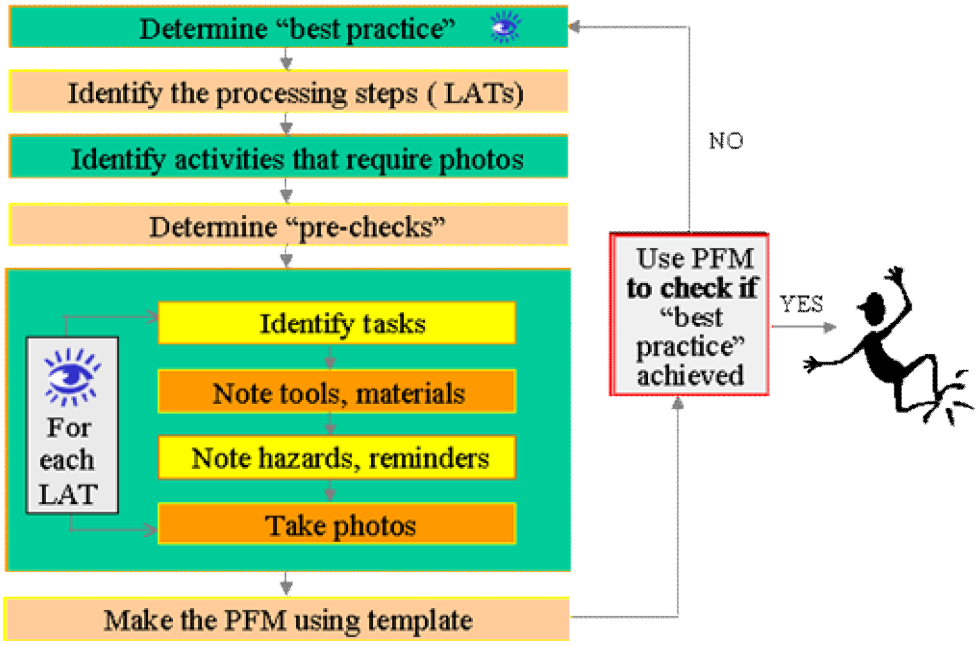

Figure 5.2: Steps used to develop the PFM: Experimental and testing procedures

Table 5.1: Porous ceramic manufacturing procedure

University of Zululand

Procedure Overview **Instructions & Explanations**

UTBAC Ceramic Water Filters

Safety

Use lab coat for processing and finishing steps

Surgical gloves when handling final product

Leather gloves or clamp tool when loading and off-loading kiln

☐ Picture on front side

☐1 Jar Mill

☐2 Plaster molds

☐3 Slip Casting

☐4 Packing for Firing

⌖1 Enlarged picture on reverse side

⌖1 Milled PSD

⌖2 Firing schedule

⌖3 Finishing

⌖4 Testing

⌖5 Filter operation

Related SOPs,.

PFM 1: Microbiological Testing

PFM 2: Constant Head Permeability

PFM 3: AP, WA, ASG, BD testing by boiling water

PFM 4: PSD

1 Source and prepare raw materials

1.1 Source raw materials (RM) from suppliers
1.2 Test the particle size distribution (PSD) ⌖1
1.3 Develop recipe and then batch the RM
1.4 Prepare RM by ball milling for 15h and 30h ☐1
1.5 Add carbon source to milled fractions and condition for 1-2 h in ball mill.
1.6 Remove from mill and pour into slow RPM planetary mixer (Kenwood).
1.7 Test for flow time and slip density (SG)

2 Make and condition mold

2.1 Clean master mold
2.2 Position master on clean glass plate and centralize PVC pipe ring around master.
2.3 Close all gaps with sticky plaster
2.4 Mix plaster into water (2:1 ratio), remove all lumps. Cast into mold and wait for hydration to start (plaster heats-up)
2.5 Remove master using a twisting action
2.6 Leave overnight to set then dry for 24 hr at 50°C
2.7 Condition by pouring water into mold and decanting immediately☐2

3 Cast the slip into plaster molds

3.1 Pour slip from mixer into plaster molds
3.2 Keep mold full and leave slip in mold until sufficient wall thickness has been achieved !!!
3.3 Decant excess slip and leave upside down for casting to dry and excess slip to drain☐3
3.4 Strip product, and place in drier at 90°C ☐2

4 Dry and burn-out the green body

4.1 Remove product from drier (24 hr)
4.2 Pack filters on expanded metal trays in kiln
4.3 Pre-fire using pre-determined firing cycle ⌖2
4.4 Ensure kiln is well ventilated for removal of volatiles ☐4

5 Fire the body

5.1 Check for cracks or defects
5.2 Cover kiln trays with 3-5mm layer of fused ☐4 silica fines. Re-pack with gaps onto kiln trays
5.3 Fire using pre-determined firing cycle ⌖2

6 Finish and glue filter to plastic fitting

6.1 Inspect for cracks or defects
6.2 Finish filter evenly on disk sander⌖3
6.3 Drill 1.5mm hole in plastic flange
6.4 Heat-seal screen onto flange opening.
6.5 Clean plastic with acetone to remove oil layer.
6.6 Brush primer (Primer 3-N) on filter base. Leave to stand for 2 hours.
6.7 Fill ceramic with activated carbon granules.
6.8 Glue ceramic onto plastic fitting and remove excess glue. Leave to dry for 24 hr and package.

7 QA Test the filters

7.1 Determine porosity using 3 methods: water immersion, Hg porosimetry and SEM
7.2 Carry out XRD analysis on the sintered product
7.3 Perform constant head permeability test ⌖4
7.4 Conduct microbiological testing on filtrate

8 Assemble filter system

8.1 Drill holes in buckets and lid for filters and tap. Assemble and package⌖5

☐1 **1.5** Jar (Ball) mill

☐2 **2.6** Master- and plaster molds and product after stripping

☐3 **3.3** Slip casting process

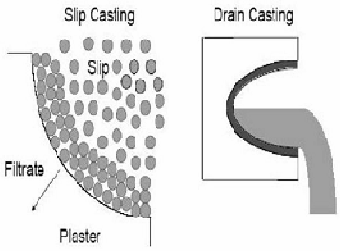

☐4 **4.4** Packing for pre (A)- and final firing (B)

✓ Pre-Checks (Things to check before starting this process)

- ☐ Raw material particle size distribution
- ☐ Plaster mold cleanliness and state of drying

Equipment & Materials Required

ID	Qty	Description	Step
	3	☐ Raw materials	1
	1	☐ Ball Mill	1
	1	☐ Planetary Mixer	1 & 3
		☐ Dryer & Kiln	4 & 5
		☐ Test equipment (See)	7
		☐ Containers & parts for filter assembly	8

✓ Post-Checks (Things to check after completion)

- ☐ 100% Inspection for cracked items (reject all items with cracks)
- ☐ Porosity by water immersion (BD & SG) and SEM tests
- ☐ Pore Size Distribution using Hg
- ☐ Constant head permeability tests
- ☐ Microbiological test results

1 PSD requirement for milled raw material

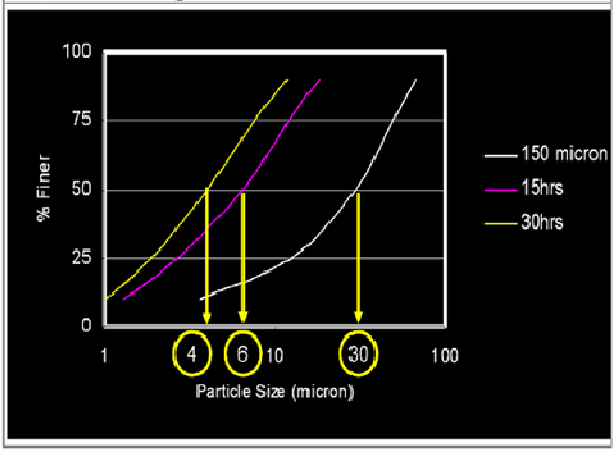

2 7 Burn-out (---) and sintering (——) schedules

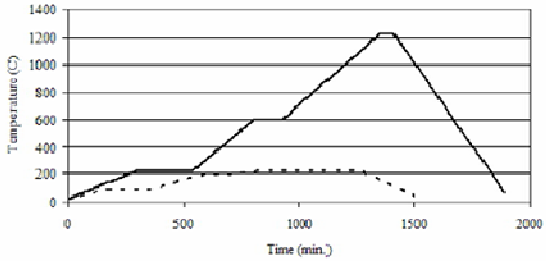

3 6 Finishing of the filter

4 7 Constant head permeability testing of filter

5 8 Operating the filter

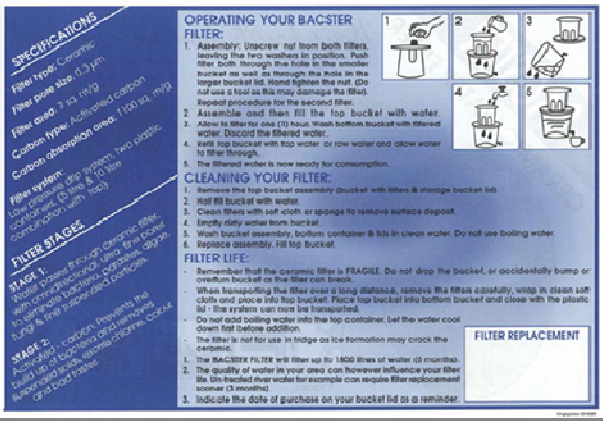

5.3 Raw materials selection and preparation

Based on the literature review, the aim was to select raw material suitable for the preparation of an acceptable slip with possible dilatant or shear thickening rheology (where particle collisions intensify as shear rate increases). Dilatancy would maintain the viscosity at a level that would support the largest grains, ensure a homogenous suspension, prevent segregation and give a high density cast, strong enough for further processing steps.

SWOT analysis, personal experience, as well as the following factors from literature study was used in selecting the most suitable raw material:

- high temperature properties of materials
- chemical and physical properties of RM
- PSD of the raw material components
- green body particle packing
- maximum slip solids content
- slip (de)flocculation status (no additives required)
- particle-particle collision intensity
- settling from the slip

5.3.1 SWOT Analysis for material selection

The SWOT analysis, as shown in Figure 5.3, was performed to narrow down the number of raw material possibilities. The responses for the analysis came from personal experience as well as from the extensive literature survey presented in the previous chapters. The chemical analyses and datasheets for the final selection (containing PSD) were sourced from the suppliers and are presented in Chapter 6.

	Favourable Properties	Unfavourable Properties
	Strengths	**Weaknesses**
Internal	a) What is the material's strengths? b) Why does it work better than other materials? c) What unique capabilities and properties does the material possess? d) What is the material's perceived strengths from literature?	a) Material weaknesses? b) Why does it not perform better than other materials? c) What can be done to improve the material? d) What are the perceived weaknesses of the material from literature?
External	**Opportunities** a) What material trends or conditions may positively impact manufacturing? b) What opportunities are available for using the material?	**Threats** a) What material trends or conditions may negatively impact manufacturing? b) How can materials used by low cost competitors impact manufacturing? c) How will material price hikes or shortages impact manufacturing? d) What impact do material weaknesses have on manufacturing?

Figure 5.3: Raw materials selection process using a SWOT analysis

5.3.2 Heat-resistant porous ceramic

The thermal shock resistance of the product was important in the raw material selection process. Normally ceramic materials have improved high temperature properties compared with metallic or high molecular materials (Park *et al* 2010). Materials with heat resistant properties are, however, not sensitive to thermal shock which allows the green body to be fired and cooled at a more rapid rate than materials susceptible to thermal shock.

Critical also to the process is the first firing process (burn-out) where huge amounts of volatiles are generated requiring sufficient time for the process to be completed. The process is exothermic and therefore difficult to control the temperature and therefore the use of thermal shock resistant materials is important.

Free silica (quartz) in the raw materials was limited due to its volume expansion at 570°C and 870°C. This volume expansion is shown in Figure 5.4.

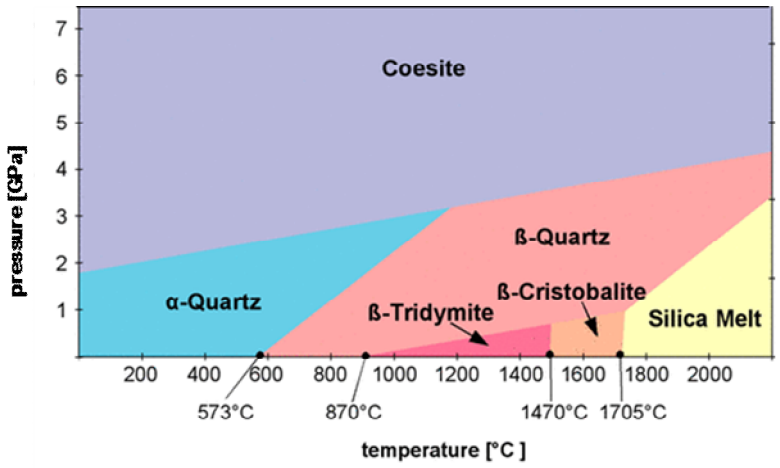

Figure 5.4: Quartz (silica) phase inversions at various temperature and pressures (The Quartz Page, 2012)

To overcome the quartz inversions (Figure 5.4) the LAS (Li_2O-Al_2O_3-SiO_2) system was looked at for the preparation of slip and product with thermal shock resistance properties. Based on Hummel (1951), lithium alumino silicate was selected because of its zero thermal expansion ("ZTE"- acronym) at 1250ºC and therefore its superior thermal shock resistance in ceramics, its price and availability in South Africa as well as its particle size range (-200 mesh). Cenospheres, part of the ash discards from coal fired power stations, was looked at to act as a heat resistant filler (already been exposed to heat treatment), particle shape (spherical) and as coarse particle size contributor to the slip PSD.

Initially slip was prepared by ball milling lithium alumino silicate (Li_2O-Al_2O_3-$8SiO_2$) and cenospheres (Al_2O_3-$2SiO_2$- $0.2Fe_2O_3$) until suitable PSD was obtained. The slip was cast into plaster moulds, stripped, dried and the green product fired to 1250ºC as prescribed by Hummel (1951).

The thermal shock resistance of the fired product was determined by using a direct heating method (LPG-gas flame) to simulate extreme differential thermal expansion before inserting into water at room temperature. The sample was then inspected for defects (cracks). The process was repeated 3 times.

5.3.3 PSD requirements using ball milling

The raw materials selected required further processing to obtain a better particle size distribution, agglomerate reduction and particle shape for the final batching (recipe) step. A laboratory-sized jar (ball) mill that operates on a rotating mill rack was developed for the purpose of further milling of the raw materials.

The mill was made with a steel shell of which the inside, including the inside of the lid, had to be covered with a food-grade, polyurethane liner. This prevented contamination from the steel lining affecting the slip. The other parts of the mill included a clamping mechanism for sealing the lid to the shell. Another mill could be acquired to double production. The mill has a capacity of 8-10 l. See the Table 5.1 for a photograph of the jar mill.

For the milling rack, a strong steel frame was welded together and 3 rubberised rollers with bearings were fitted to the rack. An electric motor (single phase) was then fitted with a pulley system supplying the correct rotation speed to the mill.

5.3.4 Size distribution analysis

As discussed in Chapters 2 and 3 a precise grading of the particle sizes enables one to make a slip with good mixing, casting properties and with good mechanical properties. Particle size analysis, as explained previously, can be performed using the following methods:

- Sieving
- Hydrometer sedimentation technique
- Laser light scattering technique (Particle size range 0.02-2000µm)
- X-Ray scattering method
- Microscopy

Hydrometer sedimentation and laser light scatttering analyses were used to best determine particle size distribution of the raw materials.

The other methods were not used due to their particular limitations in measurement of particle size. The microscope was only used in pore size identification because of the severe limitation of optical microscopy which was its small depth of focus at large magnification and its diffraction effects that increase and causes blurring at the edges for particles < 3µm in size. For submicron particles (0.001-5µm) it is necessary to use either, TEM (Transmission Electron Microscopy) or SEM (Scanning Electron Microscopy). Sieving was also not practical because the materials were already smaller than 75 micron (200 mesh) in size. Figure 5.5 furthermore illustrate some of the problems of trying to force a particle through the welded mesh of the screen.

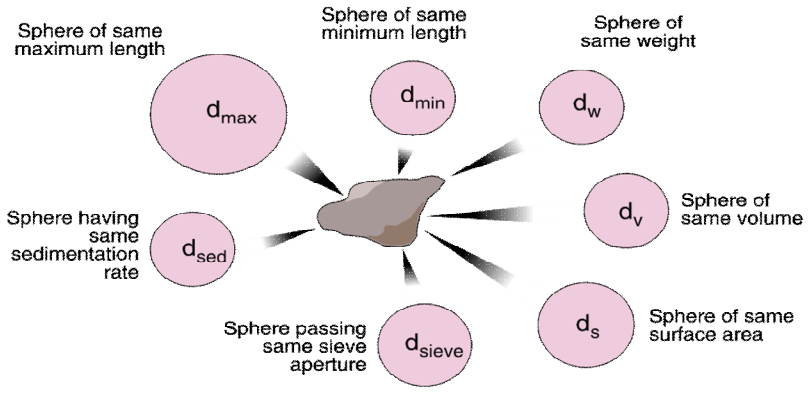

Figure 5.5: Particle shape and density issues related to a screen analysis

For some of the materials the PSD's were also obtained from the raw material suppliers' datasheets. The hydrometer is discussed using the PFM: Hydrometer Particle Size Analysis in Table 5.2.

5.3.4.1 Hydrometer method

The PSD of the fine material was determined by examining the settling from a suspension of the powder (Table 5.2). The method required two categories of measurement:

1. incremental: concentration of the suspension at known depths over a set time period was measured. The method used is either a fixed time or a fixed depth technique. Fixed depth method was used.

2. cumulative: the rate at which the powder is settling from the suspension was calculated; the accumulation of particles was measured at specified depth.

Advantages

- Equipment required was relatively simple, available and inexpensive.
- Accurate and reproducible measurement of a wide range of sizes.

Disadvantages

- Large particles created turbulence, slowed down and were therefore recorded as undersize.
- Sediment analyses were determined at low concentrations for interaction between particles to be reduced so that their terminal settling velocities could be taken as equal to those of isolated particles.
- Particle size lower limit had to be set due to increasing Brownian motion.
- Careful temperature control was necessary to reduce convective movement.
- Particle re-aggregation during extended measurements could have occurred.
- Particles had to be completely insoluble in the suspending liquid thereby limiting the analyses to the inorganic particles only.

Table 5.2: Hydrometer test procedure

Hydrometer Particle Size Distribution (PSD)

PFM-1

University of Zululand

UTBAC Ceramic Water Filters

Procedure Overview **Instructions & Explanations**

GMP guidelines apply

Std Site Clothing and PPE Req'd for CALGON

Rubber gloves for CALGON

Warning

i_1 Special note

Additional person(s) required

$\square_1$ Picture on front side

$\square_3$ Dispersion

$\square_4$ Measuring cylinder with hydrometer

$\#_1$ SG correction

$\#_2$ Viscosity/T corrections

$\#_3$ T recording

Obtain all tools & materials listed on reverse side

Related PPMs

ASTM D3360-96

ASTM D 422-63

1 Disperse sample

1.1 Stir 40g sodium hexametaphospahate into 1 l distilled water.

1.2 Weigh out 30g of dry material into mixing cup.

1.3 Add 125ml of dispersant water into 250 ml mixing cup to cover sample. Soak overnight. $\square_3$

1.4 Add more distilled water while stirring until cup is half full. Stir for 1 m

2 Test with hydrometer

2.1 Immediately after dispersion, transfer sample slurry into cylinder making sure that full sample transfer occurs (wash cup with water) $\square_2$ $\square_4$

2.2 Close cylinder with hand palm and invert a number of times for 1 m (60 times)

2.3 Slowly insert hydrometer and take readings (SG) at the following time intervals: 1, 3, 5, 10, 20, 30 m and 1, 2, 4, 7, 14, and 24 h, reading from the top of meniscus. $\square_4$

2.4 After every reading remove hydrometer, rinse and float in blank reference cylinder

2.5 Record, T, time and reading on attached form

3 Perform Calculations

3.1 Calculate % sample remaining in suspension at the measuring depth of hydrometer, P = (Ra/W) x 100 $\square_1\square_2$

3.2 Calculate diameter of sample at time T, D = K*SQRT L/T $\square_1$

4 Report

4.1 Record readings on table $\square_4$

4.2 From table plot a graph of particle diameter on the x- axes (Log scale)

4.3 % Smaller than corresponding diameter on y- axes using a normal scale

5 Calibrate

5.1 Hydrometer is calibrated at 20°C, variations in temperature produces inaccuracies in readings

5.2 Readings should be taken at bottom, therefore correction have to be applied when taking reading at top of meniscus

5.3 Prepare cylinder filled with dispersant and water (ratio) and 2 ranges of temperatures. Read at top of meniscus at T1 subtract from 0, repeat for T2

$\square_1$ **StepNumber** Variable description

- a: correction factor (Table 1)
- P: % material remaining in suspension
- R: hydrometer reading
- W: sample mass (oven dried)
- D: diameter of particle, mm
- n: coefficient of suspension viscosity
- L: effective reading depth (Table 2)
- T: cumulative time at taking of reading
- K: constant depending on T and SG of sample

$\square_2$ **StepNumber** PSD by application of Stokes Law

- test accuracy depends on obtaining complete and stable deflocculating of sample
- apply law by sedimentation of particulate material from initial homogeneous suspension
- use any systematic set of measurements which permit determination of suspension density (% solid)
- measured at some defined distance beneath surface of suspension
- measured at some appropriately selected series of sedimentation time durations, can be converted into PSD
- observe suspension density at effective distance below surface of center of gravity of floating hydrometer at a series of convenient time intervals (exponential)

$\square_3$ **StepNumber** Dispersion

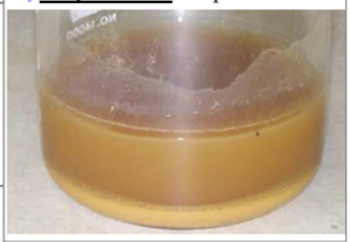

$\square_4$ **StepNumber** Hydrometer

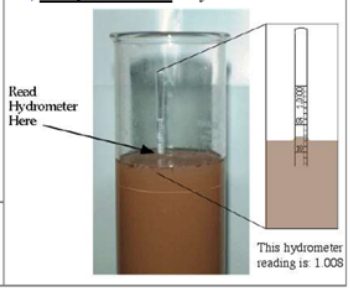

✓ Pre-Checks (Things to check before starting this process)

- ☐ Distilled water at constant temperature of 20°C
- ☐ Deflocculated sample

Tools & Materials Required

Quantity & Description	Step
☐ Sedimentation cylinder	
☐ Thermometer	
☐ Stopwatch	
☐ High speed stirrer	
☐ Dispersant	
☐ Hydrometer	

#1 StepNumber SG Correction

TABLE 1 Values of Correction Factor, α, for Different Specific Gravities of Soil Particles[A]

Specific Gravity	Correction Factor[A]
2.95	0.94
2.90	0.95
2.85	0.96
2.80	0.97
2.75	0.98
2.70	0.99
2.65	1.00
2.60	1.01
2.55	1.02
2.50	1.03
2.45	1.05

[A] For use in equation for percentage of soil remaining in suspension when using Hydrometer 152H.

#2 StepNumber Viscosity, temperature correction

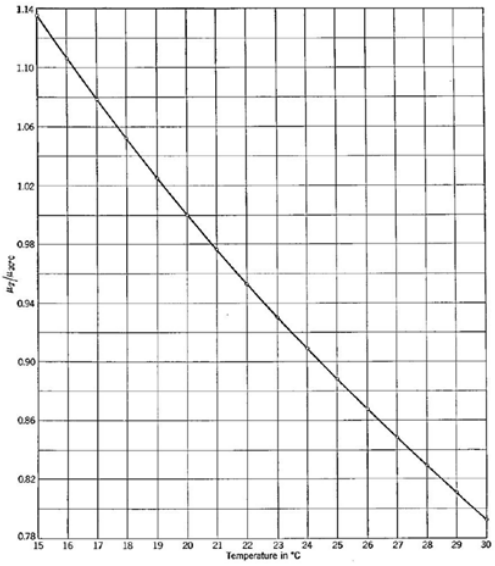

#3 StepNumber Temperature recording

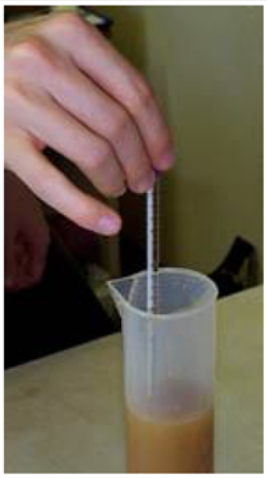

Performance Points

ITEM	C	Step
1.		
2.		
3.		

5.3.4.2 Laser diffraction

Particle size distributions for all raw materials as well as the ball milled fractions were determined using the MALVERN laser diffraction analysis for determining particle size distributing following Stokes Law. Laser diffraction analysis was performed by a laboratory (Syncat, Richards Bay). The particles fall through a laser beam and the light scatter is collected for a range of angles. The angles of diffraction are inversely related to the particle size. Distribution of scattered light intensity is then calculated by computer software to yield the PSD.

Advantages:

- Fast and typically took about 5 minutes to take a measurement and analyse.
- Precise and wide range of 64 size bands could be displayed covering a wide range in particle size.
- It is an absolute measurement, which required no calibration
- Simple to use

Disadvantages:

- Expensive
- Assumes spherical particles
- There had to be a difference in refractive indices between particles and suspending medium

5.3.5 Application of the packing models

Previous packing models (Furnas and Andreassen) have shown that a slip with a particle size distribution that follows the models (best fit PSD) pack into a dense body. The packing model and best fit PSD depends on the chosen distribution coefficient, q-value (assuming constant water addition and a well dispersed system) as explained in Section 3.1.2.12.2: Packing model. Previous authors (Dinger and Funk 1993) found a q-value of 0.30 to give good flow and dense packing.

5.3.5.1 Spreadsheet: composite PSD

Using the EMMA Mix Analyser programme (EMMA 2012), composite particle size distributions of the raw materials was prepared. By manipulating the particle size distribution, it was possible to fit the composite distribution to the packing model of Funk and Dinger (1993) and thereby predict the flowability and packing of the selected raw materials. Using the spreadsheet, it was also possible to reduce the number of raw material fractions by using overlapping fraction sizes. By using this method, raw material recipes for the slip could be prepared according to a predetermined PSD. The predetermined PSD either worked well (casting and body density) or had another mixture property that could be repeated using alternative raw materials. Should a milled fraction change its characteristics (new batch number), the recipe can be adjusted to the desired PSD and therefore correct inter particle spacing (IPS). The results for the selected the raw materials fractions are shown in Chapter 6: Results.

5.3.5.2 Slip recipe

Recipe determination was applied by investigation the PSD of a combination of materials, each with its known PSD. The steps used in obtaining the recipe are described as follows:

1. A library of particle size distributions for different materials (use the particle size distributions from laboratory work or from the supplier's datasheets) was created (Appendix A: PSD for raw materials)

2. The volume per cent (not the weight %) of each fraction was calculated using the density of each material.

3. The composite particle size distribution (EMMA spreadsheet program) for any combination of these materials using the quantity of the individual materials was determined. The parameters q-value and maximum particle size as required by the Andreasen Model (Andreasen and Anderson 1930) were used as input.

4. The distribution in a graphical format was plotted

5. The graph was compared with the graph of the Andreasen model.

The distribution was adjusted to best fit the Andreasen curve by modifying the recipe (Repeat steps 1-4 until closest fit to model can be obtained).

With only a limited number of raw material components available, some sizes were therefore not available in the mix. A "perfect" fit was therefore not always possible, as the distribution of Andreasen is based on a continuous feed of finer-and-finer material (Andreasen and Anderson 1930).

5.3.6 Raw material selection

From the developmental testing of various combinations based on the SWOT analysis, thermal expansion and composite PSD study which included castability tests and rheological measurements, the list of raw materials used in the testing process are presented in the following section. Some of the main properties of the materials are highlighted.

5.3.6.1 Baco-95 Alumina Al_2O_3

Alumina has stable chemical and physical characteristics, and is used widely in ceramic. Various grades of high-purity alumina such as calcined, low-soda calcined, tabular and fused, hydrated, reactive, activated, and cement aluminas are available in the market and can be selected for slip casting (Naito *et al* 2003).

Calcined aluminas in the form of α-A1203 are very stable. The aluminas are produced as a low soda content alumina with particle size and calcination to fit the needs of the ceramics industry. Calcined alumina is ball milled to produce a fine powder, which is called a reactive alumina.

5.3.6.2 Zirconia ZrO2

According to Naito *et al* (2003), zirconia with high purity has an extreme melting temperature of 2700°C which provides for good thermal shock properties. The pure zirconia crystal structure is monoclinic at room temperature but transforms to a tetragonal structure at 1170°C and cubic structure at 2370°C. Unfortunately the monoclinic structure to tetragonal structure transformation is accompanied by a change in volume which results in cracks forming within the sintered structure.

The structure can be stabilized (volume change reduced) by the adding oxides stabilizers (CaO, MgO and $Y_20_{3)}$. The stabilisers form solid solutions with zirconia which makes the tetragonal crystal structure stable at 1170°C. This eliminates the negative phase transformation (volume change) when heating and cooling ceramics.

5.3.6.3 Flyash: Cenospheres

- Cenolite is a lightweight ceramic hollow sphere (balloon), made from SiO_2 and Al_2O_3. Also referred to as microspheres, micro balloons, hollow ceramic microspheres or glass beads, they are separated from flyash by electrostatic followed by flotation methods. Advantages well-rounded geometry increases material flow
- reduced water absorption of the closed spheres
- lightweight with the inorganic hollow spheres controlling slip specific gravity and therefore increasing thermal resistance

5.3.6.4 ZTE: Lithium alumino silicate

Lithium alumino silicate can be used as a source of Lithia (LiO) ceramics where it acts as a powerful flux that reduces the melting point and lowers thermal expansion. As explained earlier it strongly reduces the coefficient of thermal expansion (less than 1×10^{-6} °C), thereby increasing resistance to thermal shock and increasing the number of firing cycles possible without cracking. Lithium alumino silicate is available only in 200 mesh (smaller than 75 micron) size and therefore requires further milling to obtain sufficient amount of fines (less than 1 micron fraction) for rheology and strength development during slip casting.

5.3.6.5 Metakaolin: Casting clays

Casting clays are normally used in the production of traditional ceramic 'white wares' and consists of ball clay, china clay, filler and flux in various proportions depending upon the application (WBB Datasheet). The ball clay dispersion is difficult and therefore has to be mixed and aged before casting. As mentioned in previous chapters the deflocculant used reduced the amount of water needed, which reduced problems such as shrinkage and warping. The clay body needs 0.3% to 1.5% (by weight) deflocculant.

Complications when using casting clays include the allowance for ageing of a body which depends on the compositional make-up. The biggest problem is the usual time delay for the clay to age in order to become stable for casting. Other factors to consider included: poor filling (too long to fill moulds), flabby casts (soft casts – difficult to handle), brittle casts (hard casts – difficult to fettle), poor draining after casting, wreathing (small uneven fringes on slip side of cast), pinholes (small holes just below surface on mould side of cast piece), cracking, casting spot (poor flow), and casting flash (discoloured patch occurring on the mould side of the article)- WBB Datasheet.

Three metakaolin clays were investigated for possible use in ceramic filter manufacture: CS5, Superwhite and Terradura (G&W Base Minerals)- Table 5.3.

Procedure used in mixing the clay:

1. Add 1 liter of water for every 1 kg of casting clay into a mixer
2. Initially add the minimum amount of required deflocculant to the mixing water
3. Slowly add and mix casting clay powder and pore former to water until no lumps are present
4. Leave the slip to stand for 15 minutes, if the clay thickens add a few more drops of deflocculant. Repeat until correct consistency (test slip specific gravity and flow rate) is obtained.
5. Dry and fire the samples to bisque[52] firing temperature. Test for water absorption and strength.

[52] initial firing to a porous state for application of glaze. After glaze application sample is fired to glaze temperature (see datasheet)

Table 5.3: Physical and ceramic properties of the casting clays (G&W Base Datasheet)

	CASTING SLIP 5	SUPERWHITE	TERRADURA
Powder Colour	Light grey	Light grey	Light grey
Fired Colour	White	Off-White	White
Deflocculant:			
Sodium Silicate (ml)	85–110	80–120	60–80
Alcosperse 150 (ml)	85–110	75–120	60–80
Bisque temp °C	1000-1040	1000-1040	1000–1040
Glaze temp °C	1100–1140	1100–1120	1100–1140
Green Shrinkage %	2–4	3–5	2–3
Total shrinkage %	3–4	3-5	3–5
Water absorption %	10–15	12–18	10–15
Strength (MOR) Mpa	30–34	30–34	45–55

5.3.6.6 Activated carbon

According to the supplier (Haycarb 2012) datasheet, activated carbon is made from carbonised coconut husks, wood, peat, coal, bituminous coal, and various other materials. The carbonised material is heated to high temperatures before being chemically or steam activated. This results in a highly porous adsorptive medium with a complex structure composed of carbon atoms. It is the pore network within a rigid carbon skeleton with its disordered layers of carbon atoms linked by random chemical or carbon bonds that makes it highly absorptive.

Activated carbon removes impurities from gases or liquids through a process of adsorption where molecules are attracted into this network of pores. Adsorption is responsible for the performance of activated carbon in water. One gram of carbon has a pore surface area of 1200– 2500 m^2 and this large surface area gives it an exceptional ability to adsorb taste, odour, and chemicals on to its surface (Figure 5.6). Activated carbon is therefore used in water purification to remove by adsorption; chloroform, chlorine, VOCs (volatile organic compounds), hazardous chemical substance, bad smell, heavy metal and pesticides from water (Haycarb 2012).

The *Outbac* candle shaped filter is filled with activated carbon after the finishing stage. After filling, the plastic fitting is glued onto the ceramic thereby encapsulating the carbon inside the filter.

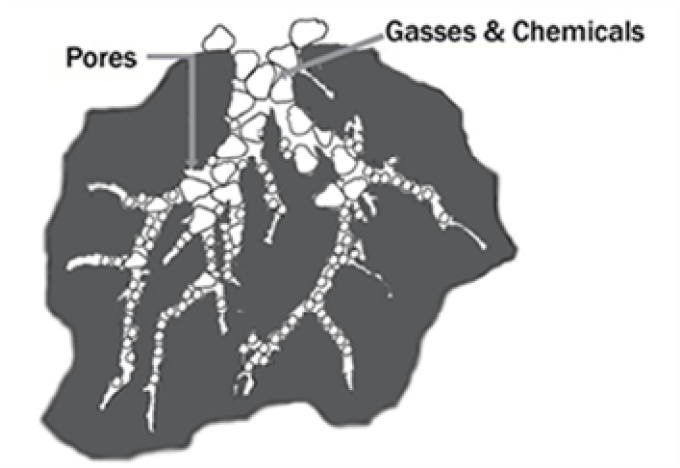

Figure 5.6: Physical property of an activated carbon particle (Haycarb Datasheet)

5.4 Filter Forming Process

5.4.1 Mould preparation

A number of master moulds were manufactured by an engineering shop from both aluminium and stainless steel. The primary concern of the mould was the final geometry and dimensions of the finished product as well as the plastic flange (diameter) that would later be glued to the ceramic to complete the filter (Table 5.). Allowance also had to be made for shrinkage caused by both drying and sintering stages. The master mould that gave minimum breakage and ease in stripping was then selected for the plaster mould making stage. The final master was manufactured with a slight taper running from top to bottom. The taper helped with the stripping as the material combination and high density achieved provided only a very small drying shrinkage.

Figure 5.7 shows a cross-section of the set-up that was used for preparing the plaster former necessary for making the plaster moulds. It was not necessary to use any release agent on the master. A polished granite slab was used as a smooth base on which the former was placed. A plaster fillet (plaster/water mixture with a plastic consistency) was prepared for attachment to the granite base as well as to prevent any plaster from escaping.

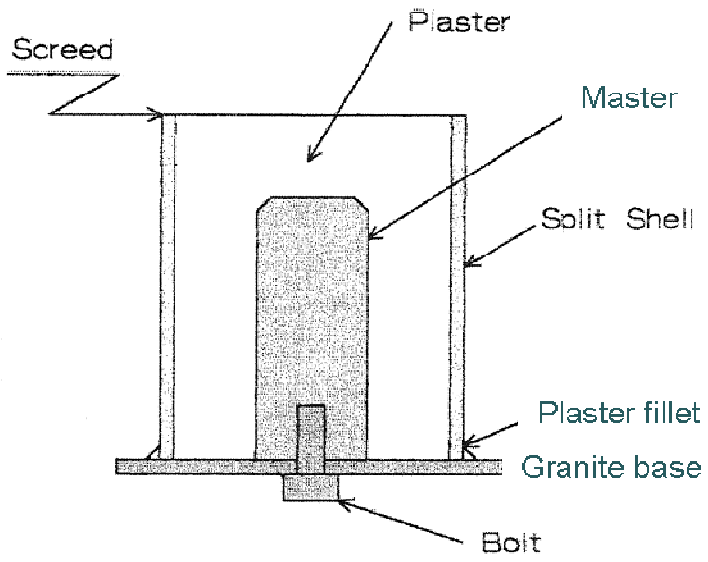

Figure 5.7: Mould former (cross-section) used for the making of plaster moulds

5.4.2 Plaster casting

Plaster of Paris (which the slip casting molds was made from) is composed of calcium sulfate ($CaSO_4 \cdot 0.5\ H_20$). Mixing plaster of Paris with water, allows the plaster to hydrate and cure into a solid, hard structure with a chemical composition of $CaSO_4 \cdot 2H_20$. The Plaster of Paris with a consistency 67 parts plaster to 33 parts water was prepared by hand mixing and poured into the prepared plaster former (Figure 5.7). After setting for about 30 minutes to an hour, the plaster mould was stripped from the former, left to hydrate overnight before drying for 12 hours at 56°C (See procedure in Table 5.1).

5.4.3 Slip preparation

The mill was opened and 35 weight % of the organic carbon (pore-former) was added. After 1-2 hrs. of milling homogenization and conditioning the slip was transferred to a planetary mixer and kept in suspension by slow mixing (stirring).

5.4.3.1 Casting procedure

1. Pour slip quickly and accurately into the mold. Over-fill mold slightly above the pouring hole.

2. Allow the ceramic slip to sit in the mould until desired thickness is reached (about 8-10mm). Keep the mould full. Allow only three castings with the same mould (monitor the wall thickness as a function of time).

3. Wait until the correct wall thickness has been achieved, decant the mould over a screen and wait until all the slip has been removed. Leave the mold inverted on a drying tray to drain and allow the green product to be released from the mould.

4. Carefully remove the casting from the mold by bumping against table with hand catching body. Use a knife with great care to remove the excess hardened slip. Put the mold in the mould drier to dry out and stay clean (Keep the drying temperatures below 57 °C).

6. Place the casting into a drier at 99°C to dry. The casting is now ready for firing.

5.4.4 Rheological measurements

The slip was then put through a number of basic production-type rheology determinations. As raw material particle size distribution changes from batch to batch, it was decided to use the measurements of SG and flow time to obtain a feeling for the inter-particle spacing (IPS) of the slip. IPS, the average distance between particles, should be held as constant as possible by making slight recipe adjustments (maintain constant material PSD) or by increasing the moisture content.

Variable shear (flow time) was taken as a measurement of viscosity by using only a cylindrical funnel with a 2 mm opening and a stopwatch, eliminating the need for expensive and sophisticated instruments and allowing for easy, on-site production measurements. The funnel opening was closed and then filled with 100 cm^3 of slip. Timed release (seconds) from the funnel was measured with a stopwatch.

The specific gravity (SG) of the slip was determined by tarring a 100 cm^3 measuring cylinder on a scale, filling it exactly to the 100 cm^3 mark, and then from the mass and volume obtaining the SG, expressed in $g.cm^{-3}$. The SG is a reflection of the water content of the slip.

5.4.5 Casting, castability and stripability testing

Every time a new batch was used, experiments had to be performed on the raw materials to obtain optimum slip density, PSD (as explained previously), maximum slip solids content and flow properties (flow time). The data was then used to optimization adjustments (PSD, packing density, proportion of raw materials and flow property), resulting in slight adjustments to the recipe. The aim was to adjust the solid content to range between 65-70 weight percent to minimise segregation of the raw materials during casting.

Due to the fact that the pore-former (organic carbon) played such an important role in the rheology of the slip, it was decided that instead of the initial plan of performing the experiments in two sets (without, and with pore-former), to include the pore-former from the outset into the process.

After thorough mixing and 2 h ball milling, the slip SG and flow time was measured and recorded and the necessary adjustments (water addition) made. The slip was then cast into plaster moulds (at room temperature) using the traditional method of drain casting.

The slip was allowed to stand for a predetermined period of time. Cake thickness was visually inspected at 5, 10 and 20 minute intervals (similar process followed by Sakar-Deliormanh and Yayla 2002) until the required thickness (wall thickness of between 8-10 mm or until no further increase occurs) was achieved. The excess slip was then poured or decanted from the mould, the mould inverted, placed in an elevated position for draining, and left until the body could be stripped. Ease of stripping is a reliable indicator of good slip properties. The stripping of the cast product was determined by looking at factors such as sticking to the mould (segregation), flabby casts (poor packing density), poor draining after casting (segregation) and cracking (excessive shrinkage).

Poor stripping, poor wall thickness development and weak green body indicate particle segregation or show that too much organic carbon has been added – requiring modification to the recipe.

After stripping from the moulds, the sample was left to dry at room temperature for one hour before being oven-dried at 90°C overnight. On completion of drying, all the filters were visually inspected for cracks. Cracked items were removed and destroyed and possible modifications were again made to the slip recipe.

5.5 Binder Burnout

5.5.1 Developing a firing schedule for both burn-out phase and sintering

Before determining the burn-out and firing cycles, the phase diagram for the LAS (Li_2O-Al_2O_3-SiO_2) system was investigated to identify the various phases of the LAS system and the conditions under which each phase exists. The phase diagram for the Li_2O-Al_2O_3-SiO_2 system is shown in Figure 5.8. The composition and position of the raw material (Lithium alumino silicate) used in the research is indicated as position in P and R in Figure 5.8. The reduction in the melting points for the end-members (SiO_2 and Al_2O_3) resulting from lithium addition to around 1100ºC is also shown.

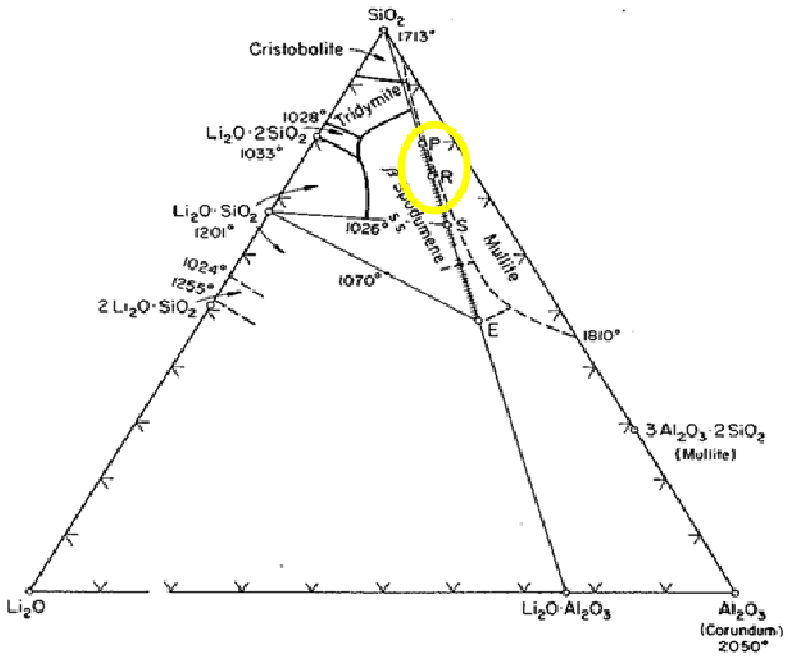

Figure 5.8: The Phase system Li_2O-Al_2O_3-SiO_2 (Levin et al 1985)

After drying, the carbon additives (pore formers) in the body had to be burned out during a special burnout cycle or during the normal sintering cycle. Burn-out considerations included:

- organic additives had to carbonised at slow heating rate and long holding times
- a separate firing cycle was allowed for the burn-out (carbonisation step)
- the burn-out step was followed by final sintering
- the firing cycles for both burn-out and final sintering were derived from the TGA results to avoid cracking during firing

The firing schedule was obtained using a modified thermal gravimetric analysis (TGA). In a thermo gravimetric analysis (TGA) a sample is heated and the loss in weight is measured as a function of temperature. With the temperature increase, chemical reactions or loss of crystal water cause it to lose weight with the release of volatiles (gasses). The results derived through use of this apparatus, in the form of a TG curve, were used to determine the optimum firing curve (ramps and holds).

The test was modified by using a makeshift apparatus using a micro-balance and small furnace. The small sample was suspended freely from the balance by a stainless steel wire into the kiln. A heating rate of 2 °C min^{-1} was maintained to observe the carbon decomposition in air.

Final sintering was then followed by using an electric kiln with a final temperature of ± 1200ºC and a holding time of ± 1 hr. (with minimum shrinkage).

5.5.2 Characterisation of the sintered samples

On completion of sintering the samples were physically tested for thermal shock, shrinkage, water absorption, porosity, pore size distribution, pore size, specific surface area (SSA) as well as hydrodynamic aspects (permeability- hydraulic conductivity).

5.6 Final product investigation

This section concerns itself with analytical, electron microscopy, XRD, microbiological and physical properties, with the emphasis on how the methods were used to characterise the materials and the densified porous filter. A comprehensive summary of these test methods are given in Table 5.1 to 5.4. Figure 5.9 gives an overview of the testing regime applied to the characterisation of the porous ceramic filter.

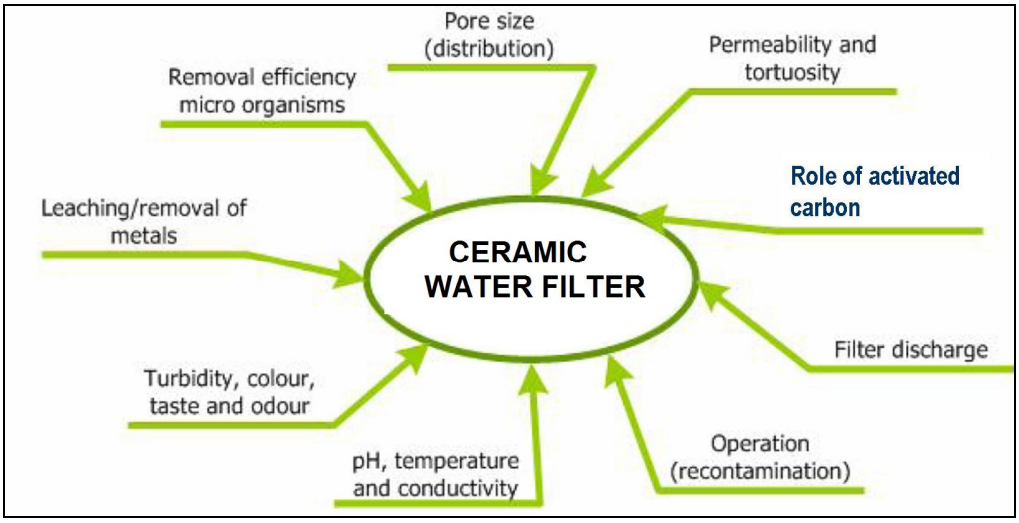

Figure 5.9: Raw material and product testing regime

5.6.1 Porous material evaluations

The evaluation of the porosity for the fired pore structures was done using three test methods: SEM, water immersion and Hg porosimetry determinations (similar evaluation process followed by Lyckfeldt and Ferreira (1998). Water immersion and Hg porosimetry were used for identifying and measuring the smaller pores and necks formed by the contact between larger spherical openings left by carbon particles (See Figure 5.10). SEM focused more on the visual identification of the larger pores left behind by burnt-out carbon particles. For use as an effective bacterial filter as well as for adequate hydraulic conductivity, the connected pores at the neck points will be the important limiting factor.

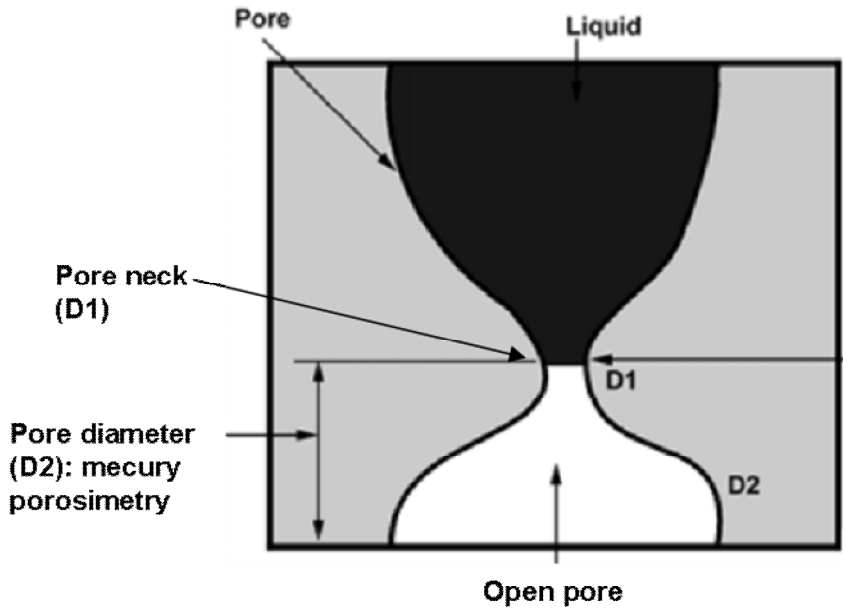

Figure 5.10: Pore-neck openings (Lyckfeldt and Ferreira 1998)

Porosity and density measurements (Table 5.4). The density and porosity of the vitrified product was also evaluated through the use of the water immersion method. The sample mass was determined on removal from the kiln to establish dry weight, after which product was placed in water and boiled for 12 h. The water was replaced by room temperature water. The sample was dried using a wet cloth (remove water drops on surface) and then weighed (wet weight). Finally mass suspended in water was determined. Apparent specific gravity (ASG), apparent porosity (AP) and water absorption (WA) were then calculated from the 5 weights, using appropriate equations (Section 5 in Table 5.4). Average values and standard deviations were determined for the results.

Table 5.4: Immersion test procedure

Immersion Test for WA, BD, AP and ASG

PFM-2

University of Zululand

Procedure Overview **Instructions & Explanations**

UTBAC Ceramic Water Filters

GMP guidelines apply

Std Site Clothing and PPE Req'd

Leather gloves for steam protection

Warning

i_1 Special note

Additional person(s) required

$\square_1$ Picture on front side

$\#_1$ Enlarged picture on reverse side

Obtain all tools & materials listed on reverse side

ASTM C20-87

ASTM C373-72 (1982)

ASTM C830-83

ASTM C1039-85

PPM 2: Permeability

1 Selecting test sample

1.1 Select 5 representative test specimens in excess mass of 50g
1.2 Naturally freshly fracture sample surface
1.3 Remove sharp edges/corners
1.4 Ensure that sample contains no cracks

2 Drying test samples

2.1 Dry samples to constant mass by heating to 150°C
2.2 Place in desiccator for weighing
2.3 Determine the dry mass, D, to nearest, 0.01g

3 Boiling test samples

3.1 Place samples in pan, covered with distilled water. Allow capillary forces to draw in water until initially saturated $\square_1\square_2\square_3$
3.2 Boil for 5h, taking care to keep sample covered at all times. $\square_1$
3.3 Keep samples away from bottom, sides and each other.
3.4 Soak for additional 24h.
3.5 Remove and blot each sample with wetted cloth to remove excess water and determine saturated mass, M, to nearest 0.01g (avoid evaporation)

4 Determine suspended mass

4.1 Tare scale with wet cotton thread suspended in water container on balance
4.2 Perform weighing by tying wet cotton thread around sample
4.3 Suspend sample in container making sure that sample is not touching bottom/sides and weigh suspended mass, S, to nearest 0.01g

5 Performing calculations

5.1 Exterior volume in cm^3: V= M – S
5.2 Volume of open pores and impervious portion:
☐ volume of open pores in cm^3: M - D
☐ volume of imperious portion, cm^3 : D – S
5.3 Apparent porosity, P as %, volume of open pores to exterior volume: P= [(M – D)/V] x 100
5.4 Water absorption A as %, relationship of mass of water absorbed to mass of dry sample: A = [M – D)/D] x 100
5.5 Apparent specific gravity, T, portion of sample impervious to water measured in g/ cm^3 T = D/(D – S)
5.6 Bulk density, B, in g/ cm^3 is the quotient of its dry mass divided by the exterior volume, including pores: B = D/V

6 Reporting

6.1 For each property, report average of values obtained with 5 specimens
6.2 Test another 5 samples if large differences occur between individual values.
6.3 Report individual and average of all 10 determinations

$\square_1$ **StepNumber** Importance of proper saturation

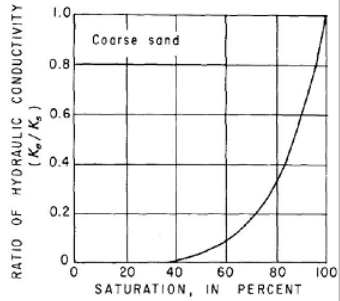

$\square_2$ **StepNumber** Capillary rise in porous material

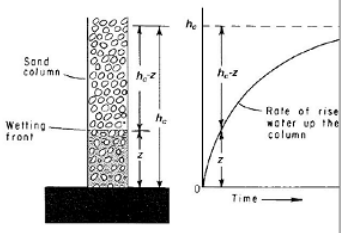

$\square_3$ **StepNumber** Capillary rise for granular material

APPROXIMATE HEIGHT OF CAPILLARY RISE (h_c) IN GRANULAR MATERIALS

Material	Rise (mm)
Sand:	
Coarse	125
Medium	250
Fine	400
Silt	1,000

$\square_4$ **StepNumber** Results of stratified flow through porous membrane

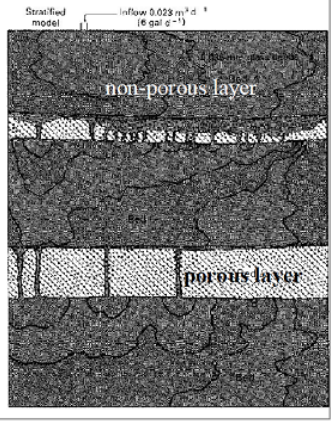

✓ Pre-Checks (Things to check before starting this process)

- ☐ Assume that 1 cm^3 of water weighs 1g
- ☐ Item

Tools & Materials Required

Quantity & Description	Step
☐ Micro-balance (weigh to 0.01g)	
☐ Drier (150C)	
☐ Plastic container for immersion of sample on scale	
☐ Pan for boiling samples	

✓ Post-Checks (Things to check after completion)

- ☐ Use wet cloth to dry samples before weighing
- ☐ Ensure that balance in water is swinging freely

#1 StepNumber Porosity definition

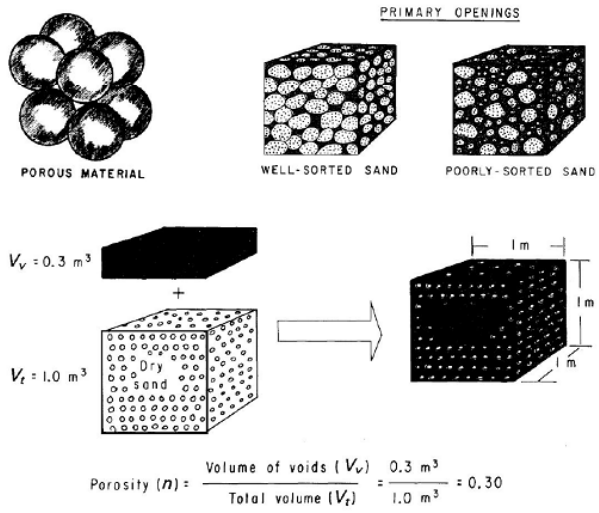

#2 StepNumber Porosity values for natural materials

SELECTED VALUES OF POROSITY
[Values in percent by volume]

Material	Primary openings	Secondary openings
Equal-size spheres (marbles):		
Loosest packing	48	--
Tightest packing	26	--
Soil	55	--
Clay	50	--
Sand	25	--
Gravel	20	--
Limestone	10	10
Sandstone (semiconsolidated)	10	1
Granite	--	.1
Basalt (young)	10	1

#3 StepNumber Immersion Test Results for medium- high & very high, K, filters

Abbreviations
AP: Apparent porosity (%)
WA: Water absorption (%)
ASG: Apparent specific gravity (g/cm^3)
BD: Bulk density (g/cm^3)

Sample	AP	WA	ASG	BD
AVE MED K	67	85	2.42	79
SD MED. K	0	0	0.01	0
AVE HIGH K	73	113	2.41	65
SD HIGH K	0	0	0.05	0
AVE V HIGH K	73	109	2.44	67
SD V HIGH K	0	1	0.01	0

Key Learning/Performance Points

ITEM	C	Step
1.		
2.		
3.		

Pore size distribution. The sintered product's pore size distribution was analysed with a Micromeritics mercury porosimeter (Micromeritics, Datasheet). The pore size distribution gave a measure of the interconnected pores left behind by the carbon particles (Tari 1999). Surface area determinations were also made after firing the product using the Micromeretics Porosimeter. This process allowed the pores in the sample to absorb single (mono) layer gas molecules.

To measure even the smaller pore structure, the gas has to be condensed in the pores before evaluation can take place, as pressure increases:

a) gas condensation fills the smallest pores first
b) pressure is further increased until all the pores are saturated with liquid
c) pressure is released incrementally, allowing evaporation of the condensed gas to take place
d) measuring the adsorption and desorption branches for preparing isotherms and hysteresis curves
e) use the isotherms and hysteresis curves for obtaining the pore size/shape, pore size distribution, pore volume, and the surface area (SSA) of the fired ceramic sample.

5.6.2 SEM investigation

The overall pore size and structure formed by the burned-off organic carbon particles were visually studied using SEM. Images were taken at two different magnifications, one at 300 x and one at 700 x magnification. The images were recorded and recorded for record keeping.

5.6.3 XRD

A standard XRD analysis was carried out on the sintered porous ceramic. A representative sample from a fired ceramic filter was taken. The sample was prepared as follows:

1. obtain an approximately 20 g section of the sample
2. wet grind the sample down to – 10 micron grain size using acetone (75-100mg of powder required)
3. load powder on to glass slide which completely occupy the square glass well, sample must be flush with top surface of glass slide. Avoid excessive agitation of sample thereby preventing preferred orientation of the sample
4. prepared sample was supplied to UKZN Material Sciences Laboratory in Durban for analysis.

5.7 Flow Testing

5.7.1 Hydraulic conductivity

The hydrodynamic aspects of the ceramic filter design and operation will be tested to ensure the proper distribution of flow through all the pores (not just the largest pores) under highest hydraulic pressure and effective retention time through the activated carbon. Hydraulic retention time will be a key parameter in the filter's performance.

The test procedure and apparatus used in the constant head permeability tests are explained shown in Table 5.5. Figure 5.11 illustrates the equation as well as the variables necessary for calculating the hydraulic conductivity permeability).

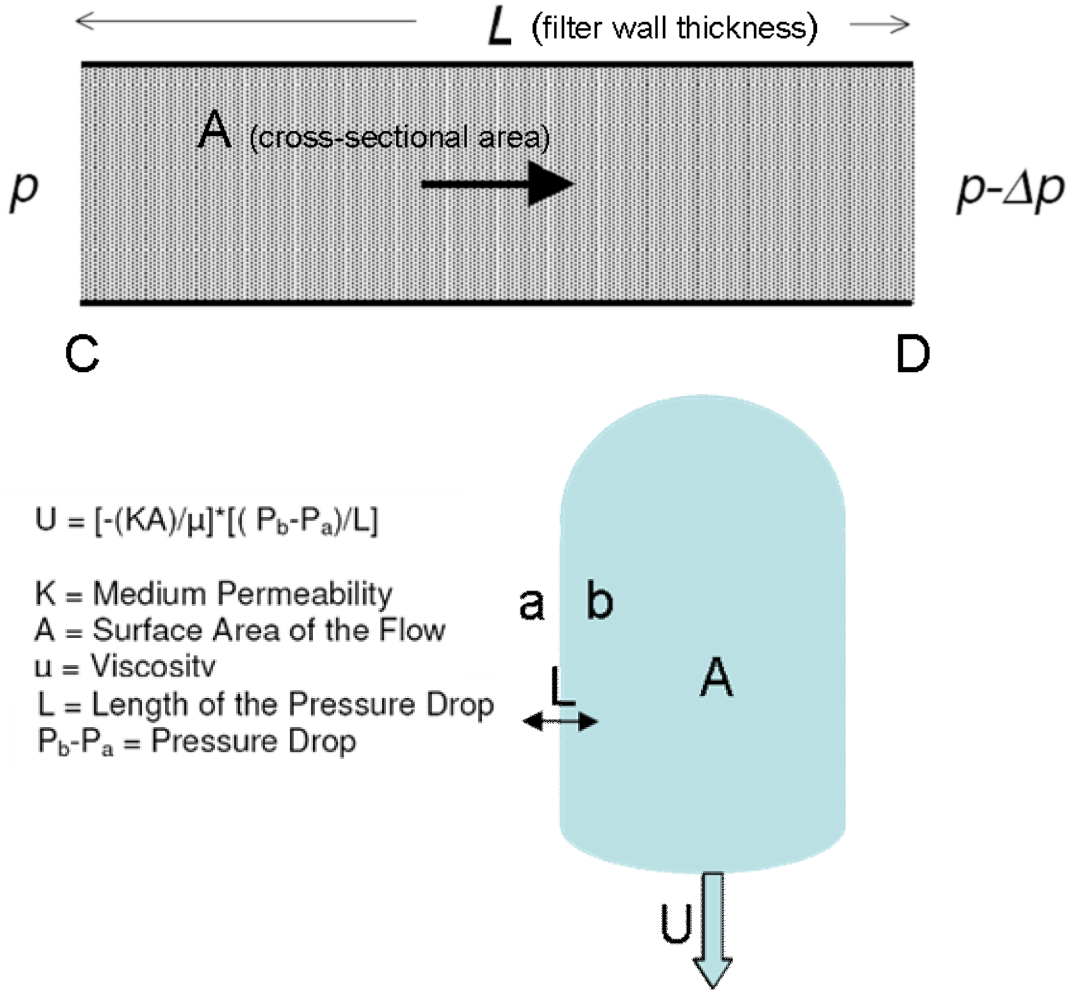

Figure 5.11: Variables relative to the filter used in determination of K

Table 5.5: Constant head permeability test procedure

Constant Head Permeability Test

PFM-3

University of Zululand

Procedure Overview

Instructions & Explanations

UTBAC Ceramic Water Filters

GMP guidelines apply

Std Site Clothing and PPE Req'd

Warning

i1 Special note

□1 Picture on front side

□1 Cross-sectional Area Calculation

□2 Darcy's Law

□3 Permeameter Gasket

□4 Membrane (filter) position

⌖1 Enlarged picture on reverse side

⌖1 Flow & K value through membrane

⌖2 Experimental Set-up

⌖3 Water Viscosity at T

Obtain all tools & materials listed on reverse side

Related PFMs

Soil Testing for Engineers (Lambe TW, 1963)

1 Describe hydraulic conductivity ⌖1

1.1 Measure ability of ceramic to conduct water under a unit hydraulic potential gradient ⌖1

1.2 Intrinsic property of the porous ceramic and is governed by pore size, total porosity, pore size distribution and degree of saturation

1.3 Express, K, in cm/sec after Darcy: K= Q.L/A▲h▲t cm/sec □2 :

- Q= volume of water, cm3, flowing through given area in a given time
- L= length of ceramic, cm (wall thickness) through which water flows
- A: cross sectional area through which water flows, cm^3 (outside surface area of ceramic membrane) □1
- ▲h= hydraulic gradient responsible for flow, measured in cm height of water column
- ▲t= time interval for flow was measurement (sec.)

2 Set up the permeameter ⌖2

2.1 Determine and record membrane h, L & ▲h

2.2 Silicone the membrane on to the rubber gasket glued to perm eater tube base, allow to dry for 90 m □3 & □4

2.3 Apply the support frame and clamps, ensuring a tight seal on the top/bottom tube gaskets ⚠

2.4 Allow the water, from the supply funnel, to saturate and fill the inside chamber of the ceramic (10-15 minutes), suction can be supplied to speed saturation of filter

3 Perform constant head test ⌖2

3.1 Adjust the flow to maintain constant head conditions in the funnel. ⌖3

3.2 Place thermometer in funnel, and record water temperature

3.3 Allow a few minutes for equilibrium conditions to be reached while taring glass beaker and zeroing stopwatch.

3.4 Start stopwatch and collect sufficient amount of filtrate water. Record volume and time in attached Recording Sheet

3.5 Record water temperature for viscosity determination

4 Perform calculations

4.1 Reduce the permeability at temperature T, K_T, to that at 20°C, $K_{20°C}$ by using:

- $K_{20°C} = K_T \mu_T/\mu_{20°C}$
- $K_{20°C}$: permeability at temperature 20°C
- K_T : permeability at temperature T
- $\mu_{20°C}$: viscosity of water at temperature 20°C
- μ_T : viscosity of water at temperature T

4.2 Obtain $\mu_T/\mu_{20°C}$ from indicated table and perform calculation ⌖3

5 Present results

5.1 Compare hydraulic conductivity to geological materials are showed in the diagram ⌖1

5.2 Use classification below as reference

Degree of permeability	K in cm/sec
High	$> 10^{-1}$
Medium	10^{-1} to 10^{-3}
Low	10^{-3} to 10^{-5}
Very low	10^{-5} to 10^{-7}

□1 1.3 Cross sectional area calculation (cone)

- m=SQRT $(D-d/2)^2+h^2$= 6.2721706
- Am= π/2. m(D + d)= 99.21 cm^2
- D= membrane base diameter (cm): 5.20cm
- d= membrane cone diameter (cm): 4.87cm
- h= filter height (cm): 6.27 & 2.1

□2 1.3 Darcy's Law

- Darcy showed that rate of water, q, flowing through sand of cross-sectional area, A, is proportional to the imposed gradient i
- q/A ~ I q= KiA
- K or hydraulic conductivity, coefficient of permeability or permeability and indicates the ease with which water will flow through a soil/sand/ceramic membrane

□3 2.2 Rubber gasket

□4 2.2 Membrane position

5.7.2 Retention time

As per the work by Fahlin (2003) who determined the tortuosity of a ceramic filter by using bromine as a tracer. This study used chloride as a tracer and measured the breakthrough (retention) time of the chloride during a filtration test. The apparatus used consisted of a similar experimental procedure followed for Constant Head Permeability Test (Table 5.5). The area of filtration and the hydraulic head was kept constant to simplify the determination of hydraulic conductivity. An Aquameter AQUAPROBE was used to measure electrical conductivity (EC in μS/cm) of the filtrate at a 1 minute recording interval. The schematic in Figure 5.12 illustrates the experimental setup for the tracer breakthrough test.

The calculations used in determining the retention time included:

a) flow through the filter: $Q = K.A.\Delta h.L^{-1}$ ($mL.min.^{-1}$) to obtain the hydraulic conductivity, with Δh set at 30cm, L at 0.8cm (wall thickness of the ceramic filter) and A set at 91 cm^2 (cross-sectional area of the ceramic filter).

b) tortuosity (ratio of the actual distance the water travels divided by the direct linear length across the filter:

   $\tilde{n} = L_e.L_s^{-1}$(unit less).

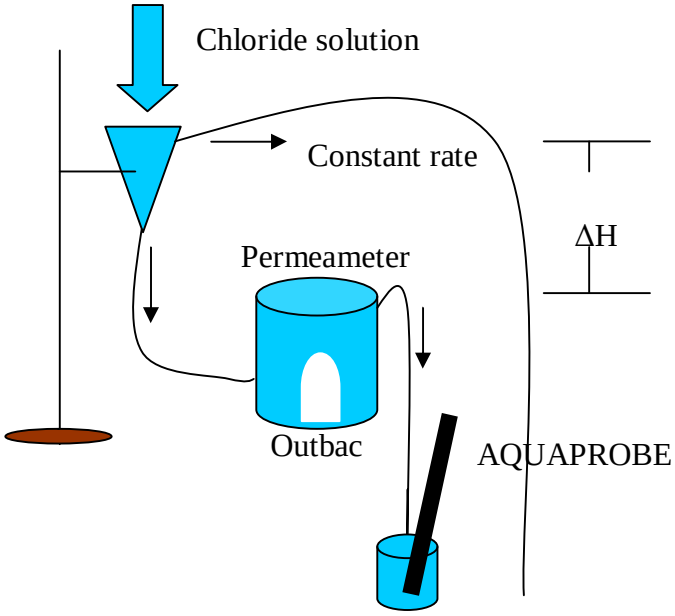

Figure 5.12: Laboratory setup for retention time of the filter using a chloride tracer

The filter was fully saturated by running 2500 cm^3 through the system. The delay volume of 330 cm^3, for water in the tube, permeameter, measuring cup, the volume first has to be displaced before the tracer could be detected. The hydraulic conductivity for each filter was used to calculate time required to displace one complete volume (bed volume) once. The delay due to the bed volume displacement was taken in consideration for determining the retention time and tortuosity.

5.7.3 Testing the cleanability of the ceramic

After the filter has been used for some time, it is important to be able to clean the filtration surface to restore the flow through the filter. Various possible cleaning methods were looked at for effective removal of biomass. Cleaning methods evaluated included:

a) flushing the surface with fast flowing water,

b) backwashing by reversing the normal flow through the filter

c) flushing the filter with citric acid to dissolve carbonate deposits on the surface

d) cleaning the filter surface using coarse water-sandpaper under running water.

5.8 Microbiological testing

Two bacteriological techniques (See Table 5.6: Bacteriological investigation) were used for the preparation and testing of influent and effluent from the CWF:

a) 100ml of broth cultures (*E. coli, S. faecalis* and *B. cereus*) of different bacterial strains (Gram positive- and Gram negative bacteria) were inoculated in 1000ml sterile distilled water for influent filtration water. The spread plate technique was used to determine the CFUs (colony forming units). Ten-fold dilutions were used for the influent water, 0.1 ml of the tenfold dilutions was aseptically conveyed, by means of a sterile pipette, onto the nutrient agar plates and spread with a sterile glass spreader. All plates were incubated at 37 ºC for 24 h. Samples were prepared in triplicate and CFU and LRV per 100ml average were calculated for each of the samples

b) Influent and effluent water samples were processed using the membrane filter (MF) technique for heterotrophic count (nutrient agar, MERCK catalogue no. HG0000C1.500), total coliforms (Eosin methylene blue agar, MERCK catalogue no. 1.01347.0500) and faecal coliforms (ChromoCult agar, MERCK catalogue no. 1.10426.0500). The filtration unit used a sterile membrane (Millipore catalogue no. 0.45) with pore sizes of smaller than 0.45 µm (Simonis and Basson 2011).

c) Natural water from three local water sources in close proximity to the University of Zululand (KwaZulu-Natal, Republic of South Africa) was used as influent water for the filters (used as a drinking water supply when the local centralised water distribution system breaks down):

- University Stream flowing into Lake Mangeza (a naturally formed lake adjacent to the Mhlatuze River) – due to informal student residences without necessary sewage connections is polluted due to informal student residences without necessary sewage connections
- Mangeza Stream also flowing into Lake Mangeza and draining rural and agricultural land-use type catchments
- Lake Mangeza

Three CWF for each filter grade (permeability: low, medium and high) filters were tested in parallel. Filters were first flushed using sterile distilled water (at least 10 volume displacements). Water influent (250ml) was completely filtered through the filters using a siphon vacuum principle. The MF technique was then used to analyse both influent water and filtered water and analysed for the presence of bacteria.

Each of the samples was filtered through the ceramic filters and the filtrate was then also filtered through a sterile membrane filtration unit containing sterile nitrocellulose membranes. Different volumes for the membrane filtration (0.1ml, 1ml and 10ml of the CWF filtrate as well as 0.01ml, 0.1ml and 1ml of the raw water samples) and raw water samples were then aseptically placed on Nutrient agar, Chromocult agar and Eosin Methylene Blue agar to conduct the heterotrophic count, total coliform count and to detect faecal coliforms. All plates were incubated at 37 ºC for 24 h. The filtered water (filtrate) and control (raw sample) were both analyzed and compared with regard to the occurrence of microorganisms and to establish whether there was any reduction in the occurrence of microorganisms in the CWF filtrate, which would indicate an increase in microbial quality.

The results were expressed in LRV units (Simonis and Basson 2011).

$$LRV = \left\{ \frac{no.ColiformsInfluent}{no.ColiformsEffluent} \right\} \log_{10}$$

Table 5.6: Microbiological test procedure

Microbiological Testing of Filtrate

PFM-4

University of Zululand

Procedure Overview | **Instructions & Explanations**

UTBAC Ceramic Water Filters

- Lab coat
- Sterile gloves
- Warning
- i1 Special note

Do not streak until medium is firm

- i2 Allow loop to cool before streaking
- i3 Final plate with 30- 300 CFU
- □1 Picture on front side
- ⌖1 Enlarged picture on reverse side
- Obtain all tools & materials listed on reverse side
- Microbiology
- Merck Microbiology Manual 12th Edition
- Manual for identification of medical bacteria (Cowan ST)
- Medical Microbiology (Cruickshank R et al)
- Microbiology Laboratory Exercises (Barnett M

1 Prepare culture media ⌖1

1.1 Suspend 31g nutrient agar) in 1l distilled autoclaved water.
1.2 Autoclave for 15 minutes at 121°C and allow to cool to between 45- 55°C
1.3 Pour plate: lift lid with left hand, pour nutrient agar with right hand into labeled petri dish covering surface completely, gently tilt and rotate. Flame to remove bubbles □1
1.4 Slant: remove screw cap (McCarthy bottle) with left hand, half fill bottle with nutrient agar. Allow to set at angle with thick butt at bottom end
1.5 After solidification, invert plates and set slants in upright position, tighten screw caps. Store in fridge for inoculation

2 Inoculate streak plate

2.1 Place gas burner and inoculation loop to righ of bench and uninoculated plates to the left of flame.
2.2 Use sterile technique to obtain loop-full of inoculum from pure culture broth.
2.3 Tilt open lid and glide loop rapidly back & forth across center of labeled plate.
2.4 Incubate streaked plate for 24 hours at 37°C
2.5 Check contamination and active growth on plate

3 Inoculate slant

3.1 Place gas burner and inoculation loop to right of bench and uninoculated slant to the left of flame
3.2 Touch one culture from streaked plate lightly with flamed-cooled inoculation loop.
3.3 With left hand remove screw cap, flame bottle, streak once from bottom to top of surface.
3.4 Incubate slant in upright position for 24 hours at 37°C
3.5 Check for contamination and active growth on slant

4 Prepare nutrient broth

4.1 Suspend 1.6g nutrient broth into 100ml of distilled autoclaved water. Shake until material is completely dissolved
4.2 Autoclave for 15 minutes at 121°C and allow cooling to between 45- 55°C.
4.3 Lightly touch slant surface colony with flamed, cooled inoculation loop. Stir broth with inoculation loop.
4.4 Incubate inoculated broth for 24 hours at 37°C

5 Prepare diluted broth for filtration

5.1 Add the 100ml of incubated broth to 2 l of distilled autoclaved water. Shake well
5.2 Add diluted broth to class beaker containing ceramic membrane
5.3 Siphon filtrate through the membrane into sterilised beaker (use sterilised syringe to draw vacuum) □2
5.4 Retain raw and filtered water for testing.

6 Use plate-count method □4 ⌖2

6.1 Prepare a range of dilutions to obtain 1 within colony range i3
6.2 Prepare initial dilution by placing 1ml in a 9ml dilution blank
6.3 Shake vigorously to obtain uniform distribution
6.4 Continue by taking 1ml measured aliquots into additional dilution blanks (10^{-5} for raw water & 10^{-2} for filtered samples)
6.5 Pipette 1ml from the dilution blanks into labeled sterile Petri dishes (triplicate) □3
6.6 Pour melted, cooled agar medium (25ml) into each dish while rotating gently
6.7 Allow medium to solidify, place in incubator at 37°C for 24 hrs

□1 **1.3** Pour plate

□2 **StepNumber** Siphoning of filtrate

□3 **StepNumber** BriefDescription

□4 **StepNumber** Counting colonies

- ☐ After incubation, select plate that contains desired no. of colonies
- ☐ Take an accurate colony count
- ☐ Calculate: colonies x dilution = CFU/ml

Repeat for duplicate and average CFU's

✓ Pre-Checks (Things to check before starting this process)

- ☐ Ensure that filter connection are properly sealed
- ☐ Area is continuously flamed (gas burner)
- ☐ All glassware/water autoclaved
- ☐ Agar medium properly melted and temperature maintained
- ☐ Flame bottles on opening

Tools & Materials Required

Quantity & Description	Step
☐ Bacterial suspension (raw & filtered)	
☐ 9ml dilutions	
☐ Petri dishes	
☐ Nutrient agar (Merck: 1.05450.0500)	
☐ Nutrient Broth (Merck: 1.05443.0500)	
☐ Sterile 1ml micro-pipette tips	
☐ Bacterial suspension (raw & filtered)	

#1 StepNumber Experimental Layout

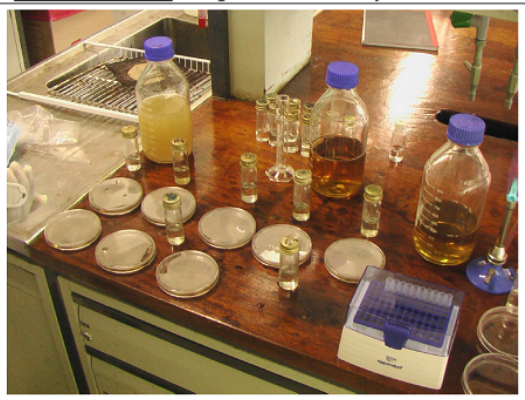

#2 StepNumber Plate count method

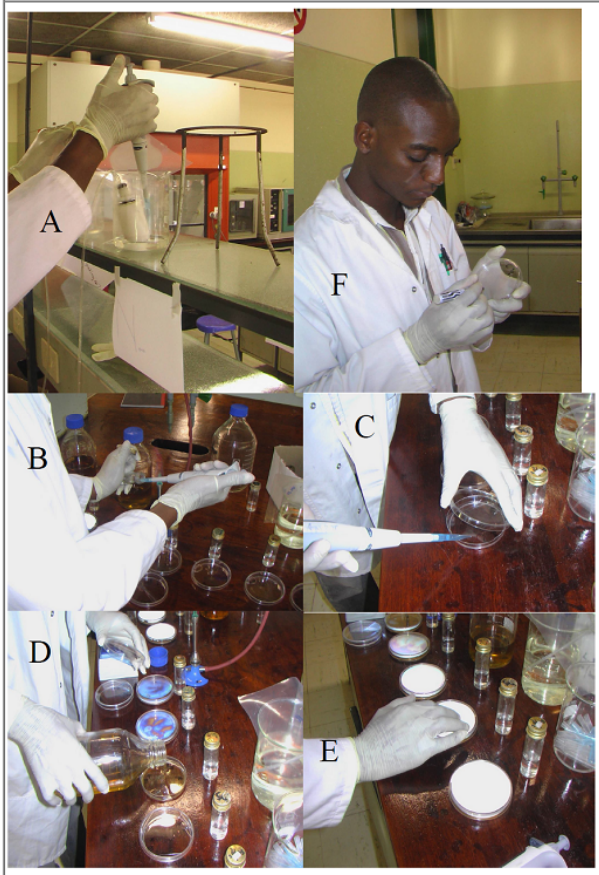

5.9 Assembly of the filtration systems

5.9.1 Finishing stage

After testing and 100% inspection of the filter for cracks and other defects, the finishing section involved the following steps (Experimental Procedure for the Finishing Section):

a) the filter is handled during all stages of manufacturing using sterile gloves

b) bottom surface (cast surface) is ground on grinding disk (to make it flat and smooth)

c) ceramic is cleaned with an air blower (to remove all dust)

d) surface to be glued treated with Sika Primer-3N and left to dry for 2 h

e) plastic flange is prepared by drilling a 3mm hole through the center, heat-sealing stainless steel mesh over the hole and cleaning the plastic surface with Sika Cleaner 205

f) ceramic unit is inverted on holding rack and the inside is filled with activated carbon

g) ceramic unit is glued to plastic flange (hole drilled and stainless screen fitted) and left to dry (set) for 24 h

h) completed filter is inserted into small plastic bag and the bag is closed by heat sealing

5.9.2 Filter system

Three types of filter systems have been developed for domestic purposes:

1. gravity system – low pressure households (BACSTER)
2. siphon system – camping (OUTBAC)
3. high pressure – high pressure households (BACOUT)

The systems components are all sourced locally, modified and fitted together to provide a variety of solutions for HWTS. Datasheets have been developed for all three filter systems and are shown in Chapter 6.

5.9.2.1 BACSTER

The *Bacster* system makes use of gravity to feed the water through the porous ceramic filter (Clasen *et al* 2006). The product name, *BACSTER*, is derived from the words *bac*teria and *ster*ilized (water), i.e. *BAC* and *STER* combined in *BACSTER*.

The system is assembled using two plastic buckets that have been sourced from a local supplier as shown in Figure 5.13:. Two holes (equal to filter outlet diameter) are drilled with a hole-saw into the bottom of the one bucket and through the lid of the other bucket. A hole is also drilled (diameter equal to the tap inlet) through the lower side of the bottom bucket. Two of the *BACSTER* porous ceramic filters were fitted with rubber washers and threaded into the two holes of the one bucket and lid of the other bucket. Nuts are used for hand tightening the filters to the bucket/lid assembly. The nuts were hand tightened to prevent untreated water leaking through into the bottom storage container. The tap is now fitted to the bottom bucket. The bucket/lid assembly is then fitted on to the bottom bucket (with attached tap). The assembly is now complete and water can be added to the top bucket. The water passes through the ceramic candles and activated carbon core (inside the ceramic) into the bottom bucket for storage. Clean, filtered water can then be removed by opening the tap. The ceramic filter lifespan is dependent on the quality of water used (datasheet).

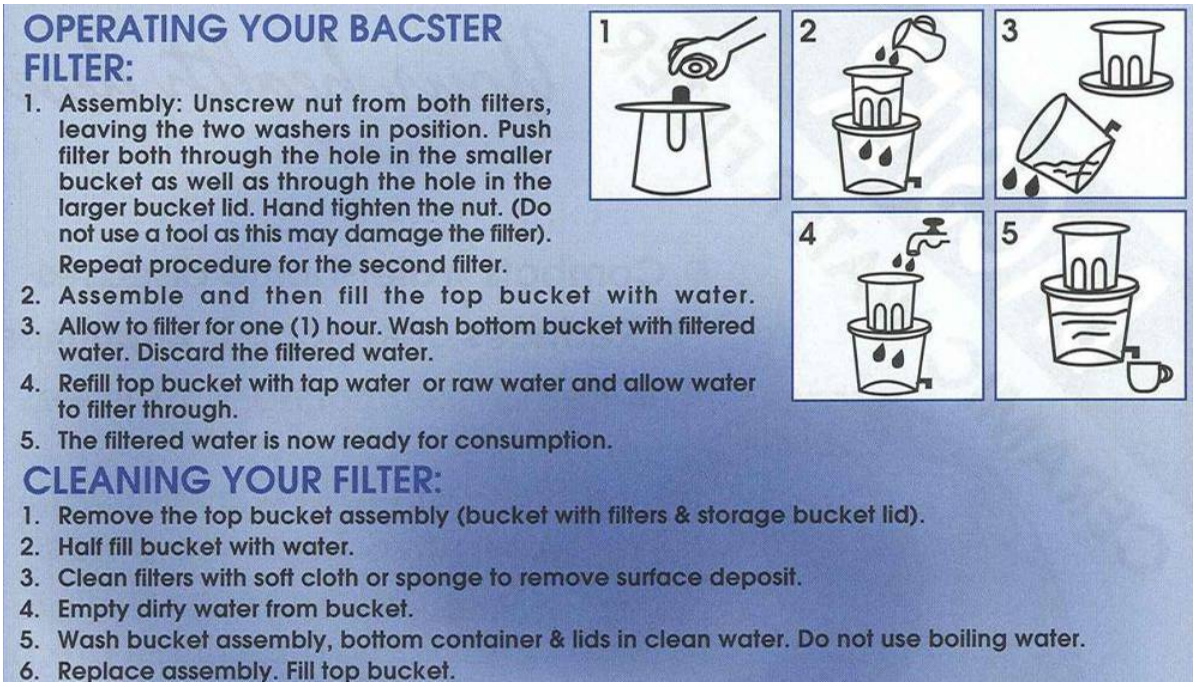

Figure 5.13: Bacster assembly, operating and cleaning instructions

5.9.2.2 BACOUT

A high pressure inline filter (*BACOUT*) assembly and application are shown in the datasheets in Chapter 6. The filter uses a cylindrical ceramic element and is fitted into filter assembly as shown in Figure 5.14. The installation and cleaning instructions are also shown in Figure 5.14.

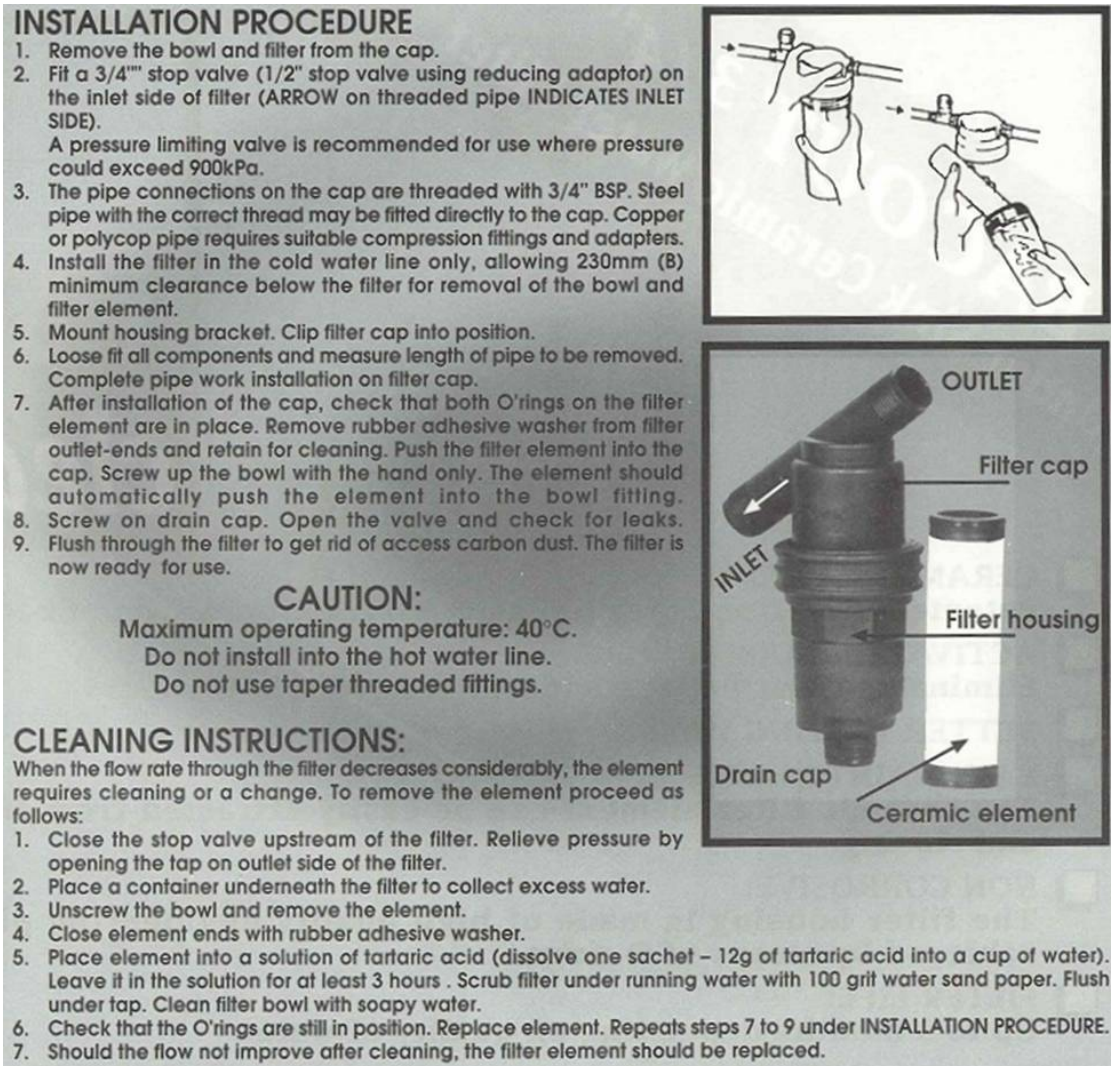

Figure 5.14: Bacout installation and cleaning instructions

5.9.2.3 Outbac

The camping and outdoors filter, *Outbac*, uses a similar ceramic element used in Bacster, fitted into a 5 liter wine gasket bag. The bag is modified by cutting one end and fitting a draw- string into the open-ended section of the bag. The *Outbac* datasheet is shown in Chapter 6.

The *Outbac* installation and cleaning instructions is shown in Figure 5.15.

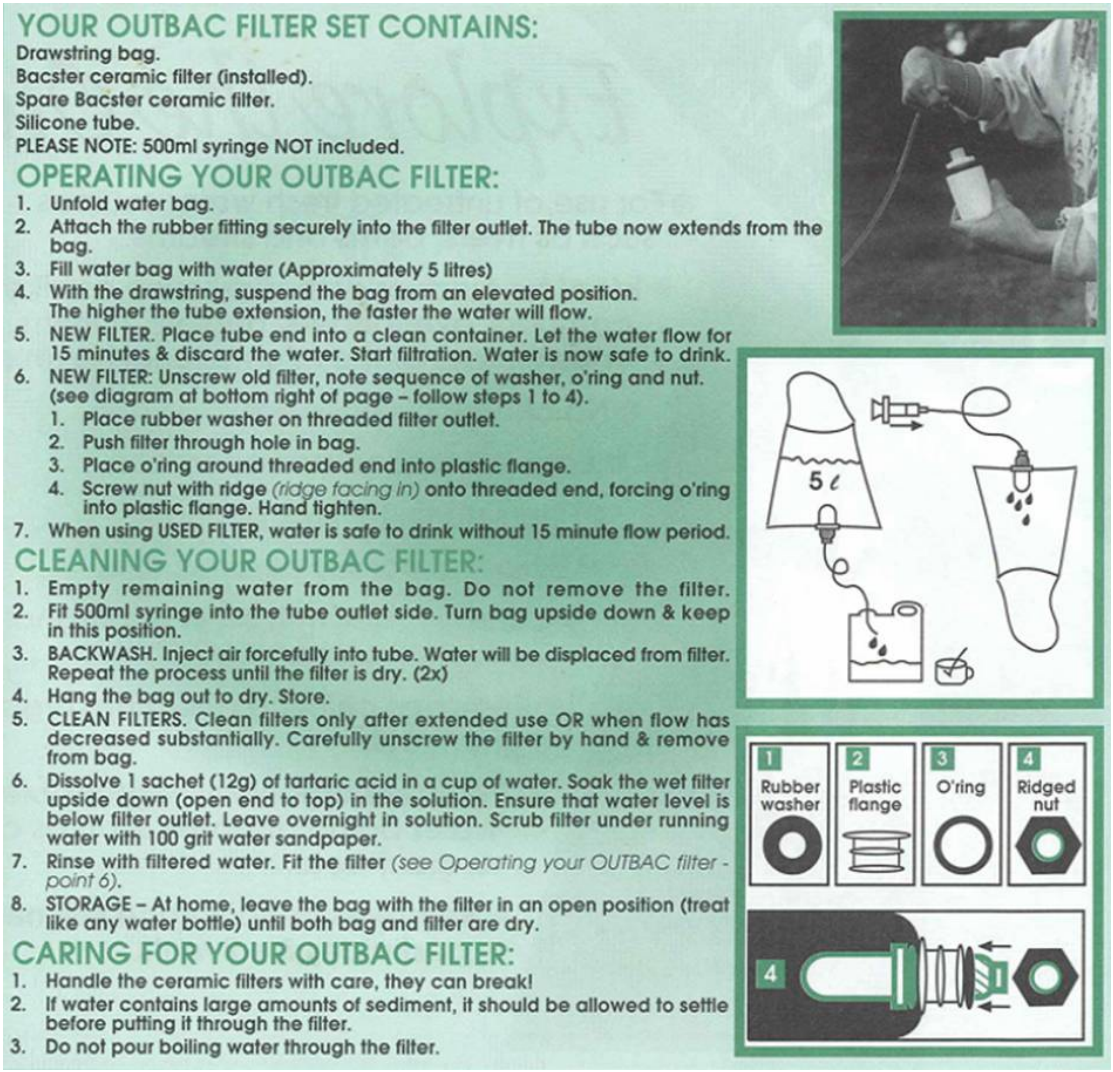

Figure 5.15: Outbac assembly, installation and cleaning instructions

5.10 Summary: material consumption (mass balance)

In this chapter the experimental procedure responsible for producing the filter was presented. The slip casting technique (Best Available Low-cost Techniques) and the conditions under which the filtration performance levels were achieved were examined.

Chapter 6: Results

6.1 Raw material selection (SWOT)

A ceramic filter was manufactured by shaping a solid article composed of inorganic nonmetallic materials by the action of heat. The major charcteristic of the ceramics is its heat resistance, large apparant porosity and effective bacteriological control.

The results from the raw material SWOT analysis are shown in Figure 6.1. It helped to highlight various strength and weaknesses of each of the materials investigated. The SWOT analysis results, the literature survey (Chapters 3 and 4) and practical experience assisted with the selection process as shown in Table 6.1.

The raw materials selected for making the ceramic filter was based on the property interplay between availability, price, rheology (in slip), special control of particle shape and particle-size distribution and thermal stability during the firing and cooling stages. The raw materials selected provided the best properties that were needed for both the forming process (slip casting) as well as for the final use of the product (filtration).

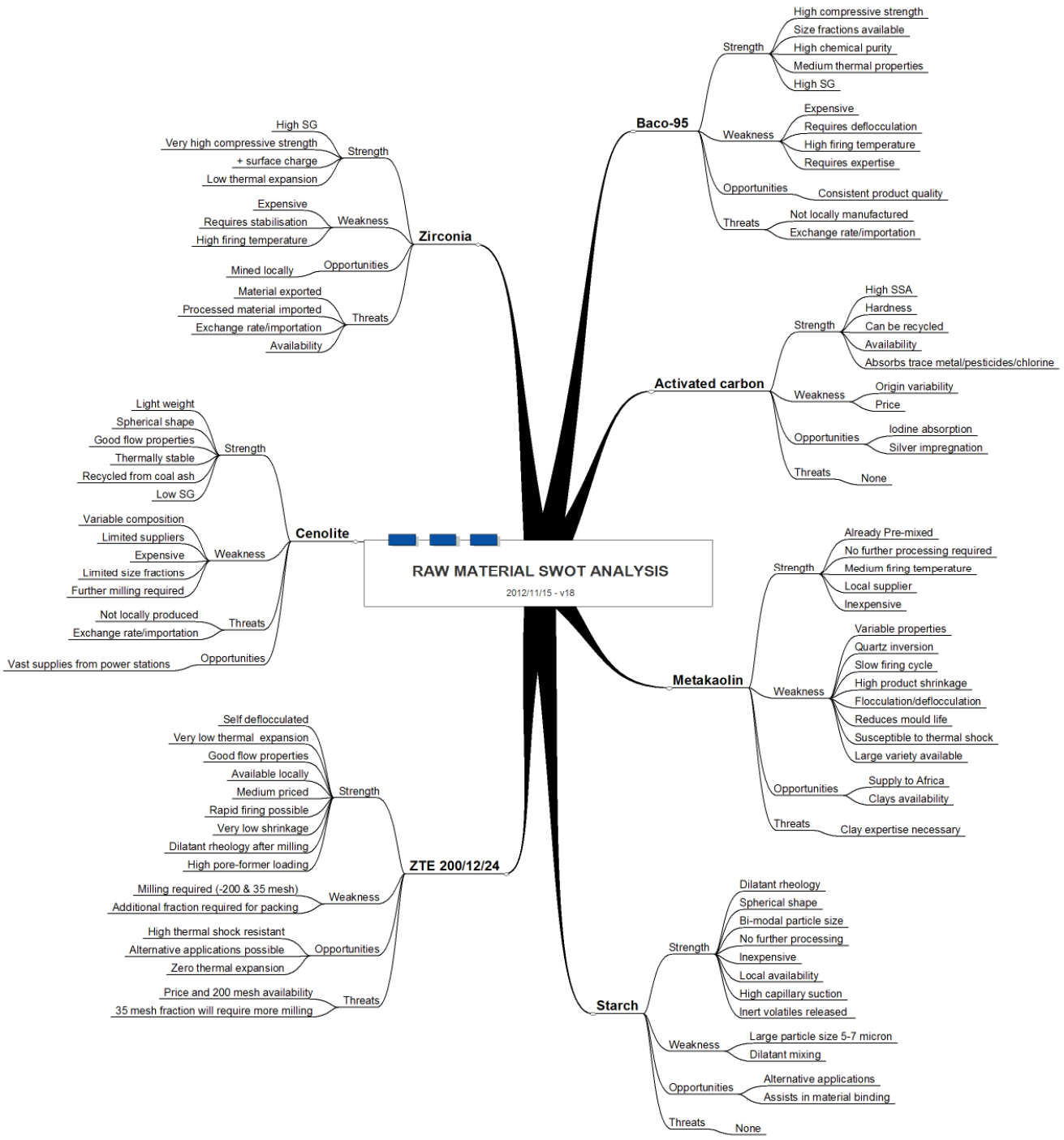

Figure 6.1: The SWOT analysis for the raw material selection process

Table 6.1: Selection criteria and selected raw material performance

Raw Materials	Thermal resistance	Firing temperature	Chemistry	Milling required	Packing density	Deflocculant required	Rheology	Selected
Alumina								
Baco-95	Medium	1400-1600°C	a Al_2O_3	More fractions	Medium	Yes	Thixotropic	No
Alphabond	Medium	600°C	a Al_2O_3	More fractions	Medium	Yes	Thixotropic	No
Zirconia	High	1400-1600°C	ZrO_2	More fractions	Medium	Yes	Thixotropic	No
Flyash								
Cenospheres	Medium	1200°C	SiO_2 and Al_2O_3	15h	N/A	N/A	N/A	Yes
Lithium alumino slicate								
ZTE 12	Very high	1200°C	LiO,SiO_2 and Al_2O_3	15h	High	No	Dilatant	Yes
ZTE 24	Very high	1200°C	LiO,SiO_2 and Al_2O_3	None	High	No	Dilatant	Yes
ZTE 200	Very high	1200°C	LiO,SiO_2 and Al_2O_3	15h &30h	N/A	No	N/A	No
Starch		N/A	C	None	High	No	Dilatant	Yes
Fume Silica	Medium	1400-1600°C	SiO_2	None	Medium	Yes	Thixotropic	No
Metakaolin								
CS 5	Low	1050°C	$Al_2Si_2O_5(OH)_4$	8h	Low	Yes	Thixotropic	No
Superwhite	Low	1050°C	$Al_2Si_2O_5(OH)_4$	8h	Low	Yes	Thixotropic	No
Terradura	Low	1050°C	$Al_2Si_2O_5(OH)_4$	8h	Low	Yes	Thixotropic	No

6.2 Selected raw material specifications

The materials that corresponded best to the basic manufacturing demands and operating conditions of the finished product, the ceramic water filter, are discussed below and the datasheets shown in Tables 6.2 to 6.5.

6.2.1 Lithium alumino silicate

Lithium, alumino silicate a local raw material provided the bulk of the product volume. The main factors for selecting lithium, alumino silicate included as follows:

- the starting (ZTE 200) particle size distribution did not provide sufficient flow properties for slip casting and had to be further ball milled to obtain the necessary sizing (15 hr. (ZTE 15) and 30 hr. (ZTE 30) milled fractions.

- the material required no addition of deflocculants or dispersants for obtaining the necessary flow properties. This advantage of not using deflocculant extends the life of the plaster moulds as well as leading to faster drying rates.

- the material was however mainly selected for its zero thermal expansion during heat treatment. This made the drying and firing rates both faster and the product stronger in terms of thermal stresses initiated during the forming and drying processes. The product also showed exceptional thermal shock results after the three heating and cooling cycles (Figure 6.2).

- the product also fired to a creamy white colour making it more appealing for household use.

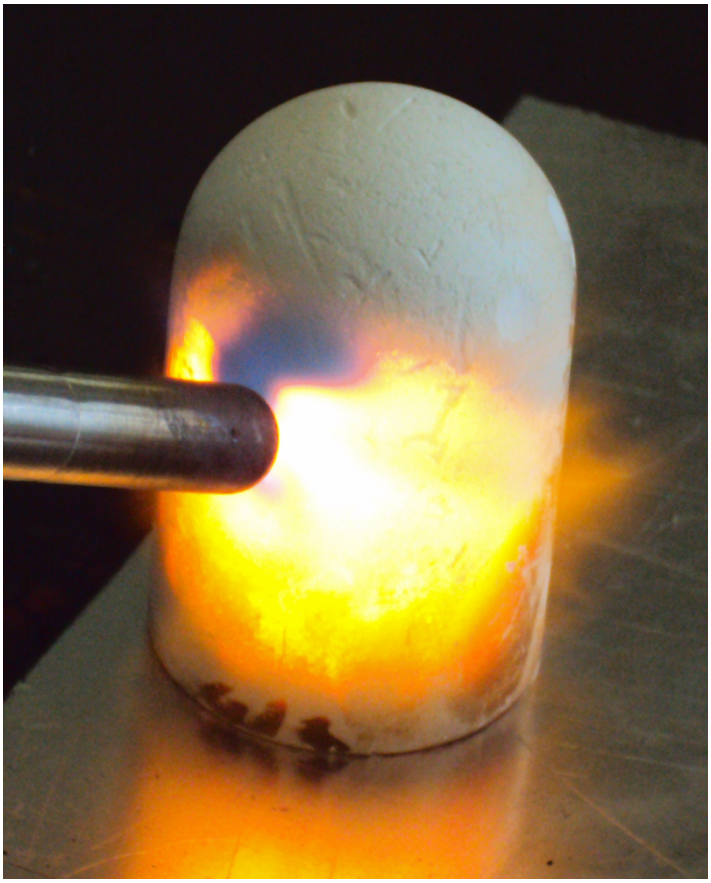

Figure 6.2: Testing Outbac for its exceptional thermal shock resistance (3 x differential heating and cooling cycles)

Table 6.2 show the chemical analysis and particle size distribution for lithium, alumino silicate from the supplier datasheet. The importance of LiO_2 concentration which is responsible for the low thermal expansion coefficient was a very important reason for choosing this material.

Table 6.2: Lithium, alumino silicate datasheet

Lithium alumino silicate (ZTE 200)

Chemical Analysis

Oxide	Units	Value
$Li0_2$	%	4.28
K_2O	%	0.12
Na_2O	%	0.53
Al_2O_3	%	17.4
Si_2O	%	73.96
Fe_2O_3 Total	%	0.03
Fe_2O_3 Inherent	%	0.02

Partice Size: Cummulative

Size	Units	Percent Retained
212 - 150	µm	Trace
150 - 106	µm	0.51
106 - 75	µm	3.64
75 - 53	µm	24.45
-53	µm	75.55

6.2.2 Flyash cenospheres (Cenolite)

Cenolite is a coal ash waste product from coal fired power stations. The main factors for selecting cenolite as filler in the recipe include the following:

- Cenolite is shaped as a perfectly spherical bead that provides the coarse size particle fraction necessary for both flow and particle packing density (Table 6.3).

- the material has to be milled for 15h to obtain a combined PSD with lithium, alumino silicate that provided a good packing density.

- the material is composed of the minerals fused alumino silicate and mullite (thermally stable) that provide a thermally stable material for inclusion into the slip

The addition of cenolite to the slip therefore assists in providing the necessary coarse fraction (PSD), perfectly spherical particle shape (enhanced flow) as well as assisting in thermal shock resistance of the product (a property that makes the filter useful in application other than for water filtration such as aerators in molten aluminium industry). The Cenolite together with the Lithium, alumino silicate also assists in lowering the firing temperature to levels where the dried product can be fired in an ordinary pottery-type kiln.

Cenolite is ball milled for 15 hrs. together with the lithium alumino silicate to ensure that all agglomerates have been properly dispersed.

Table 6.3: Raw material datasheet: cenolite

Flyash: Cenolite

Mineralogical Analysis

Mineral	Units	Value
Fused alumino silicate	%	65 - 80
Mullite	%	25 - 35
Quartz	%	0 - 1
Calcite	%	0 - 1
Particle size	μm	150 - 300
Relative density	g/cm^3	0.6 - 0.8
Bulk density	g/cm^3	0.4
pH		6 - 8

6.2.3 Organic carbon pore former

Two pore former materials used in the study were organic carbon and dextrin. The organic carbon is made up of alpha glucosidic bonds, which cause helix-shaped molecules, giving a near perfect spherical particle (Figure 3.4). The main factors for selecting organic carbon as pore-former in the slip included the following:

- showed excellent flow (spherical particle shape) and dispersal properties when mixed with the other raw materials.
- required no dispersants or flocculant which ensured high solid load concentration in the slip.
- provided the slip with a strong dilatant rheology perfectly matching the combined rheology of the other raw materials in the slip. This resulted in limited segregation and high casting density, which provided a strong green product with good stripping and handling properties.

Some of the properties of the organic carbon are shown in Table 6.4. Particle size is 99.9 per cent finer than 150 micron with a PSD that combines well with the other raw materials.

Table 6.4: Raw material datasheet: organic carbon

Chemical/Physical Property	Units	Value
Brabender viscosity @ 92°C	BU	260
Grits 150 micron	µm	0.1
Moisture	%	10 - 14
pH		5 - 6
Sulphur Dioxide	ppm	100
Amylose	%	26
Amylopectin	%	74

6.2.4 Activated carbon

Granular activated carbon (GAC) has a high surface area (SSA) and is prepared from coconut shells or coal, which has a relatively wide pore distribution ranging from micro- to mesopore size. Due to its large specific surface area as shown in Table 6.5, GAC has a wide use in water treatment. It was therefore selected for addition (added to the inside of the ceramic candle) to the final product. It is added to the final product in granular form and assists in the removal of odours, tastes and trace metals from water.

Table 6.5: Raw material datasheet: activated carbon

Activated Carbon (12 x 30 mesh)		
Property	**Units**	
Origin		coconut shell
Mesh size	US ASTM	12x30
Surface Area	m2/g	1100-1250
CTC	%mm	60-70
Iodine No.		1050-1200
AP	g/cm3	0.44-0.48
Hardness	%	95-99
pH		9-11

6.3 Process flow diagram

The flow diagram, Figure 6.3 demonstrates the process flow required for both the manufacturing as well as the testing of a porous ceramic water filter. The process was explained in Chapter 5: Experimental Procedure.

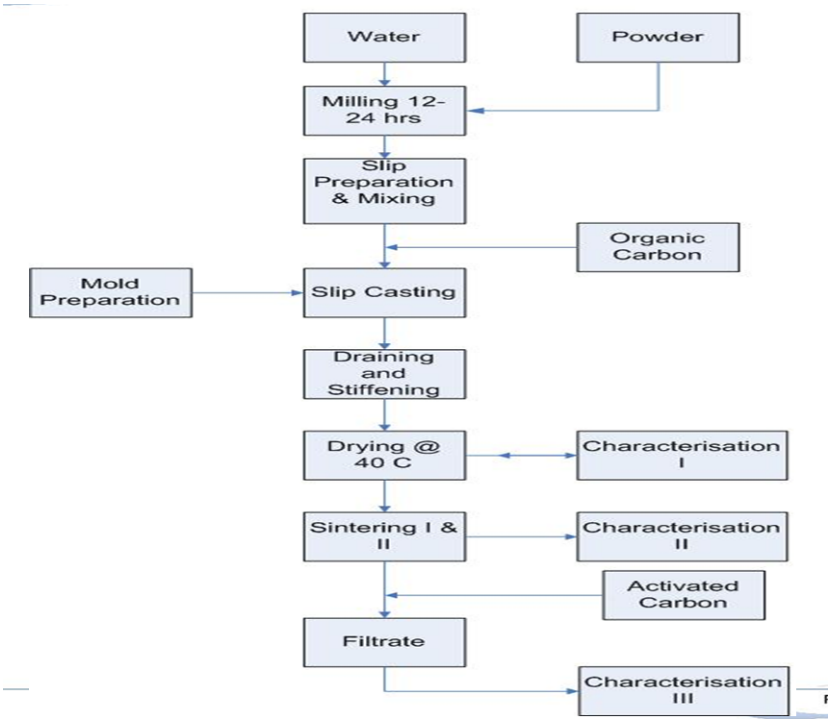

*Figure 6.3: Ceramic filter (*OUTBAC*) manufacturing and testing process flow diagram*

6.4 Milling

6.4.1 Particle size distribution for optimum packing

Milling of the lithium alumino silicate was necessary for obtaining adequate particle size and size distribution for optimum packing. The solid particle packing potential is the main parameter that influences all the other parameters as was explained in Chapter 4 and 5. Optimum packing for slip casting was obtained by comparing the PSD of the mix with a continuous distribution packing model where particle size, shape, position and orientation of particles play an important role. The Dinger and Funk model, a modification of the Andreassen model, was used in determining the optimum packing.

The particle size analysis for the distribution giving optimum packing was analyzed using a Malvern- particles size analyzer as well as the hydrometer analyses. The results are presented for both the starting material (100% finer than 75 micron) and the milled material (15 h and 30 h fractions respectively) in Figure 6.4.

The important advantage of both the 12-15h and 24-30 h milled fraction is the percentage of smaller than 1 micron (-1 micron) fraction of 5 per cent and 10 per cent respectively for the two milled fractions. The finer particles help to optimise the grading of the entire mix (slip) by fitting in between the maximum particle size grains and contributed to the green strength of the demoulded items.

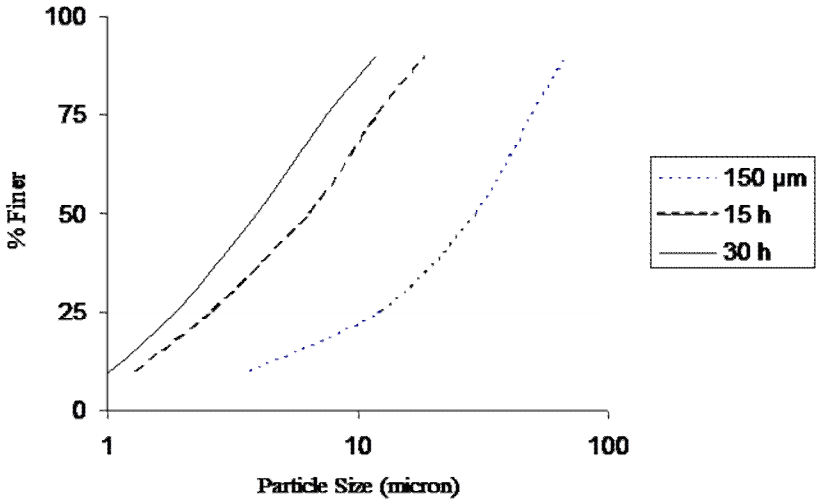

Figure 6.4: Particle size distribution of Lithium Alumino-silicate before and after milling

The optimum packing for slip casting was determined using spreadsheet software where the PSDs of various fractions were compared with the continuous packing model. The best result was obtained by using the four fractions (combined 15h milled Cenolite and ZTE 15, ZTE 30 and organic carbon) is illustrated in Figure 6.5. The amount of each fraction used, in obtaining the best fit with the model, became the mixing recipe.

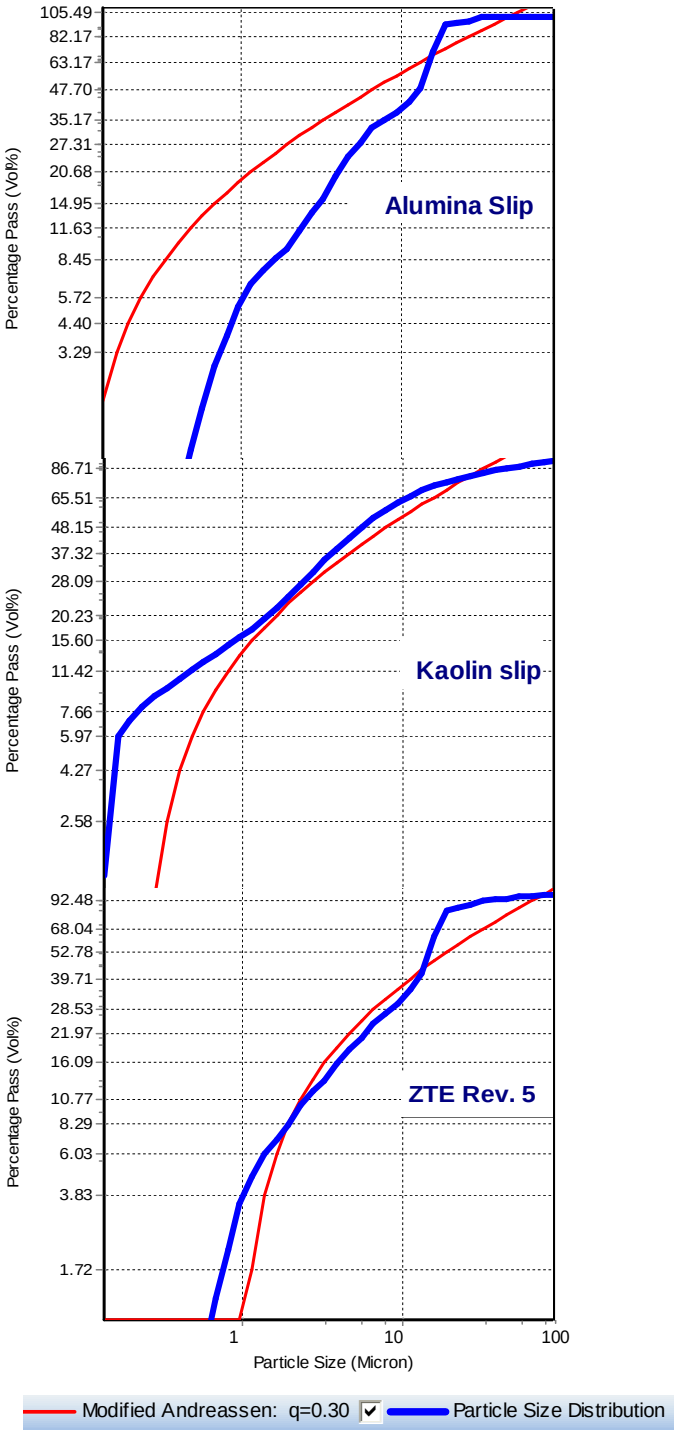

Figure 6.5: Best fit between slip recipes and modified Andreassen packing model

6.4.2 Slip recipe

From the milling tests and particle packing (best fit model) the best slip recipe and mixing procedure was derived. The recipe:

- Add 55 weight % lithium alumino silicate to 37 weight % water and bring into a suspension
- pour mixture into ball mill and mill for 15h
- decant suspension from the ball mill into a bucket
- split the suspension into two equal volumes
- add 8 weight % cenospheres to one of the suspension volumes and mill for 30h
- decant the contents of the mill into a large bucket, add the 15h suspension as well as 37 weight % pore former
- add the remainder of the water and hand mix and bring the material into suspension until all of the lumps have disintegrated
- add the suspension to the ball mill and mill for another 1h to break-up all lumps and aggregates and to condition the slip.
- decant the slip from the mill.

The solid content was adjusted to range between 65-70 weight per cent. This was followed by another 1h of milling for conditioning the slip.

6.5 Slip Rheology

As expected the slip gave a dilatant rheology with an increase in viscosity as the shear rate increased. Dilatancy increased and green body strength decreased with addition of organic carbon which limits the amount of organic carbon addition to 42% by weight. After the short 1h milling the slip was quality tested for slip SG and slip flow rate. The slip had to show a flow rates between 10-20 seconds and a SG of between and 1.53-1.72 $g.cm^{-3}$ respectively before the slip was quality passed for production (casting). These test values (flow rate and SG) was used the production standard (giving the least amount of rejects).

6.6 Shaping and stripping

Although high viscosity dilatant slips were prepared, the slip was easy to pour, which filled the mould quickly without leaving pouring marks on the outer surface. After consolidation in the mould the product stripped cleanly from the mould indicating that little or no segregation had occurred (Table 6.7). Very little shrinkage occurred but it was sufficient to release the product from the mould.

6.7 Burnout and firing schedule

Figure 6.6 illustrates the results from the modified TGA test for the burn-out cycle. The curve in Figure 6.6 can be distinguished in 3 zones:

- Zone 1 with a temperature range of 50–200°C is characterised by a 15 per cent loss in mass. The loss is due to evaporation of the mixing and bonded water.
- Zone 2 with a temperature range of 200- 300°C is characterised by 82% loss in mass. The loss is due to the loss of volatiles resulting from the oxidation of the pore-former (decarbonisation) which generates large amounts of gas, resulting in a dramatic loss in weight (Figure 6.7).
- Zone 3 with a temperature range of 300- 500ºC the weight remained constant with a 3% mass loss.

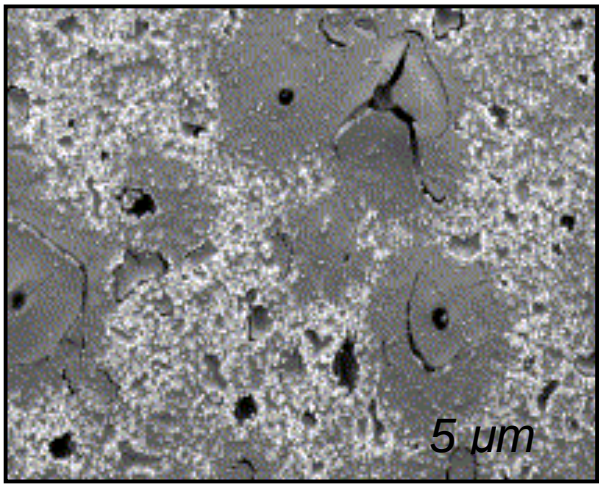

Figure 6.6: SEM image of ceramic after the Zone 2 burn-out stage at 200- 300°C (Unknown)

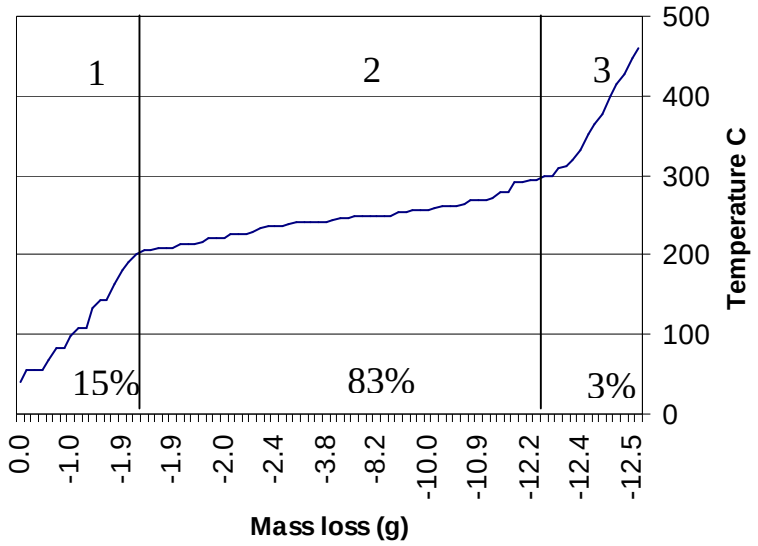

Figure 6.7: TGA curve with 3 characteristic zones and percentage weight loss for each zone during the burn-out and firing phases of the ceramic

The TGA curve was very helpful (especially Zone 2 with its 83% loss in mass) in designing the burn-out firing cycle and for contributing information (mass loss) to the design of the final sintering cycle. The design of the two firing curves used for the heat processing of the porous ceramic is presented in Figure 6.8.

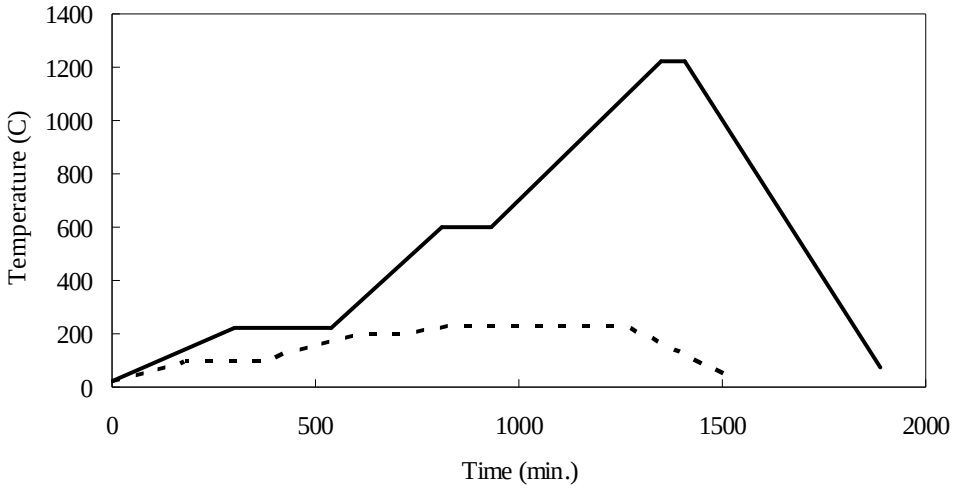

Figure 6.8: Burn-out (----) and sintering (—) heating schedules

6.8 Ceramic Filter Product Testing

6.8.1 X-ray Powder Diffraction (XRD) analysis

From the XRD diffraction analysis two crystalline phases were identified from the sintered ceramic product:

1. $LiAlSi_3O_8$ forming the dominant phase
2. SiO_2 in trace quantities but acting as internal standard

The dominant phase obtained compared best with that for tetragonal high temperature phase of $LiAlSi_3O_8$ (International Index Reference Pattern: 35-794) and forms the end member of a complete solid solution series with beta-spodumene.

6.8.2 Pore structure

6.8.2.1 Water immersion technique

Water absorption test results are shown in Table 6.6. The range of porosities and water absorption are indicative of an increase in permeability for the various CWF products. Table 6.7 indicates, from porosities and water absorption results, the limited amount of segregation that takes place during slip casting.

Samples were taken from three filter localities (top T, - casting side, middle, M, and bottom, B) as indicated in Table 6.7.

Table 6.6: Porosity and water absorption for four CWF types: Low K, Medium K, High K and Coated (Sample size, n=5)

n=5	**Sample**	**AP (%)**	**WA (%)**	**ASG (g.cm-3)**
$\bar{x}$	Low K	67	85	2.42
s	Low K	0	0	0.01
$\bar{x}$	Medium K	73	109	2.44
s	Medium K	0	0	0.05
$\bar{x}$	High K	73	113	2.41
s	High K	0	1	0.01
$\bar{x}$	Coated	30	19	2.27

Table 6.7: Sampling positions to test for segregation during slip casting using porosity and water absorption results (Sample size, n=3)

SAMPLE	(%) AP	WA	ASG	(g/cm3) BD
B3	68	87	2.44	78
B1	68	87	2.42	78
B2	70	95	2.44	74
AVE	**69**	**90**	**2.43**	**76**
SD	**1**	**4**	**0.01**	**2**
T1	68	86	2.44	79
T2	68	87	2.45	78
T3	68	87	2.44	78
AVE	**68**	**87**	**2.44**	**78**
SD	**0**	**0**	**0.01**	**0**
M1	68	86	2.44	79
M2	68	86	2.44	79
M3	68	86	2.45	79
AVE	**68**	**86**	**2.44**	**79**
SD	**0**	**0**	**0.01**	**0**

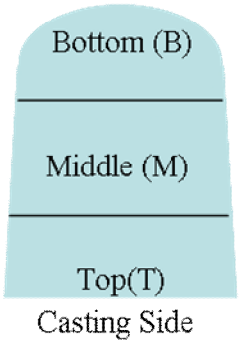

6.8.2.2 Hg porosimetry investigations

The pore size distribution of sintered samples were analysed with the use of a Micromeritics mercury porosimeter. The pore size distribution gave a measure of the interconnected pores left behind by the carbon particles. Figure 6.10: illustrates the pore size distributions for the samples milled at different times (12, 24, 35 and 40 hours).

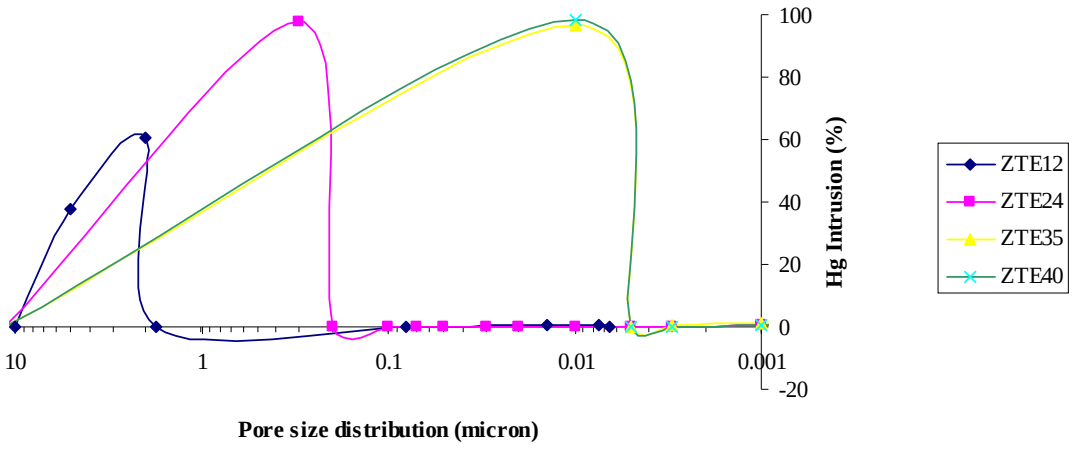

Figure 6.9: Pore size distribution for samples prepared using Lithium alumina silicate (ZTE) milled for progressively longer times (ZTE12: 12 h milling, ZTE24: 24h milling etc.)

Figure 6.10: illustrates the pore size distributions for different recipes using variety of LAS raw material fractions. Recipes consist out of a coarse fraction (d_{50} of 2.5; 3.8 or 5 micron) combined with equal amounts of the regularly 12-15 h and 24-30 h milled fractions (1224). Lastly the pore-former added amounted to either 25 or 40 per cent. Most of the pore size distributions are positioned around 3 micron. The Outbac sample however shows a pronounced bi-modal distribution around 3 (24%) and 0.008 (63%) micron.

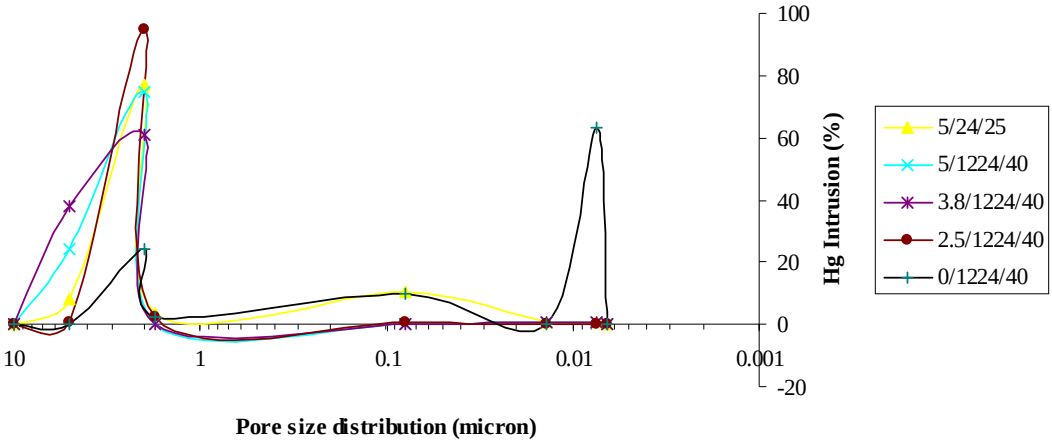

Figure 6.10: Filter pore size distributions obtained from Hg porosimetry

Table 6.8 provides a summary of the total pore area (pore specific area) as well as the average pore diameter for either the milled fractions or for the samples prepared using the recipes listed above.

Table 6.8: Total pore area and average pore diameter for selected sample blends and milled powders

Sample	Total area (m^2/g)	Ave. dia. (micron)
5/24/25	4.39	0.39
5/1224/40	7.26	0.16
3.8/1224/40	9.32	0.28
2.5/1224/40	9.16	0.52
0/1224/40	287.41	0.03
ZTE12	5.12	0.04
ZTE24	6.80	0.04
ZTE35	6.80	0.04
ZTE40	17.14	0.02

6.8.2.3 Scanning electron microscopy (SEM)

Figure 6.11 show the SEM images photographed at two scales for the microstructure of the sintered samples. The large spherical shaped pores correspond to the shape and size of the original organic carbon.

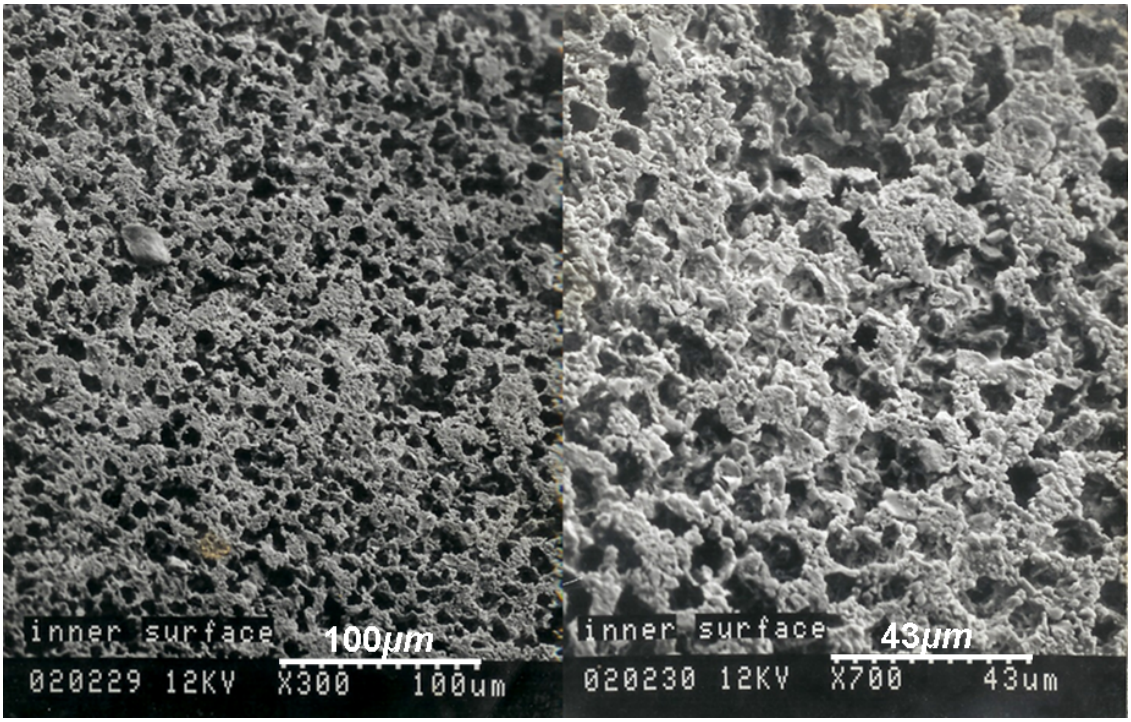

Figure 6.11: SEM images of the filters

The SEM images showed the following textural features:

1. Sintered fine grained equant particles 0.2 to 3 microns in diameter in a glassy matrix that tends to fill all the spaces between the individual particles with very few micro-pores of submicron size
2. Course vesicular structure where the rounded pore spaces are mostly between 2 to 4 microns. These pores appear to provide the main interconnecting channel ways.

6.8.3 Hydraulic conductivity (k) results

The standard organic carbon content was varied within the limits of still maintaining adequate flow properties, sufficient green strength for handling and firing. Table 6.9 shows the k values for the filter samples produced from 36.4 % (standard filter classified with a low degree of hydraulic conductivity as shown in Figure 6.12), 41.6% (low to medium flow classification) and 46.2% (medium classification) organic carbon additions.

A standard filter was dip coated with a 50h milled lithium alumino silicate, refired to 900°C before testing the hydraulic conductivity. The coated filters gave a very low k value excluding their use to highly polluted water only (Figure 6.12). The low k value obtained for the porous filter translates to a 0.5-1l h^{-1} filtration rate. The BACSTER filter with two fitted filters can therefore supply up to 2 l h^{-1} of filtered water which compares well with other low cost filter developments.

Table 6.9: Hydraulic conductivity (k) values for the CWF range

Degree of conductivity	k in $cmsec^{-1}$	CWF
High	**Above 10^{-1}**	
Medium	**10^{-1} to 10^{-3}**	**High flow**
Low	**10^{-3} to 10^{-5}**	**Standard**
Very Low	**10^{-5} to 10^{-7}**	**Coated**
Practically impermeable	**Less than 10^{-7}**	

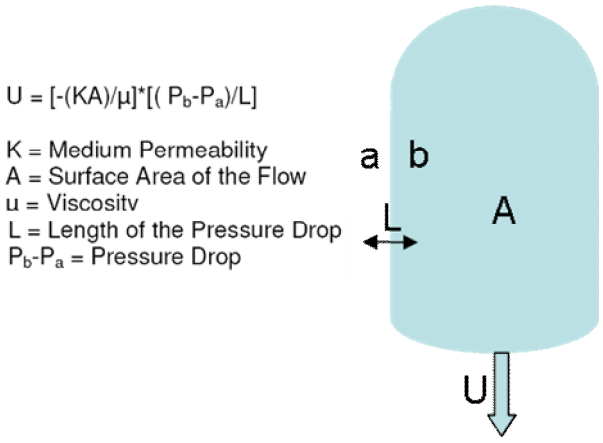

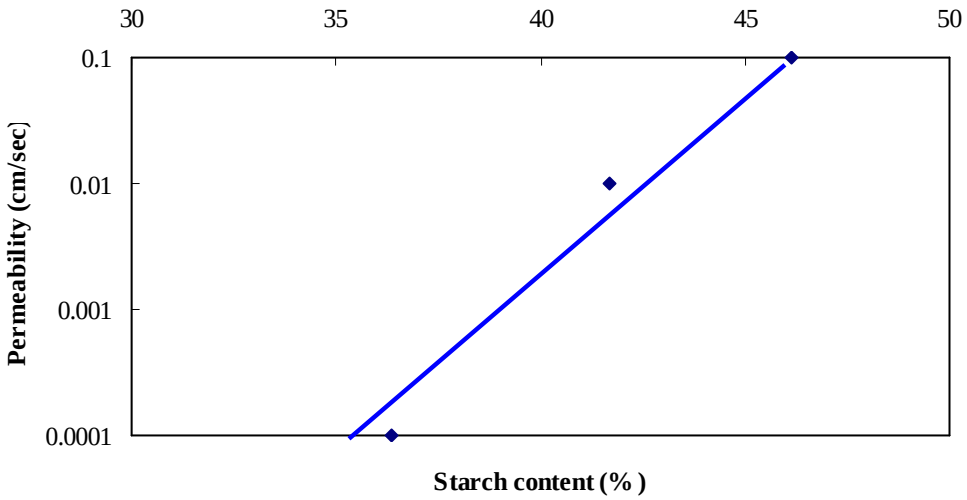

Figure 6.12: Water hydraulic conductivity ($cm.sec^{-1}$) for filters with different organic carbon contents

6.8.4 Bacster water retention time and tortuosity

The conclusion from the study indicated that for the standard filter (low flow) water spent a minimum of 32 minutes within the ceramic filter, as shown in Figure 6.13, before breakthrough of the chloride tracer occurred. The variables used for calculating tortuosity and hydraulic conductivity (constant flow rate) are shown in Table 6.10. Variables used in calculating the hydraulic conductivity (K), theoretical water travel length (Le) and tortuosity(t).

The water retention time of 32 minutes for the low flow filter compares well with the work of Fahlin (2003) where the water spent a minimum of 50 minutes within their filter before breakthrough of the tracer occurred.

The PfP filter described by Fahlin (2003) had a wall thickness of 10mm compared with the Outbac filter's thickness of 8mm which explains the slightly longer retention time of the PfP filter.

Table 6.10: Variables used in calculating the hydraulic conductivity (K), theoretical water travel length (Le) and tortuosity(t).

Parameter	Units	Description	Low flow	Medium flow	High flow
Q	mL/min.	Discharge through filter	112	170	331
K	cm/min.	Hydraulic conductivity	2.76×10^{-2}	4.9 x 10-2	8.1 x 10-2
A	cm^2	Cross sectional area of the ceramic filter	91	91	91
Δh	cm	Head difference between influent and effluent (filtrate) of the filter	31.50	31.50	31.50
L	cm	Shortest linear length of water travel through filter	0.8	0.8	0.8
t	unitless	Tortuosity as ratio of actual- divided by shortest distance linear length	1.14	1.225	0.61
Le	cm	Theoretical actual distance water travels	0.91	0.98	0.49
Ls	cm	Shortest linear length of water travel through filter	0.80	0.80	0.80
Retention	min.	Time before breakthrough of the chloride tracer occurred	32	20	6

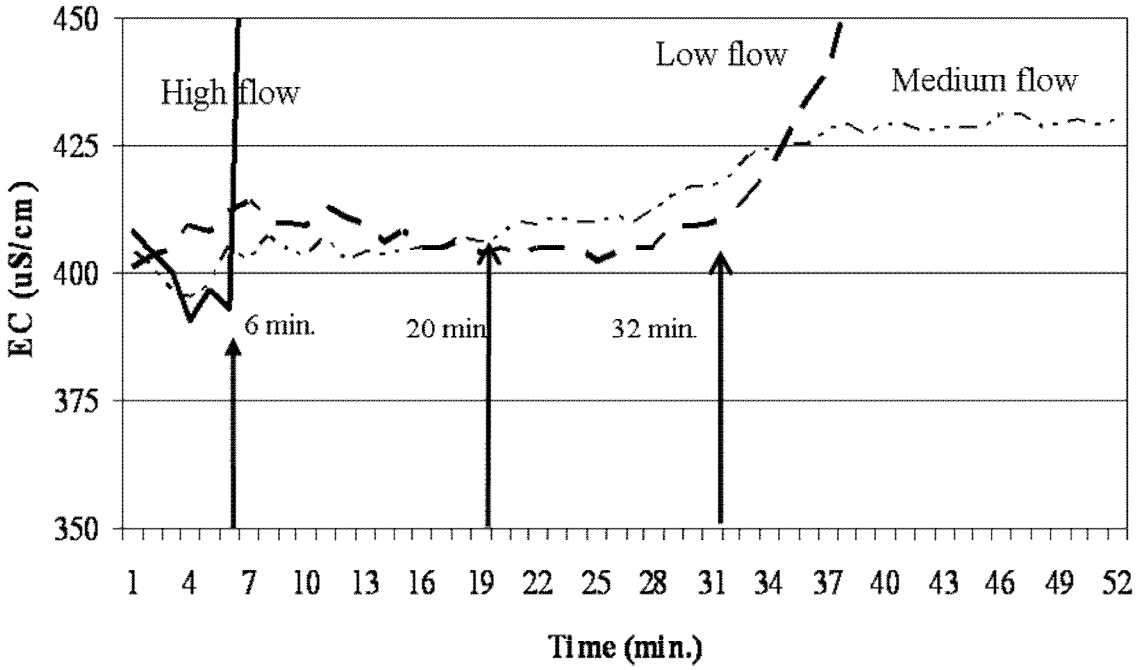

Figure 6.13: Retention time for the chloride tracer test with break through occurring after 6 minutes (high flow filter), 20 minutes (medium flow filter) and 32 minutes (standard, low flow filter)

6.9 Microbiological test results

6.9.1 Bacster effective pore size

Figure 6.14 indicates the effective pore size (determined by the pore porisimetry, Figure 6.9) for the BACSTER water filter relative to the size of pathogenic micro-organisms.

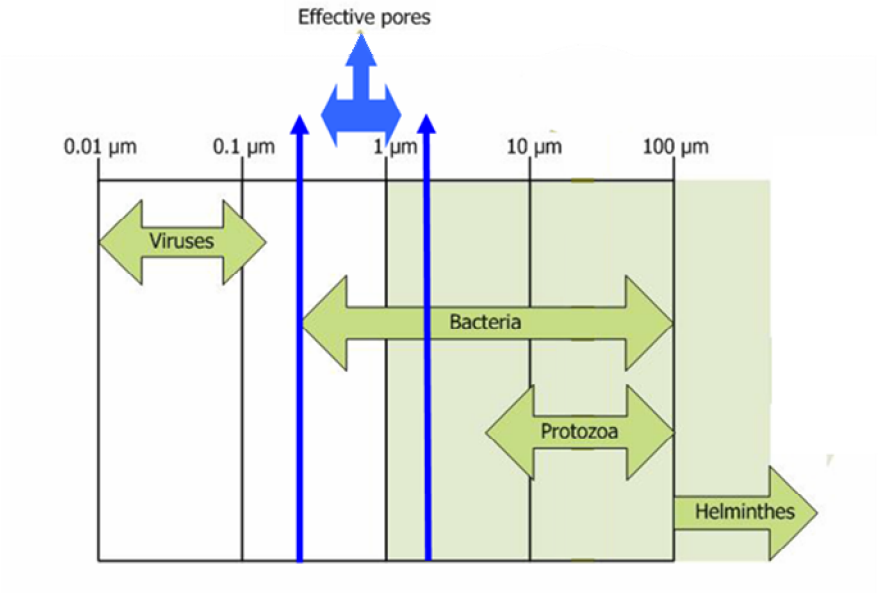

Figure 6.14: Bacster's effective pore size relative to the size of pathogenic micro-organism

6.9.2 Inoculation technique

The results for the two bacteriological techniques (Table 5.6: Bacteriological investigation) was applied and used in the preparation and testing of influent and effluent from the CWF. Table 6.11 applies to the pure culture inoculation and concentration of the influent water. The results show the micro-porous ceramic filters to be more than suitable for eliminating bacteria from highly polluted drinking water.

Table 6.11: Bacteriological test results of the filtrate (effluent water) LRV for the porous (standard) and coated filters

Bacterial species	Influent	Effluent (LRV)			
	CFU/ml	Standard	Coated	Med. Flow	High Flow
E. coli	6.0×10^6	5.5	6.8		
S. faecalis	1.5×10^4	4.2	4.2		
B. cereus	1.1×10^6	3.6	3.6		
Total coliform	1.0×10^5	> 6		5.6	4.9
Feacal coliform	5.7×10^4	> 6		> 6	> 6

Note: The $\log_{10}$ reduction value (LRV) is used to describe the bacterial removal efficiency. The LRV is calculated as: LRV=$\log_{10}$(influent CFU)-$\log_{10}$(effluent CFU). 1 LRV = 90% reduction; 2 LRV = 99%; 3 LRV = 99,9%; 4 LRV = 99,99%; 5 LRV = 99.999% & 6 LRV = 99.9999%

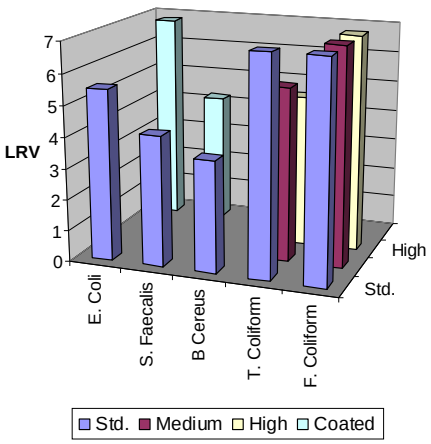

6.9.3 Membrane filter (MF) technique

Table 6.12 shows the results for both the natural water influent samples and effluent from the filter water samples processed using the membrane filter (MF) technique for heterotrophic count, total coliforms and faecal coliforms. Table 6.12 also shows the excellent results from the bacteriological testing. The results showed these micro-porous ceramic filters to be more than suitable for eliminating bacteria from polluted drinking water.

Table 6.12: Natural water influent samples and effluent processed using the membrane filter (MF) technique

		Total Coliform	*Feacal Coliform*	*Heterotrophic bacteria*
		Mangeza Stream		
	Influent (CFU/100ml)	**9×10^3**	**0**	**1.3×10^4**
Effluent (LRV)	**Standard filter**	**> 6**	**> 6**	**2.8**
	Low Flow Filter	**> 6**	**> 6**	**3.1**
	Medium Flow Filter	**> 6**	**> 6**	**2.3**
	High Flow Filter	**2.5**	**> 6**	**2.2**
		University Stream		
	Influent (CFU/100ml)	**1.0×10^7**	**5.7×10^6**	**1.8×10^7**
Effluent (LRV)	**Standard filter**	**> 6**	**> 6**	**> 6**
	Low Flow Filter	**> 6**	**> 6**	**6**
	Medium Flow Filter	**5.6**	**> 6**	**5.7**
	High Flow Filter	**4.9**	**> 6**	**5.1**
		Lake Mangeza		
	Influent (CFU/100ml)	**4.5×10^4**	**2.0×10^4**	**4.3×10^4**
Effluent (LRV)	**Standard filter**	**N/T**	**N/T**	**N/T**
	Low Flow Filter	**> 6**	**> 6**	**4.2**
	Medium Flow Filter	**> 6**	**> 6**	**3.7**
	High Flow Filter	**3.7**	**> 6**	**2.7**
	Mean	**5.3**	**6.0**	**4.0**
	σ	**1.2**	**0.0**	**1.5**
	n	**29**	**29**	**29**

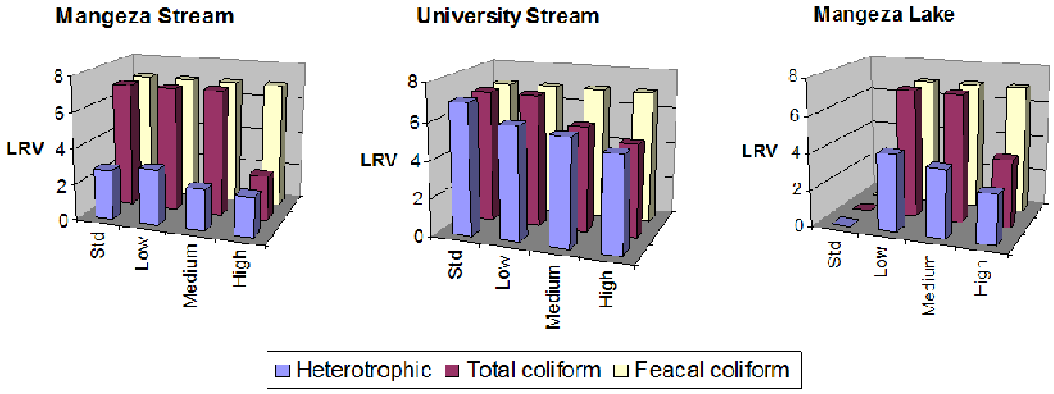

6.10 Water Filter System

Figure 6.15 to 6.17 show the 3 types of filter systems with their respective specifications, assembly instructions and cleaning hints that have been developed for domestic purposes:

a) gravity system – low pressure households (Figure 6.15: BACSTER)

b) siphon system – camping (Figure 6.16: OUTBAC)

c) high pressure – high pressure (- 2.5bar) (Figure 6.17: BACOUT)

6.10.1 BACSTER

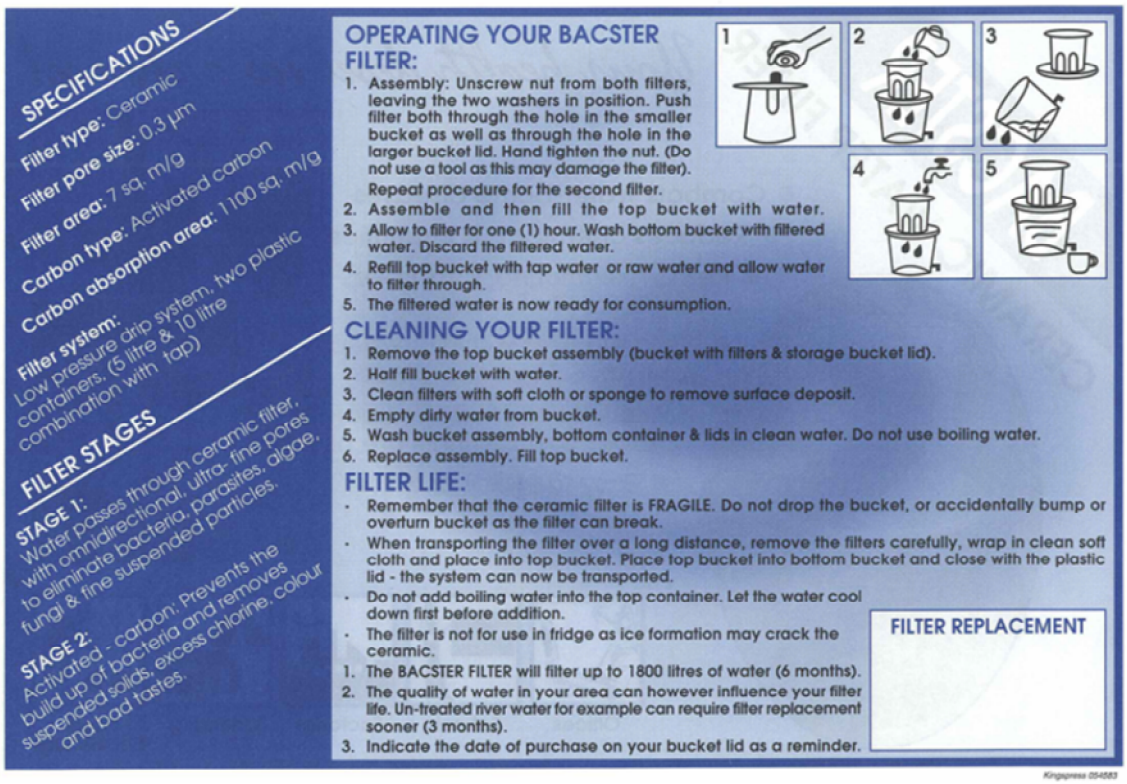

Figure 6.15: Bacster ceramic water filter datasheet

6.10.2 OUTBAC

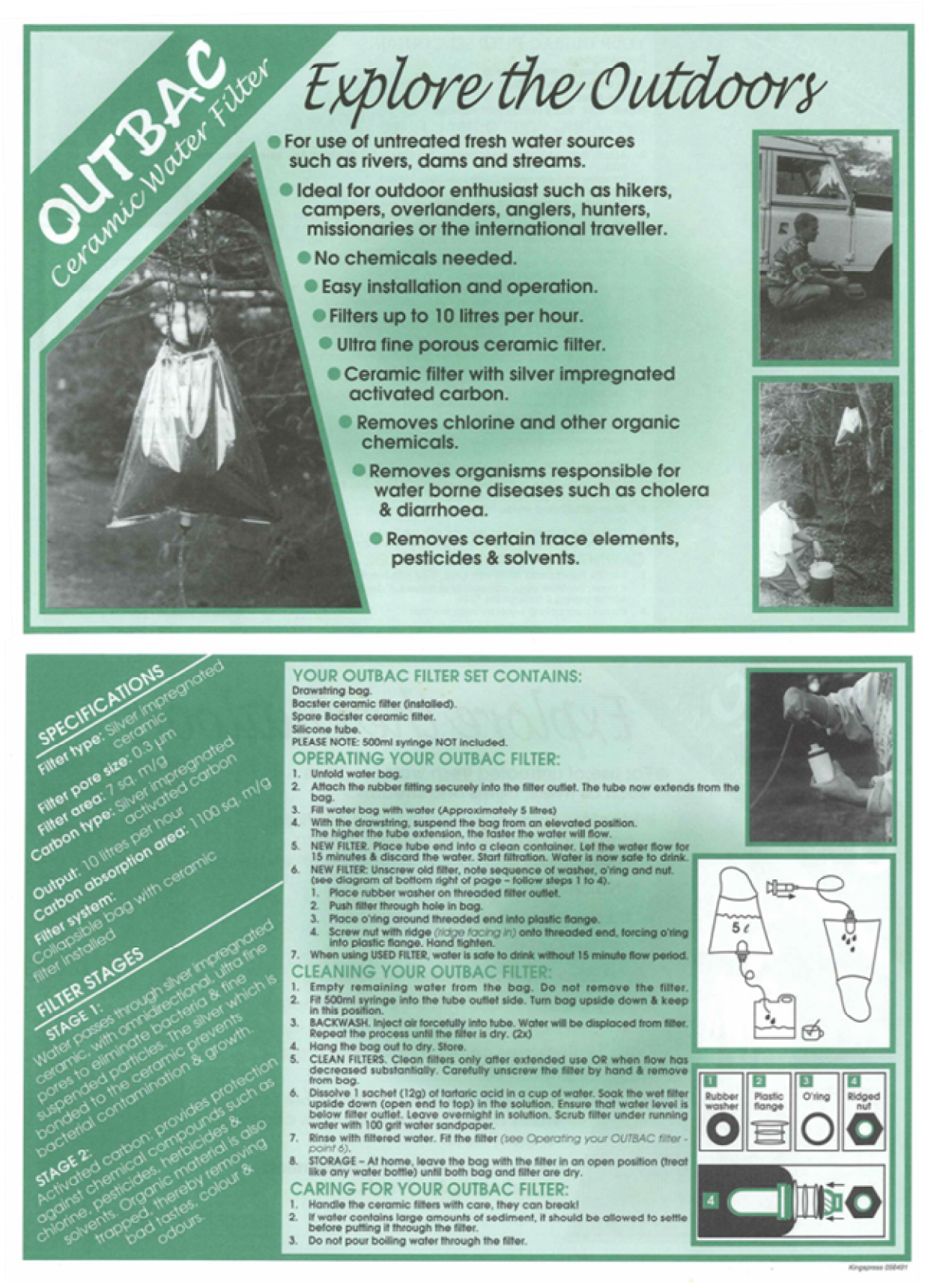

Figure 6.16: Outbac ceramic water filter datasheet

6.10.3 BACOUT

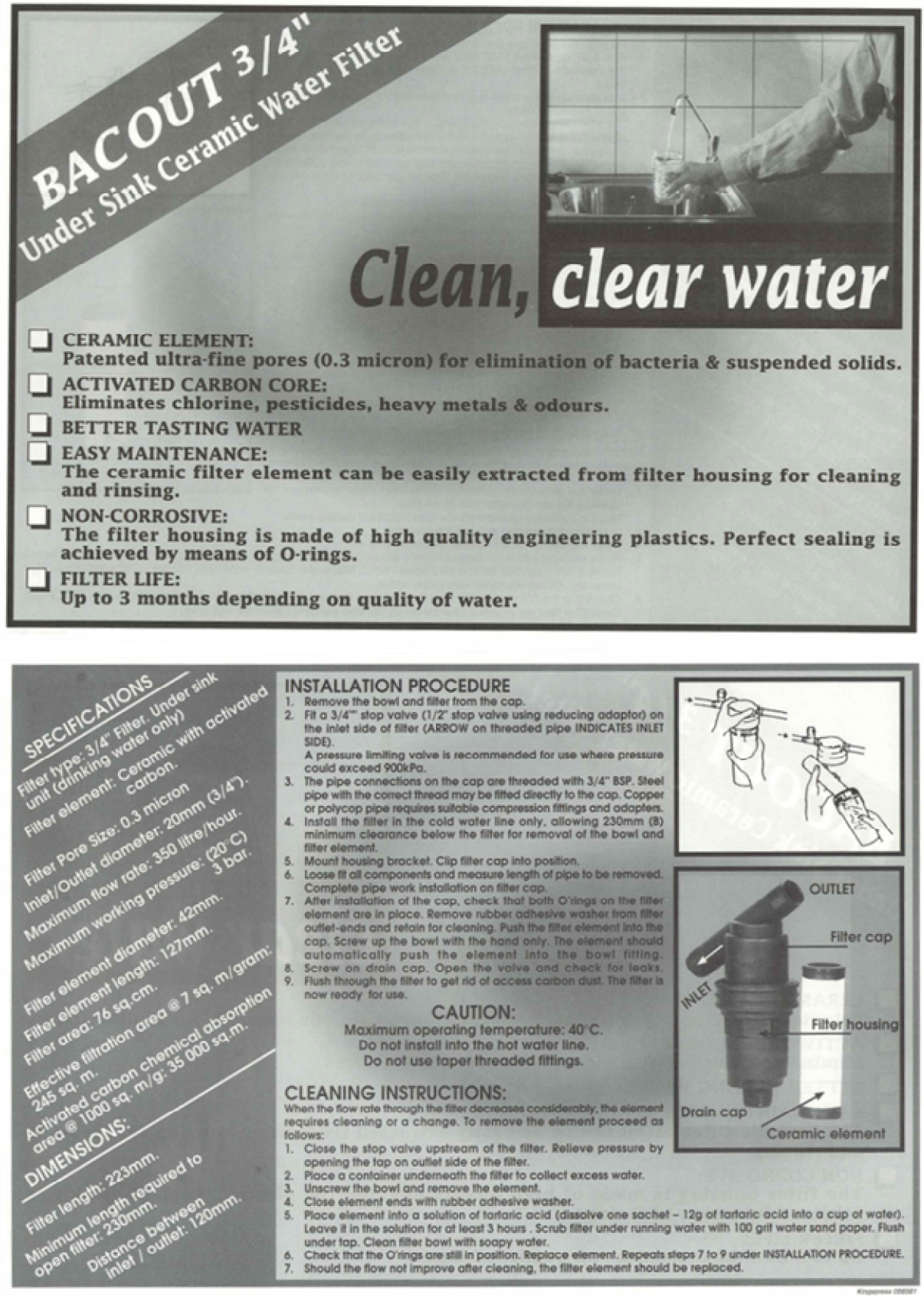

Figure 6.17: Bacout ceramic water filter datasheet

6.11 Comparison of BACSTER water filter with other low cost filters

Table 6.13 shows a summary of worldwide testing done on low cost CWF for the period 2000 to 2013. The average benchmark standard for *Escherichia coli* effectiveness was 97 per cent, whereas virus testing effectiveness was limited with a LRV[53] > 4 (99.99 per cent) as shown in Table 6.13, *Bacster/Outbac* performs far better than other low cost producers.

Table 6.13: Summary of bacterial and viral testing for low-cost CWF (References listed in Brown and Sobsey 2010 and Simonis and Basson 2011)

REFERENCE	BACTERIAL TYPE	[ ] REDUCTION %	[ ] REDUCTION LRV (log_{10})	REMARKS
Benchmark standards for low cost CWF				
Dies (2000)	*Escherichia coli*	> 98		Katadyn filter
Sagara (2000)	*Escherichia coli*			Nepalese CWF
	Giardia lamblia		4.6	
Lantagne (2001)	*Cryptosporidium parvum*		4.3	
(Lantagne 2001, Roberts 2004; Duke et al. 2006). Brown et al (2007)	*Escherichia coli*	GM 98		Brown (2007): 90- 99%
	diarrhoeal disease	mean 46		
Hwang (2002)	Total Coliform	94 - 99.9		Terafil filter (Low 2002)
	Escherichia coli	88		White Clay CWF
Dies (2003)	*Escherichia coli*	>98		White Clay CWF with CS
	Escherichia coli	>98		Hong Phuc CWF
Coulbert (2005)	*Escherichia coli*	99.8		Pozzani CWF
Franz (2005)	*Escherichia coli*	92 - 100		tested 5 types of commercial filters
McAllister (2005)	Bacteria	99		Potters for Peace with CS
	Viruses	20		
Clasen et al (2006)				mean reduction of 39 - 44% in diarrheal disease
Van Halem (2006)	*Escherichia coli*		3 - 6.8	
	Clostridium spores		3.3 -4.9	
Baumgartner (2007)	*Escherichia coli*	99.8		Filtron with CS
	Total Coliform	99.4		
WSP (2007)	*Escherichia coli*	UP TO 98	1.7	50% reduction in diarrheal disease
	Escherichia coli	boiling: 99		
Oyanedel-Craver & Smith (2008)	*Escherichia coli*	≥ 97.8		
	Viruses	< 90		
Brown (2010)	*Escherichia coli*	mean 99	2.1 - 2.9	
	Bacteriophages MS2	90 -99	1.2 - 4.1	
Momba et al (2010)	*Escherichia coli*	91.8	1.2	Used nanosilver as coating which leached at a rate of 0.5 mg/l
Momba (2013)	*Cryptosporidium oocysts*	92-98		CCF ceramic candle filter
	Giardia cysts	93-98		
	Somatic coliphages	80-100		
USA and other standards for producing drinking water				
(USEPA 1987; NSF 2003),	Bacteria		6	Specification for filters
	viruses		4	
	protozoa		3	
Brazil ABNT NBR 14908	*Escherichia coli*		2	
	Viruses			No reduction required
WQA ORD0901	*Escherichia coli*		3	
	Bacteriophages MS3		3	

[53] log reduction value, LRV= log_{10}([un-filtered].[filtrate]$^{-1}$

6.12 Input and output flows in the manufacturing of the porous ceramic filter

In this section factors such as consumption levels, associated emissions and unit costs, were determined for presentation as mass flow diagrams (Figure 6.18 and Figure 6.19). All production variables (raw material usage and costs, electricity consumption and costs, waste costs) were quantified for the presentation and for determining the unit cost of producing a low cost porous ceramic filter (EC 2007).

The manufacture of porous ceramic filter took place in an electric kiln, with a limited range of raw materials and two different shapes. The raw materials were further processed (milled) before mixing and casting (water was added for mixing and shaping) into shape using plaster moulds. The water was evaporated drying before the product was placed by hand in an electric kiln. The two-step firing required a pre-determined temperature gradient to ensure that the porous ceramic filters obtained the right treatment. After firing the kiln was allowed to cool (uncontrolled) for the product to release heat and prevent cracking of the ceramic structure.

Raw material, water and electricity consumption data for the manufacture of the porous ceramic filter are shown in, Figure 6.18, as a mass flow diagram. Emissions and process losses that arise from the manufacturing process of the porous filter are shown in Figure 6.18.

Process losses and waste

Broken ware can arise during the several manufacturing process steps (in particular shaping, drying, firing and subsequent treatment). Broken plaster moulds can arise through extended use of the moulds or during stripping of the body. Parts of the accumulated process losses mentioned above, can be recycled and re-used within process.

Filter costing

The unit cost of the filter (excluding labour costs) is shown in Figure 6.19. The diagram includes the costs for raw material, electricity costs and water costs.

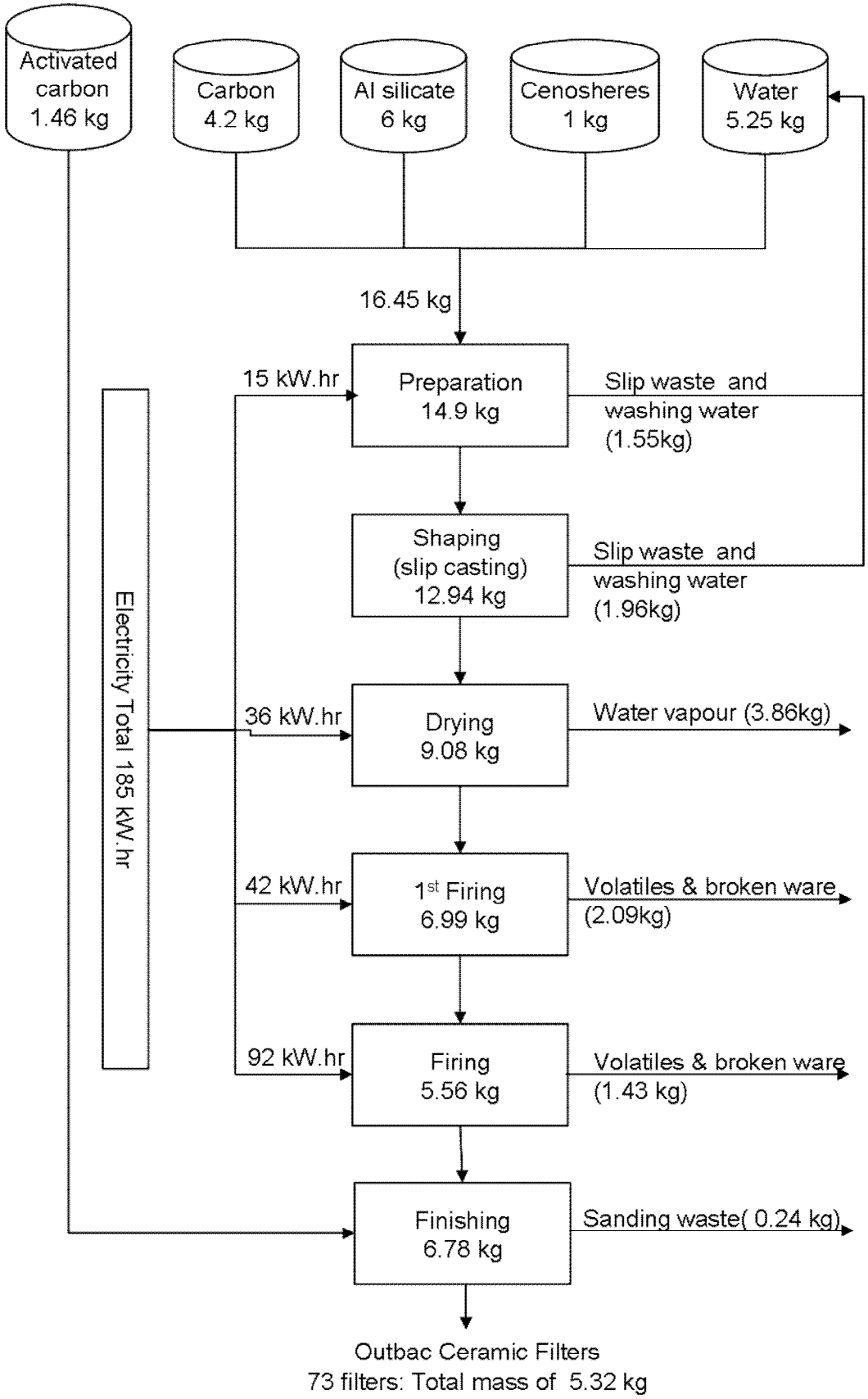

Figure 6.18: Material mass flow diagram for the manufacture of the Outbac *ceramic filter*

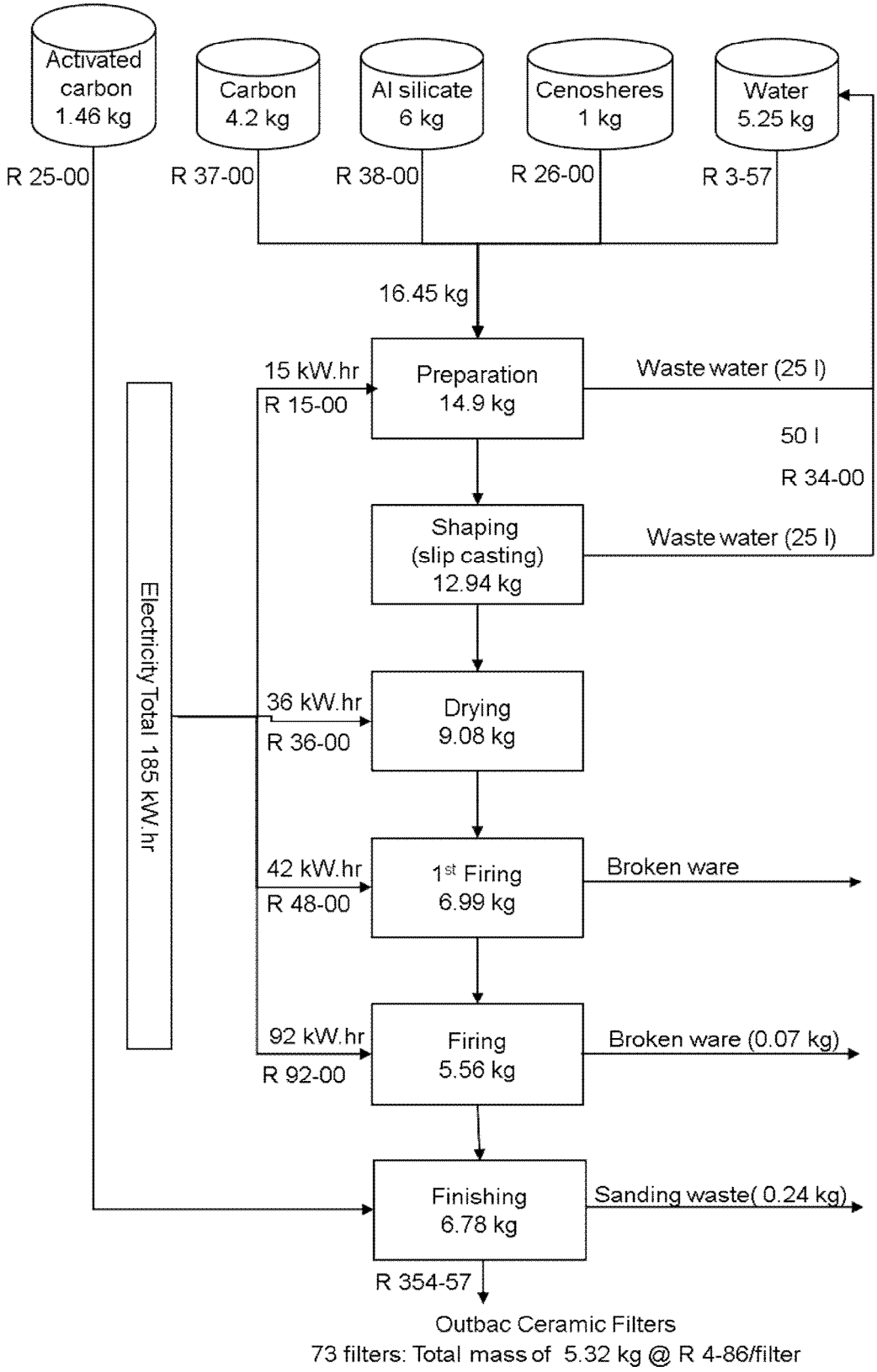

Figure 6.19: Costing diagram for the manufacture of the Outbac *ceramic filter*

Chapter 7: Summary, Conclusions and Recommendations

7.1 Summary

The slip casting shaping method was successfully used for the manufacture of a porous ceramic water filter. The method was found to be more suitable than either extrusion or die casting for manufacturing a locally suitable, low cost ceramic water filter. Slip casting, requiring limited expensive equipment, makes this the only promising method for manufacturing ceramic filters in a rural, non-technical setting.

The candle- type filter required less raw material compared to the other low cost filter such as the pot- type filter from Potters for Peace (PfP). To make the PfP filter clay, sawdust and water is mixed and then pressed into a pot shaped mould (10 l bucket size) using a press. The pressed items are large with thick walls requiring between 4-21 days for drying. The items are also large, with a 10 l storage capacity, which allow only a few to fit into the kiln space for firing as compared with *Bacster filter* shown in Figure 7.1. The low flow nano-coated filter can be effective in extreme conditions; however, low flow negates effectiveness in a gravity-fed filter system.

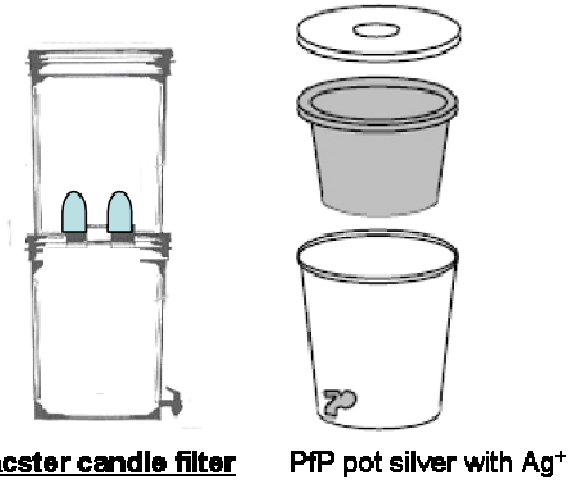

Figure 7.1: Comparison of the Bacster candle filter and the PfP pot filter, with special reference to size

Raw Material selection: Using milled lithium alumino-silicate has the main advantage of thermal shock resistance because of the material's zero thermal expansion at firing temperatures. The zero thermal expansion (adopted ZTE product name) helped to prevent damage (cracking) to the product during heating. The material also provides dilatant rheology matching the rheology of the organic carbon pore-former. The dimensional stability (low drying and firing shrinkage) of the product over the firing range also prevented unnecessary expansion and cracking of the product. Cenolite has a perfectly spherical grain shape as well as thermal stability (pre-fired in heating process in coal fired power stations). Both these materials (Cenolite and lithium alumino-silicate) were therefore selected as starting material. The organic carbon pore-former, with its dilatant rheology and spherical particle size, used also complemented the properties of the two main raw materials.

Ball milling, PSD and particle packing: A small scale, laboratory, ball-mill was developed and successfully used for obtaining the necessary PSD from the lithium alumino-silicate and cenospheres raw materials. Milling tests based on the Andreasen packing model were used for obtaining the best particle packing for the raw material recipe. The use of four raw material fractions from the milling process provided the required rheology, flow properties and high density of the green body. The fractions consisted out of the following materials:

a) lithium alumino-silicate (ZTE 15) obtained by milling for 15h,

b) Cenolite milled for 15h,

c) lithium alumino-silicate (ZTE 30) obtained by milling for 30h,

d) organic carbon pore-former

Slip casting rheology: The selection of organic carbon as the pore-former for the ceramic actually gave a number of additional benefits to the operation and manufacture. The dilatant rheology, excellent flow properties and dispersability of organic carbon when mixed with water negated the use of any dispersants or flocculants ensuring that we obtained high solid load density. This ensured that minimum segregation and maximum casting densities were obtained, giving us a sufficiently strong green product that could be stripped and handled without breakage.

The firing temperature was therefore also lowered allowing us to sinter at a temperature of 1230°C.

The particle size of the pore-former provided us with small pores around 3 microns after firing for the elimination of bacteria from drinking water. These pores were much smaller and more effective when compared with PfP's pore size of 16-25 micron.

Master mould design: For the plaster mould making stage, a master mould (shape) was selected that would result in minimum breakage and easy stripping. The final master was manufactured with a slight taper running from top to bottom. The taper helped with stripping as the material combination and high density achieved provided only very small drying shrinkage.

Slip properties: Two easy, on-site production measurements were used to fine-tune the slip rheology. The SG, as a reflection of the water content of the slip, and the variable shear (flow time), as a measurement of viscosity, were used to obtain a measurement of the relative Inter Particle Spacing (IPS) and therefore the slip rheology. It was found that the IPS could only remain constant if the solids content was varied in response to the changes in packing capability of the changing PSD from milled material. By slightly modifying the solids content (recipe) it was possible to ensure that the particle-particle interactions (particle attraction-repulsion characteristics) remained similar from milled batch-to-milled batch. This also resulted in no chemical dispersants (additives) being required. This process was repeated until we came up with a recipe that could give us the required product qualities (filtration and hydraulic conductivity requirements).

Burn-out: The decarbonisation process was carried out separately from the sintering process. The two-stage process had the advantage of both improved de-gassing by stacking on an open grid and by yielding the least number of final defects. The defects could be removed prior to further firing. Even with a wall thickness in excess of 10 mm, less than 5% of defects were obtained.

Cracking normally results from stresses generated during the decarbonisation process and the low strength of the ceramic matrix. Although the process requires more time and energy, the inspection stage built in prior to the second stage of burn-out and sintering resulted in a reduced reject rate.

Firing cycle: In general the organic carbon containing bodies were burned out without any problem. This shows the importance of using the 2 stage firing process with regard to time efficiency and crack avoidance.

Sintering was performed with limited deformation and shrinkage indicating good homogeneity of the raw materials preparation and thermal stability of the raw materials used. Limited dimensional change (shrinkage) gave accurate control of the ultimate filter size after sintering.

Filter porosity: The overall pore size, obtained from the SEM images after firing, and the pore size distribution from Hg porosimetry, agree with each other. When comparing the bi-modal pore size distribution with the size of pathogenic micro-organism, it is clear why the filter has such an excellent capability, for filtering out bacteria. The pore size of the filter covers, in size range, from bacteria, protozoa, helminthes and to viruses (the latter only to limited extent). The pore-former provided us with small pores that are much smaller and more effective when compared with PfP's pore size of 16-25 micron.

The large apparent porosity results of between 67-73 per cent provide a specific surface area of 7 m^2 g^{-1} and a high flow rate which explains the filtration efficiency of the filter. The 32 minute retention time of water further helps with the filtration effectiveness.

Hydraulic conductivity: The hydrodynamic aspects of the ceramic filter design and operation was tested to ensure the proper distribution of flow through all the pores (not just the largest or pores under highest hydraulic pressure and effective retention time through the activated carbon. Hydraulic retention time in the ceramic and activated carbon core is a key parameter in the filter's performance. Three filter types were developed with variable hydraulic conductivities, a low (standard)-, medium- and high- flow.

The balance between filtration and conductivity was tested by conducting both the conductivity (flow) tests and subsequently conducting the microbiological tests on the same filters. The best compromise was found with the medium flow filter that gave a k of 10^{-1} and 10^{-3} cm s^{-1} (flow of 1.5- 2.0 l h^{-1} for the Bacster Filter System and a water retention time of 20 minutes) and LRV for faecal coliform of > 6 (99, 9999% effective).

Microbiological testing: Bacteriological testing exceeded all expectations. The WHO (2011) recommends a performance requirement for household water treatment (HWT) technologies and associated $\log_{10}$ reduction criteria as interim, protective and highly protective for reference microbes (virus, bacteria and protozoa). The log10 reduction for bacteria specifies a $\geq$ 4 requirement. The National Sanitation Foundation (NSF) specifies that POU water treatment systems should produce potable drinking water that meets a 6 $\log_{10}$ reduction of bacteria, 4 $\log_{10}$ reductions of viruses, and a 3 $\log_{10}$ reduction of protozoa (USEPA 1987). The low cost filters developed and tested in this study came close to meeting the extreme performance criteria for the elimination of bacteria. This product can immediately be useful to families placed in situations where polluted drinking water causes distress. The PfP, with a much larger pore size, required an additional coating of silver to effectively removing only 46% of diarrhoea-causing bacteria.

The method of slip casting for the manufacture of porous ceramic used in this study has been showed to work very successfully. The filter requires fewer raw materials, energy for the shaping- and firing- process, finishing, storage space, it is small, compact, and more effective against bacterial load and has a flow rate 3-4 times faster than any other low cost manufactured filter. The low unit manufacturing cost, places *Outbac* in a strong position, to also compete on a price-only-basis with other low cost, ceramic filter producers in the world.

7.2 Conclusions

Aims

The main aim is to develop and evaluate a ceramic micro-porous filtration system using the slip casting technique for application in domestic water supply.

A micro-porous ceramic water filter with micron-sized pores was developed using the traditional slip casting process. The filter has the advantage of low cost due to the usage of locally available raw materials, labour and local expertise.

The product was tested using water contaminated with high concentrations of selected bacterial cultures as well as with locally polluted stream water. The filter was found to be highly effective in the removal of bacteria and suspended solids found in natural water. With the correct cleaning and basic maintenance this filter technology can effectively provide clean drinking water for rural families affected by polluted surface water sources.

Objectives

1. *Conduct a literature study and evaluation of the best method available for making ceramic micro-porous material*

   An exhaustive literature study identified three common forming processes suitable for shaping porous ceramics: pressing, extrusion and slip casting. Each of the fabrication methods result in a specific range of pore size, pore size distribution, porosity, as well as varying levels of interconnectedness among the pores. Furthermore the amount, size and shape of defects in the ceramic are also dependent on the processing method used. Finally, each fabrication method differs in terms of overall investment cost and cost per product and quality requirement for making a ceramic filter.

   The traditional slip casting process was selected as most suitable for the development of a porous ceramic, water filter.

2. *Source, investigate and test (rheology) ceramic materials for their suitability in the slip casting method*

   The raw materials selected and used in the development process gave the best fit for the important slip casting criteria:

   a) limited further processing was necessary
   b) rheology that formed stable suspensions with minimum segregation
   c) allowed quick release (without damage) of the product from the mould
   d) the pore former matched the slip rheology, releasing volatiles without creating any defects
   e) the product proved to be temperature insensitive (minimum thermal expansion and thermal shock) over the firing range and fused together during sintering stage to give a strong product with a maximum degree of porosity

3. *Produce ceramic samples for filtration testing and evaluation*

   Slip preparation: Particle size distribution and its related factor, the packing density, were fine-tuned with milling processes and resulted in the inclusion of two ball milled fractions. The milling reduced the d_{50} (average particle size) from 30 micron to 4 micron as well as increasing the -1 micron (fines) fraction. The organic carbon pore-former provided additional stability to the slip as a result of its dilatant rheological properties.

   Flow properties: Density and flow measurements were kept within pre-determined limits to avoid variations that could have resulted in casting defects.

   Forming: Stable slip was poured into plaster moulds and kept full of slip until the desired wall thickness had been achieved. The forming process was then stopped by inverting the moulds to remove the excess slip (drain casting). The high density achieved during casting resulted in the green product stripping within seconds after casting for overnight drying.

Pyrolising, burnout and sintering: The two stage firing process gave minimal defects (less that 5%). Although the process required slightly more time/energy, the inspection stage built in prior to the second stage of burn-out and sintering resulted in a reduced reject rate. Sintering was completed with minimal shrinkage.

Product testing: Physical tests and scanning electron microscope images provided us with the evidence why this filter is such an effective micro-sieve:

a. Course vesicular structure where the rounded pore spaces are between 2 to 4 micron in diameter with a few micro-pores of submicron size also visible. These pores provide the main interconnecting channel ways.

b. The bi-modal pore size distribution provided a combined 7 m^2 g^{-1} surface area for filtration.

c. The medium k (permeability) value obtained for the high flow type porous filter translated to 8-10 L h^{-1} filtration rate, making them suitable for providing sufficient drinking water for an average sized family.

4. *Evaluate the effectiveness of the micro filtration system for removal of pathogenic bacteria*

Two bacteriological techniques were used for the preparation and testing of influent and effluent from the filter:

a. using naturally occurring water from two streams, samples were processed using the membrane filter (MF) technique for heterotrophic count, total coliforms, and faecal coliforms

b. pure cultures of *E. coli, S. faecalis and B. cereus* were inoculated in water for the influent water.

Bacteriological testing exceeded all expectations and came close to the USEPA standards developed for developed countries, exceeded the WHO recommendation for purification units and provided better protection than

most of the previously tested low cost ceramic water solutions.

5. *Design and create an effective micro filtration systems for household use*

Three filter systems were developed benefitting from the small omni-directional, ultra-fine pores (0.3μm) creating capillary suction involving every pore in the filtration process:

a. High pressure filter: *BACOUT*
b. Gravity filter (2 bucket system): BACSTER
c. Syphon filter: *OUTBAC*

7.3 Impact

A micro-porous ceramic water filter with micron size pores was developed using the traditional slip casting process. This locally produced filter has the advantage of low cost, less raw materials, less labour, less energy, less expertise and the opportunity for local financing and innovation. Enhanced flow is obtained through this filter system. The product was tested using water inoculated with high concentrations of different bacterial cultures as well as with locally polluted stream water. The filter was found to be more than effective than other similar low cost filtration units in providing protection from bacteria and suspended solids found in natural water. With correct cleaning and basic maintenance this filter technology can effectively give drinking water to rural families affected by polluted surface water sources.

7.4 Recommendations

Low cost production: Proceed immediately with the initiation of small micro enterprises for the production of porous ceramic, assembly of OUTBAC water filter, as well as the marketing and sale of the product to needy communities suffering from a lack of potable water.

Initiate the process by both providing training in the slip casting technique. Start with a pilot programme that could provide a model for similar production unit's through-out Africa.

Viral protection: With more than 100 viruses occurring in drinking water, none of the filters indicated in Table 6.13 could effectively remove viruses. To be 100% effective further research has been initiated at Unizulu. Initially a two-step treatment is recommended:

- disinfection by bleach treatment or use of an non-chemically, nano coated CWF
- physical and chemical removal (bacteria, chlorine) using CWF system combined with activated carbon

The removal of pathogenic viruses from polluted drinking water is technologically challenging. The small particle size of viruses (25–200 nm) makes it possible to remove them using expensive nano-filtration and reverse osmosis, which are not suitable or affordable on a domestic scale. Viruses do not travel independently in water, however, but "hitch a ride" on larger host particles such as microbes. Initial results have shown that the larger hosts, to which the virus is attached, may then be removed together with the viruses, either, by filtration, or by their inactivation by incorporation of metallic ions into their enzyme system in a chemical reaction, or by a combination of the two methods.

Further research is in progress with a silver-impregnated filter tested on water samples contaminated with *Escherichia coli, Proteus mirabilis, Pseudomonas aeruginosa,* for its oligiodynamic effect, as well as somatic bacteriophages. The ceramic filters reduced the viral count by 94–99%. We believe that, with further development, our prototype is easily capable of achieving the WHO criterion at modest additional cost.

WHO recommendations for household purification systems

An added requirement is satisfying the above mentioned recommendation of the WHO for household water-treatment systems to eliminate 99.99% of microbial contamination. This is proving to be exceptionally difficult to achieve in poor countries at a cost they can afford.

Further testing as required by WHO (2011) standards for household water treatment systems for correct, consistent and continuous use should be applied to the filter for certification and will include testing using virus and protozoa reference microbes.

We therefore believe that if implemented on a large enough scale, the improved, low cost, ceramic filter offers the prospect of providing safe, affordable drinking water to millions of people in Africa who currently are at risk of waterborne diseases from microorganisms.

References

Akhond, H., Taheri, E., Sarpoolaky, H., and Taavoni, A., 2009. Gel-casting of Alumina Nanopowders Based on Gelation of Sodium Alginate. Ceramics International, 35, pp. 1033–1037.

Almeida, F.A., 2009. Influence of cassava starch content and sintering temperature on the alumina consolidation technique. Journal of European Ceramic Society, Vol. 29, pp 1587 – 1594.

Andreasen, A.H.M., and Andersen, J., 1930. Ueber die Beziehung zwischen Kornabstufung und Zwischenraum in Produkten aus losen Koernern (mit einigen Experimenten), Kolloid-Z., 50, pp. 217-228.

Aqua Rain, 1998. Emergency Water Systems for Times like these. Water Conditioning & Purification Magazine, March, pp.66.

ASTM C 20-87, 1988. 1988 Annual Book of ASTM Standards. Section 15, Vol. 15.01, pp. 5-7.

ASTM D3350-96. Particle size distribution by Hydrometer of Common White Extender Pigments.

Bae, S., and Baik, S. 1994. Critical concentration of MgO for the prevention of abnormal grain growth in alumina. J. Am. Ceram. Soc. 77: 2499-2504.

Baeuerlein, E., 2000. Biomineralization, Weinheim: Wiley-VCH.

Bai, Z. and Sharma, A., 2008. 'Sheba' – A New Low Cost Household Water Filter. 33rd International Conference, Accra, Ghana.

Balzer, B. and Gauckler, L.J., 2003. Chapter 5- Novel Colloidal Forming Technique: Direct Coagulation Casting. Handbook of Advanced Ceramics S. Somiya *et al*. (Eds.)

BAMR Quality Control Instrumentation. Viscosity measurements.

Bartuli, C., Bemporad, E., Tullianic, J.M., Tirillòa, J., Pulcia, G., and Sebastiani, M., 2009. Mechanical Properties of Cellular Ceramics obtained by Gel-casting: Characterization and Modelling. Journal of the European Ceramic Society.

Baumgartner, J., Murcott, S. and Ezzati1, M., 2007. Reconsidering 'appropriate technology': the effects of operating conditions on the bacterial removal performance of two household drinking-water filter systems. Environ. Res. Lett. 2 (2007) 024003 (6pp).

Bell, M. L. (Inventors: Kodama, Kose and Seki), 1988. Process for preparation of micro-cellular porous ceramic body. US patent: 4891174 (Application Number: 07/263924).

Bielefeldt, A.R., 2009. Bacterial Treatment Effectiveness of Point-of-use ceramic water filters. Water Research, Vol. 43, pp 3559- 3565.

Bill, J., Hoffmann, R., Fuchs, T. and Aldinger, F., 2003. Template-induced deposition of ceramic materials from aqueous solution. Chapter 5.3: Handbook of Advanced Ceramics. S. Somiya *et al*. (Eds.). Elsevier, p. 392.

Boisnolt, J.M., Tirlia, A.B.T., Holmes, C. and Marroy, P., 1999. Concrete developments in cementing technology. Oilfield Review.

Bollman, H., 1957. Unique new forming technique. Ceram. Age, 70: 36-38.

Bowen, H. J. M., 1972. The biochemistry of the trace element; in nuclear activation techniques in life sciences: Proceedings of a symposium, IAEA, Vienna, p. 393.

Brazilian Inmetro Seal of Conformity, 2004. Pressurized POU Standard 14908, and non-plumbed, gravity-fed devices are tested and certified under ABNT NBR 15176.

Brown, J. and Sobsey, M.D., 2010. Microbiological effectiveness of locally produced ceramic filters for drinking water treatment in Cambodia. Journal of Water and Health, 08.1.

Brown, J., Sobsey, M. D. and Proum, S. 2007. Use of ceramic water filters in Cambodia. Water Science and Technology 50(1):111-115.

Brunauer, S., Emmett, P. H. and Teller, E., 1938. Adsorption of gases in multimolecular layers. J. Am. Chem. Soc., 1938, 60, p.309.

Ceramica Stefani. http://www.ceramicastefani.com.br/ URL [Accessed: 17.01.2012].

Chapell, J. S., Ring, T. A., and Birchall, J. D., 1986. Particle size distribution effects on sintering rates. J. Appl. Phys. 60:383-391.

Chaudhuri, M., Verma, S.R., Anirban, G., 1994. Performance evaluation of ceramic filter candles. Journal of Environmental Engineering. Vol. 120. No. 6. 1994.

Chi, W., 2004. Sintering behaviour of porous SiC ceramics. Ceramics International, Vol. 30, pp 869- 874.

Chu, M-Y., Rahaman, M. N., and Brook, R. J., 1991. Effect of heating rate on sintering and coarsening. J. Am. Ceram. Soc. 74: 1217-1225.

Clasen, T., Parra, G., Boisson, S. and Collin, S., 2005. Household-based ceramic water filters for the prevention of diarrhea: a randomized, controlled trial of a pilot program in Colombia. Am. J. Trop. Med. Hyg. 73(4), 790–795.

Clasen, T, and Boisson, S., 2006. Household-based ceramic water filters for the treatment of drinking water in disaster response: and assessment of a pilot programme in the Dominican Republic. Water Practice & Technology, Vol. 1 No. 2.

Clasen, T., Brown, J. and Collin, S., 2006. Preventing diarrhoea with household ceramic water filters: assessment of a pilot project in Bolivia. Int. J. Environ. Health Res. 16(3), 221–239.

Clasen, T., Cairncross, S., Haller, L., Bartram, J., Damian, W., 2007a. Cost effectiveness of water quality interventions for preventing diarrhoeal disease in developing countries. Journal of Water and Health Vol. 5 No 4 pp 599-608.

Clasen, T., Schmidt, W. P., Rabie, T., Roberts, I. & Cairncross, S., 2007b. Interventions to improve water quality for preventing diarrhoea: systematic review and meta-analysis. BMJ 334(7597), 755–756.

Clopeck, K.L., Foster, L.E., Krause, C.F., Manto, J.P., Phillips, D.J, and Yamakoshi, B.L., 2006. Implementation of an appropriate household water purification system in Tourou, Cameroon. University of Virginia.

Coble, R. L., and Gupta, T. K., 1967. Sintering and Related Phenomena, p. 423, New York: Gordon and Breach.

Coble, R. L., and Cannon, R. M., 1978. Current paradigms in powder processing. Mater. Sci. Res. 11: 151-170.

Colomban, P. H., 1989. Gel Technology in Ceramics, Glass-Ceramics and Ceramic-Ceramic Compositest. Ceramics International, 15, pp. 23-50.

Colombo, P., 2008. Engineering Porosity in Polymer-Derived. Journal of the European Ceramic Society, 28, pp.1389–1395.

Coulbert, B., 2005. An Evaluation of Household Drinking Water Treatment Systems in Peru: The Table Filter and the Safe Water System. Brittany.

Cowan, R. E., 1976. Treatise on Materials Science and Technology, Vol. 9, Ceramic Fabrication processes, pp. 153-171, Wang F. F. Y., ed., New York: Academic Press.

Cutler, I. B., 1978. Active powders, Ceramic Processing before Firing, pp. 21-29, Onoda, G. Y., and Hench, L. L., eds., New York: Wiley.

Darcovich, K., Toll, F., Hontanx, P., and Roux, V., 2003. An Experimental and Numerical Study of Particle Size Distribution Effects on the Sintering of Porous Ceramics. Materials Science and Engineering, A348, pp.76-83.

Dies, R. W., 2000. Development of a ceramic water filter for Nepal. MSc. Thesis, Bachelor of Applied Science, University of British Columbia, Canada.

Dinger, R.D., 2002. Rheology for Ceramics. p. 39–40. Dinger Ceramic Consulting Services.

Dobrovolskiy, A.G., 1977. Development of slip moulding methods. Ceramurgia International, Vol. 3, No. 4.

Doulton Filters, 2009. History of the Doulton Ceramic Filter Candle. http://www.doulton.ca/ceramicwaterfilter.html> URL Accessed March 5, 2009.

Dunn, E.J., 1930. Microscopic measurements for the determination of particle size of grains and pigments. Ind. Eng. Chem. Anal. Ed., 2 (1), pp 59–62.

Du Preez, M., Venter, S.N., Theron, J., Matlala, M., Gericke, M., Sigmin, Y., 2001. Enteropathogens in water, Water Research Commission Report, No. 741/1/01, i.

Du Preez, M., Conroy, R.M., Wright, J.A., Moyo, S., Potgieter, N. and Gundry, S.W., 2008. Short Report: Use of Ceramic Water Filtration in the Prevention of Diarrheal Disease: A Randomized Controlled Trial in Rural South Africa and Zimbabwe Am. J. Trop. Med. Hyg., 79(5), pp. 696–701.

Duke, W.F., Nordin, R. and Mazumder, A., 2006. Comparative Analysis of the Filtron and Biosand Water Filters, University of Victoria, British Columbia.

DWA, 2004. National Water Resource Strategy, Chapter 2, p 21. Pretoria.

Dynys, F. W., and Holloran, J. W. 1984. Influence of Aggregates on Sintering. J. Am. Ceram. Soc. 67: 596-601.

EC (European Commission), 2007. Ceramic Manufacturing Industry. BAT reference document.

Eisenberg, J.N., Scott, J.C., Porco, T., 2007. Integrating public health control strategies: balancing water sanitation and hygiene interventions to reduce diarrheal disease burden. Am. J. Public Health. Jan. 3, 2007.

EPA, 2006. Water Health Series Filtration Facts, Sep 2006, 816-K-05-002.

Ergun, Y., 2004. Polymethyl methacrylate based open- cell porous plastics for high-pressure ceramic casting. Material Science and Engineering, A 385, pp 279- 285.

Evans, J. W., and De Jonghe, L. C., 1991. The Production of Inorganic Materials, New York: Macmillan.

Fahay, M., 2009. Sedimentation Methods, CIVIL 2121: Geomechanics. units.civil.uwa.edu.au/teaching/CIVL2122?f=255422 (URL accessed, January 17, 2012).

Fahlin, C.J., 2003 Hydraulic Properties Investigation of the Potters For Peace Colloidal Silver Impregnated, Ceramic Filter. University of Colorado at Boulder, College of Engineering, Undergraduate Independent Study Research. Available at www.pottersforpeace.org (accessed 2 August 2008).

Fewtrell, L., Kaufmann, R., Kay, D., Enanoria, W., Haller, L., Colford, J., 2005. Water, sanitation, and hygiene interventions to reduce diarrhoea in less developed countries: a systematic review and meta-analysis. Lancet Infect Diseases, 5: pp 42—52.

Fish, R., 2001. Rheology for Slip Production and Slip Casting. Old Hickory Clay Company. http://www.oldhickoryclay.com/pdf_files/Rheology_for_Slip.pdf, URL accessed January 17, 2012.

Franz, A., 2007. A Performance Study of Ceramic Candle Filters in Kenya Including Tests for Coliphage Removal. Water Practice & Technology 1.

FTE, 2008. South Africa's looming water crisis. FTE, Sunday, 9 March 2008, 21:28.

Funk, J.E., and Dinger, D.R., 1994. Predictive Process Control of Crowded Particulate Suspensions Applied to Ceramic Manufacturing. Kluwer Academic Publishers, Boston, MA, pp. 452-453.

Furnas, C. C., 1931. Grading Aggregates, Mathematical Relations for Beds of Broken Solids of Maximum Density. Ind. Eng. Chem. 23, pp. 1052-1058.

Ganesh, I., Olherob, S.M., and Torresb, P.M.C., 2009. Hydrolysis-induced Aqueous Gel-casting for near-net shape forming of ZTA Ceramic Composites. Journal of the European Ceramic Society, 29 pp. 1393–1401.

Garcia-Bordejé, E., Pinilla, J.L., and Lazaro, M., 2004. Vanadium Supported on Carbon-Coated Monoliths: effect of pore structure. Applied Catalysis B: Environmental, 50, pp. 235–242.

German, R. M., 1992. Sintering densification for powder mixtures of varying distribution widths. Acta Metall. Mater. 40: 2085-2089.

German, R. M., 1996. Sintering Theory and Practice, New York: Wiley.

Gordon, R. S., 1973. Mass transport in the diffusional creep of ionic solids. J. Am. Ceram. Soc. 56: 147-152.

Gotoh, K., and Higashitani, K., 1997. Gradient ceramic membranes. Powder Technology Handbook. Separation and Purification Technology, 32, pp. 73-79.

Grala, E. M., 1957. Further investigation of the feasibility of the freeze casting method for forming fuel-size infiltrated titanium carbide turbine blades. NACA (Nat. Adv. Comm. Aeronaut.) Tech. Notes 3769; Ceram. Abstr., p. 108.

Green by Design, 2009. Water Filter Guide. <http://greenbydesign.com/guides/>. Accessed March 5, 2009.

Gregorova, E. and Pabst, W., 2004a. Porosity and pore size control in starch consolidation casting of oxide ceramics- achievements and problems. Journal of the European Ceramic Society, Vol. 27, pp 669- 672.

Gregorova, E., Pabst, W. and Stini, J., 2004b. Rheology of ceramic suspensions with organic or niopolymeric gelling additives. Part 1: Theory of viscoelasticity. Ceramics- Silikaty, 48, pp. 93-99.

Gregorova, E., Pabst, W., and Stetina, J., 2006. Viscoelastic behaviour of Ceramic suspensions with carrageenan. Journal of the European Ceramic Society, 26, pp. 1185–1194.

Gregorova, E. and Pabst, W., 2007. Porous Ceramics prepared using Poppy Seed as a pore-forming agent. Ceramics International, 33, pp. 1385–1388.

Guo, J., and Lewis, J. A., 1999. Aggregation effects on compressive flow properties and drying behaviour of colloidal silica suspensions. J. Am. Ceram. 5oc. 82: 2345-2358.

Gyger, L.S., Kulkami, P., Bruck, H.A., Gupta, S. K., and Wilson, O. C., 2007. Replamineform inspired Bone Structures (ribs) using multi-piece moulds and Advanced Ceramic Gel-casting Technology. Materials Science and Engineering, 27(4), pp.:646-653.

Haarhof, J. and Olivier, J., 2002. GAC Performance at three Southern African Water Treatment Plants. Water SA Special Edition: WISA Proceedings, 2002.

Hamidi, A., Hamidi, S., Lattip, A., Rozita, N., and Ay Shin, O., 2008. Preparation and characterisation of Filter Support from local Silica. Solid State Science and Technology, Vol. 16, No 1, pp.14-20.

Handwerker, C. A., Morris, P. A., and Coble, R. L., 1989. Effects of chemical inhomogeneities on grain growth and microstructure in A12O3. J. Am. Ceram. Soc. 72: 130-136.

Hasselman, D. P. H., 1969. Unified Theory of Thermal Shock Fracture Initiation and Crack Propagation in Brittle Ceramics. J. Am. Ceram. Soc. 52, 11,

pp. 600-604.

Haycarb, 2012. Haycarb activated carbon solutions, http://www.haycarb.com/carbon/carbon, URL accessed September 21, 2012.

Hbalze, B. and Gaukler, L.J., 2003. Novel Colloidal forming technique: direct coagulation casting. Handbook of Advanced Ceramics, Chapter 5.5.

Hegenbart, S., 1995. Truth of a grain. Food product design. Weeks Publishing Company.

Holdridge, D.A. and Moore, F., 1952. The Significance of Clay-Water Relationships in Ceramics. British Ceramic Research Association, Penkhull, Stoke-On-Trent.

Holmes, S., 1996. South African Water Quality Guidelines, Volume 1: Domestic Water Use, DWA.

Hotta, T., Abe, H., and Naito, M., 2005. Effect of Coarse Particles on the Strength of Alumina made by Slip Casting. Powder Technology, 149, pp. 106– 111.

Howard, R. E., and Lidiard, A. B., 1964. Matter transport in solids. Rept. Progr. Phys. 27: 161-240.

Hsieh, H. P., 1996. Inorganic Membranes for Separation and Reaction, Amsterdam: Elsevier.

Hummel, F.A., 1951. Thermal Expansion Properties of Some Synthetic Lithia Minerals. Journal of the American Ceramic Society, Vol. 34, Issue 8, pp. 235-239.

Hung, I., Hung, D., Fung, K., and Hon, M-H., 2006. Effect of Calcination Temperature on Morphology of Mesoporous YSZ. Journal of the European Ceramic Society, 26, pp. 2627–2632.

Hunter, R. J., and White, L. R., 1987. Foundations of colloid science. Oxford Oxfordshire New York: Clarendon Press; Oxford University Press.

Hüsken, G. and Brouwers, H.J.H., 2008. A new mix design concept for earth-moist concrete: A theoretical and experimental study. Cement and Concrete Research 38, pp. 1246–1259.

Hwang, R., 2003. Six month field monitoring of point-of-use ceramic water filter by using H2S paper strip most probable number method in San Francisco Libre, Nicaragua. Master of Environmental Engineering Thesis, MIT, Civil and Environmental Engineering Department. Cambridge, Massachusetts.

Jackson, P.J., 1998. Protocol for Testing Cartridge Filters for Treatment of Private Water Supplies. DWI, 4480/I May 1998.

Janney, M. A., 1990. Method for forming ceramic powder into complex shape. US Patent 4.894.194.

Jena, A., Gupta, K., Sarkar, P and Rho, H., 2003. Porosity Characterization of Microporous small Ceramic components. Ceramic Bulletin, Vol. 82, December, 2003, pp. 9401-9406.

Jenkins, R., 1984. X-ray Fluorescence Analysis. Analytical Chemistry, 56 (9), pp. 1099A-1106A.

Jimbo, G., 1992. Chemical engineering analysis of fine grinding phenomenon and process. J. Chem. Eng. Jpn, 25, pp.117-127.

Karagedov, G.R.; Shatskaya, S.S. and Lyakhov, N.Z., 2006. Nature of a Mechanically Stimulated Phase change in Zirconia. Chemistry for Sustainable Development, 14, pp. 345-353.

Kichkailo, O.V. and Levitskii, L.A., 2005. Lithium Bearing Heat Resistant Ceramics. Glas & Ceramics, Vol. 62, No.5-6.

King, A.G., 2002. Ceramic Technology and Processing. William Andrew Publishing, pp 211-215.

Kingery, W.D., and Francois, B., 1967. Sintering of crystalline oxides, I. Interactions between grain boundaries and pores. Sintering and Related Phenomena, pp. 471-498, Kuczynski, G. C., Hooton, N. A., and Gibbon, G. F., eds., New York: Gordon & Breach.

Kingery, W.D., Bowen, H.K., and Uhlmann, D. R. (1976). Introduction to Ceramics, 2nd edn, New York: Wiley.

Kupper, T.E., Kupper, A.H., Schoffl, V, and Milledge, J.S., 2009. Water Disinfection in the Mountains, State of the Art Recommendation. Paper of the Union Internationale Des Associations D'alpinisme Medical Commission. Travel Medicine and Infectious Disease, 7, pp. 7-14.

Landham, R. R., Nahass, P., Leung, D. K., Ungureit, M., Rhine, W. E., Bowen, H. K., and Calvert, P. D., 1987. Potential use of polymerizable solvents and dispersants for tape-casting of ceramics. Am. Ceram. Soc. Bull. 66: 1513-1516.

Lange, F. F., Davis, B. I., and Aksay, I. A. 1983. Processing-Related Fracture Origins: I, Observations in Sintered and Isostatically Hot-Pressed $A1_20_3/ZrO_2$ Composites. J. Am. Ceram. Soc. 66: 407-408.

Lange, F. F., 1989. Powder Processing Science and Technology of Increased Reliability. J. Am. Ceram. Soc. 72 pp. 3-15.

Lantagne, D.S., 2001. Investigation of Potters for Peace colloidal silver impregnated ceramic filter Report 1: Intrinsic effectiveness. USAID P.O. 524-0-00-01-00014-5362.

Lantagne, C.E., 2005. Research on Colloidal Silver Impregnated Pot. Enrique Campbell Consultant.

Lemons, A., 2009. Maji Salama: Implementing ceramic water filtration technology in Arusha, Tanzania. MPH Candidate thesis.

Levin, E.M., Robbins, C.R., and McMurdie, H.F., 1985. Phase diagrams for ceramists. National Bureau of Standards, Vol. 1, p.166.

Li, W., Xing, W., and Xu, N., 2006. Modelling of Relationship between Water Permeability and Microstructure Parameters of Ceramic Membranes. Desalination, 192, pp. 340–345.

Liu, D.M., 1991. Influence of Solid Loading and Particle Size Distribution on the Porosity Development of Green Alumina Ceramic Mouldings. Ceramics International, 23, pp. 513-520.

Liu, Y., Liu, X-Q, Wei, H. and Meng, G-Y., 2001. Porous Mullite Ceramics from National Clay produced by Gel-casting. Ceramics International, 27, pp 1-7.

Low, C.S., 2002. Appropriate Microbial Indicator Tests for Drinking Water in developing Countries and Assessment of Ceramic Water Filters, M Thesis, 2002, MIT.

Lowenstam, H. A., and Weiner, S., 1989. On Biomineralization, New York: Oxford University Press.

Lu, P.K., and Lannutti, J.J., 2000. Effect of density gradients on dimensional tolerance during binder removal. J. Am. Ceram. Soc. 83: 2536-2542.

Lyckfeldt, O., and Ferreira, J.M.F., 1998. Processing of porous ceramics by starch consolidation. Journal of the European Ceramic Society 18 (1998) pp 131-140.

Mandal, S., 2007. Synthesis of low expansion ceramics in lithia-alumina-silica system with zirconia additive using the power precursor in the form of hydroxyhydrogel. Ceramics International, 33, pp 123-132.

Mann, S., Webb, J., and Williams, R.J.P., 1989. Biomineralization, Weinheim: VCH Verlagsgesellschaft.

Martin, L.P., Nagle, D., and Rosen, M., 1998. Effect of Particle Size Distribution upon Specific Surface Area and Ultrasonic Velocity in Sintered Ceramic Powders. Materials Science and Engineering, A246, pp. 151–160.

Masaaki, T.M. and Kurita, S., 1997. Development of Self-Hardening Slip Casting. Journal of European Cer. Soc., 17, pp. 415 419.

Masuda, T., Sato, A., and Hara, H., 1994. Preparation of a Dense Zeolite Film on the outer surface of an Alumina Ceramic Filter. Applied Catalysis, General 111, pp.143-150.

Mathibela, N.G., 2012. Bacteriological efficiency of low-cost point-of-use ceramic water filter units of low, medium and high flow rates. Hon. Project, Department of Biochemistry and Microbiology, UNIZUL.

Maxwell, W.A., Gurnick, R. S., and Francisco, A. C., 1954. Preliminary investigation of the freeze casting method for forming refractory powders. NACA (Nat. Adv. Comm. Aeronaut.) Res. Memo E 53L21, p. 19.

McAllister, S., 2005. Analysis and comparison of sustainable water filters. Epd. 397 technical report. Undergraduate Engineering Review, University of Wisconsin.

Micromeretics Internet Website: Gas sorption analysis. < http://www.micromeretics.com> Accessed March 9, 2009

Mohd, B., 2002. Estimating some Pore-Related Properties of Limestone from Bulk Density and Water Absorption Data. Natural Resources and Chemical Engineering Department, Applied Tafila College.

Momba, M.N.B., Offringa, G., Nameni G. and Brouckaert, B., 2010. Nanotechnology-based clay filter pot to purify water in rural homes, WRC Report No. KV 244/10, pp. 46.

Momba, M.N.B., 2013. Selection criteria and use of hwts by rural communities without improved water sources, PowerPoint presentation, TUT Water Research Group, Faculty of Science, Research day. Pretoria: University of Pretoria. http://www.wrc.org.za> Accessed April 15, 2013

Morris, J., 2004. Ceramic Water Purifier National Roll-Out Strategy and Quality Assurance Plan, IDE 2004.

Moszynski, P., 2006. Worldwide water crisis is a 'silent emergency', UN agency says. Brit. Med. J. 333, 986.

Mulder, M., 1996. Basic Principles of Membrane Technology, Dordrecht: Kluwer Academic Publishers.

Mutsuddy, B.C., and Ford, R.C., 1995. Ceramic Injection Moulding; Materials Technology Series, London: Chapman & Hall.

Naito, M., Hotta, T., Hayakawa, O., Shinohara, N., and Uematsu, K., 1998. Ball milling conditions of a very small amount of large particles in silicon nitride powder. J. Ceram. Soc. Jpn 106: 811-814.

Naito, M., and Jimbo, G., 1985. Effect of additives on the powder mechanical properties and its application for mechanical processing. Funsai 29: 104-114.

Naito, M., Shinohara, N. and Uematsuet, K., 2003. Chapter 2.1: Raw Materials. Handbook of Advanced Ceramics, S. Somiya *et al*. (Eds.). Elsevier Inc.

Narula, C. K., 1995. Ceramic Precursor Technology and its Applications, New York: Marcel Dekker.

Neirinck, B., Fransaer, J., Van der Biest, O., and Vleugels, J., 2009. A novel route to produce porous ceramics. Journal of the European Ceramic Soc., 29 pp. 833-836

NSF (National Sanitation Foundation, now NSF-International), 2003. Microbiological Water Purifiers, NSF P231, Ann Arbor, accessed from

Ohmori, H., 2003. Chapter 7.1: Grinding. Handbook of Advanced Ceramics. S. Somiya *et al*. (Eds.). Elsevier.

Ohring, M., 2000. The Materials Science of Thin Films, Boston, MA: Academic Press.

Okada, K., Uchiyama, S., Isobea, T., Kameshimaa, Y., Nakajimaa, A., and Kurata, T., 2009. Capillary rise properties of Porous Mullite Ceramics prepared by an Extrusion Method using Organic Fibres as the Pore Former. Journal of the European Ceramic Society, 29, pp. 2491–2497.

Omatete, O.O., Strehlow, R.A., and Walls, C.A., 1992. Drying of gelcast ceramics, in Ceramic Transactions, Vol. 26: Forming Science and Technology for Ceramics, pp. 101-107, Cima M. J., ed., Westerville, OH: American Ceramic Society.

Oyanedel-Craver, V.A. and Smith, J.A., 2008 Sustainable colloidal-silver-impregnated ceramic filter for point-of-use water treatment. Environ. Sci. Technol. 42, 927–933.

Ozgur, C. and San, O., 2009. Fine Particle Migration during Slip Casting. Ceramics International.

Padilla, S., Vallet-Regí, M., Ginebra, M.P., and Gil, F.J., 2005. Processing and Mechanical Properties of Hydroxyapatite pieces obtained by the Gel-casting Method. Journal of the European Ceramic Society, 25, pp. 375–383.

Palacio, L., Bouzerdib, Y., Ouammoub, M., Albizaneb, A., Bennazhab, J., Hernándeza, A., and Calvo, J.I., 2009. Ceramic Membranes from Moroccan Natural Clay and phosphate for Industrial Water Treatment. Desalination, 245, pp. 501–507.

Palmour, H., Geho, M., Russell, R. L., and Hare, T. M., 1992. Study of Do effects on subsequent densification behaviour in spinel and alumina ceramics, Sintering '91, pp. 37-44, Chaklader, A. C. D., and Lund, J. A., eds., Brookfield, VT: Trans Tech.

Park, C-L, Kim, B-G, Jeon, H-S and Lee, J-R., 2010. Heat-resistant ceramics based on LAS-system non-metallic mineral and its thermal shock resistance. Journal of the Ceramic Society of Japan, 118, pp. 220-225.

Patterson, B.R., and Benson, L.A., 1983. The effect of powder size distribution on sintering. Progr. Powder Met. 39: 215-230.

Poehls, D. J. and Smith, G. J., 2009. Encyclopaedic Dictionary of Hydrogeology. Elsevier, pp. 1-517.

Pruss, A., Kay D., Fewtrell L. and Bartram J., 2002. Estimating the burden of disease from water, sanitation, and hygiene at a global level. Environ. Health Perspective. 110(5), 537–542.

Puyate, Y.T., 2009. Models for predicting drying stress: An alternative approach. Chemical Engineering Science, Vol. 64, pp 1820-1831.

Rahaman, M. N., De Jonghe, L. C., and Chu, M., 1991. Effect of green density on densification and creep during sintering. J. Am. Ceram. Soc. 74: 514-519.

Rahaman, M. N., 1995. Ceramic Processing and Sintering, First Edition, New York: Marcel Dekker.

Rahaman, M. N., and Zhou, Y., 1995. Effect of dopants on the sintering of ultra-fine CeO_2 powder. J. Eur. Ceram. Soc. 15: 939-950.

Rahaman, M. N., 2003. Ceramic Processing and Sintering, Second Edition, New York: Marcel Dekker.

Raj, R., 1987. Analysis of the sintering pressure. J. Am. Ceram. Soc. 70: C210-C211.

Ramachandra, R and Rao, R.R., 1999. Characterisation of Aqueous Silicon Slips. Journal of the European Ceramic Society, 19, pp. 2763-2771.

Readey, D. W., 1966. Mass transport and sintering in impure ionic solids. J. Am. Ceram. Soc. 49: 366-369.

Reed, J. S., 1995. Principles of Ceramics Processing, 2nd edn, New York: Wiley, pp. 215, xxii, 658.

Rhodes, W. H., and Wench, B.J., 1973. J. Am. Ceram. Soc. 56: 495.

Rhodes, W. W., 1981. Agglomerate and particle size effects on sintering of yttria-stabilized zirconia. J. Am. Ceram. Soc. 64, pp. 19-22.

Ring, T. A., 1996. Fundamentals of Ceramic Powder Processing and Synthesis, San Diego, CA: Academic Press.

Rumpf, H., 1959. Beanspruchungstheorie der Prallzerkleinerung Chemie-Ing-Techn. 39: 323-337.

Ruoff, A. L., 1965. Mass transfer problems in ionic crystals with charge neutrality. J. Appl. Phys. 36: 2903-2907.

S-14.10: Particle Size Analysis Hydrometer Method. 2003. S - 14.10 WCC-103 Publication, WREP-125, 2nd Edition

Sakar-Deliormanh, A. and Yayla, Z., 2002. Effects of calcium hydroxide on slip casting behaviour. Applied Science 24, 2004, 237 -243.

Sarkar, N., and Greminger Jr., G. K., 1983. Methylcellulose polymers as multifunctional processing aids in ceramics. Am. Ceram. Soc. Bull. 62: 1280-1288.

Schoenert, K., and Steier, K., 1971. Die Grenze der Zerkleinerung bei kleiner Korngroessen. Chemie-Ing-Techn. 43: 773-777.

Segal, D., 1989. Chemical Synthesis of Advanced Ceramic Materials, Cambridge: Cambridge.

Shui, A., Kato, Z., Tanaka, S., Uchida, N., and Uematsu, K., 2001. Isotropic sintering shrinkage in pressed compact of near-spherical alumina particles. Am. Ceram. 5oc. Bull. 80: 29-32.

Sigmund, W. M., Bell, N. S., and Bergstrom, L., 2000. Novel powder-processing methods for advanced ceramics. J. Am. Ceram. Soc. 83, pp. 1557-1574.

Silakate, P., Nuntiya, A. and Larpkiattaworn, S., 2008. Effect of Flocculation of Alumina Slip on the Pore Size Distribution of Cast Alumina by Polyacrylamide (PAM). Chiang Mai J. Sci., 35(1), pp. 17-22

Simonis, J.J. and Basson, A.K., 2011. Evaluation of a low-cost ceramic micro-porous filter for elimination of common disease microorganisms. Physics and Chemistry of the Earth, Elsevier, 36, pp. 1129-1134.

Simonis, J.J. and Basson, A.K., 2012. Manufacturing a low-cost ceramic water filter and filter system for the elimination of common pathogenic bacteria. Physics and Chemistry of the Earth, Elsevier, 5--52, pp. 269-276.

Singh, P., Daniel, I., Joseph, D., Sathish, C.I., Gurupathama, S.K., Dalala, B. and Nudurupatia, S., 2009. Spontaneous dispersion of particles on liquid surfaces. PNAS, vol. 106, no. 47, pp. 19761-19764.

Sobsey, M. D., 2002. Managing Water in the Home: Accelerated Health Gains from Improved Water Supply. WHO, Geneva. Sobsey MD, 2000.

Soil Moisture and Porous Ceramics Catalog, 2008. Soilmoisture Equipment Corp.

Sphere Project, 2004. URL http://www.sphereproject.org/. Accessed June 27, 2012

Subbanna, M., Kapur, P.C., and Pradip, P., 2002. Role of Powder Size, Packing, Solid Loading and Dispersion. Colloidal Processing of Ceramics. Ceramics International, 28, pp. 401–405.

Takahashi, M. and Kurita, S., 1997. Development of self-hardening slip casting. Journal of the European Ceramic Society, vol. 17, pp. 415-419.

Takahashi, M., Menchavez, R.L., Fuji, M., and Takegami, H., 2009. Opportunities of Porous Ceramics Fabricated by Gel-casting. Mitigating Environmental Issues. Journal of the European Ceramic Society, 29, pp. 823–828.

Tari, G., 1999. Influence of particle size and particle distribution on drying-shrinkage behaviour of alumina slip cast bodies. Ceramics International, Vol. 25, pp 577 – 580.

Tarton, A., 2008. Key Note Address: A clean South Africa. Presented at the CSIR Conference: Science Real and Relevant, Pretoria.

The Quartz Page, 2012. The silica group, http://www.quartzpage.de/gen_mod.html#pdsp, URL accessed September 21, 2012.

Thompson, R.A., 1981. Mechanics of powder pressing: I Model for powder densification. Bull. Am. Ceramic Soc., 60, pp 244 – 251.

Thompson, A. M., and Harmer, M. P., 1993. Influence of atmosphere on the final stage sintering kinetics of ultra-high-purity alumina. J. Am. Ceram. Soc, 76, pp. 2248-2256.

Tormey, E. S., Pober, R. L., Bowen, H. K., and Calvert, P. D., 1984. Tape-casting future developments, in Advances in Ceramics, Vol. 9: Forming of Ceramics, pp. 140-149, Mangels, J. A., and Messing G.L., eds., Columbus, OH: American Ceramic Society.

Tsuru, T., 2003. Chapter 10: Porous Ceramics for Filtration, Handbook of Advanced Ceramics, S. Somiya *et al* (Eds.)

Tulliani, J-M., Bartuli, C., Bemporad, E., Naglieria, V., and Sebastiani, M., 2009. Characterization of Dense and Porous Zirconia Produced by Gel-casting with Gelatin as a Gelling Agent. Ceramics International, 35, pp. 2481–2491.

Uematsu, K., Ito, H., Zhang, Y., and Uchida, N., 1995. Novel characterization method for the processing ceramics by polarized light microscope with liquid immersion technique. Ceram. Trans. 54: 83-89.

Uematsu, K., 1996. Immersion Microscopy for Detailed Characterization of Defects in Ceramic Powders and Green Bodies. Powder Technol. 88: 291-298.

USEPA (United States Environmental Protection Agency), 1987.Guide Standard and Protocol for Testing Microbiological Water Purifiers. USEPA, Office of Drinking Water, Washington, DC.

USFilter, 2012. Filtration Product Handbook, US Filter - Plymouth Pro. www.thewaterexchange.net/water-filters-basics.htm, URL accessed January 17, 2012.

Van Halem, D., 2006. Ceramic Silver Impregnated Pot Filters for Household Drinking Water Treatment in Developing Countries. MSc. Thesis, Delft University of Technology.

Van Halen, D., van der Laan, H., Heijmana, S.J.G., van Dijk, J.C., and Amy, G.L., 2009. Assessing the Sustainability of the Silver-Impregnated Ceramic Pot Filter for Low-Cost Household Drinking Water Treatment. Physics and Chemistry of the Earth, 34, pp. 36–42.

Van Vuuren, L., 2008. Eutrophication - Microscope Refocused on SA water Quality Threat. The Water Wheel, DWAF, Sept./Oct. 2008, Pretoria.

Vidal, D., Ridgway, C., Pianet, G., Schoelkopf, J., Roy, R., and Bertrand, F., 2009. Effect of Particle Size Distribution and Packing Compression on Fluid Permeability as Predicted by Lattice-Boltzmann Simulations. Computers and Chemical Engineering, 33, pp. 256–266.

Von Hoy, C., Barda, A., Griffith, M., and Halloran, J. W., 1998. Micro fabrication of ceramics by co-extrusion. J. Am. Ceram. Soc. 81: 152-158.

Wegmann, M., Michen, B., and Graule, T., 2008a. Nanostructured Surface Modification of Microporous Ceramics for Efficient Virus Filtration. Journal of the European Ceramic Society, 28, pp. 1603–1612.

Wegmann, M., Luxbacher, T., Fritsch, J., and Graule, T., 2008b. Modification of Ceramic Microfilters with Colloidal Zirconia to Promote the Adsorption of Viruses from Water. WRC., 42, pp. 1726 – 1734.

Weiguang, C., Dongliang, J., Zhengren, H., Shouhong, T., 2005. Sintering behaviour of porous SiC ceramics. Ceramics International 30 (2004), pp 869–874.

Wittemore, O.J., 1999. Method for the extrusion of ceramic filter media. USA Patent 5925309

WHO and UNICEF, 2000. Global Water Supply and Sanitation Assessment Report, Geneva.

WHO, 2006. Guidelines for Drinking-Water Quality, First Addendum to Third Edition, Volume 1 Recommendations, Geneva.

WHO and UNICEF, 2006. Joint Monitoring Programme for Water Supply and Sanitation. Available at: http://www.wssinfo.org/en/233_wat_africaS.html. Accessed July 16, 2008 Latest

WHO, 2007. Combating waterborne disease at the household level. 2007. <http://www.who.int/household_water/en/> Accessed March 5, 2009

WHO, 2009. <http://www.who.int/household_water/en/> Accessed March 5, 2009.

WHO, 2011. Evaluating Household Water Treatment Options: Health-Based Targets and Microbiological Performance Specifications. World Health Organization; 1st edition (November 2011)

World Health Report, 2008. Primary Health Care Now More Than Ever http://www.who.int/whr/2008/whr08_en.pdf >Accessed March 5, 2009

WQA (Water Quality Association), 2012. ORD 0901: Microbiological Testing Protocol- Tap Water Sources for Developing Countries- Pour Through Products. http://www.wqa.org/goldseal/34.html. Accessed January 2012.

Wright, J. F., Jr, and Reed, J. S., 2001. Polymer-plasticized ceramic extrusion. Part 1.Am. Ceram. Soc. Bull. 80: 31-35.

Yamaguchi, T., and Kosha, H., 1981. Sintering of acicular Fe_20_3 particles. J. Am. Ceram. Soc. 64: C84-C85.

Yang, G. and Tsai, C., 2008. Effects of Starch Addition on Characteristics of Tubular Porous Ceramic Membrane Substrates. Desalination, 233, pp. 129–136.

Yang, J-F., Hayashi, I., Zhang, G.J., and Ohji, J., 2005. Effects of Pore Morphology on the Fabrication and mechanical Properties of Porous Si3N4 Ceramics. Azjomo Journal of Materials Online.

Yang, Y., Laarz, E., Kaushik, S., Mueller, E., and Sigmund, W., 2003. Chapter 3-Forming and Drying, Handbook of Advanced Ceramics S. Somiya *et al*. (Eds.), pp 131- 186.

Yeh, An.-I. and Li, J.-Y., 1996. A continuous measurement of swelling of rice starch during heating. Journal of Cereal Science, 23, 277–283.

Yin, L., Penga, H.X., Dharab, S., Yangc, L., and Su, B., 2009. Natural additives in protein coagulation casting for improved microstructural controllability of cellular ceramics. Composites, Part B

Yokoyama, T., Urayama, K., Naito, M., Kato, M., and Yokoyama, T., 1987. The Angmill Mechanofusion System and its applications. KONA 5: 59-68.

Yokoyama, T., Urayama, K., Naito, M., Kato, M., and Yokoyama, T., 1988. Ultra-fine grinding by a new attrition type mill and its application to the particle reformation. Proc. 2. "Japan-Soviet Symposium on Mechanochemistry," pp. 281-290, March, Tokyo.

Young, A. C., Omatete, O. O., Janney, M. A., and Menchhofer, P. A., 1991. Gel-casting of Alumina. J. Am. Ceram. Soc. 74: 612-618.

Zand, A., Sikorski, Y., Sanders, M., and Navaz, H., 2007. A simple laboratory experiment for the measurement of single phase permeability. Journal of Physical and General Sciences, Volume 1, Issue 2.

Zaspalis, V.T., Kikkinides, E.S., Kolenbrander, M. and Mauczok, R., 2003. Method for the Morphological characterization Of Powder Raw Materials for the Manufacturing of Ceramics. Journal of Materials Processing Technology, 142, pp. 267–274.

Zhang, Y. and Binner. J., 2002. Enhanced Casting Rate by Dynamic Heating during Slip Casting. Journal of the European Ceramic Society, 22, pp. 135–142.

Zheng, J., and Reed, J. S., 1989. Effects of particle packing characteristics on solid-state sintering. J. Am. Ceram. Soc. 72, pp. 810-817.

Zhou, Y., and Rahaman, M. N., 1993. Hydrothermal synthesis and sintering of ultra-fine CeO2 powders. J. Mater. Res. 8: 1680-1686.

Zivcova, Z., Gregorová, E., Pabst, W., Smith, D.S., Michot, A., and Poulier, C., 2009. Thermal Conductivity of Porous Alumina Ceramics Prepared Using Starch as a Pore-Forming Agent. Journal of the European Ceramic Society, 29, pp. 347–353.

Zuberi, B., Liu, J.J., Carty, W.M., and Pillai, S.C., 2009. Low Coefficient of Thermal Expansion Materials including nonstoichiometric Cordierite Fibres and Methods of Manufacture. Patent C04b3503FI.